

بِسْمِ اللّٰهِ الرَّحْمٰنِ الرَّحِیْمِ

SUDAN UNIVERSITY OF SCIENCE AND TECHNOLOGY
COLLAGE OF GRADUATE STUDIES

**QSAR Study of 2-Phenyl – and 2,3 - Diphenyl
Quinoline – 4- Carboxylic Acid Derivatives as
Biologically Active Compounds**

دراسة العلاقة الكمية بين البنية و الفعالية لمشتقات 2- فينيل و 2،3 -
- ثنائي فينيل كينولين - 4- حمض الكربوكسيليك كمركبات نشطة
بيولوجياً

by

TAWASSL TAJ ELSIR HASSAN HAG ALSIDDIG

(MSc. Chemistry, BSc. Chemistry)

*A thesis submitted in fulfillment of the requirements of the Ph.D
degree in chemistry at Sudan University of Science and Technology.*

Supervisor:

Prof. Dr. Ahmed Elsadig Mohammed Saeed

Chemistry Department

College of Science

March.2019



Approval Page

(To be completed after the college council approval)

Name of Candidate:

Thesis title:

Degree Examined for: Ph.D. (Chemistry)

Approved by:

1. External Examiner

Name: Prof. Younis M. H. Younis

Signature: Date: 07/03/2019

2. Internal Examiner

Name: Dr. Mohamed EL Mukhtar Abdell Aziz

Signature: Date: 07/03/2019

3. Supervisor

Name: Ahmed Elsadig Mohammed Saed

Signature: Date: 07/03/2019

قال الله تعالى :

رَبِّ أُرْوِ عَنِّي ذُرًّا تُشْكِرُ فَسَتَكِرُ لِي أَنِّي أُنْفِسُ عَلَيَّ وَعَلَى وَالِدِيَّ

ذُرًّا أُرْعِيهِ صَالِحًا نُرْضَاهُ وَأُرْوِي لِي بِرَحْمَتِكَ فِي عِبَادَتِكَ

(الصالحين)

Dedication

This work is dedicated

To soul of my father

To My mother for always loving and supporting me

To my wonderful children Lina and Gaffer

To my brother and sister

To my friends

To anyone who helped me

Tawassul

ACKNOWLEDGMENTS

First of all thanks for ALLAH for everything and my sincere thanks
to my supervisor:

Prof. Dr. Ahmed Elsadig Mohammed Saeed, for suggesting the idea
of this work and guidance during all stages of research.

Astaza. Hiba Hashim Mahgoub, Department of Chemistry, College of
Science, Sudan University of Science and Technology

Dr. Mayson Mohammed Almahdi, Department of Chemistry, College
of Education, Alzaiem Alazhari University

Ibrahim Khalifa, College Pharmacy, King Saud University

I am deeply indebted to them for their useful help.

I am also grateful to any person worked with me in any way in
research Lab in Sudan University and all technical staff of the
Chemistry department, Sudan University of Science and Technology
for their help.

Abstract

Quinoline derivatives are very important in synthetic medicinal chemistry because of their wide biological range in natural products and drugs; this importance led to consider the activity of newly designed and synthesized quinoline-4-carboxylic acid derivatives as human dihydroorotate dehydrogenase (DHODH) enzyme inhibitors.

In this work set of data used to study quantitative structure activity relationship (QSAR) of quinoline-4-carboxylic acids derivatives were obtained from previous published article containing biological activity of quinoline derivatives having similar skeleton.

Thus the models obtained can be used to predict the activity of newly designed derivatives against vesicular stomatitis virus (VSV) replication as dihydroorotate dehydrogenase (DHODH) enzyme inhibitor. A highly descriptive and predictive QSAR model was obtained through calculation of alignment-independent descriptors using MOE2009.10 software. The 25 quinoline derivatives of data set divided into training set and test set. A training set composed of 20 compounds and obtained by partial least squares (PLS) analysis resulted in a model displaying a squared correlation coefficient r^2 of 0.913. Validation of this model was performed using leave-one-out method (LOO) giving q^2 of 0.842 and r^2_{pre} of 0.873, for a test set of 5 compounds. This model was used to predict the biological activity of 180 new designed quinoline-4-carboxylic acid derivatives and brequinar as a reference. The 87 compounds showed higher predicted activity than that for brequinar. Lipinski's rule of five (RO5) was applied to select compounds from the 86 new designed derivatives for synthesis and elevated pharmacokinetic for them. Therefore 16 compounds were selected for synthesis possessing higher predicted activity and agreeing with rule of five.

New quinolines were synthesized from three-component of different types of arylaldehyde, p-amino-acetophenone and phenyl pyruvic acid using Doebner-

Miller reaction. Quinoline-4-carboxylic acids were reacted by Claisen-Schmidt condensation with arylaldehydes in the presence of sodium hydroxide in order to give the corresponding α,β -unsaturated carbonyl derivatives which were condensed with urea, thiourea, hydrazine, phenyl hydrazine, semicarbazide hydrochloride and monoethanolamide to produce good yield of 2-pyrimidinone, 2-pyrimidinethion, pyrazoline-1-phenyl, pyrazoline, pyrazoline-1-carboxamide and 1,4-oxazepines derivatives, respectively. The purity and identities of products were elucidated through thin layer chromatography (TLC), melting point and spectroscopic data (IR, ^1H NMR, ^{13}C NMR, GC-Mass).

Docking study was performed by MOE2009.10 software for each data set, 16 synthesized compounds and 70 compounds having high predicted activity to evaluate their interactions with protein of (DHODH) enzyme. In this study a number of compounds showed higher interactions than this of stranded reference brequinar.

الخلاصة

مشتقات الكينولين مهمة جداً في الكيمياء الدوائية الإصطناعية بسبب نطاقها البيولوجي الواسع في المنتجات الطبيعية والأدوية، وقد أدت هذه الأهمية إلى دراسة نشاط مشتقات حمض كينولين-4-كاربوكسيليك المصممة والمخلقة الجديدة كمثبطات إنزيم ثنائي هيدروروتيت ديهيدروجينيز (DHODH).

في هذه الدراسة، تم الحصول على مجموعة البيانات من مقالة منشورة وتحتوي على نشاط بيولوجي لمشتقات كينولين تمتلك هيكل أساسي مماثل لأحماض الكينولين-4-كربوكسيليك لإجراء دراسة كمية لعلاقة البنية بالفعالية (QSAR) من أجل الحصول على النماذج التي يمكن إستخدامها للتنبؤ بنشاط المشتقات المصممة الجديدة ضد تكاثر فيروسات الفطور الحويصلية (VSV) كمثبط إنزيم ثنائي هيدروروتيت ديهيدروجينيز (DHODH). تم الحصول على نموذج QSAR ذو وصفية وتنبؤية عالية من خلال حساب واصفات مستقلة بإستخدام برنامج MOE2009.10. حيث أن 25 مركب لمجموعة البيانات قسمت إلى مجموعة تدريب ومجموعة إختبار. من خلال مجموعة التدريب التي تتكون من 20 مركباً، تم تكوين نموذجاً بطريقة تحليل المربعات الصغرى (PLS) يعرض مربع معامل الارتباط r^2 مقداره 0.913. تم إجراء التحقق من صحة هذا النموذج بإستخدام طريقة leave-one-out (LOO) وحسبت قيمة q^2 ومقدراها 0.842 وقيمة r^2_{pre} وقدرها 0.873 لمجموعة الإختبار المكونة من 5 مركبات. تم إستخدام هذا النموذج للتنبؤ بالنشاط البيولوجي لـ 180 مشتق لأحماض الكينولين-4-كاربوكسيليك الجديدة المصممة و brequinar كمرجع. أظهرت 86 مركباً فعالية حيوية متوقعة أعلى من brequinar وطبقت عليها قاعدة Lipinski (RO5) من أجل اختيار مركبات مناسبة للتخليق من الـ 86 مركباً ودراسة الحركية الدوائية لها. لذلك تم إختيار 16 مركباً تمتلك نشاطاً متوقعاً أعلى من ذلك لـ brequinar وتتفق مع قاعدة Lipinski.

تم تخليق مركبات الكينولين الجديدة عن طريق تفاعل دوبنر- ميلر (Doebner-Miller)، من ثلاثة مكونات هي الالدهيدات، بارا-أمينو-أسيوفينون و حامض الفنيل بيروفيك. مشتقات أحماض الكينولين-4-كاربوكسيلية الناتجة تفاعلت بواسطة تكاثف Claisen-Schmidt مع الالدهيدات في وجود هيدروكسيد الصوديوم من أجل إنتاج مشتقات، α - β الكربونيل غير المشبعة المقابلة والتي تتفاعل مع اليوريا، ثيوريا، هيدرازين، فينيل هيدرازين، سيمي كربازيد واحادي الإيثانول أمين لتكوين مشتقات لحقات 2-بيريميدينون، 2 بيريميدينون، بيرازولين-1-فينيل، بيرازولين، بيرازولين-1-كربوزاميد و 1، 4 أوكسازيبين، على التوالي مع ناتج جيد. تم إجراء التحاليل الكيميائية التأكيدية من درجة الإنصهار و كروماتوغرافيا الطبقة الرقيقة والطرق الطيفية (IR، $^1\text{H-NMR}$ ، $^{13}\text{CNMR}$ و GCMS) وقد أظهرت نتائج جيدة.

تم تنفيذ دراسة الإلتحام الجزيئي بواسطة برنامج MOE2009.10 لكل من مركبات مجموعة البيانات و86 مركب من المركبات المصممة التي تمتلك نشاطاً حيويًا متوقعًا عاليًا من أجل دراسة إرتباطها مع بروتين إنزيم (DHODH). خلال هذه الدراسة أظهرت بعض المركبات ارتباطًا عاليًا مقارنة بـ .brequinar

TABLE OF CONTENTS

Dedication	i
Acknowledgment	ii
Abstract (English)	iii
Abstract (Arabic)	v
Table of contents	vii
List of tables	xiii
List of figures	xv
List of Schemes	xxii
List of abbreviations	xxiii

CHAPTER ONE

Introduction

1.	Introduction	1
1.1	Quinolines	1
1.1.1	Structure and nomenclature of quinolone	1
1.1.2	Properties of quinoline	1
1.1.3	Quinoline Synthesis	1
1.1.3.1	Skraup synthesis	1
1.1.3.2	Doebner-Miller ring synthesis	2
1.1.3.3	Friedlander synthesis	2
1.1.3.4	Combes synthesis	3
1.1.3.5	Conrad–Limpach synthesis	3
1.1.3.6	The Pfitzinger synthesis	3

1.1.4	Importance of Quinolines	4
1.1.4.1	Antimalarial Activity	4
1.1.4.2	Anticancer Activity	5
1.1.4.3	Antimycobacterial Activity	6
1.1.4.4	Antimicrobial Activity	7
1.1.4.5	Antiinflammatory Activity	7
1.1.4.6	Antifungal Activity	8
1.1.4.7	HIV inhibitor Activity	8
1.2	Computational Chemistry	9
1.3	Chemoinformatics	9
1.3.1	Drug Design	10
1.3.1.1	Structure-Based Drug Design (SBDD)	10
1.3.1.2	Molecular Docking	10
1.3.1.3	Virtual Screening (VS)	11
1.3.2	Property Prediction (QSAR/QSPR)	12
1.3.2.1	Aims and objectives of QSPR	12
1.3.2.2	Development of QSPR model	13
1.3.2.3	Molecular descriptors	13
1.3.2.3.1	Quantifying Structure in terms of Lipophilicity	14
1.3.2.3.2	Quantifying Structure in terms of Electronic Parameters	15
1.3.2.3.3	Steric Parameters	15
1.3.2.3.4	Molar Refractivity (MR)	16
1.3.2.3.5	Molecular Connectivity	16

1. 3. 2. 4	Regression Analysis (Hansch Analysis)	16
1. 3. 2. 4.1	Application of Statistics	18
1. 3. 2. 4.2	Methodology and Precautions	18
1. 3. 2. 4.2.1	Biological activity	18
1. 3. 2. 4.2.2	Number of independent variables	18
1. 3. 2. 5	Comparative Molecular field Analysis (CoMFA)	18
1. 3. 2. 6	Application of QSAR	19
1. 3. 2. 7	Objectives of QSAR	19
1. 3. 2. 8	Importance in Drug Research	20
1.4	Rational drug design	21
1.4.1	computer-aided drug discovery (CADD)	22
1.5	Lipinski,s Rule	24
1.6	Aim and objective of current study	24

CHAPTER TWO

Materials and Methods

2.	Materials and Methods	26
2.1	Materials, Software's and instruments	26
2. 1. 1	Data Set	26
2. 1. 2	Chemicals	26
2. 1. 3	Software	27
2. 1. 3. 1	ACD labs Software	27
2. 1. 3. 2	ChemDraw Software	27
2. 1. 3. 3	MOE Software	27

2. 1. 3. 4	SPSS Software	28
2. 1.4	Glass ware	28
2. 1.5	Apparatus and equipment's	29
2. 1.5.1	Instrumentations	28
2. 1.5.2	Infra-red spectroscopy	28
2. 1.5.3	¹ H Nuclear magnetic resonance spectroscopy	28
2. 1.5.4	¹³ C Nuclear magnetic resonance spectroscopy	28
2. 1.5.5	Gas chromatography- mass spectroscopy	29
2. 1.5.6	Thin layer chromatography (TLC)	29
2.2	Methods	29
2.2.1	Preparation for QSAR modeling study	29
2.2.1.1	Molecular modeling descriptors	29
2.2.1.2	Model development	30
2.2.1.3	Validation Model	31
2.2.2	Modeling of quinoline derivatives	31
2.2.2.1	Predict the biological activity of new designed quinoline derivatives:	31
2.2.2.2	ADMET studies	31
2.2.3	Synthesis	31
2.2.3.1	General method for synthesis 2,3-di phenyl/2--(furan-2-yl)-3-phenylquinoline-4-carboxylic acid derivatives (I and IX)	32
2.2.3.2	General method for synthesis α,β -unsaturated carbonyl derivatives (II and X)	32
2.2.3.3	General method for synthesis 2- Pyrimidinone / Pyrimidinethion derivatives (III, IV, XI and XII)	32
2.2.3.4	General method for synthesis pyrazoline/ pyrazoline-1- phenyl/ pyrazoline -1-carboxamide derivatives derivatives (V, VI, VII, XIII, XIV and XV)	32
2.2.3.5	General method for synthesis 1, 4-oxazipines derivatives (VIII and XVI)	33

2.2.4	In silico molecular docking studies	33
2.2.4.1	Preparation of Ligands	33
2.2.4.2	Preparation of Protein	33
2.2.4.3	Docking protocol	34
2.2.4.4	Analysis of docking	34

CHAPTER THREE

Discussion

3.	DISCUSSION	139
3.1	QSAR Study	145
3.2	ADME study	148
3.3	Docking study	149
3.4	Synthetic design	158
3.5	Reaction mechanism of quinoline	161
3.6	α,β -unsaturated carbonyl derivatives from Claisen-Schmidt condensation	162
3.7	Reaction mechanism of pyrimidinone/thione	162
3.8	Reaction mechanism of pyrazolines	163
3.9	Reaction mechanism of oxazipine	163
3.10	Spectral characterization	164
3.11	Conclusion and Recommendations	166

CHAPTER FOUR

References

4.	REFERENCES	168
-----------	-------------------	------------

Appendixes

Appendix A.	Infra-red spectroscopy (IR) data of the prepared 2, 3-diphenyl/ 2 (furan-2-yl), 3-phenylquinoline-4-carboxylic acid derivatives	176
Appendix B.	¹ H Nuclear magnetic resonance (¹ HNMR) spectrum of the prepared 2, 3-diphenyl/ 2 (furan-2-yl), 3-phenylquinoline-4-carboxylic acid derivatives.	190
Appendix C.	¹³ C Nuclear magnetic resonance (¹³ C NMR) spectrum of the prepared 2, 3-diphenyl/ 2 (furan-2-yl), 3-phenylquinoline-4-carboxylic acid derivatives.	206
Appendix D.	Gas chromatography- mass spectroscopy (GCMS) spectrum of 2, 3-diphenyl/ 2 (furan-2-yl), 3-phenylquinoline-4-carboxylic acid derivatives	222
Appendix E.	Gas chromatography- mass spectroscopy (GCMS) spectrum of 2, 3-diphenyl/ 2 (furan-2-yl), 3-phenylquinoline-4-carboxylic acid derivatives	231

LIST OF TABLES

Table .No	Name of Table	Page
2.1	Experimental EC ₅₀ , experimental pEC ₅₀ , predicted pEC ₅₀ and residual values of quinoline derivatives of 25 compounds used in training and test sets for inhibit in vitro VSV replication in MDCK epithelial cells (Das et al, 2013).	39
2.2	Value of chemical descriptors used in QSAR of quinoline data set.	41
2.3	Models with descriptors used in predict the biological activity of quinoline data set.	43
2.4	The Statistical parameter for five equations have greater r ² .	44
2.5	Value of chemical descriptors used in QSAR of new quinoline compounds set.	45
2.6	The values of chemical descriptors used in ADMET study of new quinoline derivatives selected from.	71
2.7	Chemical names of the prepared compounds	97
2.7.1	Chemical names of 2, 3-diphenylquinoline-4-carboxylic acid derivatives.	97
2.7.2	Chemical names of 2 (furan-2-yl), 3-diphenylquinoline-4-carboxylic acid derivatives	98
2.8	Reaction conditions of the prepared compounds	99
2.8.1	Reaction conditions of the prepared 2, 3-diphenylquinoline-4-carboxylic acid derivatives	99
2.8.2	Reaction conditions of the prepared 2 (furan-2-yl), 3-diphenylquinoline -4- carboxylic acid derivatives	100
2.9	Infra - red spectral data (IR) of the prepared compounds	101
2.9.1	Infra - red spectral data (IR) of the prepared 2, 3-diphenylquinoline-4-carboxylic acid derivatives	101
2.9.2	Infra - red spectral data (IR) of the prepared 2 (furan-2-yl), 3-phenylquinoline-4-carboxylic acid derivatives	103
2.10	¹ H Nuclear magnetic resonance (¹ HNMR) data of the prepared compounds	105
2.10.1	¹ H Nuclear magnetic resonance (¹ HNMR) of the prepared 2, 3-diphenylquinoline-4-carboxylic acid derivatives	105

2.10.2	¹ H Nuclear magnetic resonance (¹ HNMR) of the 2 (furan-2-yl), 3-phenylquinoline-4-carboxylic acid derivatives	110
2.11	¹³ C Nuclear magnetic resonance (¹³ CNMR) data of the prepared compounds	115
2.11.1	¹³ C Nuclear magnetic resonance (¹³ CNMR) of the prepared 2, 3-diphenylquinoline-4-carboxylic acid derivatives	115
2.11.2	¹³ C Nuclear magnetic resonance (¹³ CNMR) of the 2 (furan-2-yl), 3-phenylquinoline-4-carboxylic acid derivatives	120
2.12	Gas chromatography- mass spectroscopy (GCMS) data of the prepared compounds.	125
2.12.1	Gas chromatography- mass spectroscopy (GCMS) 2, 3-diphenylquinoline-4-carboxylic acid derivatives	125
2.12.2	Gas chromatography- mass spectroscopy (GCMS) of prepared 2 (furan-2-yl), 3-phenylquinoline-4-carboxylic acid derivatives	129
2.13	Thin layer chromatography (TLC) data of the prepared compounds	134
2.13.1	Thin layer chromatography (TLC) data of the prepared 2, 3-diphenylquinoline-4-carboxylic acid derivatives.	134
2.13.2	Thin layer chromatography (TLC) data of the prepared 2 (furan-2-yl), 3-phenylquinoline-4-carboxylic acid derivatives	135
2.14	Binding energy, bond interaction and Amino acid interaction of quinoline derivatives data set	136
2.15	Binding energy, Amino acid interacted, Type interaction and Bonds length for synthesized compounds with portion (iuuo) pocket as inhibition of human dihydroorotate dehydrogenase enzyme (DHODH):	138
2.16	Binding energy, Amino acid interacted, Type interaction and Bonds length for docking a new designed compounds with portion (iuuo) pocket as inhibition of human dihydroorotate dehydrogenase (DHODH)	140

LIST OF FIGURES

Fig No	Name of figures	Page
1.1	Structure of quinoline ring	1
1.2	Skraup synthesis	1
1.3	Doebner-Miller ring synthesis	2
1.4	Friedlander synthesis.	2
1.5	Combes synthesis	3
1.6	Conrad–Limpach synthesis	3
1.7	Pfitzinger synthesis	4
1.8	Structures of quinoline derivatives with antimalarial activity	5
1.9	Structures of quinoline derivatives with anticancer activity	6
1.10	Structures of quinoline derivatives with Antimycobacterial activity	6
1.11	The Structures of quinoline derivatives with antimicrobial activity	7
1.12	Structures of quinoline derivatives with antiinflammatory activity	7
1.13	Structures of quinoline derivatives with antifungal activity	8
1.14	Structure of quinoline compound has HIV inhibitor activity	8
2.1	Correlation matrix for chemical descriptors	38
3.1	plot of predicted training set versus experimental pEC ₅₀ values for model ¹	147
3.2	plot of cross validation prediction versus experimental pEC ₅₀ values for model ¹	147
3.3	plot of predicted test set versus experimental pEC ₅₀ values for model ¹	148
3.4	Structure of human (DHODH) protein (PDB code: 1UUO).	150
3.5	(a) Active sites of human (DHODH) protein with brequinar ligand. (b) Ligand interaction with protine.	151

3.6	2D and 3D models of biochemical interactions of compound L44 with DHODH enzyme.	151
3.7	2D and 3D models of biochemical interactions of compound III with DHODH	153
3.8	2D and 3D models of biochemical interactions of compound XVI with DHODH	153
3.9	2D and 3D models of biochemical interactions of compound VI with DHODH	153
3.10	2D models of biochemical interactions of other synthesized compounds with	154
3.11	2D and 3D models of biochemical interactions of compound D16 with DHODH	155
3.12	2D and 3D models of biochemical interactions of compound C11 with DHODH	156
3.13	2D and 3D models of biochemical interactions of compound C27 with DHODH	156
3.14	2D and 3D models of biochemical interactions of compound E10 with DHODH	157
3.15	2D and 3D models of biochemical interactions of compound E13 with DHODH	157
3.16	Retrosynthetic analysis of 2,3-diphenyl/2-(furan-2-yl)-3-phenyl quinoline-4-carboxylic acid derivatives	159
3.17	Retrosynthetic analysis of α,β -unsaturated carbonyl derivatives	160
3.18	Retrosynthetic analysis of pyrimidinone/thione derivatives	160
3.19	Retrosynthetic analysis of pyrazoline derivatives	160
3.20	Retrosynthetic analysis of oxazepines derivatives	161
3.21	synthesis mechanism of quinolines derivatives	161
3.22	synthesis mechanism of α,β -unsaturated carbonyl derivatives	162
3.23	synthesis mechanism of the pyrimidinone\thione derivatives	162
3.24	synthesis mechanism of the pyrazoline derivatives	163
3.25	synthesis mechanism of the oxazepine derivatives	163
A.1	IR spectrum of 6-acetyl-2,3-diphenylquinoline-4-carboxylic acid (I).	176

A.2	IR spectrum of 6-cinnamoyl-2,3-diphenylquinoline-4-carboxylic acid(II)	177
A.3	IR spectrum of 6-(2-oxo-6-phenyl-1,2-dihydropyrimidin-4-yl)-quinoline -4-carboxylic acid (III).	178
A.4	IR spectrum of 2,3-diphenyl-6-(6-phenyl-2-thioxo-1,2-dihydropyrimidin-4-yl)quinoline-4-carboxylic acid (IV).	179
A.5	IR spectrum 2,3-diphenyl-6-(5-phenyl-4,5-dihydro-1H-pyrazol-3-yl)quinoline-4-carboxylic acid (VI).	180
A.6	IR spectrum of 6-(1-carbamoyl-5-phenyl-4,5-dihydro-1H-pyrazol-3-yl)-2,3-diphenylquinoline-4-carboxylic acid (VII).	181
A.7	IR spectrum of 2,3-diphenyl-6-(7-phenyl-2,3,6,7-tetrahydro-1,4-oxazepin-5-yl)quinoline-4-carboxylic acid (VIII).	182
A.8	IR spectrum of 6-acetyl-2-(furan-2-yl)-3-phenylquinoline-4-carboxylic acid (X).	183
A.9	IR spectrum of 2-(furan-2-yl)-6-(6-(furan-2-yl)-2-oxo-1,2-dihydropyrimidin-4-yl)-3-phenylquinoline-4-carboxylic acid (XI).	184
A.10	IR spectrum of 2-(furan-2-yl)-6-(6-(furan-2-yl)-2-thioxo-1,2-dihydropyrimidin-4-yl)-3-phenylquinoline-4-carboxylic acid (XII).	185
A.11	IR spectrum of 2-(furan-2-yl)-6-(5-(furan-2-yl)-1-phenyl-4,5-dihydro-1H-pyrazol-3-yl)-3-phenylquinoline-4-carboxylic acid (XIII)	186
A.12	IR spectrum of 6-(1-carbamoyl-5-(furan-2-yl)-4,5-dihydro-1H-pyrazol-3-yl)-2-(furan-2-yl)-3-phenylquinoline-4-carboxylic acid (XIV).	187
A.13	IR spectrum spectrum of 6-(1-carbamoyl-5-(furan-2-yl)-4,5-dihydro-1H-pyrazol-3-yl)-2-(furan-2-yl)-3-phenylquinoline-4-carboxylic acid (XV).	188
A.14	IR spectrum of 2-(furan-2-yl)-6-(7-(furan-2-yl)-2,3,6,7-tetrahydro -1,4-oxazepin-5-yl)-3-phenylquinoline-4-carboxylic acid (XVI)	189
B.1	¹ HNMR spectrum of 6-acetyl-2,3-diphenylquinoline-4-carboxylic acid (I).	190
B.2	¹ HNMR spectrum of 6-cinnamoyl-2,3-diphenylquinoline-4-carboxylic acid (II)	191
B.3	¹ HNMR spectrum of 6-(2-oxo-6-phenyl-1,2-dihydropyrimidin-4-yl)-quinoline -4-carboxylic acid (III).	192
B.4	¹ HNMR spectrum of 2,3-diphenyl-6-(6-phenyl-2-thioxo-1,2-dihydropyrimidin-4-yl)quinoline-4-carboxylic acid (IV).	193

B.5	¹ HNMR of 6-(1,5-diphenyl-4,5-dihydro-1H-pyrazol-3-yl)-2,3-diphenylquinoline-4-carboxylic acid (V).	194
B.6	¹ HNMR spectrum 2,3-diphenyl-6-(5-phenyl-4,5-dihydro-1H-pyrazol-3-yl)quinoline-4-carboxylic acid (VI).	195
B.7	¹ HNMR spectrum of 6-(1-carbamoyl-5-phenyl-4,5-dihydro-1H-pyrazol-3-yl)-2,3-diphenylquinoline-4-carboxylic acid (VII).	196
B.8	¹ HNMR 2,3-diphenyl-6-(7-phenyl-2,3,6,7-tetrahydro-1,4-oxazepin-5-yl)quinoline-4-carboxylic acid (VIII).	197
B.9	¹ HNMR of 6-acetyl-2-(furan-2-yl)-3-phenylquinoline-4-carboxylic acid (IX).	198
B.10	¹ HNMR spectrum of 6-acetyl-2-(furan-2-yl)-3-phenylquinoline-4-carboxylic acid (X).	199
B.11	¹ HNMR spectrum of 2-(furan-2-yl)-6-(6-(furan-2-yl)-2-oxo-1,2-dihydropyrimidin-4-yl)-3-phenylquinoline-4-carboxylic acid (XI).	200
B.12	¹ HNMR spectrum of 2-(furan-2-yl)-6-(6-(furan-2-yl)-2-thioxo-1,2-dihydropyrimidin-4-yl)-3-phenylquinoline-4-carboxylic acid (XII).	201
B.13	¹ HNMR spectrum of 2-(furan-2-yl)-6-(5-(furan-2-yl)-1-phenyl-4,5-dihydro-1H-pyrazol-3-yl)-3-phenylquinoline-4-carboxylic acid (XIII).	202
B.14	¹ HNMR spectrum of 6-(1-carbamoyl-5-(furan-2-yl)-4,5-dihydro-1H-pyrazol-3-yl)-2-(furan-2-yl)-3-phenylquinoline-4-carboxylic acid (XIV).	203
B.15	¹ HNMR spectrum spectrum of 6-(1-carbamoyl-5-(furan-2-yl)-4,5-dihydro-1H-pyrazol-3-yl)-2-(furan-2-yl)-3-phenylquinoline-4-carboxylic acid (XV).	204
B.16	¹ HNMR spectrum of 2-(furan-2-yl)-6-(7-(furan-2-yl)-2,3,6,7-tetrahydro-1,4-oxazepin-5-yl)-3-phenylquinoline-4-carboxylic acid (XVI).	205
C.1	¹³ C NMR spectrum of 6-acetyl-2,3-diphenylquinoline-4-carboxylic acid (I).	206
C.2	¹³ C NMR spectrum of 6-cinnamoyl-2,3-diphenylquinoline-4-carboxylic acid (II).	207
C.3	¹³ C NMR spectrum of 6-(2-oxo-6-phenyl-1,2-dihydropyrimidin-4-yl)-quinoline-4-carboxylic acid (III).	208
C.4	¹³ C NMR spectrum of 2,3-diphenyl-6-(6-phenyl-2-thioxo-1,2-dihydropyrimidin-4-yl)quinoline-4-carboxylic acid (IV).	209
C.5	¹³ C NMR of 6-(1,5-diphenyl-4,5-dihydro-1H-pyrazol-3-yl)-2,3-diphenylquinoline-4-carboxylic acid (V).	210

C.6	¹³ C NMR spectrum 2,3-diphenyl-6-(5-phenyl-4,5-dihydro-1H-pyrazol-3-yl)quinoline-4-carboxylic acid (VI).	211
C.7	¹³ C NMR spectrum of 6-(1-carbamoyl-5-phenyl-4,5-dihydro-1H-pyrazol-3-yl)-2,3-diphenylquinoline-4-carboxylic acid (VII).	212
C.8	¹³ C NMR 2,3-diphenyl-6-(7-phenyl-2,3,6,7-tetrahydro-1,4-oxazepin-5-yl)quinoline-4-carboxylic acid (VIII).	213
C.9	¹³ C NMR of 6-acetyl-2-(furan-2-yl)-3-phenylquinoline-4-carboxylic acid (IX).	214
C.10	¹³ C NMR spectrum of 6-acetyl-2-(furan-2-yl)-3-phenylquinoline-4-carboxylic acid (X).	215
C.11	¹³ C NMR spectrum of 2-(furan-2-yl)-6-(6-(furan-2-yl)-2-oxo-1,2-dihydropyrimidin-4-yl)-3-phenylquinoline-4-carboxylic acid (XI).	216
C.12	¹³ C NMR spectrum of 2-(furan-2-yl)-6-(6-(furan-2-yl)-2-thioxo-1,2-dihydropyrimidin-4-yl)-3-phenylquinoline-4-carboxylic acid (XII).	217
C.13	¹³ C NMR spectrum of 2-(furan-2-yl)-6-(5-(furan-2-yl)-1-phenyl-4,5-dihydro-1H-pyrazol-3-yl)-3-phenylquinoline-4-carboxylic acid (XIII).	218
C.14	¹³ C NMR spectrum of 6-(1-carbamoyl-5-(furan-2-yl)-4,5-dihydro-1H-pyrazol-3-yl)-2-(furan-2-yl)-3-phenylquinoline-4-carboxylic acid (XIV).	219
C.15	¹³ C NMR spectrum of 6-(1-carbamoyl-5-(furan-2-yl)-4,5-dihydro-1H-pyrazol-3-yl)-2-(furan-2-yl)-3-phenylquinoline-4-carboxylic acid (XV).	220
C.16	¹³ C NMR spectrum of 2-(furan-2-yl)-6-(7-(furan-2-yl)-2,3,6,7-tetrahydro-1,4-oxazepin-5-yl)-3-phenylquinoline-4-carboxylic acid (XVI).	221
D.1	GC-MS spectrum of 6-acetyl-2,3-diphenylquinoline-4-carboxylic acid (I).	222
D.2	GC-MS spectrum of 6-cinnamoyl-2,3-diphenylquinoline-4-carboxylic acid (II).	223
D.3	GC-MS spectrum of 6-(2-oxo-6-phenyl-1,2-dihydropyrimidin-4-yl)-quinoline-4-carboxylic acid (III).	224
D.4	GC-MS spectrum of 2,3-diphenyl-6-(6-phenyl-2-thioxo-1,2-dihydropyrimidin-4-yl)quinoline-4-carboxylic acid (IV).	224
D.5	GC-MS of 6-(1,5-diphenyl-4,5-dihydro-1H-pyrazol-3-yl)-2,3-diphenylquinoline-4-carboxylic acid (V).	225
D.6	GC-MS spectrum 2,3-diphenyl-6-(5-phenyl-4,5-dihydro-1H-pyrazol-3-yl)quinoline-4-carboxylic acid (VI).	225

D.7	GC-MS spectrum of 6-(1-carbamoyl-5-phenyl-4,5-dihydro-1H-pyrazol-3-yl)-2,3-diphenylquinoline-4-carboxylic acid (VII).	226
D.8	GC-MS 2,3-diphenyl-6-(7-phenyl-2,3,6,7-tetrahydro-1,4-oxazepin-5-yl)quinoline-4-carboxylic acid (VIII).	226
D.9	GC-MS of 6-acetyl-2-(furan-2-yl)-3-phenylquinoline-4-carboxylic acid (IX).	227
D.10	GC-MS spectrum of 6-acetyl-2-(furan-2-yl)-3-phenylquinoline-4-carboxylic acid (X).	227
D.11	GC-MS spectrum of 2-(furan-2-yl)-6-(6-(furan-2-yl)-2-oxo-1,2-dihydropyrimidin-4-yl)-3-phenylquinoline-4-carboxylic acid (XI).	228
D.12	GC-MS spectrum of 2-(furan-2-yl)-6-(6-(furan-2-yl)-2-thioxo-1,2-dihydropyrimidin-4-yl)-3-phenylquinoline-4-carboxylic acid (XII).	228
D.13	GC-MS spectrum of 2-(furan-2-yl)-6-(5-(furan-2-yl)-1-phenyl-4,5-dihydro-1H-pyrazol-3-yl)-3-phenylquinoline-4-carboxylic acid (XIII).	229
D.14	GC-MS spectrum of 6-(1-carbamoyl-5-(furan-2-yl)-4,5-dihydro-1H-pyrazol-3-yl)-2-(furan-2-yl)-3-phenylquinoline-4-carboxylic acid (XIV).	229
D.15	GC-MS spectrum of 6-(1-carbamoyl-5-(furan-2-yl)-4,5-dihydro-1H-pyrazol-3-yl)-2-(furan-2-yl)-3-phenylquinoline-4-carboxylic acid (XV).	230
D.16	GC-MS spectrum of 2-(furan-2-yl)-6-(7-(furan-2-yl)-2,3,6,7-tetrahydro-1,4-oxazepin-5-yl)-3-phenylquinoline-4-carboxylic acid (XVI).	230
E.1	Interactions of compound (A11)	231
E.2	Interactions of compound (A25)	231
E.3	Interactions of compound (A29)	232
E.4	Interactions of compound (B2)	232
E.5	Interactions of compound (B8)	233
E.6	Interactions of compound (B35)	233
E.7	Interactions of compound (C)	234
E.8	Interactions of compound (C9)	234
E.9	Interactions of compound (C13)	235
E.10	Interactions of compound (C15)	235
E.11	Interactions of compound (C30)	236

E.12	Interactions of compound (C31)	236
E.13	Interactions of compound (C32)	237
E.14	Interactions of compound (D11)	237
E.15	Interactions of compound (D18)	238
E.16	Interactions of compound (D20)	238
E.17	Interactions of compound (D21)	239
E.18	Interactions of compound (D29)	239
E.19	Interactions of compound (E11)	240
E.20	Interactions of compound (E14)	240
E.21	Interactions of compound (E25)	241
E.22	Interactions of compound (E26)	241
E.23	Interactions of compound (E29)	242
E.24	Interactions of compound (E35)	242

LIST OF SCHEMES

Scheme. No	Name of Scheme	Page
2.1	Chemical structure of 2,3-diphenyl/2-(furan-2-yl)-3-phenyl-6-acetyl-quinoline-4-carboxylic acid derivatives.	35
2.2	Chemical structure of 2,3-diphenyl/2-(furan-2-yl)-3-phenyl-6-(3-aryl-prop-2-enon-1-yl)-quinoline-4-carboxylic acid	36
2.3	Chemical structure of (III) to (VIII) synthesized from α,β -unsaturated carbonyl derivative (II)	37
2.4	Chemical structure of (XI) to (XVI) synthesized from α,β -unsaturated carbonyl derivative (X)	38

ABBREVIATIONS

ABBREVIATION	MEANING
ADMET	Absorption, Distribution, Metabolism, Excretion and Toxicity
Ala	Alanine
Arg	Arginine
CADD	Computer Aided Drug Design
CAMD	Computer Aided Molecular Design
CAMM	Computer Aided Molecular Modeling
CoMFA	Comparative Molecular field Analysis
Chi ₀	Atomic Connectivity Index Order Zero
¹³ C NMR	Carbon Nuclear Magnetic Resonance
d	Doublet
dd	Doublet of Doublet
DNA	Deoxyribonucleic acid
DHODH	Dihydroorotate Dehydrogenase
Dipole	Dipole Moment
DMPK	Drug, Metabolism and Pharmacokinetics
EC ₅₀	Half Maximal Effective Concentration
Es	Steric parameter
FGI	Function Group Interaction
FT-IR	Fourier Infra-Red
GA	Genetic algorithms
GCMS	Gas Chromatography Mass Spectrometer
Gly	Glycine
H. acc	Number of Hydrogen Bond Acceptor Protons
H. donor	Number of Hydrogen Bond Donor Protons
HB	Hydrogen Bond
HF	Heat of Formation
His	Histidine
HIV	Human Immunodeficiency Virus
¹ H NMR	Proton Nuclear Magnetic Resonance
HOMO	Highest Occupation Molecular Orbital
HTS	High Throughput Screening

Ile	Isoleucine
IR	Infra-Red
IP	Ionization Potential
F	F-test
LBVS	Ligand Based Virtual Screening
Log P _(O/W)	Logarithmic Octanol Water Partition Coefficient
Log S	Logarithmic Solubility in Water
LOMO	Lowest Occupation Molecular Orbital
LOO	Leave One Out
m	Multiplet
MOE	Molecular Operating Environment
m.p.	Melting Point
MR	Molar Refractivity
Mwt	Molecular Weight
P	Total Polar Surface Area
PDB	Protein Data Bank
PLS	Partial Last Squares
Pro	Proline
q ²	Cross Validation Regression Coefficient
QSAR	Quantitative Structural Activity Relationship
QSPR	Quantitative Structural Property Relationship
r	Correlation Coefficient
r ²	Square of the Correlation Coefficient
RO5	Rule of Five
RMSE	Root Mean Square Error
RNA	Ribonucleic acid
s	Singlet
S	Free Binding Energy
SBDD	Structure-Based Drug Design
SBVS	Structure Based Virtual Screening
SPSS	Statistical Package for Social Sciences
t	Triplet
TLC	Thin Layer Chromatography
TMS	Tetramethylsilane

T-PSA	Topological polar area in Square Angstroms
Tyr	Tyrosine
Val	Valine
VS	Virtual Screening
VSV	Vesicular Stomatitis Virus
VSVG	Vesicular Stomatitis Virus glycoprotein G

CHAPTER ONE

Introduction

1. Introduction

1.1 Quinolines

1.1.1 Structure and nomenclature of quinoline

Quinoline also known as 1-azanaphthalene, 1-benzazine or benzo[b] pyridine is a heterocyclic organic compound, with formula C_9H_7N (Figure 1.1) and it is a colorless liquid with strong odour. It was first extracted from coal tar in 1834 by Friedlieb Ferdinand Runge (Kannappan *et al.*, 2009).

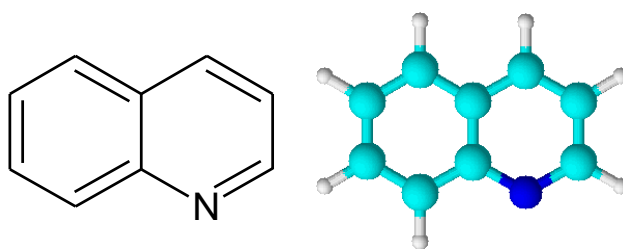


Fig 1.1: Structure of quinoline ring

1.1.2. Properties of quinoline

Molecular weight of quinoline is 129.16. The $\log P$ value is 2.04 and has an acidic pK_b of 4.85 and a basic pK_a of 9.5. Quinoline is a weak tertiary base. It can form salt with acids and displays reactions similar to those of pyridine and benzene. It shows both electrophilic and nucleophilic substitution reactions. It is nontoxic to humans on oral absorption and inhalation (Marella *et al.*, 2013).

1.1.3 Quinolines Synthesis

1.1.3.1 Skraup synthesis

Quinoline is produced when aniline as starting material (Ginelle *et al.*, 2015), concentrate sulfuric acid, glycerol and mild oxidizing agent are heated together. The reaction proceeds via dehydration of glycerol to acrolein (Figure 1.2). It is the best reaction for synthesis of quinoline (Madapa *et al.*, 2008).

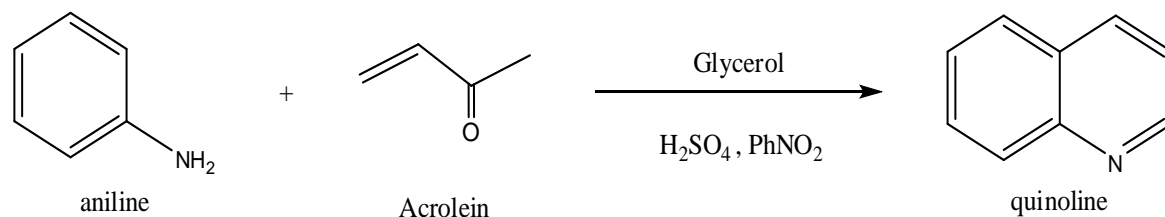


Fig. 1 .2 Skraup synthesis of quinoline

1.1.3.2 Doebner-Miller ring synthesis

The interaction of enone group with aniline takes place producing quinoline derivatives. Improvement to this reaction includes the use of 2 phase organic or aqueous acid system as shown in Figure 1.3 (Pandeya *et al.*, 2011).

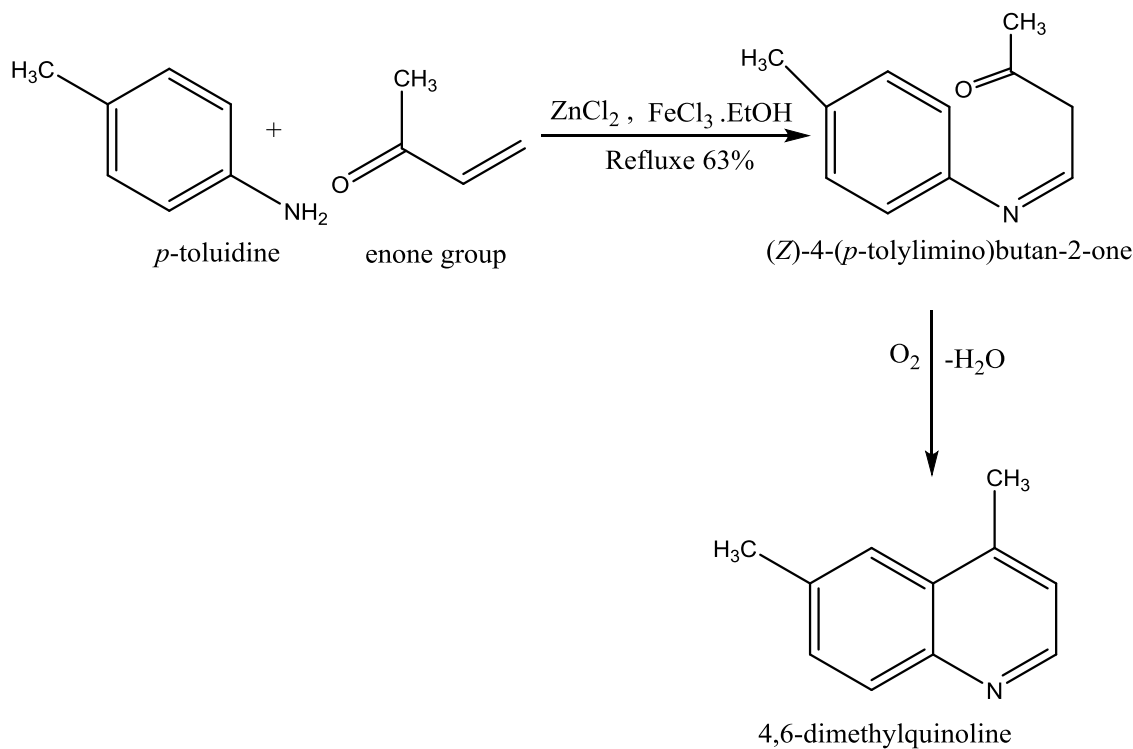


Fig. 1. 3 Doebner-Miller ring synthesis of quinoline

1.1.3.3 Friedlander synthesis

The reaction proceeds through Aldol type condensation. *o*-amino aryl aldehyde are reacted with a ketone carrying an alpha methylene group as shown in Figure 1.4 (Chaudhur *et al.*, 2006).

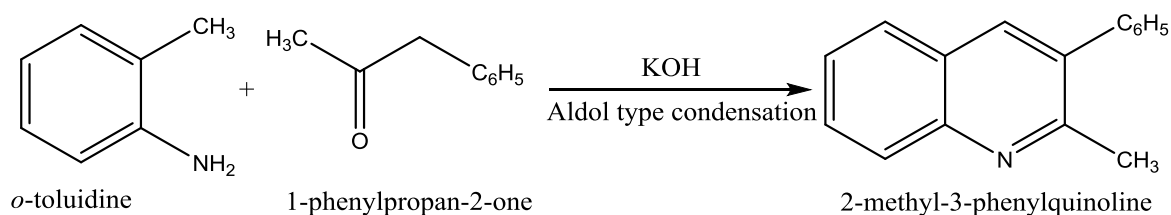


Fig. 1.4 Friedlander synthesis of quinoline

1.1.3.4 Combes synthesis

Condensation of 1,3 dicarbonyl compounds with the arylamine gives high yield of amino enone, which can be cyclized with concentration acid. In order to access 4-unsubstituted quinoline as shown in Figure 1.5, a 1,3 keto aldehyde, guarantees the regioselectivity (Pandeya *et al.*, 2011).

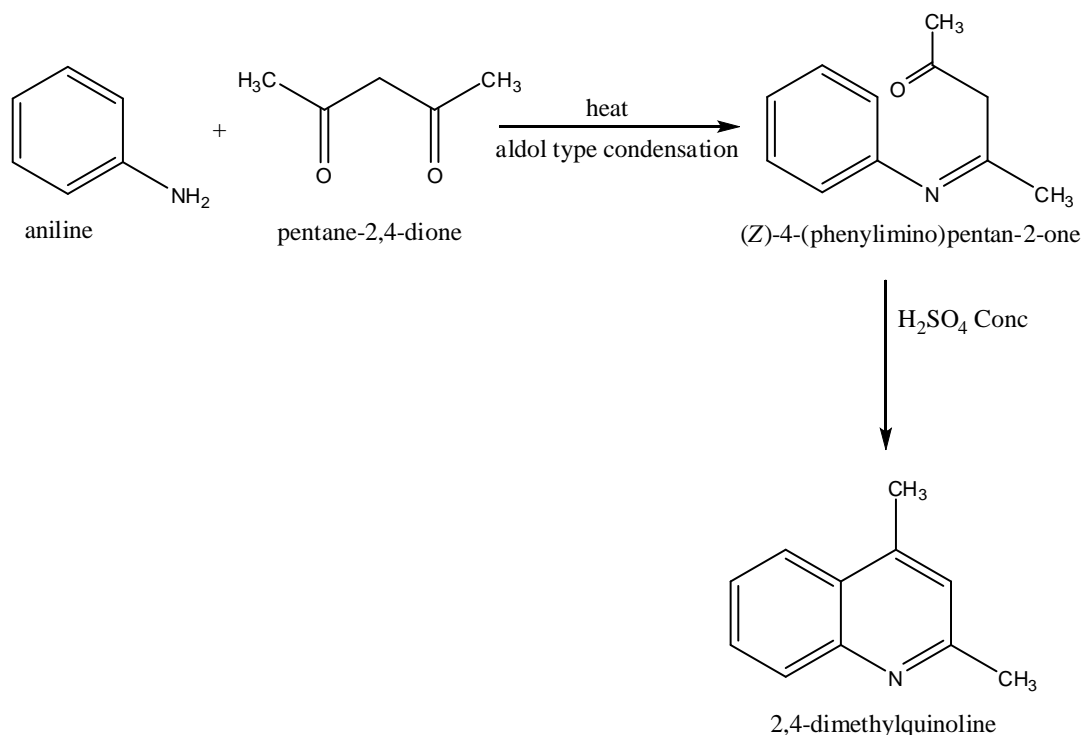


Fig.1. 5 Combes synthesis of quinoline

1.1.3.5 Conrad–Limpach synthesis

The Conrad–Limpach synthesis is similarly useful for the synthesis of quinolines. The Conrad–Limpach reaction, used to prepare 4-quinolones, by cyclization of aniline with enol tautomer as shown in Figure 1.6 (Jean *et al.*, 2009).

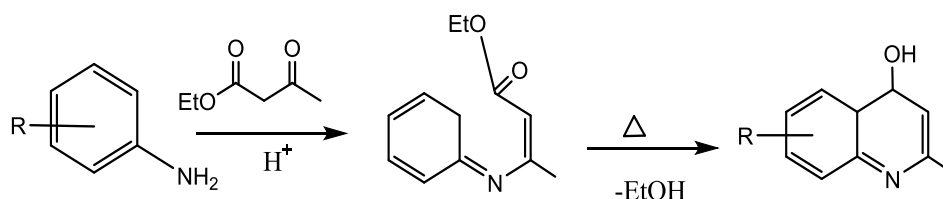


Fig.1. 6 Conrad–Limpach synthesis of quinoline

1.1.3.6 Pfitzinger synthesis

The Pfitzinger reaction is a chemical reaction of isatin with strong nucleophiles, i.e., base such as sodium hydroxide or potassium hydroxide and methyl ketones to yield substituted quinoline-4-carboxylic acids (Sangshetti *et al.*, 2014). The Pfitzinger reaction used for the

synthesis of active derivatives of substituted quinoline-4-carboxylic acids as shown in Figure 1.7 (Vatsala *et al.*, 2014).

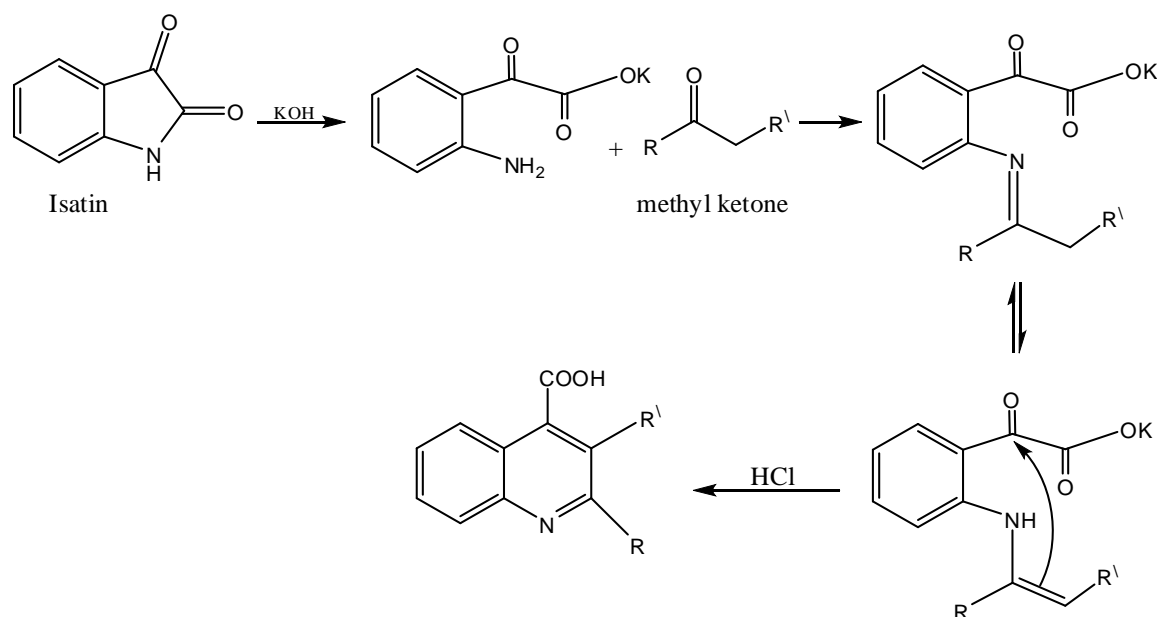


Fig.1. 7 Pfitzinger synthesis of quinoline

1.1.4 Importance of Quinolines

Quinolines are well known compounds in synthetic chemistry as well as medicinal chemistry and served the mankind in several forms, majorly as antibiotic drugs. Quinolines were discovered and several varieties have been synthesized from decades to treat several diseases and infections. However, the increased resistance of microbials to the existing quinolines is an alarming problem now.

The structural core of quinoline derivatives is frequently associated with medicinal applications, such as anti-cancer (Kouznetsov *et al.*, 2012), anti-bacterial (Turel *et al.*, 2000), anti-fungal (Wang *et al.*, 2010), anti-tumor (Aghera *et al.*, 2008). An interesting quinoline derivatives which inhibited HIV-1 (Makki *et al.*, 2012), antileishmanial activity (Ali, 2008) and antimalarial (Kumar *et al.*, 2010).

1.1.4.1 Antimalarial Activity

There are numbers of natural products of quinoline skeleton used as a medicine or employed as lead molecule for the development of newer and potent molecules. Antimalarial drugs contain quinoline derivatives such as 4-aminoquinolines like chloroquine and amodiaquine, 8-aminoquinolines such as primaquine, 4-quinolinemethanols e.g., mefloquine and quinoline-containing cinchona alkaloids, e.g., quinine as shown in Figure 1.8 (Nqoro *et al.*, 2017).

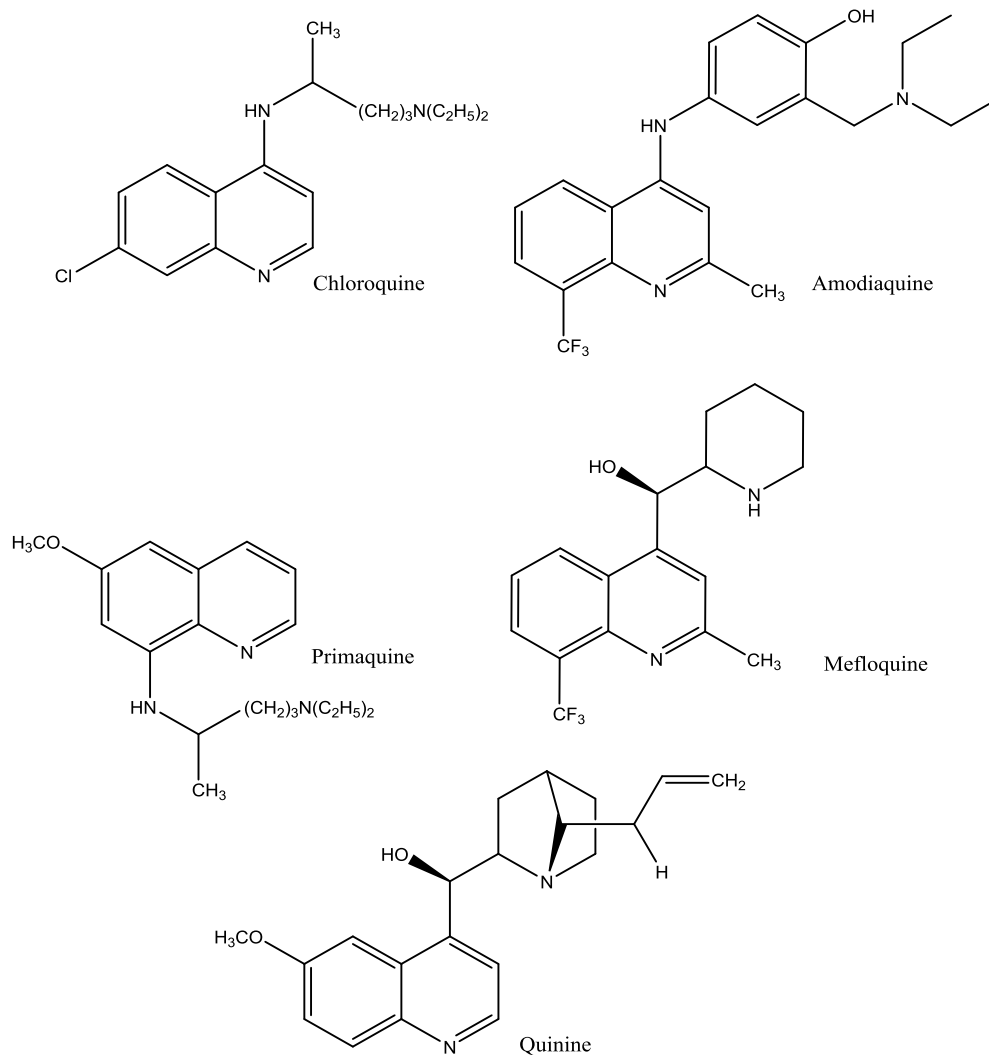


Fig. 1.8 Structures of quinoline derivatives with antimalarial activity

1.1.4.2 Anticancer activity

Quinoline derivatives fused with various heterocycles have displayed potent anticancer activity targeting different sites like topoisomerase I, telomerase, and fused quinoline derivative was found to be act on telomerase with IC₅₀ 16 μ M (Gao *et al.*, 2011).

Several derivatives of cinchoninic acid (quinoline-4-carboxylic acid) are important quinoline derivatives, including the abandoned analgesic agent cinchophen and brequinar sodium (Figure 1.9) that has been discovered as an anticancer agent and later found to have immunosuppressive activity (Massoud *et al.*, 2014).

Several quinoline analogues have anticancer activity against HeLa (human cervix cancer cell line) and MDA-MB-435 (human breast cancer cell line) (Ahsan *et al.*, 2015).

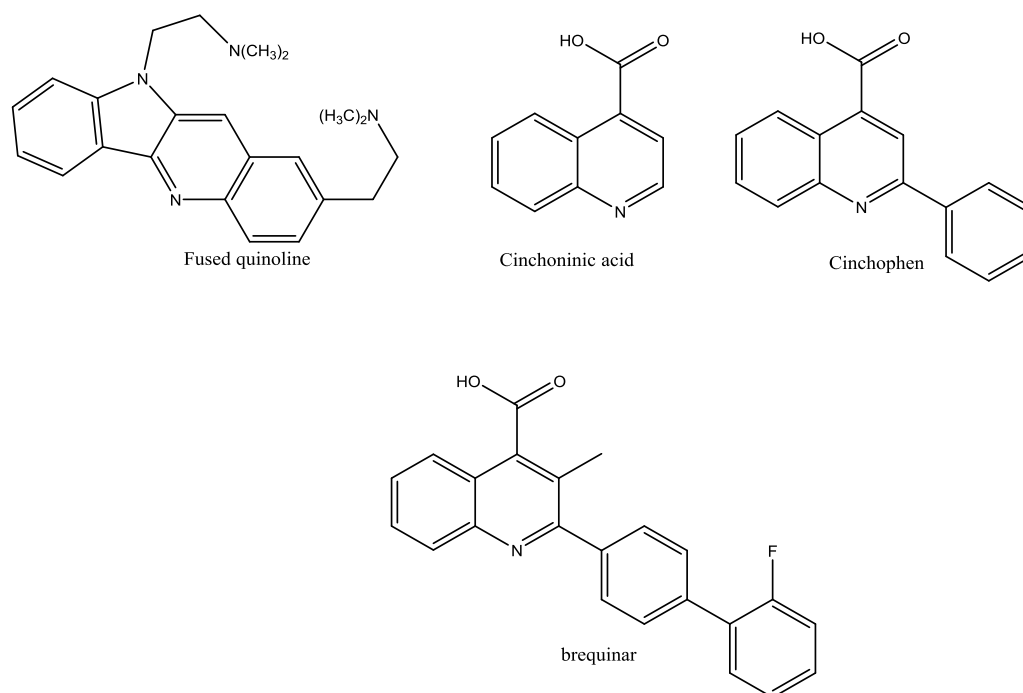


Fig. 1.9 Structures of quinoline derivatives with anticancer activity

1.1.4.3 Antimycobacterial Activity

Some synthesized aryl piperazinyl fluoro-quinolines were studied for anti-tubercular activity, some of their derivatives were found to possess significant anti-mycobacterium activity (Selvam, 2012).

Several compounds, such as 1-(4-amino-2-fluorophenyl)-6-fluoro-4-oxo-7-(piperazin-1-yl)-1,4-dihydro-quinoline-3-carboxylic acid is able to completely inhibit the growth of *M.tuberculosis* at a concentration of 6.25 $\mu\text{g/ml}$ (Zhao *et al.*, 2005). Also A number of 4-amino substituted 2,8 - bis (trifluoromethyl) quinoline derivatives were evaluated for their *invitro* antimycobacterial activity against *Mycobacterium tuberculosis* as shown in Figure 1.10 (Mital *et al.*, 2005).

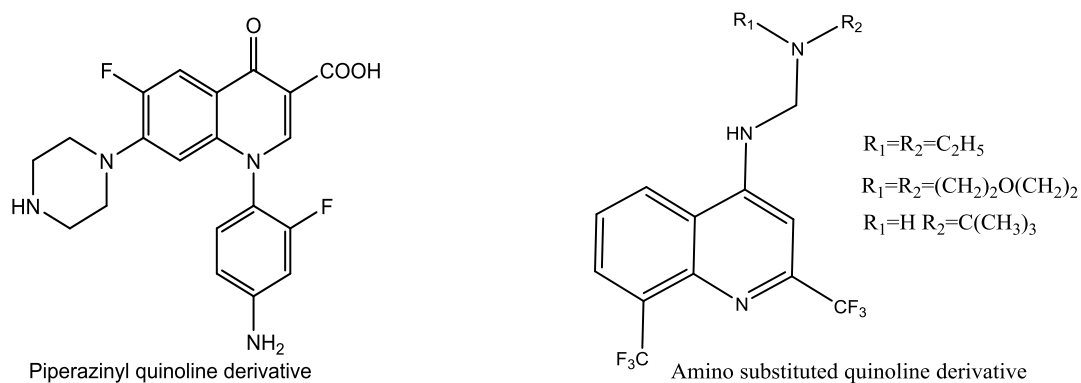


Fig. 1.10 Structures of quinoline derivatives with antimycobacterial activity

1.1.4.4 Antimicrobial Activity

Quinolones is a special structural class of quinoline antimicrobial agents. Have been established on quinoline nucleus and resulted in number of currently marketed synthetic antimicrobial agent like ciprofloxacin, ofloxacin and sparfloxacin as shown in Figure 1.11.

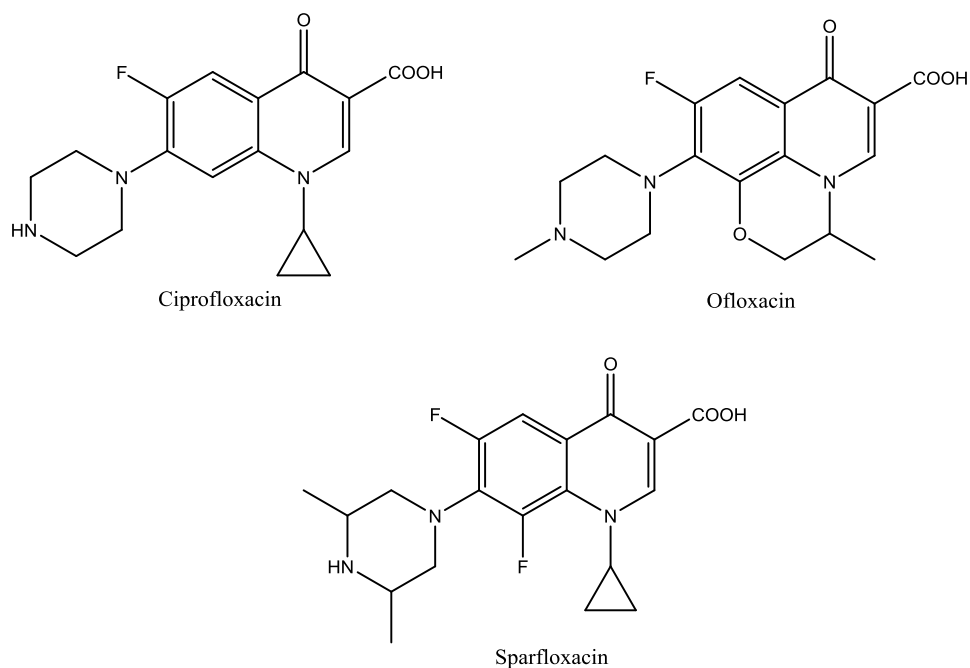


Fig.1. 11 Structures of quinoline derivatives with antimicrobial activity

1.1.4.5 Antiinflammatory Activity

Certain 4-anilino furo[2,3-b]quinoline and 4-phenoxy furo[2,3-b]quinoline derivatives acted as anti-inflammatory agent, of and proved to be more potent with IC_{50} values of 6.5 and 16.4 mM, respectively as shown in Figure 1.12 (Chen *et al.*, 2004).

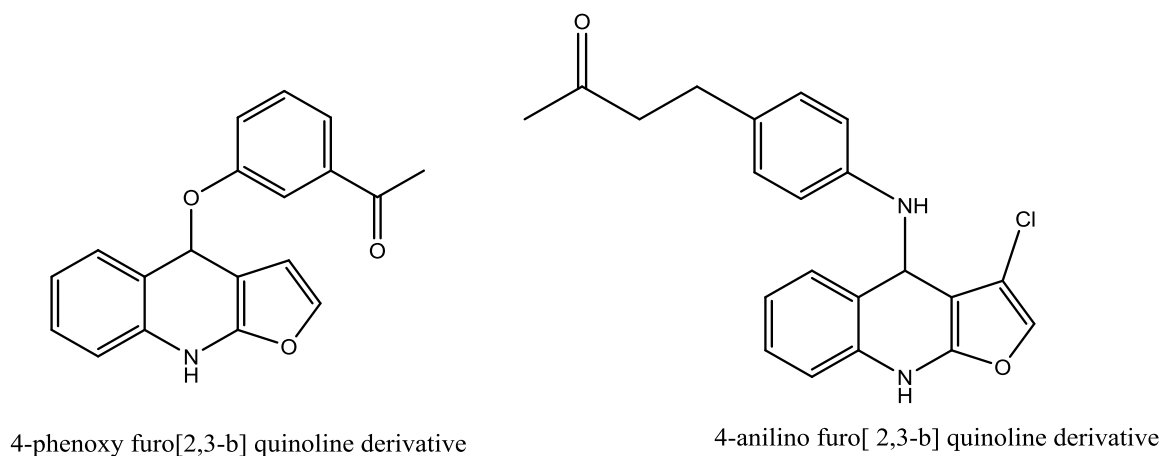
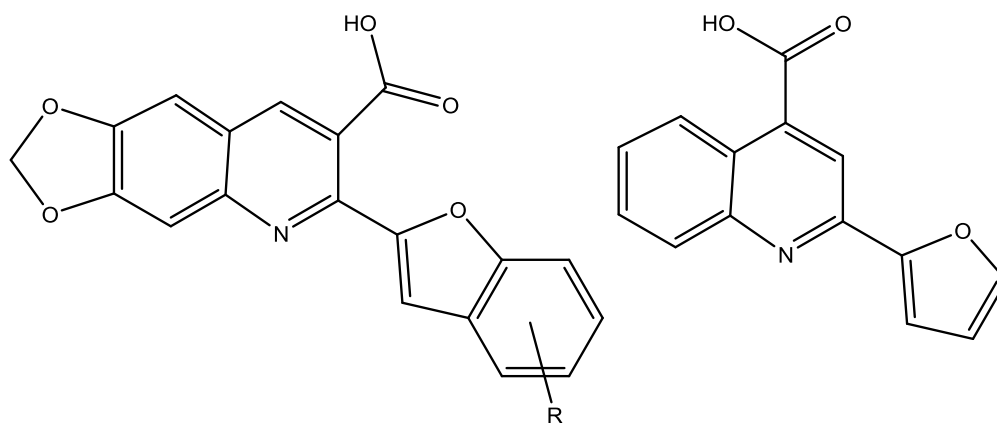


Fig. 1.12 Structures of quinoline derivatives with antiinflammatory activity

1.1.4.6 Antifungal activity

The 2-(furan-2-yl) quinoline-4-carboxylic acid (and analogues) (Figure 1.13) are widely distributed in nature and have been reported to have antifungal activities (Gao *et al.*, 2011). Cinchophen (2-Phenylquinoline-4-carboxylic acid) has been proved to be a powerful antibacterial, antifungal activity and have diverse biological activities (Wadher *et al.*, 2009).

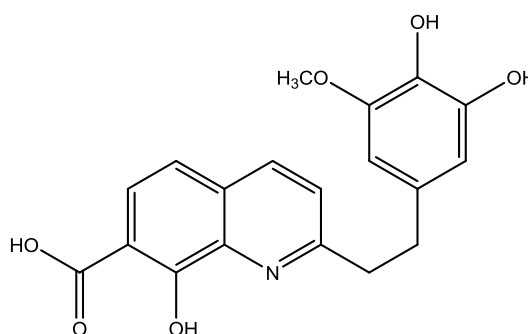


2-(furan-2-yl)quinoline-4-carboxylic acid and analogues

Fig. 1.13 Structures of quinoline derivatives with antifungal activity

1.1.4.7 HIV inhibitor activity

A series of compounds derived from 8-hydroxyquinolines potential HIV-1 integrase inhibitors were synthesized. In addition A series of compounds derived from 8-hydroxyquinolin and styryl quinoline derivatives (Figure 1.14) have gained strong attention due to their activities as perspective HIV integrase inhibitors and also, for their extensive biological activities (El-Agrody *et al.*, 2011).



8-hydroxyquinolines derivative

Fig. 1.14 Structure of quinoline derivative with HIV inhibitor activity

1.2 Computational Chemistry

The term computational chemistry is generally used when a mathematical method is sufficiently well developed that it can be automated for implementation on a computer (Youg, 2001), which deals with the modeling and the computer simulation of systems such as biomolecules, polymers, drugs, inorganic and organic molecules, and so on. Since its advent, computational chemistry has grown to the state it is today and it became popular being immensely benefited from the tremendous improvements in computer hardware and software during the last several decades. With high computing power using parallel or grid computing facilities and with faster and efficient numerical algorithms, computational chemistry can be very effectively used to solve complex chemical and biological problems (Ramachandran *et al.*, 2008).

Computational chemistry allows one to calculate molecular geometries, reactivities, spectra, and other properties. It employs:

- I- Molecular mechanics – based on a ball-and-springs model of molecules;
- II- Ab initio methods – based on approximate solutions of the Schrödinger equation without appeal to fitting to experiment;
- III- Semiempirical methods – based on approximate solutions of the Schrödinger equation with appeal to fitting to experiment (i.e. using parameterization);
- IV- DFT methods – based on approximate solutions of the Schrödinger equation, bypassing the wave function that is a central feature of ab initio and semiempirical methods;
- V- Molecular dynamics methods-study of molecules in motion (Lewars, 2004).

1.3 Chemoinformatics

Chemoinformatics provides computer methods for learning from chemical data and for modeling tasks a chemist is facing. The field has evolved in the past 50 years and has substantially shaped how chemical research is performed by providing access to chemical information on a scale unattainable by traditional methods. Many physical, chemical and biological data have been predicted from structural data. For the early phases of drug design, methods have been developed that are used in all major pharmaceutical companies. However, all domains of chemistry can benefit from chemoinformatics methods; many areas that are not yet well developed, but could substantially gain from the use of chemoinformatics methods. The quality of data is of crucial importance for successful

results. Computer-assisted structure elucidation and computer-assisted synthesis design have been attempted in the early years of chemoinformatics. Because of the importance of these fields to the chemist, new approaches should be made with better hardware and software techniques.

1.3.1 Drug Design

By far the largest number of applications of chemoinformatics has been made in drug design. Methods have been developed for: , lead discovery (both ligand- and structure-based methods) , lead optimization , modeling of ADMET properties (adsorption, distribution, metabolism, excretion and toxicity). Chemoinformatics has made substantial contributions to the development of a variety of new drugs. This approach has matured to a point that all major drug companies have a chemoinformatics department, and practically all drugs that have newly been developed have involved in one or another step chemoinformatics methods (Gasteiger, 2016).

1.3.1.1 Structure-Based Drug Design (SBDD)

Understanding the principles by which small-molecule ligands recognize and interact with macromolecules is of great importance in pharmaceutical research and development (R & D). SBDD refers to the systematic use of structural data (e.g., macromolecular targets, also called receptors), which are usually obtained experimentally or through computational homology modeling. The purpose is to conceive ligands with specific electrostatic and stereochemical attributes to achieve high receptor binding affinity. Selective modulation of a validated drug target by high affinity ligands interferes with specific cellular processes, ultimately leading to the desired pharmacological and therapeutic effects.

1.3.1.2 Molecular Docking

Molecular docking is one of the most frequently used methods in SBDD because of its ability to predict, with a substantial degree of accuracy, the conformation of small-molecule ligands within the appropriate target binding site.

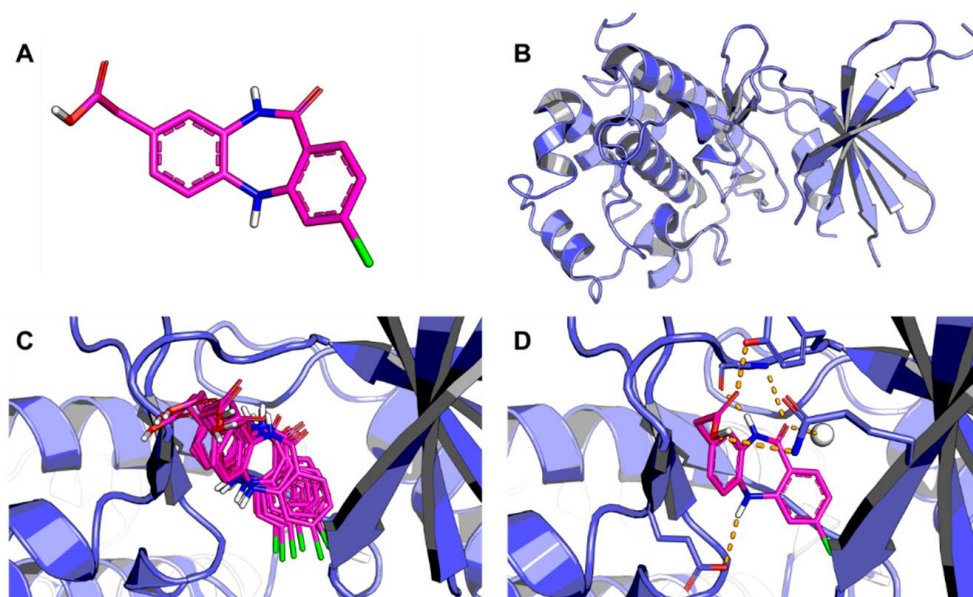


Fig. 1.15. Outline of the molecular docking process. (A) Three-dimensional structure of the ligand; (B) Three-dimensional structure of the receptor; (C) The ligand is docked into the binding cavity of the receptor and the putative conformations are explored; (D) The most likely binding conformation and the corresponding intermolecular interactions are identified. The protein backbone is represented as a cartoon. The ligand (carbon in magenta) and active site residues are shown in stick representation. Water is shown as a white sphere and hydrogen bonds are indicated as dashed lines.

1.3.1.3 Virtual Screening (VS)

Virtual screening is the application of *in silico* methods for selecting promising compounds from chemical databases. It can be regarded as the computational counterpart of experimental biological evaluation methods, such as high-throughput screening (HTS). In drug discovery, the use of large and chemically diverse compound libraries for computational and biological screening is one of the most widespread strategies. This has stimulated the use of VS as a fast and cost-effective method for the evaluation of a variety of compound collections. Usually, VS strategies fall into two main types: (i) ligand- and (ii) structure-based virtual screening (LBVS and SBVS, respectively).

- i. LBVS is based on the exploration of molecular descriptors gathered from compounds known to be active. In general, a set of mutual characteristics of a compound series is identified, which are subsequently applied as molecular filters. These database filtering methods are used to select compounds for experimental evaluation and reduce the chemical space to be explored in further screening steps.

ii. In SBVS, the compound database is docked into a previously selected target binding site. Along with the prediction of the binding mode, SBVS provides a ranking of the docked molecules. This ranking can be used as the sole criterion for selecting promising molecules, or it can be combined with other evaluation methods. The selected compounds are experimentally evaluated to determine their biological activity on the molecular target under investigation. In general, SBVS consists of the following steps: (a) molecular target preparation; (b) compound database selection; (c) molecular docking; and (d) post-docking analysis. Rigorous review of the available information regarding the target and known ligands, as well as a careful analysis of the advantages and pitfalls of the selected docking algorithms, are required in delineating the most appropriate strategies (Ferreira *et al.*, 2015).

1.3.2 Property Prediction (QSAR/QSPR)

Quantitative structure-activity relationship (QSAR) and quantitative structure-property relationship (QSPR) makes it possible to predict the activities/properties of a given compound as a function of its molecular substituent. Essentially, new and untested compounds possessing similar molecular features as compounds used in the development of QSAR/QSPR models are likewise assumed to also possess similar activities/properties (Nantasenamat *et al.*, 2009).

A large number of constitutional, topological, geometric, electrostatic, and quantum indices were introduced in theoretical chemistry with the aim to express in a numerical form the chemical structure. Such structural descriptors can be used to model physical, chemical, or biological properties with quantitative structure-property relationships (QSPR) and quantitative structure-activity relationships (QSAR) (Ivanciuc *et al.*, 2002).

1.3.2.1 Aims and objectives of QSPR

A major goal of Quantitative Structure-Activity Relationship (QSAR) or Quantitative Structure Property Relationship (QSPR) studies is to find a mathematical relationship between the activity or property under investigation (e.g., LD₅₀, pKa, etc.), and one or more descriptive parameters (descriptors) related to the structure of the molecule. While such descriptors can themselves be experimental properties of the molecule, it is generally more useful to use descriptors derived mathematically from either the 2D or the 3D molecular structure, since this allows any relationship so derived to be extended to the prediction of the property or activity for unavailable compounds. If an acceptable model of this type can

be found, it can guide the synthetic chemist in the choice between alternative hypothetical structures. More fundamentally, such studies can illuminate, or even elucidate, the 'mechanism' by which the property or activity in question is related to the chemical structure (katrizky *et al.*, 1995).

1.3.2. 2 Development of QSPR model

The construction of QSAR/QSPR model typically comprises of two main steps: (i) description of molecular structure and (ii) multivariate analysis for correlating molecular descriptors with observed activities /properties. An essential preliminary step in model development is data understanding. Intermediate steps that are also crucial for successful development of such QSAR/QSPR models include data preprocessing and statistical evaluation. A schematic representation of the QSAR process is illustrated in Figure 1.6 (Nantasenamat *et al.*, 2009).

1. 3. 2. 3 Molecular descriptors

Molecular descriptors can be defined as the essential information of a molecule in terms of its physicochemical properties such as constitutional, electronic, geometrical, hydrophobic, lipophilicity, solubility, steric, quantum chemical, and topological descriptors (Dudek *et al.*, 2006).

To make the structure activity relationship quantitative, both chemical structure and the biological activity must be quantified. Although biological activity can be measured in quantitative terms, it is not easy to quantify the chemical structure. So the crucial question is: how to quantify the chemical structure? The method used in QSAR to quantify the structure is to express it in terms of physico-chemical properties that can be measured easily. Most often, medicinal chemist works on a set of derivatives where only a part of the molecule varies and a large part remains constant. In such cases, one has to quantify only the substituents instead of the whole molecule (Gasteiger, 2016).

One of the important contribution of Hansch and his coworkers is the development and standardization of a number of such substituent constants based on physico-chemical properties.

Many others have also developed various substituent constants. Today a QSAR practitioner has a large number of such constants to choose from. Using some of these constants, one can also calculate the physico-chemical properties of the complete molecule. Some of the important and frequently used physico-chemical properties and the related substituent constants are brief described below (Malik *et al.*, 2013).

1. 3. 2. 3.1 Quantifying Structure in terms of Lipophilicity

Lipophilicity is the affinity of drug molecules for a lipophilic environment, and is often considered as a key property in the transport processes of drugs in human beings. These include intestinal absorption, membrane permeability, protein binding, and distribution among different tissues. It is usually defined as the partition coefficient (P) of a compound distributed between octanol and water phases, and is commonly expressed as logP, its logarithmic form. Since then large number of reports have correlated various biological activities with the partition coefficient (Raevsky, 2004). Hansch and Fujita (1964) recognized that partition coefficient is an additive constitutive property, that is, the partition coefficient of a molecule is the sum of the contributions from various parts of the molecule. It also means that, for example, if a methyl group is added to any molecule, the partition coefficient will increase to the same extent in all the molecules (Fujita *et al.*, 1964). By studying the partition coefficients of a large number of molecules, the contribution of each substitution was calculated. The hydrophobic parameter thus calculated for a substituent was called 'π'. It can be calculated as follows:

$$\pi_x = \log P_x - \log P_H$$

π_x is the hydrophobic constant of the substituent X. $\log P_x$ is the log partition coefficient of the molecule with the substitution X and $\log P_H$ is the log partition coefficient of the parent molecule that is, the unsubstituted molecule. For example,

$$\pi_{Cl} = \log P (\text{Chlorobenzene}) - \log P (\text{Benzene}) = 2.84 - 2.13 = 0.71$$

Thus pi value for chloro substituent is 0.71. It means that the introduction of a chloro group will result in the increase of log P by 0.71 (Pattan *et al.*, 2011).

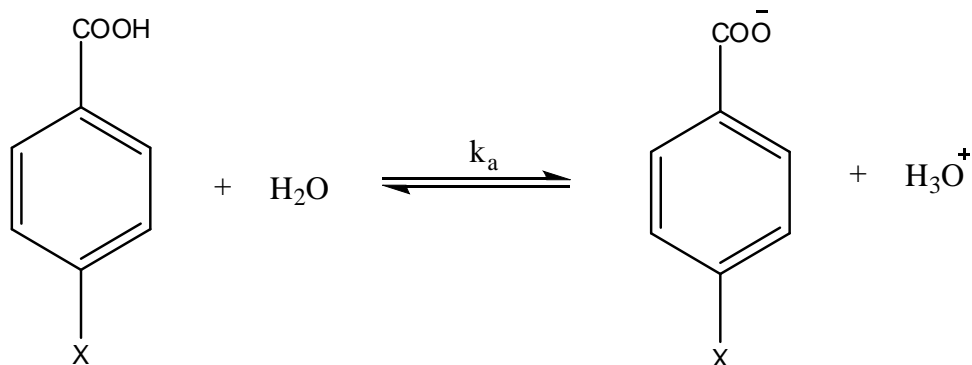
Although many organic solvents can be used to measure the partition coefficient, Hansch and his group (1971) has standardized the method using n- octanol-water system (leo *et al.*, 1971).

However, there is a computer program calculating log P from a set of empirical rules devised after examining thousands of compounds.

1. 3. 2. 3.2 Quantifying Structure in terms of Electronic Parameters

Extensive studies using electronic parameters reveal that electronic attributes of molecules are intimately related to their chemical reactivities and biological activities.

Early work examining the electronic role of substituents on rate constants was established by Hammett. Hammett employed, as a model reaction, the ionization in water of substituted benzoic acids and determined their equilibrium constants K_a (Pattan *et al.*, 2011). These constants were very useful in predicting a number of reaction rates (Malik *et al.*, 2013).



His equation has been successfully applied in studying a very large of diverse reaction. The Hammett constant (σ , sigma) can be easily calculated by the equation:

$$\sigma_X = (pK_a)_H - (pK_a)_X$$

σ_X is the Hammett constant of the substituent X, $(pK_a)_H$ is the pka of the benzoic acid with the substituent X and $(pK_a)_H$ is the pka of benzoic acid, that is, the unsubstituted parent molecule (Selassie, 2003).

1. 3. 2. 3. 3 Steric Parameters

Taft introduced the steric parameter, E_s , which was calculated using rate of ester hydrolysis. But the method could not be used to determine the values for many substituents whose esters were not stable. Kuffer and Hansch utilized the relationship between E_s and the Van Der Waal radii, which was calculate the E_s value of large number of substituents. Verloop developed a multidimensional steric parameter using a computer program based on the standard values of van der wall radii, bond lengths and bond angles. These parameters are labeled as B_1 , B_2 , B_3 , B_4 and L . L is the length of the substituent and B_1 to B_4 are width parameters where B_1 is the minimum and B_4 is the maximum width. Moriguchi developed van der waal volume V was another steric parameter which is easy to calculate (Kutter and Hansch, 1969).

1. 3. 2. 3.4 Molar Refractivity (MR)

Molar refractivity is an additive constitutive property of a compound which can be calculated easily. It is connected with the molar volume. But it is not purely a steric parameter. It also reflects drug receptor dispersion interactions. It is generally assumed that a positive coefficient with an MR term in a correlation equation suggests a binding action via dispersion forces. A negative coefficient with MR has been assumed to reflect steric hindrance. It has been found that MR and log P are highly correlated in a homologous series. But, if the series is designed to include different types of substituents, the MR and log P are not correlated and can give useful information.

1. 3. 2. 3. 5 Molecular Connectivity

Petroleum chemists have frequently used calculations based on branching in molecules to predict many physical properties like boiling point, viscosity, etc. This approach was quantified in the form of matrices. Kier has extensively used these methodologies in QSAR. The main advantage of this method is that these values can be calculated easily and no physical properties have to be measured. Large numbers of correlation have been reported between various indices of molecular connectivity and physical and biological properties. But one fundamental problem with the concept of connectivity is that while it is designed to parameterize molecular shape in a more sophisticated manner it falls short of consideration of the three-dimensional array of atoms in space. It is this topography rather than topology which is probably essential at the molecular level. It also does not give any information to medicinal chemist for further design unlike other parameters. Recently Kier and his coworkers have developed a new parameter called electro topological state index from graph theory (Gozalbes *et al.*, 2002).

Other chemical descriptors have been used to model other properties, or to improve the QSAR models with log P. The attempt has been to avoid the errors of the QSAR models. Indeed, some chemicals were not correctly modeled, and other descriptors have been introduced, producing multilinear relationships. The theoretical assumptions were modeled keeping into account other physico-chemical parameters, such as chemical reactivity, through chemical descriptors, such as the energy of the highest occupied molecular orbital (HOMO) and the lowest unoccupied molecular orbital (LUMO)

1. 3. 2. 4 Regression Analysis (Hansch Analysis)

Relationship between biological activity and physic-chemical parameter can be expressed through linear equations of the type:

$$Y = a + bx \dots\dots (1)$$

Where **Y** is the biological activity, **a** is the intercept and **x** is the Physico-chemical parameter and **b** is the slope or regression coefficient. For QSAR studies, the equation (1) can be appropriately modified as,

$$\text{Log (1/C)} = a + b (\text{log P}) \dots\dots (2)$$

Here, biological activity is expressed as log (1/C) where **C** is the molar concentration of the compound which gives specific response say IC₅₀, LD₅₀, etc. It is essential to express the concentration in logarithmic scale because the right side of the equation contains parameters which are derived from logarithmic scale like log P, Pi, sigma, Es, etc

Hansch observed that the relationship between partition coefficient and activity is not always linear. A linear relationship is observed only when the range of partition coefficient studied is small. Activity cannot increase indefinitely with the increase in partition coefficient. After a certain limit, there will be a decrease in the activity. Such a nonlinear relationship can be expressed as a parabolic equation.

$$\text{Log (1/C)} = a + b (\text{log P}) + c (\text{log P})^2 \dots\dots (3)$$

Statistically better equations were derived with a parabolic model compared to linear model. This model was further improved by Kubinyi who suggested a bilinear model

$$\text{Log (1/C)} = a + b (\text{log P}) + c \text{log}(\text{BP} + 1)^2 \dots\dots (4)$$

Here, B is a nonlinear term to be derived by a stepwise process or by other mathematical methods.

Another important contribution of Hansch is the recognition that biological activity will not depend on a single physico-chemical parameter but on many. Hence a generalized equation was suggested.

$$\text{Log (1/C)} = a + b\pi + c\sigma + dEs \dots\dots (5)$$

Here, π , σ and Es are Hansch hydrophobic constant, hammett constant and Tafts steric parameter respectively. The number of parameters in the equation can be increased or decreased. The coefficients “b, c, d” and the intercept “a” are to be calculated using multiple regression analysis. The equation (5) can also have a parabolic term as.

$$\text{Log (1/C)} = a + b\pi + c\pi^2 + d\sigma + eEs \dots\dots (6)$$

1. 3. 2. 4. 1 Application of Statistics

The significance of the equation is tested by using a number of statistical parameters. Most frequently used statistical parameters are correlation coefficient(r), standard deviation from regression (s) and F-test. In addition to the above, r^2 statistics and t- test are also used. r^2 statistics give the fraction of the total variance in the data explained by the regression and t – test gives the significance of the coefficient.

1. 3. 2. 4. 2 Methodology and Precautions

Today, simple linear regression analysis can be performed using calculators. But for more complex problems use of computer is essential. Before performing the regression analysis certain precautions are be considered.

1. 3. 2. 4.2.1 Biological activity

The biological activity data must be obtained at different doses. The log dose response must be converted to ED_{50} or ED_{30} , etc. The dose in mg/kg should also be converted to moles/kg for comparison. If the activity is calculated based on one single dose the data must be converted to log it units. The following calculation can be used.

$$BA = (M_w/d) \log (P/100 - P) BA$$

BA is biological activity, M_w is molecular weight of the compound, d is the dose in mg/kg and P is the percent activity obtained dose d . form the above equation BA can be directly used for QSAR studies. However, biological activity data from a single dose is less accurate than the ED_{50} , etc., which are obtained from multiple doses.

1. 3. 2. 4. 2. 2 Number of independent variables

In a multi regression analysis, good correlation can be obtained by including large number of parameters. If number of compounds are two, than one gets correlation coefficient = 1. The number of parameters to be included depends on the number of compounds we are analyzing. It has been shown that for sample size less than 20, when the number of variable is about one fifth of the number of compounds, one is likely to get good correlation which is only a chance correlation and not a true correlation.

1. 3. 2. 5 Comparative Molecular field Analysis (CoMFA)

The Comparative Molecular Field Analysis (CoMFA) uses electrostatic (Coulombic) and steric (van der Waals) energy fields defined by the inspected compound. The aligned molecule is placed in a 3D grid. In each point of the grid lattice a probe atom with unit

charge is placed and the potentials (Coulomb and Lennard-Jones) of the energy fields are computed. Then, they serve as descriptors in further analysis, typically using partial least squares regression. This analysis allows for identifying structure regions positively and negatively related to the activity in question (Dudek *et al.*, 2006).

1. 3. 2. 6 Application of QSAR

The ability to predict a biological activity is valuable in any number of industries. Whilst some QSARs appear to be little more than academic studies, there are a large number of applications of these models within industry, academia and governmental (regulatory) agencies. A small number of potential uses are listed below:

- The rational identification of new leads with pharmacological, biocidal or pesticidal activity.
- The optimization of pharmacological, biocidal or pesticidal activity.
- The rational design of numerous other products such as surface-active agents, perfumes, dyes, and fine chemicals.
- The identification of hazardous compounds at early stages of product development or the screening of inventories of existing compounds.
- The designing out of toxicity and side-effects in new compounds.
- The prediction of toxicity to humans through deliberate, occasional and occupational exposure.
- The prediction of toxicity to environmental species.
- The selection of compounds with optimal pharmacokinetic properties, whether it be stability or availability in biological systems. Quantitative Structure–Activity Relationships (QSARs).
- The prediction of a variety of physico-chemical properties of molecules (whether they be pharmaceuticals, pesticides, personal products, fine chemicals, etc.).
- The prediction of the fate of molecules which are released into the environment.
- The rationalization and prediction of the combined effects of molecules, whether be in mixtures or formulations. The key feature of the role of in silico technologies in all of these areas is that predictions can be made from molecular structure alone (Puzyn *et al.*, 2010).

1. 3. 2. 7 Objectives of QSAR

Mostly all the QSAR methods focus on the following goals:

1. To quantitatively correlation between the structure and physiochemical properties of substances and their biological activity are being used as the foundation stone in search of new medicines. The mathematical and statistical analysis helps us to predict the drug activity.
2. To reach easily the conclusion for any of the congener that still not in process, in way that whether it will be optimal and profitable or not.
3. To quantitatively correlate and recapitulate the relationships between trends in chemical structure alterations and respective changes in biological endpoint for comprehending which chemical properties are most likely determinants for their biological activities.
4. To optimize the existing leads so as to improve their biological activities.
5. To predict the biological activities of untested and sometimes yet unavailable compounds (Jhanwar *et al.*, 2011).

1. 3. 2. 8 Importance in Drug Research

Nowadays, rational drug design efforts widely rely on building extensive QSAR models which currently represent a substantial part of modern research. Due to inability of the fundamental laws of chemistry and physics to directly quantify biological activities of compounds, computational chemists are led to research for simplified but efficient ways of dealing with the phenomenon, such as by the means of molecular descriptors. The QSAR descriptors came to particular demand during last decades when the amounts of chemical information started to grow explosively. Nowadays, scientists routinely work with collections of hundreds of thousands of molecular structures which cannot be efficiently processed without use of diverse sets of QSAR parameters. Modern QSAR science uses a broad range of atomic and molecular properties varying from merely empirical to quantum-chemical. The most commonly used QSAR arsenals can include up to hundreds and even thousands of descriptors readily computable for extensive molecular datasets. Such varieties of available descriptors in combination with numerous powerful statistical and machine learning techniques allow creating effective and sophisticated structure-bioactivity relationships.

Nevertheless, although even the most advanced QSAR models can be great predictive instruments, often they remain purely formal and do not allow interpretation of individual factors influencing activity of drugs Topliss suggested an empirical scheme for the selection of substituents for the synthesis. This scheme is based on the physico- chemical

parameters like hydrophobic, electronic and steric parameters. In this scheme, each compound is synthesized and tested (Cherkasov, 2005).

Based on the comparative activity with the previous compound, the scheme suggested the next substituents to be selected for the synthesis. Then that compound will be synthesized and tested. The scheme suggests further substituents for the next synthesis. The scheme is called Topliss scheme (Malik *et al.*, 2013).

1.4 Rational drug design

Rational drug design can be broadly divided into two categories: (A) Development of small molecules with desired properties for targets, biomolecules (proteins or nucleic acids), whose functional roles in cellular processes and 3D structural information are known. This approaching drug design is well established and is being applied extensively by the pharmaceutical industries. (B) Development of small molecules with predefined properties for targets, whose cellular functions and their structural information may be known or unknown. Knowledge of unknown targets (genes and proteins) can be obtained by analyzing global gene expression data of samples untreated and treated with a drug using advanced computational tools. Once a target is identified, then both approaches (A) and (B) for development of small molecules require examination of several aspects. These aspects include, but are not limited to, the evaluation of binding scores (affinity/specificity), balance between hydrophilicity, lipophilicity, absorption, distribution, metabolism, and excretion, electrophilic, nucleophilic, and radical attack (biodegradation), toxicity of the parent small molecules, and products due to biotransformation in the different phases of metabolism, quantitative structure–activity relationship (QSAR), and quantitative structure–property relationship (QSPR) respectively. Most of these aspects including design of a small molecule could be performed initially using computational tools. After the initial evaluation and identification of lead molecules, gene expression profiling and bioinformatics analysis would be particularly important to gain insights in gene expression patterns. In turn, this knowledge can be utilized to improve drugs to accomplish desirable attributes such as disease free survival, eradication of disease, elimination or minimization of toxic side effects, reduction of undesirable biotransformation, improvement in distribution (bioavailability), overcoming of drug resistance, and improvement of immune responses. Therefore, rational drug design would be an integral approach to drug development and discovery (Mandal *et al.*, 2009).

1.4.1 Computer-aided drug discovery (CADD)

Bringing a new drug into the market is a costly process in terms of money, manpower, and time. Innovations in chemistry that led to the increase of compound databases covering large chemical spaces aided in the expansion of drug discovery and the development of high-throughput screening (HTS).

To this end, employment of computer-aided drug discovery (CADD) techniques by top pharmaceutical companies and other research groups became essential for the preliminary stage of drug discovery to expedite the drug development process in a more cost-efficient way and to minimize failures in the final stage.

The use of rational drug design, as applied in CADD, provides a knowledge-driven approach that can yield valuable information about the interaction pattern between protein and ligand (complex), as well as the binding affinity. Furthermore, the availability of supercomputers, parallel processing, and advanced softwares have greatly facilitated the rate of lead identification in pharmaceutical research (Macalino *et al.*, 2015).

Different terms are being applied to this area, including computer-aided drug design (CADD), computational drug design, computer-aided molecular design (CAMD), computer-aided molecular modeling (CAMP), rational drug design, in silico drug design, computer-aided rational drug design (Kapetanovic, 2009).

Strategies for CADD vary depending on the extent of structural and other information available regarding the target (enzyme/receptor) and the ligands. “Direct and indirect” designs are the two major modeling strategies currently used in the drug design process. In the indirect approach the design is based on comparative analysis of the structural features of known active and inactive compounds. In the direct design the three-dimensional features of the target (enzyme/receptor) are directly considered (Kore *et al.*, 2012).

The current scenario of the drug discovery process involves several disciplines such as chemical and structural biology, computational chemistry, organic synthesis, and pharmacology. Accordingly, it is comprised of several stages:

- (a) Target identification involves the discovery and isolation of individual targets to investigate their functions and association with a specific disease.
- (b) Target validation is the stage where the drug target is linked to the disease of interest, as well as their capacity to regulate biological functions in the body after binding to a partner molecule. Numerous studies are performed to ascertain that the target macromolecule is linked to the diseased state.

(c) Lead identification entails the discovery of a synthetic chemical that shows a degree of potency and specificity against a biological target and is assumed to have the makings of a drug that can cure the intended disease.

(d) Lead optimization covers the improvement of potency and other significant properties through iterative cycles of evaluation of the lead compound(s) and their analogs. Thus, both *in vitro* and *in vivo* experiments are conducted to prioritize and select candidates with optimum potential for development as a safe and efficient drug. Moreover, structure–activity relationships (SARs) are developed to determine pertinent pharmacokinetic and pharmacodynamic properties that can be applied to analogs that will be synthesized for evaluation

(e) Preclinical stage involves drug synthesis and formulation research, *in vivo* animal studies for potency and toxicity, and characterization of mechanistic toxicity.

(f) Clinical trials include three phases that investigate safety, adverse side effects, dosage, efficacy, and pharmacokinetic and pharmacological properties of the candidate drug on human volunteers.

In general, modeling approaches are categorized into structure-based and ligand-based methods.

The structure-based approach consists of using the 3D structure of the target (enzyme/receptor) for the generation or screening of potential ligands (modulators), followed by synthesis, biological testing, and optimization. In contrast,

Ligand-based approach consists of subjecting a collection of molecules with diverse structures and known potency to computational modeling methods to develop theoretical predictive models. These models are then used for structural optimization to enhance potency and for identification of new chemical entities through virtual screening of a large chemical database.

Over the decades, these two types of CADD approaches continued to improve and evolve separately. However, combining different structure-based and ligand-based design strategies in the drug discovery effort have been established to be more effective than any single approach since both methods are able to complement their strengths and weaknesses (Macalino *et al.*, 2015).

CADD is usually used for three major purposes: (1) filter large compound libraries into smaller sets of predicted active compounds that can be tested experimentally; (2) guide the optimization of lead compounds, whether to increase its affinity or optimize drug metabolism and pharmacokinetics (DMPK) properties including absorption, distribution,

metabolism, excretion, and the potential for toxicity (ADMET); (3) design novel compounds, either by "growing" starting molecules one functional group at a time or by piecing together fragments into novel chemotypes (Sliwoski *et al.*, 2015).

1.5 Lipinski's Rule

Lipinski's rule of five also known as the Pfizer's rule of five or simply the Rule of five (RO5) is a rule of thumb to evaluate drug likeness or determine if a chemical compound with a certain pharmacological or biological activity has properties that would make it a likely orally active drug in humans. The rule was formulated by Christopher A. Lipinski in 1997. The rule describes molecular properties important for a drug's pharmacokinetics in the human body, including their absorption, distribution, metabolism, and excretion (ADME) Components of the Lipinski's rule:

- Not more than 5 hydrogen bond donors (nitrogen or oxygen atoms with one or more hydrogen atoms)
- Not more than 10 hydrogen bond acceptors (nitrogen or oxygen atoms)
- A molecular mass less than 500 daltons
- An octanol-water partition coefficient log P not greater than 5
- No more than one number of violation (Singh *et al.*, 2013).

1.6 Aim and objective of current study

Quinoline and its fused heterocyclic derivatives tested with diverse pharmacological activity constitute an important class of compounds for new drug development. Further, these compounds are used as building blocks of various other compounds such as (α,β -unsaturated carbonyl derivatives) chalcones, pyrazolines, cyanopyridines, isoxazoles, sulphonamides, arylamides, thiopyrimidines, amino pyrimidines etc. These compounds are known to possess biological activities (Baluja *et al.*, 2015). The increased resistance of microbials to known quinolines is constantly demanding to generate novel quinolines to meet the requirements

The main objective of this study is to design and develop new derivatives of quinoline-4-carboxylic acids by using computational methods and then conventional methods in the laboratory. The specific objectives of this study are to:

- Generate QSAR models with good Statistical parameters that can be used to predict the activity of newly designed derivatives against vesicular stomatitis virus

(VSV) replication as dihydroorotate dehydrogenase (DHODH) enzyme inhibitor by using dataset compounds.

- Design new quinoline-4-carboxylic acid derivatives using the computer software to predict their biological activity by generated model.
- Study QSAR model of interest in the prediction of the activity as (DHODH) enzyme inhibitor.
- Carry out Lipinski's rule of five (RO5) for newly designed quinoline derivatives.
- Select some of the new designed derivatives for synthesis that agreeing with Lipinski's rule and possess higher predicted biological activity than that for stander reference.
- Synthesize some starting product structural derivatives of quinoline-4-carboxylic acids using by Doebner-Millar reaction and corresponding α , β unsaturated carbonyl derivatives obtained by Caisen Schmidt condensation of quinoline with aldehydes which react with some reagents (urea derivative, hydrazine derivatives and monoethanolamine) in different manners to give pyrimidinone /thiones , pyrazoline, and oxazepines compounds
- Analyze the synthesized compounds using some spectral analysis, (IR, ^1H NMR, ^{13}C NMR and GCMS).
- Predict interactions of quinoline derivatives with receptor (DHODH) enzyme protein through molecular docking study.

CHAPTER TWO

Martials and Methods

2. Materials and Methods:

2.1 Materials, Software's and instruments:

2.1.1 Data Set

Data set of biological activities for 25 quinoline derivatives was collected from (Das *et al.*, 2013). These derivatives were evaluated for their ability against vesicular stomatitis virus VSV replication in MDCK (Madin Darby canine kidney) epithelial cells in terms of EC₅₀ (Half maximal effective concentration) values as inhibitor dihydroorotate dehydrogenase (DHODH) enzyme.

2.1.2 Chemicals

- Absolute ethanol, C₂H₆O, Density 0.790 – 0.793g/cm³, Assay 98%, BDH chemicals Ltd, England.
- Acetic anhydride, C₂H₄O₃, Density 1.079 – 1.081g/cm³, Assay 98%, BDH chemicals Ltd, England.
- Acetone, C₃H₆O, Density 0.789 - 0.792g/cm³, Assay 98%, CDH Laboratory reagent, India.
- Acetyl acetone, C₅H₈O₂, Density 0.971 – 0.974g/cm³, Assay 98%, BDH Laboratory reagent, England.
- Anhydrous sodium acetate, C₂H₃O₂Na, Assay 98%, QualiKems fine chemical, India.
- Benzaldehyde, C₇H₆O, Density 1.044 - 1.047g/cm³, Assay 98.5%, Loba chemie Pvt. Ltd, India.
- Chloroform, CHCl₃, Density 1.474 – 1.480g/cm³, Assay 99.5%, Loba chemie Pvt. Ltd, India.
- Ethanol, C₂H₆O, Density 0.789g/cm³, Assay 96%, Honeywell, Brazil.
- Ethanolamine, C₂H₇NO, Density 1.01g/cm³, Assay 96%, Sigma-Aldrich, Germany.
- Furfural, C₅H₄O₂, Density 1.158 – 1.160g/cm³, Assay 98%, Loba chemie Pvt. Ltd, India.
- Glycine, C₂H₅NO₂, Assay 99%, Scientific limited, Northampton, UK.
- Hydrazine mono hydrochloride, H₄N₂.HCl, Assay 97%, Sigma-Aldrich, Germany.
- Hydrochloric acid, HCl, Density 1.18g/cm³, Assay 35–38%, Loba chemie Pvt. Ltd, India.

- Methanol, CH₄O, Density 0.790 – 0.793g/cm³ , Assay 99.5%, Loba chemie Pvt. Ltd, India.
- P-amino acetophenone, C₈H₉NO, Assay 99.9%, Blulux Laboratories (P) Ltd, India.
- Phenyl hydrazine hydrochloride, C₆ H₈N₂.HCl, Assay 99%, Sigma-Aldrich, Germany.
- Semicarbazide hydrochloride, C H₅N₃O.HCl, Assay 99%, Sigma-Aldrich, Germany.
- Sodium hydroxide, NaOH, CDH Laboratory reagent, India.
- Silica Gel-G for TLC, Techno pharmchem, India.
- Thiourea, CH₄N₂S, Assay 99%, Techno pharmchem, India.
- Urea, CH₄N₂O, Assay 99%, Loba chemie, India.

2.1.3 Softwares

2.1.3.1 ACD labs Software

ACD/ChemSketch Freeware (Version 12.01, run for Windows) for is the powerful all-purpose chemical drawing and graphics package from ACD/Labs developed to help chemists quickly and easily draw molecular structures, reactions, and schematic diagrams, calculate chemical properties, and design professional reports and presentations. Copyright © 1994-2010 for Advanced Chemistry Development, Inc. Toronto, On, Canada.

2.1.3.2 ChemDraw Software

ChemDraw (Version 16.0.0.82, run for Windows) is a program that allows drawing intuitively and efficiently simple two- dimensional representations of organic molecules. Copyright©1996-2016 for PerkinEmler informatics,Ins. Waltham, United States.

2.1.3.3 MOE Software

MOE (Version 110, run for Windows) is a drug discovery software platform that integrates visualization, modeling and simulations, as well as methodology development, in one package. MOE scientific applications are used by biologists, medicinal chemists and computational chemists in pharmaceutical, biotechnology and academic research. Main application areas in MOE include structure-based design, fragment-based design, pharmacophore discovery, medicinal chemistry applications, biologics applications, protein and antibody modeling, molecular modeling and

simulations, cheminformatics and QSAR. Copyright © 1997-2009 for Chemical Computing Group ULC. Montreal, QC, Canada.

2.1.3.4 SPSS Software

SPSS (Version 11.5.0, run for Windows) is a software package used for interactive or batched, statistical analysis. Long produced by SPSS Inc. Quarry Bay, Hong Kong.

2.1.4 Glass ware

All glasswares were Pyrex type.

2.1.5 Apparatus and equipments

- Hot plate stirrer, Stuart, Bibby sterilin LTD, UK.
- Melting point apparatus, Gallenkamp, England.
- Sensitive balance, A&D-GR-120, Japan.

2.1.6 Instrumentations

2.1.6.1 Infra-red spectroscopy

Infra-red spectroscopy (IR) was recorded on FTIR-8400s instrument (Shimadzu, Japan) using KBr disc.

2.2.6.2 ¹H Nuclear magnetic resonance spectroscopy

¹H Nuclear magnetic resonance spectroscopy (¹HNMR) was recorded on Ultrashield - 500 plus instrument (BRUKER, Germany) using chloroform (dimethyl sulfoxide) as solvent and operating at 500.13MHz for protons. Employing 5mm high-resolution broad-band TMS gradients. The zg30 pulse program was used. Spectra were recorded over a sweep width of (10330.57 Hz) at 293.4k temperature and time domain data points giving an acquisition time of 1.00 seconds.

2.2.6.3 ¹³C Nuclear magnetic resonance spectroscopy

¹³C Nuclear magnetic resonance spectroscopy (¹³CNMR) was recorded on Ultrashield - 500 plus instrument (BRUKER, Germany) using CDCl₃ as solvent and operating at 100.62MHz for protons. Employing a 5mm high-resolution broad-band TMS gradients probe. The zg30 pulse program was used. Spectra were recorded over a sweep width of (24038.46 Hz) at 298.8k temperature and time domain data points giving an acquisition time of 2.00 seconds.

2.2.6.4 Gas chromatography- mass spectroscopy

Gas chromatography mass (GCMS) was recorded on QP 2010 GC instrument (Shimadzu, Japan) and the following conditions have been adopted:

- Column oven temp=100C°
- Injection temp = 290C°
- Injection mode= split
- Total flow= 1.24ml/min
- Ion source temp = 200C°
- Solvent cut time =2.5 min
- Start time= 3min
- Oven temp program was illustrated below:

Rate	Temperature (C°)	Hold time (min)
-	100	0.00
30	160	0.00
15	92	20,00

2.1.5 Thin layer chromatography (TLC)

TLC was carried out using silica gel 60 GF 254 (Merck Germany) precoated plates or coated over glass with different mobile phases.

2.2 Methods

2.2.1 Preparation for QSAR modeling study

The 25 quinoline derivatives of data set in terms EC₅₀ (μM) converted to EC₅₀ (M), calculate pEC₅₀ (log1/EC₅₀) and then divided into training and test sets. The compounds of training set of 20 and test set of 5 compounds by random selection were drawn using ACD /Lab.12.01 freeware and saved in mol. file format see (Table 2.1).

2.2.1.1 Molecular modeling descriptors

The mol. files were opened by MOE 2009.10 software was used minimized energy, the different molecular 25 descriptors were calculated and decreased the redundancy existing in the descriptors data matrix, the correlations of descriptors with each other and with pEC₅₀ of the molecules were examined, and collinear descriptors (R < 0.9) were detected. Those descriptors which had the pair wise correlation coefficient above

0.9 and having the lower correlation with pEC₅₀ values were removed from the data matrix.

8 descriptors were left in clouding:

- i. AM1-.HF. heat of formation.
- ii. ASA-P. Total polar surface area.
- iii. AM1-. Dipol. Dipol moment.
- iv. AM1-IP. Ionization potential.
- v. Chi₀. Atomic connectivity index order zero
- vi. Density. Mass density.
- vii. MR. Molar Refractivity
- viii. Log P_(o/w). Logarithm of its partition coefficient between n-octanol and water (Table 2.2) and (Figure 2.1).

	1	2	3	4	5	6	7	8	9
1. pEC ₅₀	100	-40	-7	-47	79	-58	74	-22	67
2. AM1_dipole	-40	100	33	38	11	26	6	46	11
3. AM1_IP	-7	33	100	59	-5	43	21	56	37
4. ASA_P	-47	38	59	100	-48	61	-15	41	1
5. logP(o/w)	79	11	-5	-48	100	-58	82	-18	76
6. density	-58	26	43	61	-58	100	-42	9	-25
7. mr	74	6	21	-15	82	-42	100	9	96
8. AM1_HF	-22	46	56	41	-18	9	9	100	5
9. chi0	67	11	37	1	76	-25	96	5	100

Figure (2.1): Correlation matrix for chemical descriptors

2.2.1.2 Model development

The QSAR models were constructed based on the partial least square method (PLS) using to descriptors in MOE as an independent variables and pEC₅₀ as a dependent variable by forward regression analyses. The quality of each regression model was evaluated using a squared correlation coefficient r^2 (> 0.7) and root mean square error (RMSE) (Xu *et al.*, 2015).

About 19 QSAR models were generated by using partial least square regression method coupled with stepwise forward backward method (Table 2.3).

2.2.1.3 Validation Model

To determine the reliability of model it was validated by:

- Internal validation of training set in terms of cross validated q^2 (>0.5) carried by leave one out (LOO) as default option (Choudhary *et al.*, 2015).
- External validation of test set for external prediction r^2_{pred} (Wang *et al.*, 2009)

Goodness of fit of the models was assessed by examining the multiple correlation coefficient r^2 , Root mean square error (RMSE), the standard deviation (s), the F-ratio between the variances of calculated and observed activities (F) (Sharma² *et al.*, 2010). The acceptable F (F-test) or p -value showed value higher, so this is better for models (Wongrattanakamon *et al.*, 2016) (Table 2.4).

2.2.2 Modeling of quinoline derivatives

The set of 180 new quinoline derivatives were designed using the computer software ACD /Lab.12.01 freeware, bond lengths and bond angles standardized by clean structure and then saved as (mol) format. These compounds were not used in the developed QSAR model, but sketched to predict their activity against VSV replication as inhibitor dihydroorotate dehydrogenase (DHODH) enzyme.

2.2.2.1 Predict the biological activity of new designed quinoline derivatives

The mol. files of 180 designed derivatives were opened by MOE 2009.10 software, energy minimized and the different 4 descriptors of the best model-1 were calculated. The fit of model-1 was evaluated to predict biological activity of new quinoline derivatives in the term pEC_{50} see (Table 2.5).

2.2.2.2 ADMET studies

MOE 2009.10 software was used also to carry out ADMET by predict the Lipinski's rule, Log S and T_PSA see (Table 2.6).

2.2.3 Synthesis

The 16 quinoline derivatives selected from newly designed quinoline derivatives, having higher predicted biological activity than brequinar and agreeing with Lipinski's rule of five (RO5), were synthesized by conventional methods in the laboratory.

2.2.3.1 General method for synthesis of 2,3-di phenyl /2- (furan-2-yl) -3-phenyl - quinoline -4-carboxylic acid derivatives (I and IX)

In round bottom flask equipped with a reflux condenser, 0.236 mol of the required aromatic aldehyde, 0.25 mol of freshly distilled phenyl pyruvic acid and 200 ml of absolute ethanol were placed. The mixture was heated on a boiling water-bath and a solution of 0.248 mol of P-amino acetophenone in a 100 ml of absolute ethanol was added slowly with frequent shaking within 1 hour. The mixture was refluxed on a water-bath for 3 hours and left to stand overnight, filtered, washed with little ether and recrystallized from ethanol; for their physical and chemical properties (Tables 2.7.1, 2.7.2, 2.8.1, 2.8.2, 2.9.1, 2.9.2, 2.10.1, 2.10.2, 2.11.1, 2.11.2, 2.12.1, 2.12.2, 2.13.1 and 2.13.2).

2.2.3.2 General method for synthesis of α,β -unsaturated carbonyl derivatives (II and X):

A mixture of 0.01 mol of the required aromatic aldehyde and 0.01 mol of substituted quinoline was stirred in 30 ml of ethanol at room temperature in the presence of 10 ml of 20% sodium hydroxide solution. The mixture was stirred for 24 hours at RT and kept for overnight at RT. The mixture was poured into crushed ice and acidified with dilute hydrochloric acid. The α,β -unsaturated carbonyl derivatives were precipitated out as solid, filtered, dried and recrystallized from ethanol; for physical and chemical properties (Tables 2.7.1, 2.7.2, 2.8.1, 2.8.2, 2.9.1, 2.9.2, 2.10.1, 2.10.2, 2.11.1, 2.11.2, 2.12.1, 2.12.2, 2.13.1 and 2.13.2).

2.2.3.3 General method for synthesis of 2- Pyrimidinone/Pyrimidinethion derivatives (III, IV, XI and XII)

To a solution of 0.01 mol of α,β -unsaturated carbonyl products II or X, 50 ml absolute ethanol, 0.01mol of urea/thiourea and 6 ml of aqueous sodium hydroxide 10% was added. The reaction mixture was heated under reflux for 3h and poured in ice-cold water. The product obtained was filtered washed with water and recrystallized from ethanol; for physical and chemical properties (Tables 2.7.1, 2.7.2, 2.8.1, 2.8.2, 2.9.1, 2.9.2, 2.10.1, 2.10.2, 2.11.1, 2.11.2, 2.12.1, 2.12.2, 2.13.1 and 2.13.2).

2.2.3.4 General method for synthesis of pyrazoline/ pyrazoline-1- phenyl/ pyrazoline-1-carboxamide derivatives (V, VI, VII, XIII, XIV and XV)

A mixture of 0.01 mol of α,β -unsaturated carbonyl products II or X, 0.01 mol of hydrazine hydrochloride, phenyl hydrazine hydrochloride or pyrazoline-1-carboxamide dissolved in 25 mL of ethanol and 1 mL of ethanolic sodium hydroxide 0.1 mol was added. The reaction mixture was heated under reflux for 2h. TLC monitoring was extensively done. The product when cool was poured in ice-cold water. The solid mass which separated out was filtered washed with water and recrystallized from ethanol; for physical and chemical properties (Tables 2.7.1, 2.7.2, 2.8.1, 2.8.2, 2.9.1, 2.9.2, 2.10.1, 2.10.2, 2.11.1, 2.11.2, 2.12.1, 2.12.2, 2.13.1 and 2.13.2).

2.2.3.5 General method for synthesis 1, 4-oxazepines derivatives (VIII and XVI):

A mixture of 0.01 mol of α,β -unsaturated carbonyl products II or X, 0.01 mol of monoethanolamine dissolved in 25 mL of ethanol and 0.5 mL of ethanolic sodium hydroxide 0.1 mol was added. The reaction mixture was heated under reflux for 3h. TLC monitoring was extensively done. The product when cool was poured in ice-cold water. The solid mass which separated out was filtered washed with water and recrystallized from ethanol; for physical and chemical properties (Tables 2.7.1, 2.7.2, 2.8.1, 2.8.2, 2.9.1, 2.9.2, 2.10.1, 2.10.2, 2.11.1, 2.11.2, 2.12.1, 2.12.2, 2.13.1 and 2.13.2).

2.2.4 In silico molecular docking studies:

Molecular docking studies of quinoline derivatives with the protein receptors was carried out by using MOE 2009.10 software which distributes simulation from molecular operating environment to studies for the target site prediction for inhibitor human dihydroorotate dehydrogenase enzyme (DHODH) activity.

2.2.4.1 Preparation of Ligands

The mol. files of 25 ligands data set and 86 ligands selected from 180 new quinoline derivatives designed according to their higher predicted biological activity were opened in MOE 2009.10. The 3-D protonated structures of ligands were energy minimized. Then ligands were saved in a molecular database (mdb) file ready for run docking (Thangavelu *et al.*, 2018).

2.2.4.2 Preparation of Protein

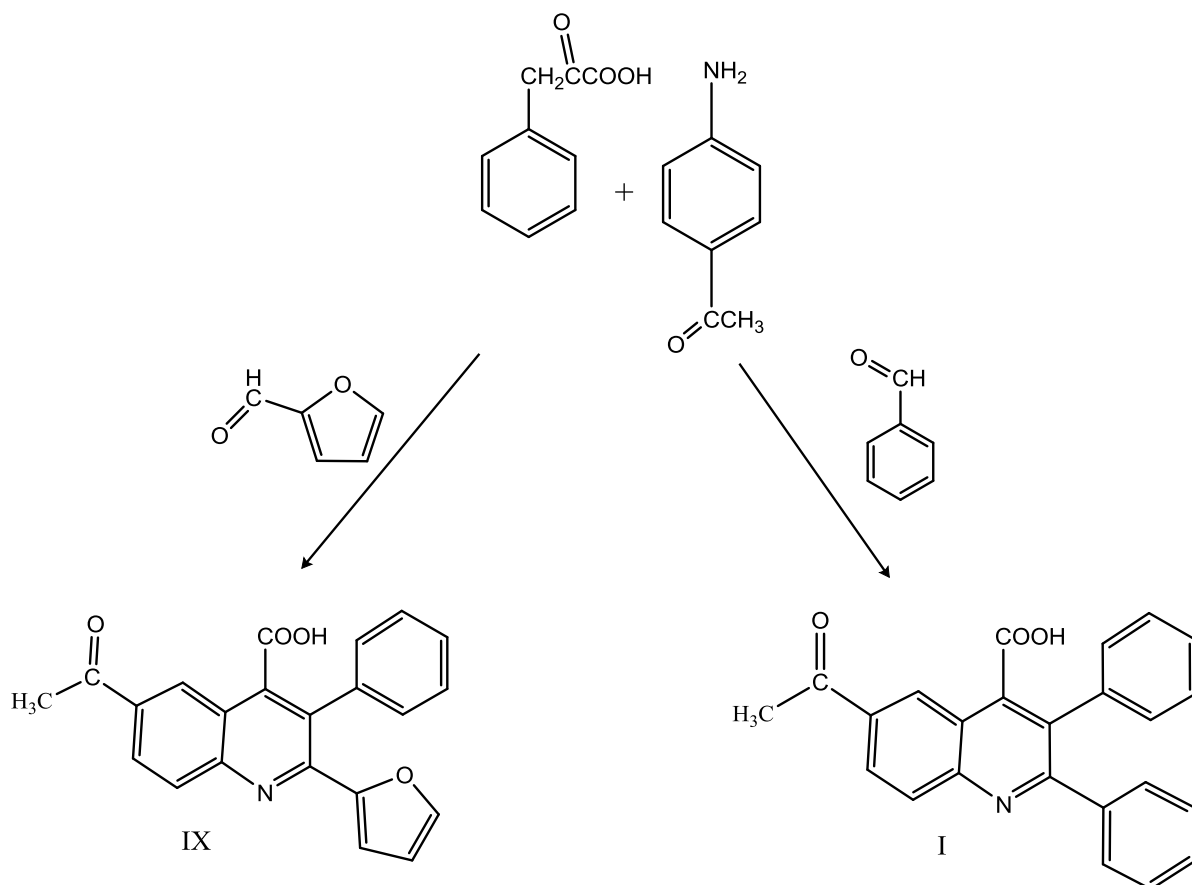
The crystal structure of the complex of human dihydroorotate dehydrogenase (DHODH) protein (PDB code: 1UUO) was retrieved from a protein data bank. The pdb file was imported to MOE suite where receptor preparation module was used to prepare the protein. All the bound water molecules were removed from the complex; 3D protonation and the active site identification were done.

2.2.4.3 Docking protocol

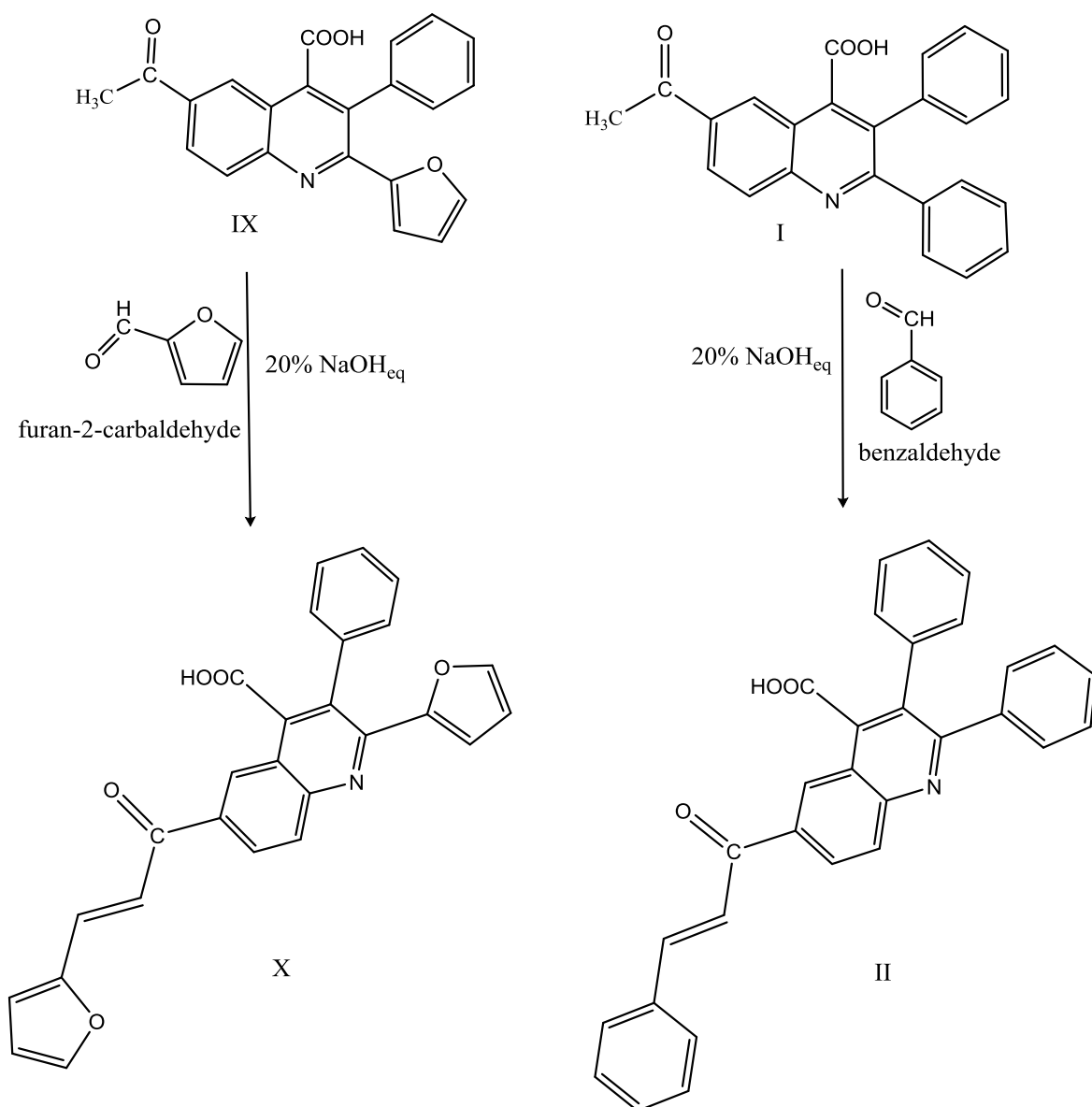
MOE docking simulation program was used to perform the total of 10 independent docking; docked poses were inspected, and the top scored pose for each compound was reserved for further studies of interaction evaluation (Arif, *et al.*, 2017).

2.2.4.4 Analysis of docking

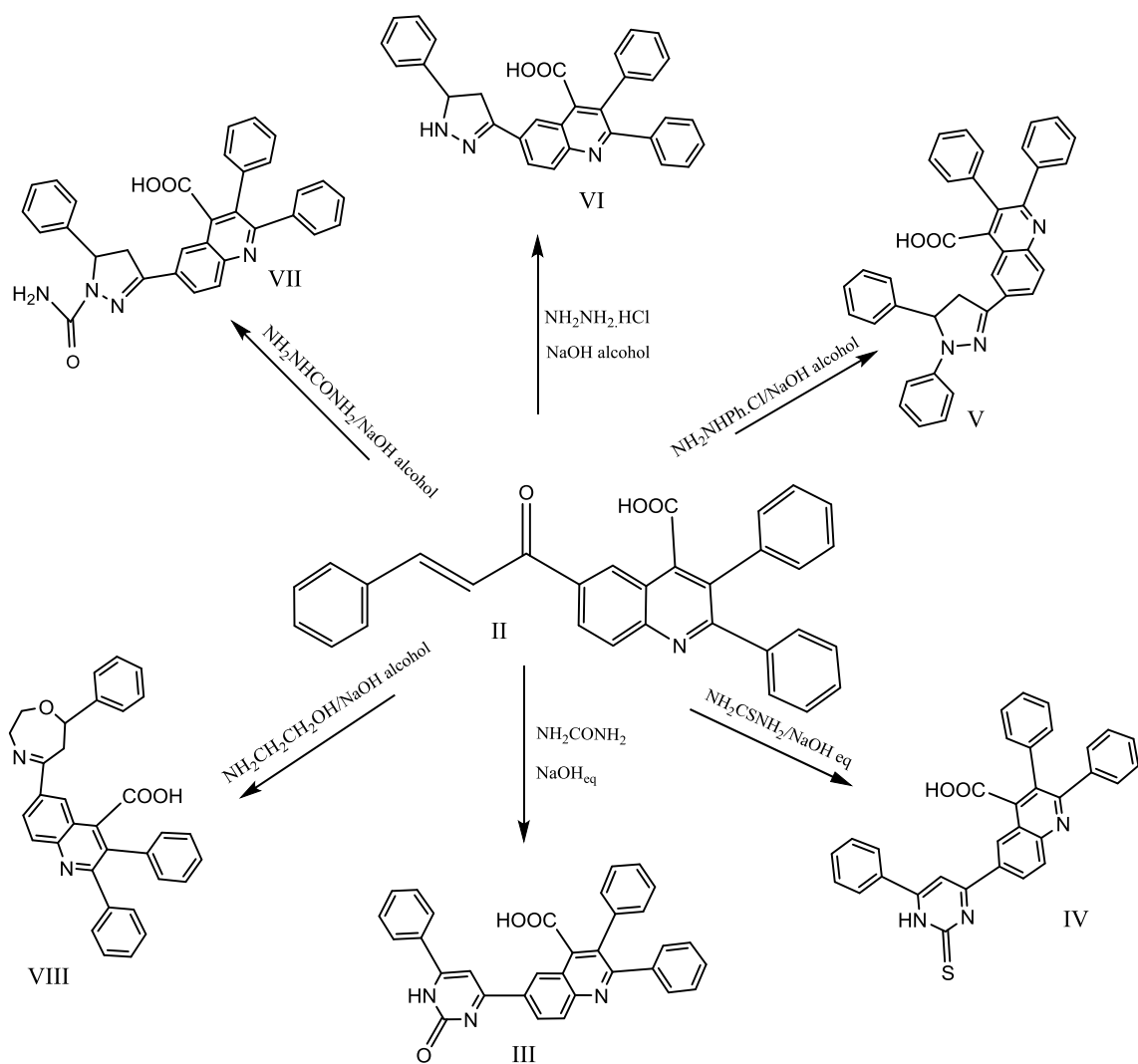
The ligand-protein interactions were visualized in 2-dimensional space by making use the MOE ligand interactions program. The Binding energy (S), length of the bonds between ligand and amino acids in receptor were calculated (Tables 2.14 and 2.15).



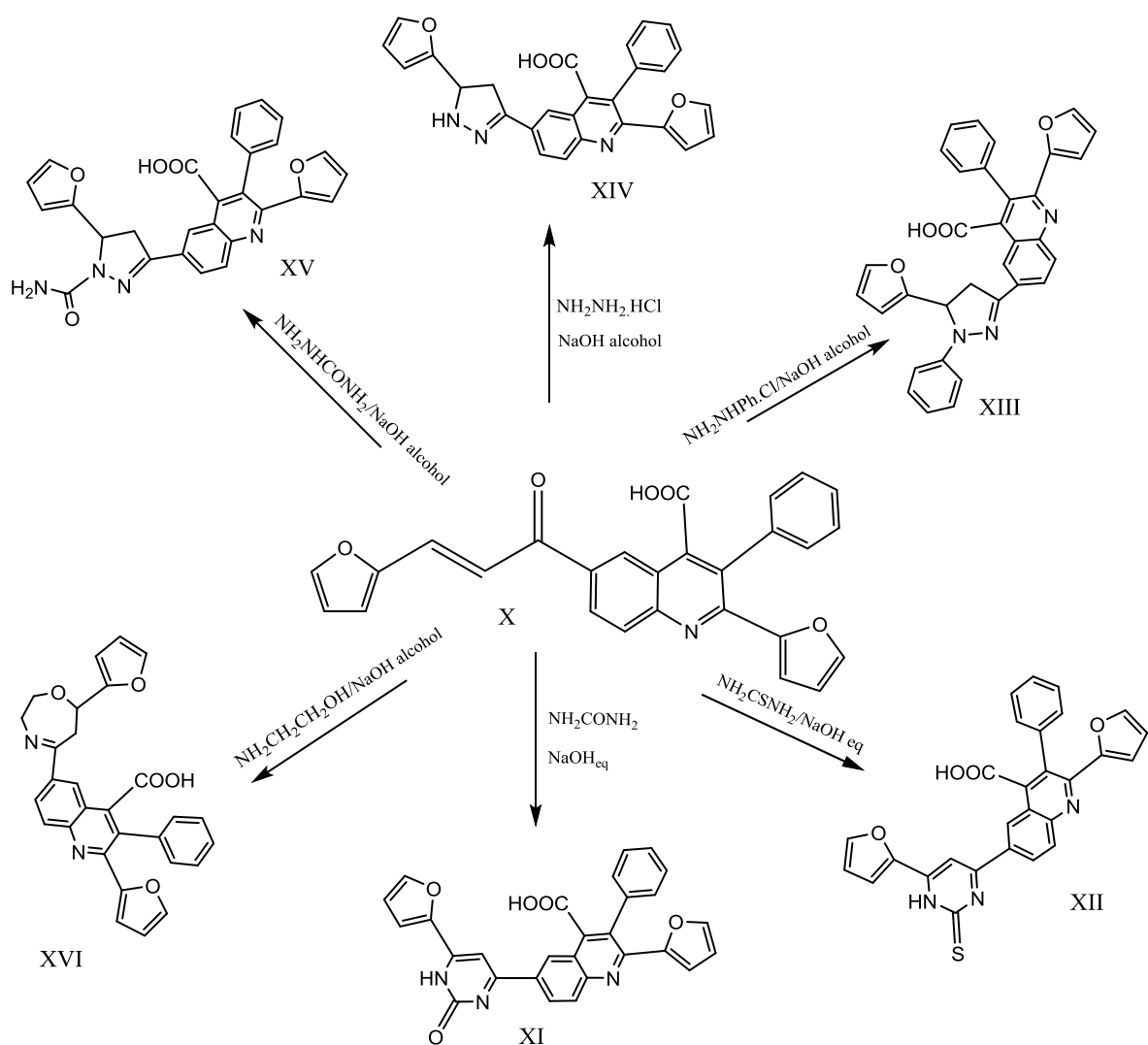
Scheme (2.1): Chemical structure of 2,3-diphenyl/2-(furan-2-yl)-3-phenyl-6-acetyl-quinoline-4-carboxylic acid derivatives.



Scheme (2.2): Chemical structure of 2,3-diphenyl/2-(furan-2-yl)-3-phenyl-6-(3-aryl-prop-2-enon-1-yl)-quinoline-4-carboxylic acid.

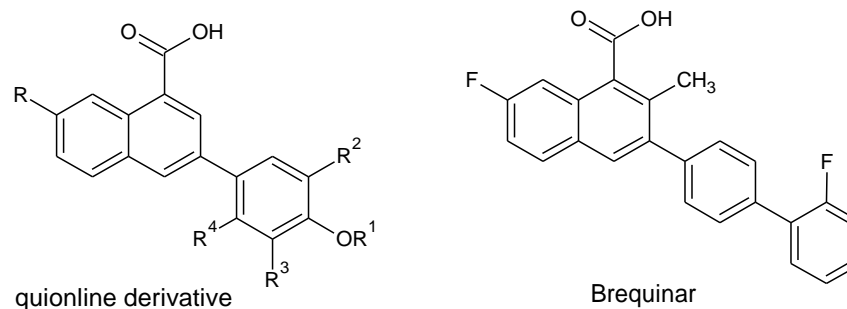


Scheme (2.3): Chemical structure of (III) to (VIII) synthesized from α,β -unsaturated carbonyl derivative (II)



Scheme (2.3): Chemical structure of (XI) to (XVI) synthesized from α,β -unsaturated carbonyl derivative (X)

Table 2.1: Experimental EC₅₀, experimental pEC₅₀, predicted pEC₅₀ and residual values of quinoline derivatives of 25 compounds used in training and test sets for inhibit in vitro VSV replication in MDCK epithelial cells (**Das et al., 2013**).



No.	compd	R	R ¹	R ²	R ³	R ⁴	EC ₅₀ (μM) exp	pEC ₅₀ exp	pEC ₅₀ pred.	Residual
1	brequinar	F	See figure 1				0.3	6.52	6.61	-0.09
2	L1	Cl	(CH ₂) ₂ CH ₃	H	H	H	4.7	5.33	5.52	-0.19
3	L2	Cl	CH ₃	H	H	H	7.1	5.15	4.99	0.16
4	L3	Cl	CH ₂ CH ₃	H	H	H	5.7	5.24	4.97	0.27
5	L4 ^T	Cl	(CH ₂) ₃ CH ₃	H	H	H	6.3	5.20	5.47	-0.26
6	L11 ^T	Cl	Ph	H	H	H	1.3	5.89	7.18	-1.29
7	L12	F	Ph	H	H	H	0.1	7.00	6.54	0.46

(continued)

8	L16	NO ₂	Ph	H	H	H	2.0	5.70	5.41	0.29
9	L18	H	Ph	H	H	H	1.0	6.00	6.50	-0.50
10	L22	F	CH ₃	H	H	H	6.4	5.19	5.05	0.14
11	L24	F	(CH ₂) ₂ CH ₃	H	H	H	19.0	4.72	5.25	-0.53
12	L26 ^T	F	CH ₂ (C ₂ H ₅)	H	H	H	6.8	5.16	5.17	0.01
13	L29	F	Ph-4-NO ₂	H	H	H	4.9	3.31	5.53	-0.22
14	L30	F	Ph-3,4-(OCH ₃ O)	H	H	H	0.9	6.04	6.23	0.19
15	L31	F	Ph-2-F	H	H	H	0.3	6.52	5.94	0.58
16	L32	F	Ph-3-F	H	H	H	0.1	7.00	7.04	-0.04
17	L33 ^T	F	Ph-4-F	H	H	H	1.0	6.00	6.80	-0.82
18	L34	F	Ph-2-pyridyl	H	H	H	22.9	4.64	4.639	0.001
19	L35	F	Ph-3-pyridyl	H	H	H	2.5	5.60	5.73	-0.13
20	L36	F	Ph-2-thiazolyl	H	H	H	14.6	4.84	4.91	-0.08
21	L39	F	CH ₂ -Ph	H	H	H	0.232	6.69	6.56	0.13
22	L40 ^T	F	3,5-dimethyl-phenyl	H	H	H	0.522	6.28	7.06	0.78
23	L42	F	Ph-3-C(CH ₃) ₃	H	H	H	0.062	7.18	7.66	-0.48
24	L43	F	Ph	CH ₃	CH ₃	H	0.023	7.63	7.73	-0.10
25	L44	F	Ph	CH(CH ₃) ₂	H	CH ₃	0.002	8.69	8.18	0.51

T= test set exp=experimental EC₅₀= value of Half maximal effective concentration

Table 2.2 value of chemical descriptors used in QSAR modeling of quinoline derivatives data set

No.	comp	AM1_Dipole	AM1_HF	AM1_IP	ASA_P	Chi ₀	mr	logP _(o/w)	Density
1	brequinar	4.82	-86.57	8.95	76.12	19.84	10.58	7.40	0.76
2	L1	3.39	-63.08	8.90	113.38	17.10	9.50	5.28	0.78
3	L2	2.96	-50.81	8.93	142.51	15.69	8.55	4.33	0.80
4	L3	3.25	-56.28	8.89	115.68	16.40	9.02	4.67	0.79
5	L4 ^T	2.30	-10.72	8.97	104.69	18.80	10.57	5.98	0.78
6	L11 ^T	2.18	-48.26	8.94	102.78	18.80	10.14	5.54	0.77
7	L12	5.37	1.97	9.26	187.70	20.38	10.59	5.32	0.79
8	L16	2.45	-3.20	8.93	104.83	17.93	10.07	5.35	0.73
9	L18	1.56	-88.06	8.93	142.71	15.69	8.12	3.89	0.78
10	L22	2.59	-99.27	8.85	113.75	17.10	9.07	4.84	0.76
11	L24	3.90	-72.52	8.89	159.81	17.97	9.45	5.01	0.76
12	L26 ^T	4.79	-43.76	9.35	188.86	21.25	10.66	5.48	0.82
13	L29	2.14	-103.4	8.90	156.98	20.66	10.72	5.25	0.80
14	L30	3.00	-91.77	9.03	104.41	19.67	10.18	5.69	0.80
15	L31	1.43	-93.74	9.08	102.43	19.67	10.17	5.73	0.80
16	L32	1.37	-90.91	9.02	104.58	19.67	10.17	5.69	0.80
17	L33 ^T	3.79	-26.18	9.20	125.27	18.80	9.98	4.71	0.78
18	L34	1.54	-38.35	9.10	123.41	18.80	9.98	4.31	0.78

(continued)

19	L35	2.80	21.34	9.17	135.70	18.10	9.84	4.52	0.83
20	L36	2.43	-59.56	8.87	117.75	19.51	10.62	5.68	0.76
21	L39	2.59	-63.06	8.93	102.59	20.54	11.04	6.25	0.75
22	L40 ^T	1.74	-28.34	8.74	104.74	21.37	11.75	6.76	0.76
23	L42	2.99	-67.37	8.88	106.26	22.17	11.94	7.04	0.73
24	L43	1.35	-60.40	9.11	104.60	20.54	11.05	6.21	0.75
25	L44	1.94	-70.03	8.92	101.77	22.12	11.97	7.05	0.73

T= test set

Table 2.3 Models with descriptors used to prediction biological activity of quinoline derivatives data set

no	eq	Residual descriptors	RMSE	R ²
1	$pEC_{50} = 0.111305 - 0.56687AM1.dipole + 1.12247logP + 0.00702AM1.HF + 0.00732ASA.P$	mr, Chi ₀ , density and AM1-IP	0.311	0.913
2	$pEC_{50} = 1.38478 - 0.49189AM1.dipole + 0.85383logP + 0.00642AM1.HF + 0.09659Chi_0$	mr, ASA.P, density and AM1-IP	0.328	0.904
3	$pEC_{50} = -4.38843 - 0.51373AM1.dipole + 1.010011logP + 0.00616AM1.HF + 0.09659 AM1-IP$	mr, ASA.P, density and Chi ₀	0.335	0.899
4	$pEC_{50} = 1.40898 - 0.47655AM1.dipole + 0.8546logP + 0.00565AM1.HF + 0.170832mr$	Chi ₀ , ASA.P, density and AM1-P	0.338	0.897
5	$pEC_{50} = 2.45482 - 0.49542AM1.dipole + 1.00982logP + 0.0073AM1.HF + 0.02096 density$	Chi ₀ , density, mr and AM1-P	0.349	0.891
6	$pEC_{50} = 0.2058 - 0.47060AM1.dipole + 0.87696logP + 0.2847 mr + 0.00504 ASA.P$	Chi ₀ , ASA.P, density and AM1-IP	0.351	0.889
7	$pEC_{50} = -5.43939 - 0.44733AM1.dipole + 0.77979logP + 0.71086 AM1-IP + 0.21288mr$	Chi ₀ , ASA.P, density and AM1-IP	0.353	0.888
8	$pEC_{50} = -4.33632 - 0.50252AM1.dipole + 1.04519logP + 0.60981 AM1-IP + 0.00553 ASA.P$	mr, Chi ₀ , density and AM1.HF	0.355	0.887
9	$pEC_{50} = -0.81665 - 0.43022AM1.dipole + 0.73885logP + 0.2847 mr + 1.5688 density$	Chi ₀ , ASA.P, AM1.HF and AM1-IP	0.351	0.889
10	$pEC_{50} = -4.65126 - 0.45280AM1.dipole + 0.83979logP + 0.66525AM1-IP + 0.007731 Chi_0$	density, ASA.P,E, mr and AM1-IP	0.360	0.883
11	$pEC_{50} = 0.49761 - 0.41982AM1.dipole + 0.70671logP + 0.24876 mr + 0.02169 Chi_0$	density, ASA.P, AM1.HF and AM1-IP	0.362	0.882
12	$pEC_{50} = -7.94416 - 0.46574AM1.dipole + 0.96013logP + 1.15033AM1-IP + 0.28017 density$	Chi ₀ , ASA.P, mr and AM1-HF	0.367	0.879
13	$pEC_{50} = 0.111305 - 0.56687AM1.dipole + 1.12247logP + 0.00702AM1.HF$	mr, Chi ₀ , density, ASA.P and AM1-IP	0.348	0.891
14	$pEC_{50} = 0.73271 - 0.50048AM1.dipole + 1.07175logP + 0.00773 ASA.P$	mr, Chi ₀ , density, AM1.HF and AM1-IP	0.360	0.883

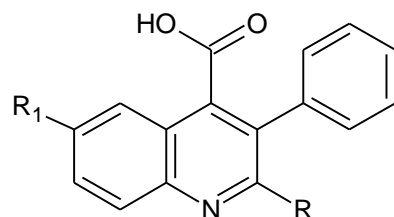
(continued)

15	$pEC_{50} = 0.47579 - 0.41800AM1.dipole + 0.70246logP + 0.29335mr$	ASA.P, Chi ₀ , density, AM1.HF and AM1-IP	0.362	0.882
16	$pEC_{50} = 0.829834 - 0.42887AM1.dipole + 0.76135logP + 0.12271 Chi_0$	ASA.P, mr, density, AM1.HF and AM1-IP	0.366	0.879
17	$pEC_{50} = -8.02239 - 0.46719AM1.dipole + 0.96509logP + 1.13233 AM1-IP$	ASA.P, mr, density, AM1.HF and Chi ₀	0.367	0.878
18	$pEC_{50} = -0.15648 - 0.44288AM1.dipole + 1.00027logP + 2.66002 density$	ASA.P, mr, AM1-IP, AM1.HF and Chi ₀	0.392	0.861
19	$pEC_{50} = 2.11692 - 0.42239AM1.dipole + 0.95099logP$	ASA.P, mr, AM1-IP, density, AM1.HF and Chi ₀	0.396	0.859

Table 2.4 The Statistical parameter for fives models have greater r^2

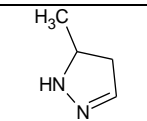
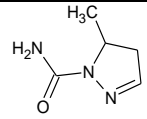
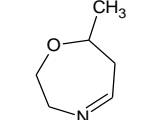
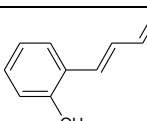
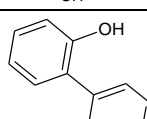
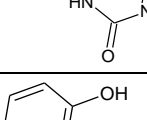
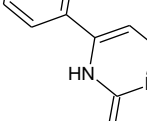
	n _{training}	n _{test set}	r^2	q^2	r^2_{pred}	RMSA	F- value	p- value	SEE
Equation (1)	20	5	0.913	0.842	0.873	0.311	39.283	<0.0001	0.359
Equation (2)	20	5	0.904	0.821	0.902	0.328	35.064	<0.0001	0.379
Equation (3)	20	5	0.899	0.805	0.885	0.337	32.776	<0.0001	0.390
Equation (13)	20	5	0.891	0.804	0.855	0.348	43.641	<0.0001	0.389
Equation (19)	20	5	0.859	0.782	0.894	0.397	51.702	<0.0001	0.429

Table 2.5: The values of chemical descriptors and predicted pEC₅₀ values of new quinoline derivatives designed

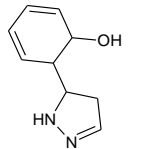
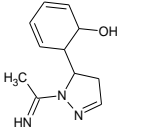
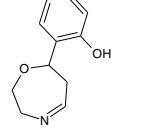
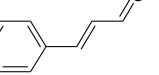
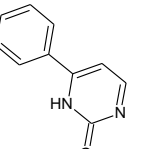
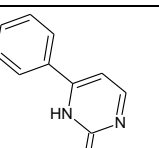
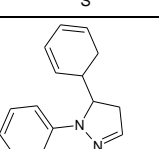


No	R	R1	AM1_ dipole	AM1_ HF	AM1_ IP	ASA_P	chi0	MR	logP(o/w)	Density	predicted pEC ₅₀
brequinar			4.82	-86.52	8.96	76.91	19.84	10.58	7.40	0.76	6.64
1	A	CH ₃ 	2.77	-45.64	9.53	16.56	129.18	8.88	3.89	0.74	4.53
2	A1	CH ₃ 	2.85	-30.18	9.45	17.97	140.52	9.78	4.53	0.72	5.4
3	A2	CH ₃ 	7.02	-6.04	9.44	19.84	185.28	10.57	4.22	0.75	3.19
4	A3	CH ₃ 	7.99	47.04	8.6	19.84	205.3	11.16	4.24	0.76	3.18
5	A4	CH ₃ 	3.15	71.00	8.29	22.24	98.65	12.55	6.58	0.71	7.93

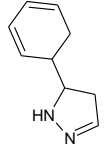
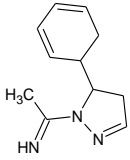
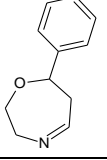
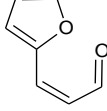
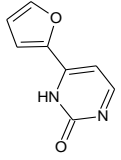
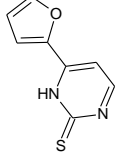
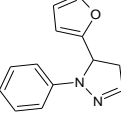
(continued)

6	A5	CH ₃		2.64	31.6	8.73	18.26	144.6	10.06	4.4	0.73	5.84
7	A6	CH ₃		3.72	2.78	8.88	20.71	205.35	10.9	3.64	0.75	4.62
8	A7	CH ₃		2.34	-40.07	9.28	19.67	127.16	10.89	3.93	0.72	4.85
9	A8	CH ₃		4.28	-13.92	9.01	21.96	125.21	11.93	5.88	0.73	6.11
10	A9	CH ₃		8.72	-14.46	9.14	23.82	210.69	12.75	5.57	0.76	3.87
11	A10	CH ₃		8.52	38.14	8.64	23.82	234.34	13.35	5.59	0.77	4.54
12	A11	CH ₃		1.85	102.31	8.41	26.23	128.34	14.74	6.55	0.72	9.08

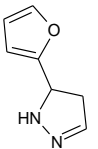
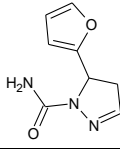
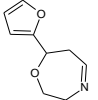
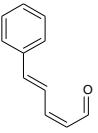
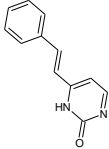
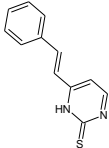
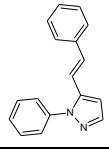
(continued)

13	A12	CH ₃		2.18	21.69	8.78	22.24	191.31	12.25	4.37	0.73	6.34
14	A13	CH ₃		3.81	-7.03	8.93	24.69	249.46	13.08	3.61	0.75	4.78
15	A14	CH ₃		2.6	-51.55	9.04	23.66	115.59	13.07	5.07	0.73	5.81
16	A15	CH ₃		4.9	3.87	9.43	21.09	126.19	11.8	6.19	0.72	6.24
17	A16	CH ₃		7.5	28.33	9.3	22.95	177.09	12.61	5.89	0.74	4.96
18	A17	CH ₃		8.58	80.83	8.56	22.95	202.69	13.2	5.9	0.75	4.93
19	A18	CH ₃		0	-	-	25.35	94.25	14.59	8.03	0.71	-

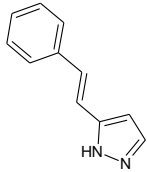
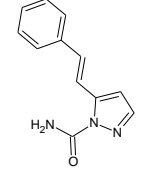
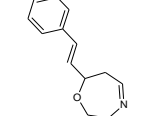
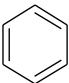
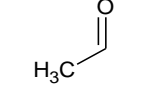
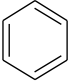
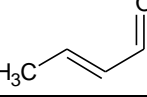
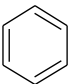
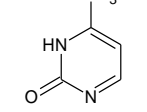
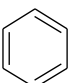
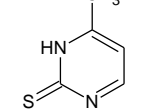
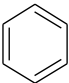
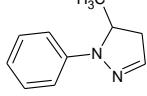
(continued)

20	A19	CH ₃		3.25	66.58	8.75	21.37	138.49	12.1	5.85	0.72	7.32
21	A20	CH ₃		5.45	55.8	8.84	23.82	198.41	12.94	5.09	0.74	5.58
22	A21	CH ₃		2.37	-3.1	9.27	22.79	110.1	12.93	5.38	0.72	6.59
23	A22	CH ₃		2.06	-11.38	8.9	20.38	120.93	11.1	4.91	0.74	6.26
24	A23	CH ₃		7.44	11.64	9.2	22.24	182.5	11.91	4.6	0.77	3.48
25	A24	CH ₃		7.62	64.37	8.62	22.24	206.02	12.51	4.62	0.78	3.94
26	A25	CH ₃		3.35	114.61	8.36	24.65	105.95	13.9	6.74	0.73	8.37

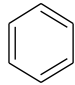
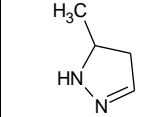
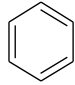
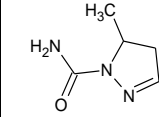
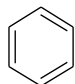
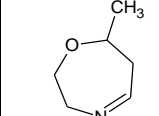
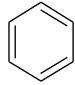
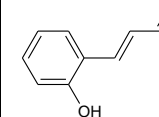
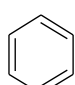
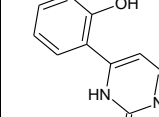
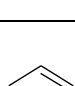
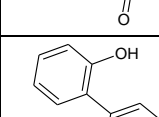
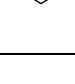
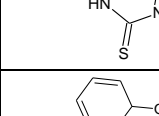
(continued)

27	A26	CH ₃		2.68	46.69	8.88	20.66	149.44	11.41	4.57	0.75	6.14
28	A27	CH ₃		5.61	23.66	8.87	23.11	207.91	12.24	3.81	0.77	3.89
29	A28	CH ₃		2.00	-21.61	9.25	22.08	113.23	12.23	4.09	0.74	5.25
30	A29	CH ₃		1.53	16.55	8.85	22.5	116.37	12.69	6.84	0.71	8.89
31	A30	CH ₃		7.82	63.7	9.26	24.36	185.34	13.5	6.53	0.73	5.81
32	A31	CH ₃		9.1	94.86	8.54	24.36	209.42	14.09	6.55	0.74	5.5
33	A32	CH ₃		2.62	138.75	8.59	26.77	102.34	15.48	8.19	0.71	10.55

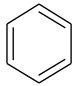
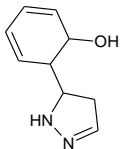
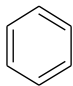
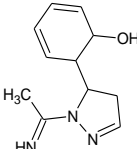
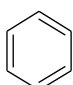
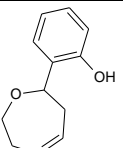
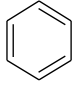
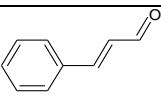
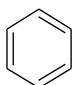
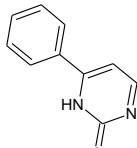
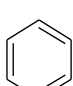
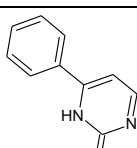
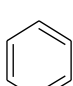
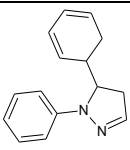
(continued)

34	A33	CH ₃		2.75	98.96	8.64	22.79	146.07	13	7.15	0.72	9.35
35	A34	CH ₃		5.96	77.77	8.89	25.23	204.31	13.84	6.11	0.74	6.63
36	A35	CH ₃		2.05	10.61	9.07	24.2	122.25	13.81	6.02	0.71	7.68
37	B(I)			2.9	-9.18	9.43	19.67	130.21	10.91	5.55	0.73	6.59
38	B1			1.92	6.08	9.34	21.09	136.46	11.81	6.19	0.72	8.02
39	B2			6.81	30.53	9.44	22.95	181.38	12.61	5.89	0.74	5.4
40	B3			7.9	83.29	8.6	22.95	207.2	13.2	5.9	0.75	5.36
41	B4			2.63	108.16	8.31	25.35	99.2	14.59	8.24	0.71	10.36

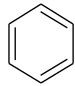
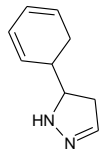
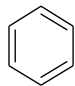
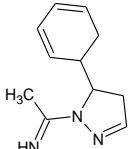
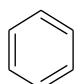
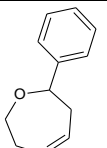
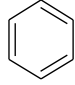
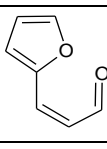
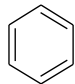
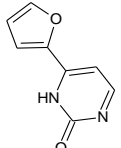
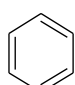
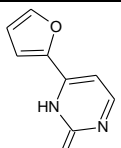
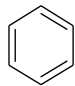
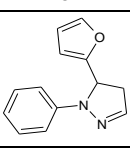
(continued)

42	B5			3.36	32.23	8.73	18.26	147.01	10.06	4.4	0.73	5.46
43	B6			3.72	2.77	8.89	20.71	205.54	10.9	3.64	0.75	4.62
44	B7			3.68	-0.34	9.28	22.79	123.45	12.93	5.59	0.72	6.2
45	B8			4.24	10.34	9.02	25.07	121.76	13.97	7.55	0.73	8.15
46	B9			7.23	26.58	9.47	26.93	214.22	14.78	7.24	0.75	6.89
47	B10			7.33	75.82	8.66	26.93	232.58	15.38	7.25	0.76	7.33
48	B11			3.3	106.23	8.56	29.34	130.64	16.77	8.21	0.72	10.16

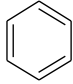
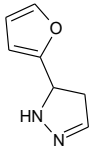
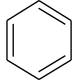
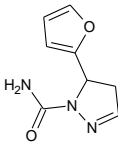
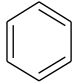
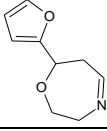
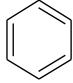
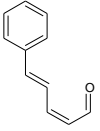
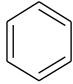
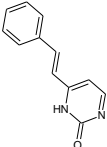
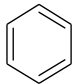
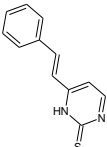
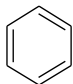
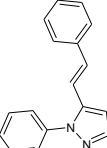
(continued)

49	B12			2.08	57.98	8.78	25.35	192.91	14.29	6.03	0.73	8.53
50	B13			5.72	38.78	8.91	27.8	249.31	15.12	5.27	0.75	5.89
51	B14			3.1	-10.22	8.96	26.77	111.49	15.11	6.73	0.73	7.65
52	B15(II)			3.93	39.67	9.34	24.2	114.35	13.82	7.86	0.71	8.82
53	B16(III)			7.37	79.86	9.34	26.06	179.09	14.64	7.55	0.73	9.28
54	B17(IV)			8.46	117.29	8.57	26.06	200.37	15.23	7.56	0.74	8.1
55	B18(V)			2.93	156.25	8.33	28.47	116.52	16.62	8.87	0.70	11.36

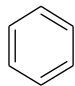
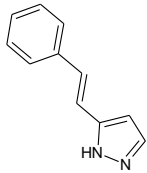
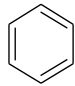
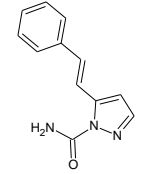
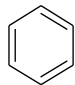
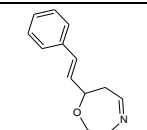
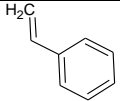
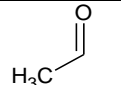
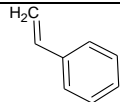
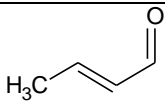
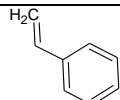
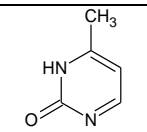
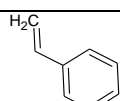
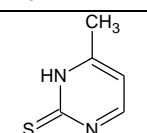
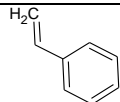
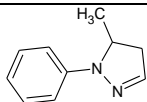
(continued)

56	B19(VI)			3.17	101.01	8.72	24.48	162.68	14.14	6.69	0.71	8.73
57	B20(VII)			3.79	108.74	8.88	26.93	213.39	14.98	5.93	0.73	7.95
58	B21(VIII)			3.68	34.89	9.34	25.9	112.09	14.96	7.04	0.71	7.99
59	B22			3.52	23.94	8.98	23.49	131.72	13.13	6.57	0.73	7.63
60	B23			7.18	80.62	9.21	25.35	184.81	13.94	6.26	0.75	5.99
61	B24			8.23	101.17	8.64	25.35	208.89	14.54	6.28	0.76	5.73
62	B25			2.83	168.77	8.73	27.76	107.69	15.94	7.92	0.73	10.38

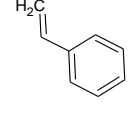
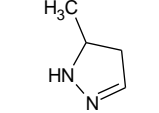
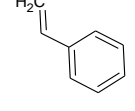
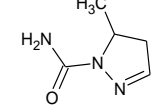
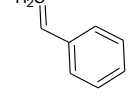
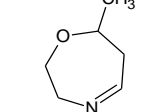
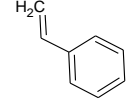
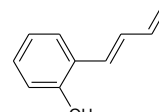
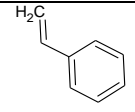
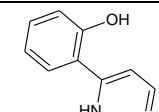
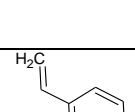
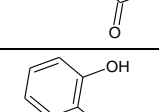
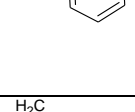
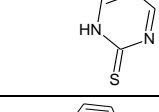
(continued)

63	B26			2.48	104.79	8.74	23.78	148.07	13.45	6.89	0.74	6.26
64	B27			4.65	93.36	8.93	26.23	210.36	14.29	5.84	0.76	7.23
65	B28			2.26	34.81	9.24	25.19	136.18	14.27	5.75	0.73	7.53
66	B29			1.57	57.01	8.95	25.61	109.5	14.71	8.5	0.71	10.97
67	B30			7.66	78.67	9.25	27.48	185.39	15.53	8.19	0.73	7.88
68	B31			9.02	95.01	8.54	24.36	204.37	14.09	6.55	0.74	5.51
69	B32			2.68	174.58	8.61	29.88	100.71	17.51	9.85	0.70	12.62

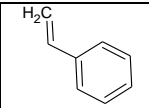
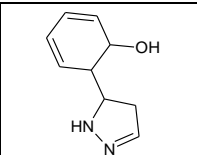
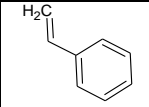
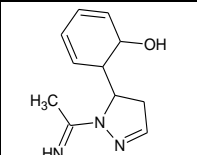
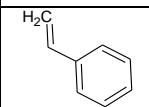
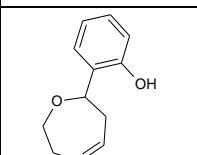
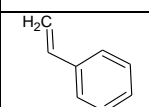
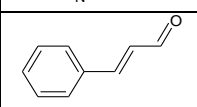
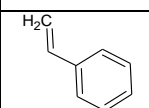
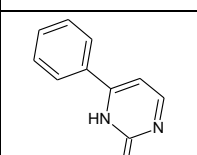
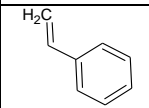
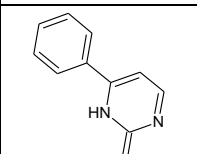
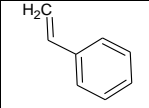
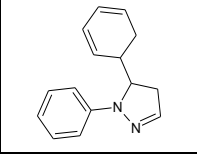
(continued)

70	B33			2.61	133.7	8.65	25.9	142.15	15.03	8.82	0.71	11.51
71	B34			5.86	113.95	8.87	28.35	204.05	15.87	7.77	0.73	8.8
72	B35			2.24	45.24	9.08	27.31	115.2	15.85	7.68	0.71	9.63
73	C			3.51	1.48	8.9	21.09	133.23	11.8	6.19	0.72	7.06
74	C1			0	-	-	22.5	132.64	12.69	6.84	0.71	-
75	C2			6.65	40.91	8.85	24.36	187.64	13.5	6.53	0.73	6.34
76	C3			7.71	94.01	8.58	24.36	206.53	14.09	6.55	0.74	6.26
77	C4			2.44	118.47	8.3	26.77	102.62	15.47	8.89	0.70	11.29

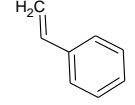
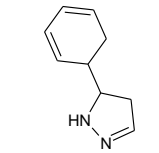
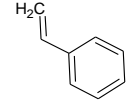
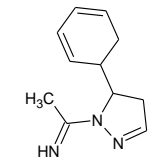
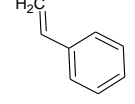
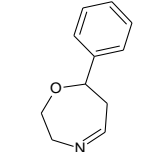
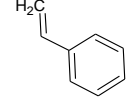
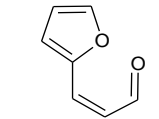
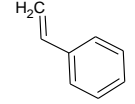
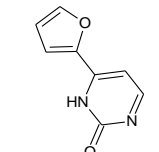
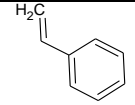
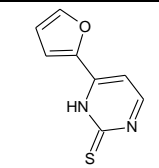
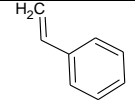
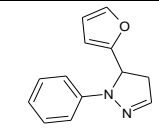
(continued)

78	C5			3.06	79.16	8.53	22.79	147.95	12.99	6.71	0.71	8.55
79	C6			5.13	89.47	8.59	25.23	210.36	13.83	5.95	0.73	7.05
80	C7			2.36	17.41	8.76	24.2	134.7	13.81	6.24	0.71	7.88
81	C8			0	-	-	26.48	134.44	14.85	8.19	0.72	-
82	C9			4.98	49.16	9.06	28.35	220.15	15.67	7.88	0.74	9.09
83	C10			0	-	-	28.35	190.44	16.27	7.9	0.75	-
84	C11			1.61	158.4	8.51	30.75	138.41	17.67	9.54	0.72	13.03

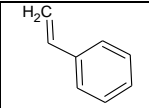
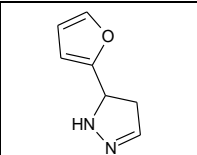
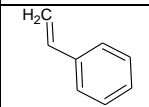
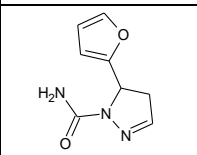
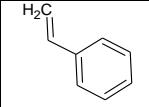
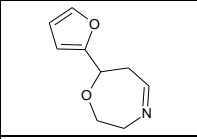
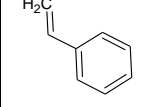
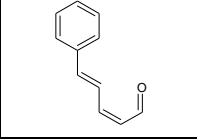
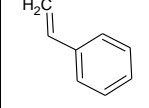
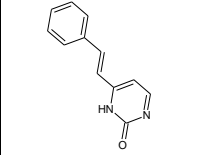
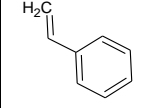
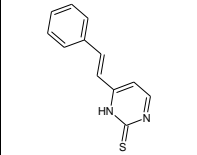
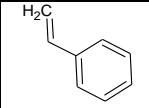
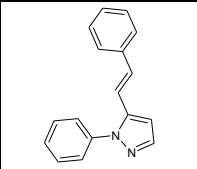
(continued)

85	C12			3.97	86.46	8.45	26.77	179.97	15.18	8.51	0.73	10.34
86	C13			3.33	69.55	8.81	29.22	235.32	16.02	7.46	0.74	9.81
87	C14			4.61	1.20	8.78	28.18	163.94	15.99	7.37	0.72	6.99
88	C15			2.51	56.86	9.05	25.61	116.91	14.71	8.5	0.71	10.49
89	C16			6.44	77.99	9.03	27.48	183.72	15.53	8.19	0.73	5.55
90	C17			6.18	130.52	8.57	27.48	212.06	16.12	8.21	0.73	9.29
91	C18			1.65	171.64	8.33	29.88	98.85	17.5	10.34	0.70	13.71

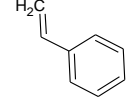
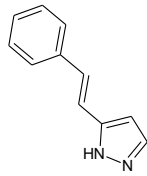
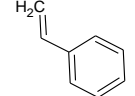
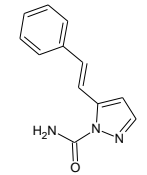
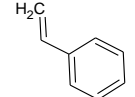
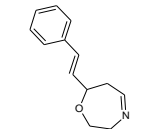
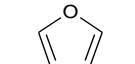
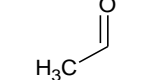
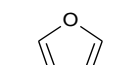
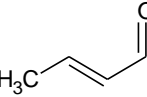
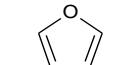
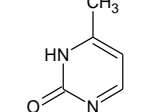
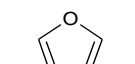
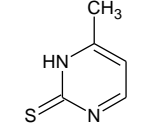
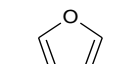
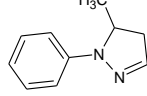
(continued)

92	C19			1.18	119.12	8.76	25.9	146.53	15.02	8.16	0.71	11.51
93	C20			0	.	.	28.35	181.38	15.87	7.4	0.73	-
94	C21			3.71	46.03	8.82	27.31	130.5	15.85	7.68	0.71	8.91
95	C22			2.91	38.48	8.93	24.91	122.21	14.02	7.22	0.73	8.73
96	C23			6.27	61.82	9.04	26.77	191.13	14.84	6.91	0.75	7.14
97	C24			6.24	113.63	8.62	26.77	211.03	15.44	6.92	0.75	7.69
98	C25			2.06	141.87	8.29	29.17	107.84	16.82	9.05	0.72	11.89

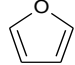
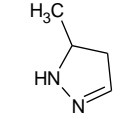
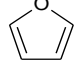
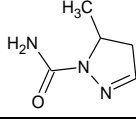
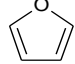
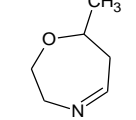
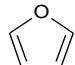
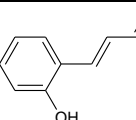
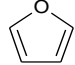
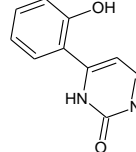
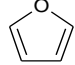
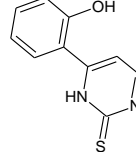
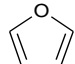
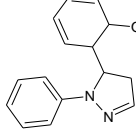
(continued)

99	C26			2.65	95.51	8.61	25.19	154.18	14.34	6.87	0.73	9.13
100	C27			3.15	67.59	8.7	27.64	202.5	15.17	6.11	0.75	8.15
101	C28			2.14	26.49	8.77	26.61	141.99	15.16	6.40	0.72	8.31
102	C29			2.53	69.79	8.88	27.03	103.81	15.6	9.14	0.70	11.19
103	C30			6.09	92.14	9.02	28.89	180.6	16.42	8.84	0.72	9.55
104	C31			7.11	145.39	8.52	28.89	200.81	17.01	8.85	0.73	9.51
105	C32			1.98	169.8	8.32	31.3	94.7	18.39	10.98	0.70	14.2

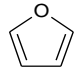
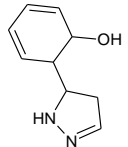
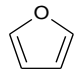
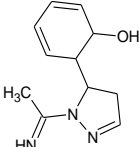
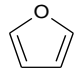
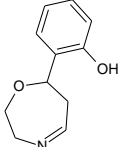
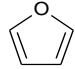
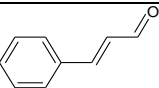
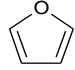
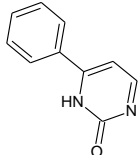
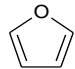
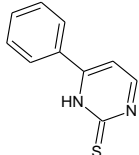
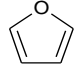
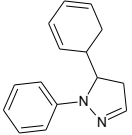
(continued)

106	C33			3.46	133.24	8.71	27.31	146.89	15.91	8.8	0.70	11.04
107	C34			3.16	102.08	8.77	29.76	197.13	16.76	8.04	0.72	10.51
108	C35			1.71	60.33	8.95	28.73	135.14	16.73	8.33	0.70	10.91
109	D(IX)			2.94	-24.53	9.21	18.97	132.02	10.21	4.26	0.75	8.03
110	D1			2.3	1.84	9.1	20.38	140.05	11.11	4.91	0.74	6.36
111	D2			5.74	14.11	9.08	22.24	199.02	11.91	4.6	0.77	4.58
112	D3			6.94	68.87	8.61	22.24	212.91	12.51	4.62	0.78	4.4
113	D4			4.02	96.25	8.37	24.65	102.92	13.9	6.96	0.73	8.07

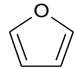
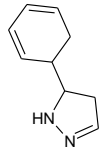
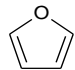
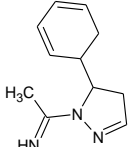
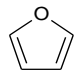
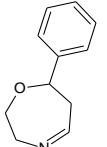
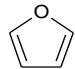
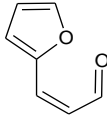
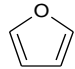
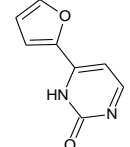
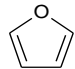
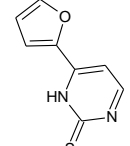
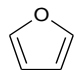
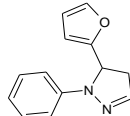
(continued)

114	D5			2.47	52.82	8.78	20.66	149.07	11.41	4.78	0.75	6.54
115	D6			2.97	24.7	8.78	23.11	203.12	12.24	4.02	0.77	5.6
116	D7			0.92	9.65	9.1	22.08	135.71	12.23	4.31	0.74	6.49
117	D8			3.76	-20.19	9.02	24.36	118.77	13.26	6.26	0.75	6.74
118	D9			5.21	6.44	9.16	26.23	214.85	14.08	5.95	0.77	6.46
119	D10			6.13	59.55	8.68	26.23	239.28	14.69	5.97	0.78	6.51
120	D11			2.62	85.04	8.1	28.63	128.11	16.08	8.1	0.74	10.25

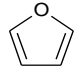
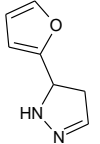

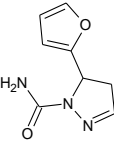
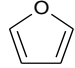
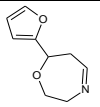
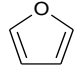
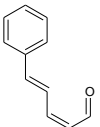
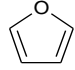
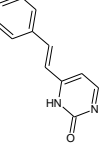
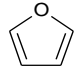
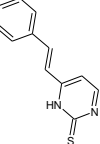
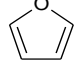
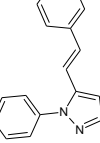
(continued)

121	D12			4.02	44.03	8.89	24.65	166.45	13.59	5.92	0.75	7
122	D13			6.06	32.89	8.77	27.1	240.5	14.42	5.16	0.77	5.46
123	D14			1.43	-28.28	9	26.06	164.11	14.41	5.44	0.75	7.42
124	D15(X)			3.56	31.13	9.22	23.49	120.03	13.13	6.57	0.73	7.57
125	D16			5.2	48.49	9.14	25.35	180.33	13.94	6.26	0.75	6.86
126	D17			7.49	102.32	8.57	25.35	207.11	14.54	6.28	0.76	7.10
127	D18			1.61	126.8	8.29	27.76	97.29	15.94	8.41	0.72	11.24


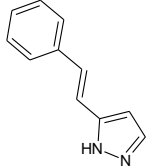
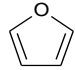
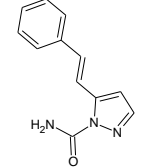
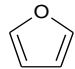
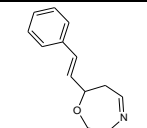
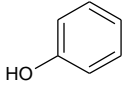
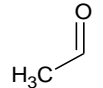
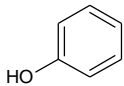
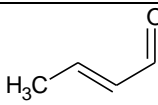
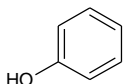
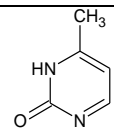
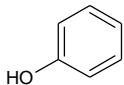
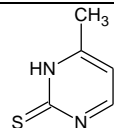
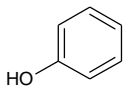
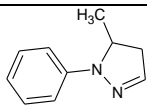
(continued)

128	D19			3.43	94.59	8.77	23.78	145.11	13.45	6.23	0.74	7.89
129	D20			2.98	84.55	8.75	26.23	201.15	14.28	5.47	0.76	7.63
130	D21			1.25	16.66	9.07	25.19	130.19	14.27	5.75	0.73	7.93
131	D22(XI)			2.22	24.73	8.93	23.49	118.44	13.13	6.57	0.73	8.27
132	D23(XII)			5.39	46.67	9.21	25.35	185.21	13.94	6.26	0.75	8.77
133	D24(XIII)			6.39	99.63	8.58	25.35	209.6	14.54	6.28	0.76	9.74
134	D25 (XIV)			1.85	125.96	8.22	27.76	98.58	15.94	8.41	0.72	11.11

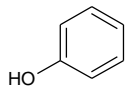
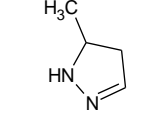
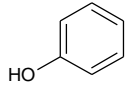
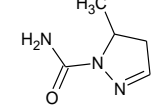
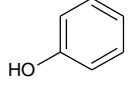
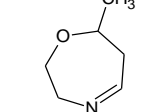
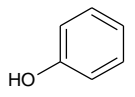
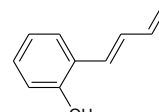
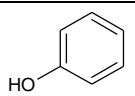
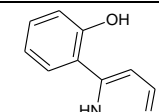
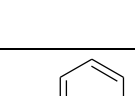
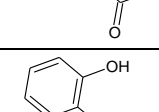
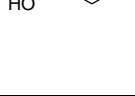
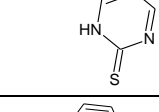
(continued)

135	D26(XV)			2.59	85.35	8.83	23.78	151.06	13.45	6.23	0.74	8.34
136	D27(XVI)			3.06	57.96	8.87	26.23	198.24	14.28	5.47	0.76	8.54
137	D28			0.76	53.74	9.18	25.19	132.59	14.27	5.75	0.73	8.49
138	D29			1.87	41.24	8.82	24.91	122.07	14.02	7.22	0.73	9.34
139	D30			7.01	62.52	9.11	26.77	197.01	14.84	6.91	0.75	6.77
140	D31			9.06	115.64	8.56	26.77	224.3	15.44	6.92	0.75	6.2
141	D32			2.66	140.39	8.06	29.17	115.59	16.82	9.05	0.72	11.6

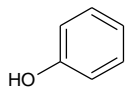
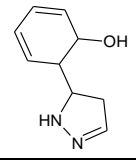
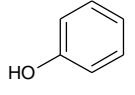
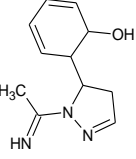
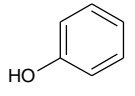
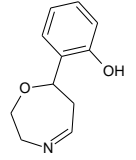
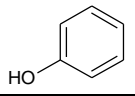
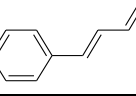
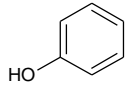
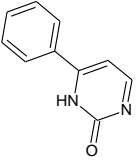
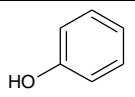
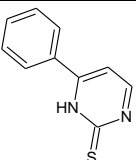
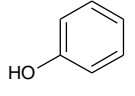
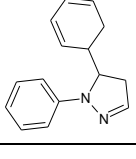
(continued)

142	D33			3.44	103.21	8.69	25.19	166.89	14.34	6.87	0.73	8.83
143	D34			6.24	98.72	8.75	27.64	219.09	15.17	6.11	0.75	6.73
144	D35			0	-	-	26.61	134.16	15.16	6.4	0.72	-
145	E			1.62	-52.75	9.18	20.54	156.39	11.05	5.24	0.75	6.85
146	E1			1.98	-37.87	9.2	21.96	164.4	11.95	5.88	0.73	7.53
147	E2			4.73	-13.57	9.11	23.82	208.67	12.75	5.57	0.76	6.12
148	E3			4.63	59.57	8.64	23.82	230.6	13.35	5.59	0.77	6.87
149	E4			2.23	83.84	8.16	26.23	120.93	14.74	7.93	0.72	10.23

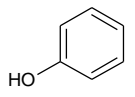
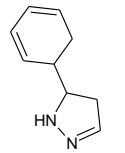
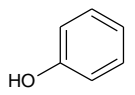
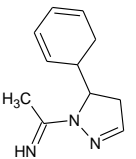
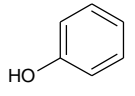
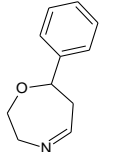
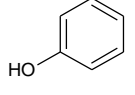
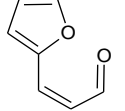
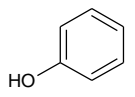
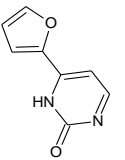
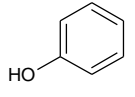
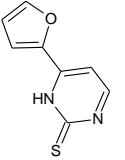
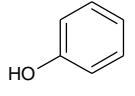
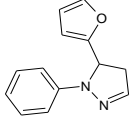
(continued)

150	E5			4.1	49.82	8.84	22.24	170.27	12.25	5.76	0.74	6.85
151	E6			2.72	-4.34	8.99	24.69	229.46	13.08	4.99	0.76	6.83
152	E7			2.14	-41.31	9.12	23.66	157.54	13.07	5.28	0.73	6.69
153	E8			5.21	-45.8	9.13	25.94	142.94	14.1	7.24	0.74	7.01
154	E9			8.46	-23.49	9.16	27.8	229.51	14.92	6.93	0.76	5.61
155	E10			4.92	31.02	8.69	27.8	263.47	15.53	6.94	0.77	8.26
156	E11			3.54	56.02	8.29	30.21	156.28	16.92	9.07	0.73	10.83

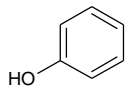
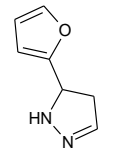
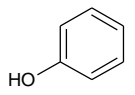
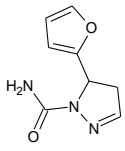
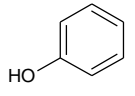
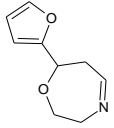
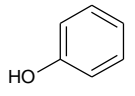
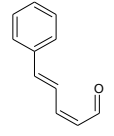
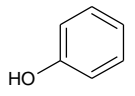
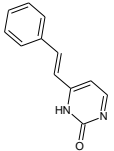
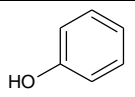
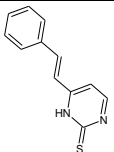
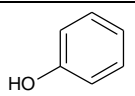
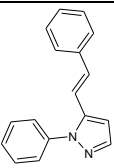
(continued)

157	E12			2.82	15.08	9.01	26.23	185.14	14.43	6.89	0.75	8.71
158	E13			1.64	-12.38	8.94	28.67	257.78	15.26	6.13	0.76	8.87
159	E14			2.69	-54	9.12	27.64	174.45	15.24	6.42	0.74	7.69
160	E15			4.44	-2.89	9.15	25.07	146.7	13.97	7.55	0.73	8.12
161	E16			5.89	20.26	9.19	26.93	203.8	14.78	7.24	0.75	7.53
162	E17			5.58	73.13	8.61	26.93	231.67	15.38	7.25	0.76	8.3
163	E18			2.5	121.95	8.23	29.34	119.64	16.77	9.38	0.72	11.96

(continued)

164	E19			1.72	59.82	8.77	25.35	164.74	14.29	7.2	0.73	9.85
165	E20			2.98	30.62	9.03	27.8	221.02	15.12	6.44	0.75	8.49
166	E21			2.37	-11.65	9.16	26.77	151.44	15.11	6.73	0.73	8.35
167	E22			3.67	-22.46	9.08	24.36	154.05	13.26	6.26	0.75	7.03
168	E23			6.23	47.85	9.21	25.35	179.43	13.94	6.26	0.75	6.26
169	E24			6.71	104.09	8.61	25.35	204	14.54	6.28	0.76	6.58
170	E25			4.16	86.61	8.34	28.63	124.34	16.08	8.1	0.74	9.36

(continued)

171	E26			2.96	46.29	8.99	24.65	176.79	13.59	5.92	0.75	7.70
172	E27			3.87	50.84	9.03	27.1	225.54	14.42	5.16	0.77	6.72
173	E28			2.05	-24.68	9.19	26.06	161.14	14.41	5.44	0.75	7.07
174	E29			1.37	9.26	8.88	26.48	141.37	14.86	8.19	0.72	10.63
175	E30			8.27	33.93	9.15	28.35	200.74	15.67	7.88	0.74	6.98
176	E31			9.28	89.17	8.6	28.35	225.71	16.27	7.9	0.75	7.00
177	E32			2.52	149.8	8.31	30.75	124.07	17.66	10.03	0.71	12.9

(continued)

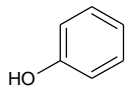
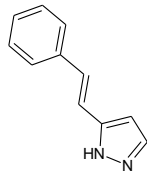
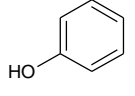
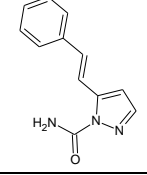
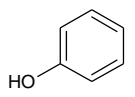
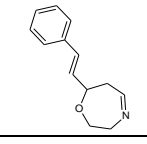
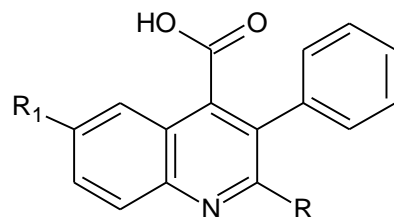
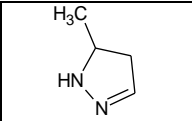
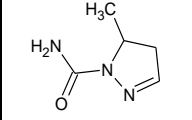
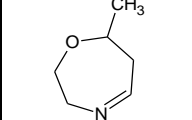
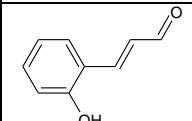
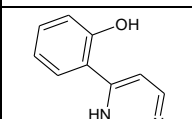
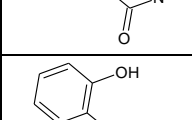
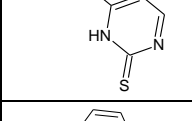
178	E33			2	73.58	8.83	26.77	170.57	15.17	7.85	0.72	10.56
179	E34			2.15	46.52	8.83	29.22	222.79	16.01	7.09	0.74	9.81
180	E35			1.95	2.4	9.03	28.18	147.3	15.99	7.37	0.72	9.38

Table 2.6: The values of chemical descriptors used in ADMET study of new quinoline derivatives selected from

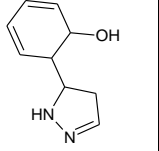
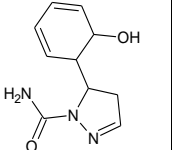
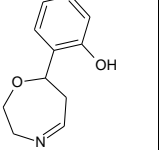
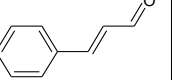
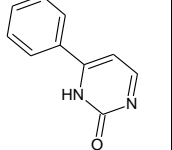
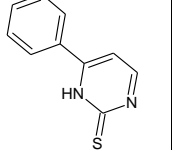
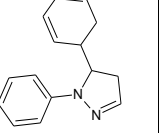


No	R	R1	logP(o/w)	H.acc	H.don	Mwt	Log S	TPSA	
brequinar		F		7.40	2	2	374.39	-9.15	374.39
1	A	CH ₃		3.89	4	2	305.333	-4.99	67.26
2	A1	CH ₃		4.53	4	2	331.371	-5.81	67.26
3	A2	CH ₃		4.22	5	3	371.396	-6.04	91.65
4	A3	CH ₃		4.24	5	3	387.463	-7.27	106.67
5	A4	CH ₃		6.58	4	2	421.5	-7.04	65.79

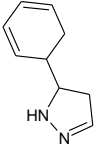
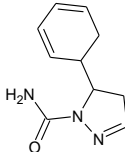
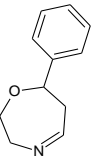
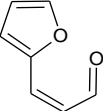
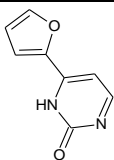
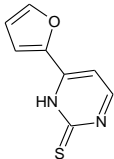
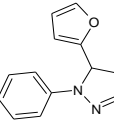
(continued)

6	A5	CH ₃		4.4	4	3	345.402	-5.14	74.58
7	A6	CH ₃		3.64	5	3	388.427	-5.57	108.88
8	A7	CH ₃		3.93	5	2	374.44	-5.58	71.78
9	A8	CH ₃		5.88	5	3	409.441	-6.90	87.49
10	A9	CH ₃		5.57	6	4	449.466	-7.44	111.88
11	A10	CH ₃		5.59	6	4	465.533	-8.67	126.9
12	A11	CH ₃		6.55	5	3	501.586	-7.42	86.02

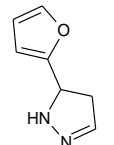
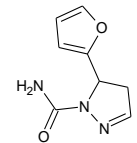
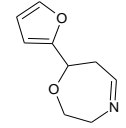
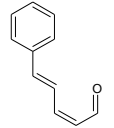
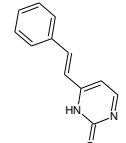
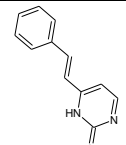
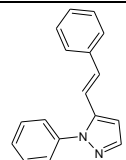
(continued)

13	A12	CH ₃		4.37	5	4	425.488	-5.52	94.81
14	A13	CH ₃		3.61	6	4	468.513	-5.95	129.11
15	A14	CH ₃		5.07	6	3	452.51	-6.66	92.01
16	A15	CH ₃		6.19	4	2	393.442	-7.26	67.26
17	A16	CH ₃		5.89	5	3	433.467	-7.80	91.65
18	A17	CH ₃		5.9	5	3	449.534	-9.03	106.67
19	A18	CH ₃		8.03	4	2	483.571	-8.48	65.79

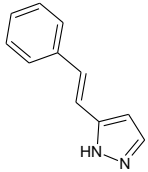
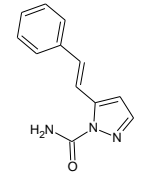
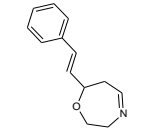
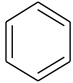
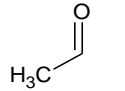
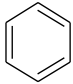
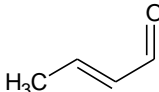
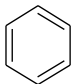
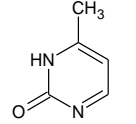
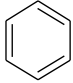
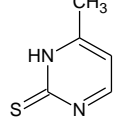
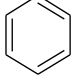
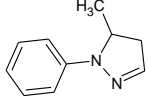
(continued)

20	A19	CH ₃		5.85	4	3	407.473	-6.58	74.58
21	A20	CH ₃		5.09	5	3	450.498	-7.01	108.88
22	A21	CH ₃		5.38	5	2	436.511	-7.02	71.78
23	A22	CH ₃		4.91	4	2	383.403	-7.01	80.4
24	A23	CH ₃		4.6	5	3	423.428	-7.55	104.79
25	A24	CH ₃		4.62	5	3	439.495	-8.79	119.81
26	A25	CH ₃		6.74	4	2	473.532	-8.23	78.93

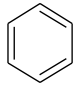
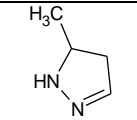
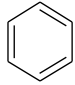
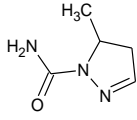
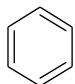
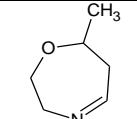
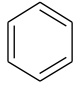
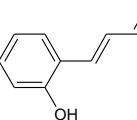
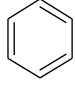
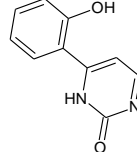
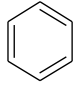
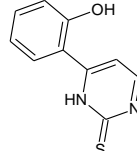
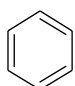
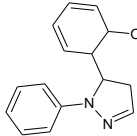
(continued)

27	A26	CH ₃		4.57	4	3	397.434	-6.33	87.72
28	A27	CH ₃		3.81	5	3	440.459	-6.76	122.02
29	A28	CH ₃		4.09	5	2	426.472	-6.78	84.92
30	A29	CH ₃		6.84	4	2	419.48	-8.39	67.26
31	A30	CH ₃		6.53	5	3	459.505	-8.30	91.65
32	A31	CH ₃		6.55	5	3	475.572	-9.54	106.67
33	A32	CH ₃		8.19	4	2	507.593	-9.63	68.01

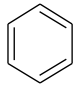
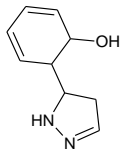
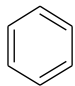
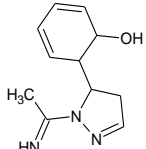
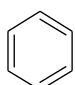
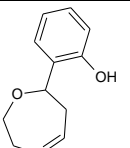
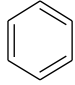
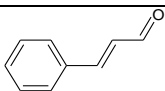
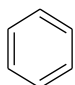
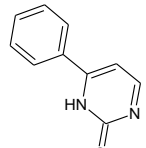
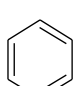
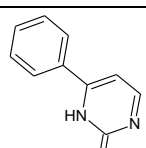
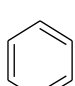
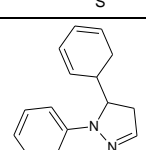
(continued)

34	A33	CH ₃		7.15	5	4	431.495	-7.91	78.87
35	A34	CH ₃		6.11	5	3	474.52	-8.14	111.1
36	A35	CH ₃		6.02	5	2	462.549	-7.53	71.78
37	B(I)			5.55	4	2	367.404	-7.08	67.26
38	B1			6.19	4	2	393.442	-7.90	67.26
39	B2			5.89	5	3	433.467	-8.12	91.65
40	B3			5.9	5	3	449.534	-9.36	106.67
41	B4			8.24	4	2	483.571	-9.12	65.79

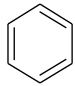
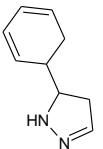
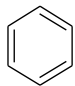
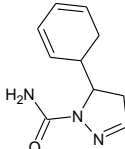
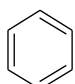
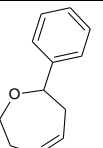
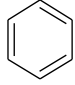
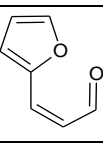
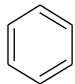
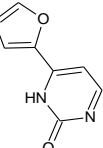
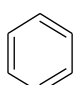
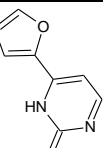
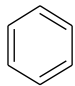
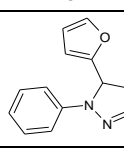
(continued)

42	B5			4.4	4	3	345.402	-5.14	74.58
43	B6			3.64	5	3	388.427	-5.57	108.88
44	B7			5.59	5	2	436.511	-7.66	71.78
45	B8			7.55	5	3	471.512	-8.98	87.49
46	B9			7.24	6	4	511.537	-9.52	111.88
47	B10			7.25	6	4	527.604	-10.75	126.9
48	B11			8.21	5	3	563.657	-9.51	86.02

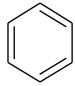
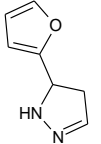
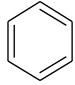
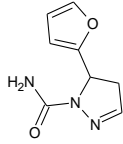
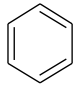
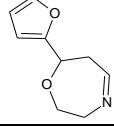
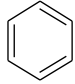
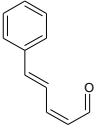
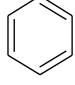
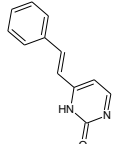
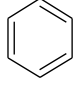
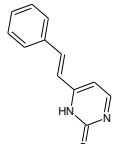
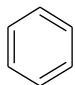
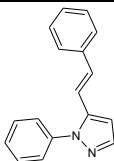
(continued)

49	B12			6.03	5	4	487.559	-7.61	94.81
50	B13			5.27	6	4	530.584	-8.03	129.11
51	B14			6.73	6	3	514.581	-8.74	92.01
52	B15(II)			4.86	4	2	455.513	-9.34	67.26
53	B16(III)			4.55	5	3	495.538	-9.88	91.65
54	B17(IV)			4.56	5	3	511.605	-11.12	106.67
55	B18(V)			4.87	4	2	547.658	-9.59	65.79

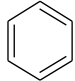
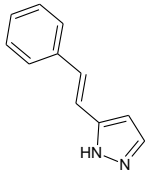
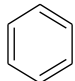
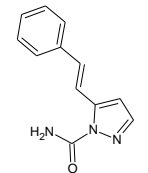
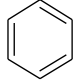
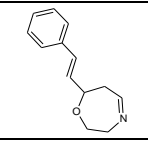
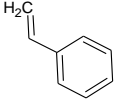
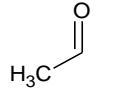
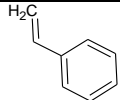
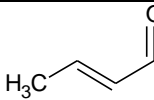
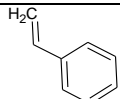
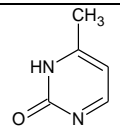
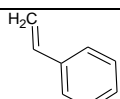
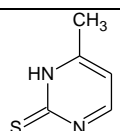
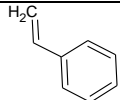
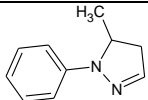
(continued)

56	B19(VI)			6.69	4	3	471.56	-7.69	74.58
57	B20(VII)			4.93	5	3	514.585	-8.12	108.88
58	B21(VIII)			7.04	5	2	498.582	-9.11	71.78
59	B22			6.57	4	2	445.474	-9.09	80.4
60	B23			6.26	5	3	485.499	-9.63	104.79
61	B24			6.28	5	3	501.566	-10.87	119.81
62	B25			7.92	4	2	533.587	-11.28	81.15

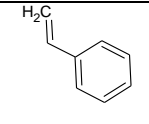
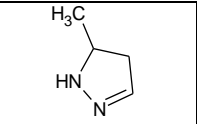
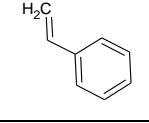
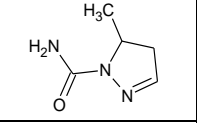
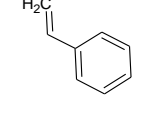
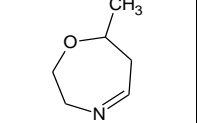
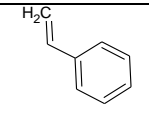
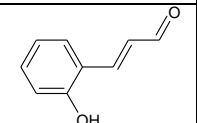
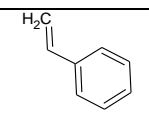
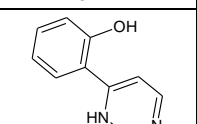
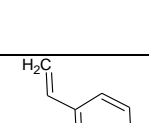
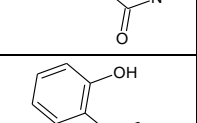
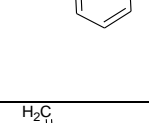
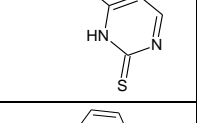
(continued)

63	B26			6.89	5	4	457.489	-9.56	92.01
64	B27			5.84	5	3	500.514	-9.79	124.24
65	B28			5.75	5	2	488.543	-8.86	84.92
66	B29			8.5	4	2	481.551	-10.48	67.26
67	B30			8.19	5	3	521.576	-10.39	91.65
68	B31			6.55	5	3	475.572	-9.54	106.67
69	B32			9.85	4	2	569.664	-11.71	68.01

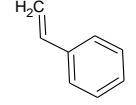
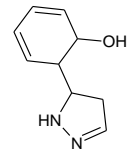
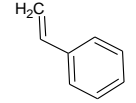
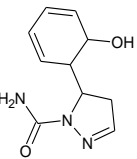
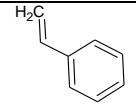
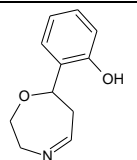
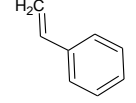
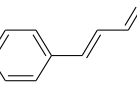
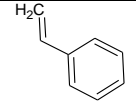
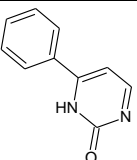
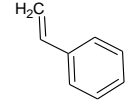
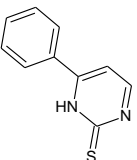
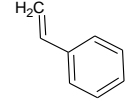
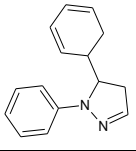
(continued)

70	B33			8.82	5	4	493.566	-10.00	78.87
71	B34			7.77	5	3	536.591	-10.22	111.1
72	B35			7.68	5	2	524.62	-9.61	71.78
73	C			6.19	4	2	393.442	-7.08	67.26
74	C1			6.84	4	2	419.48	-7.90	67.26
75	C2			6.53	5	3	459.505	-8.13	91.65
76	C3			6.55	5	3	475.572	-9.36	106.67
77	C4			8.89	4	2	509.609	-9.12	65.79

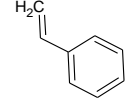
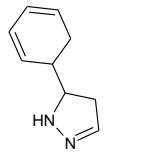
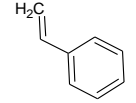
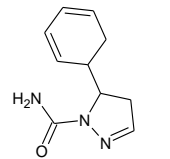
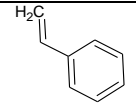
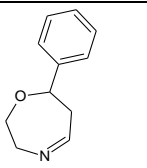
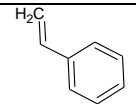
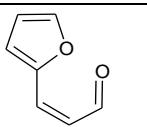
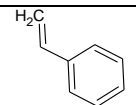
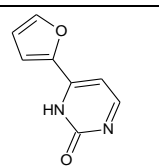
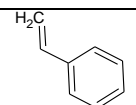
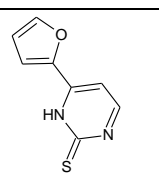
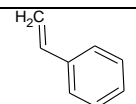
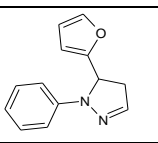
(continued)

78	C5			6.71	4	3	433.511	-7.22	74.58
79	C6			5.95	5	3	476.536	-7.65	108.88
80	C7			6.24	5	2	462.549	-7.67	71.78
81	C8			8.19	5	3	497.55	-8.99	87.49
82	C9			7.88	6	4	537.575	-9.52	111.88
83	C10			7.9	6	4	553.642	-10.76	126.9
84	C11			9.54	5	3	585.663	-11.35	88.24

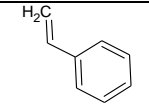
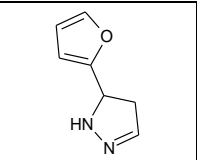
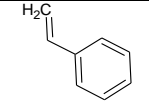
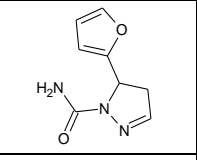
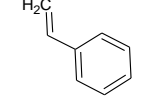
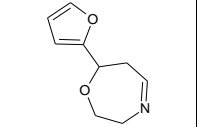
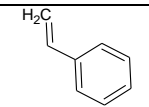
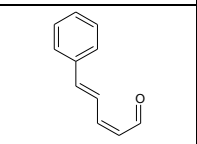
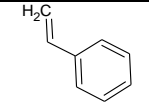
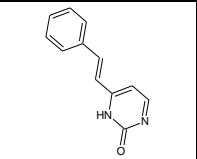
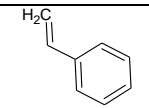
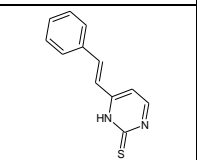
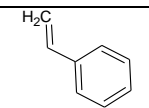
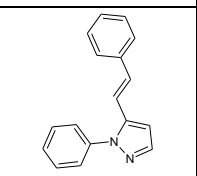
(continued)

85	C12			8.51	6	5	509.565	-9.63	99.1
86	C13			7.46	6	4	552.59	-9.86	131.33
87	C14			7.37	6	3	540.619	-8.75	92.01
88	C15			8.5	4	2	481.551	-9.35	67.26
89	C16			8.19	5	3	521.576	-9.89	91.65
90	C17			8.21	5	3	537.643	-11.12	106.67
91	C18			10.34	4	2	571.68	-10.56	65.79

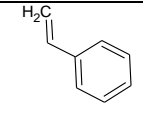
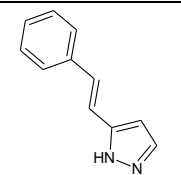
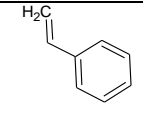
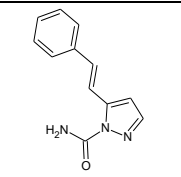
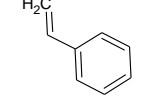
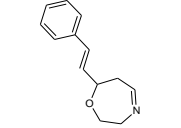

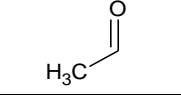
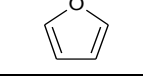
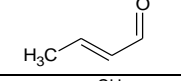

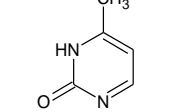
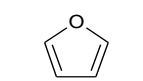
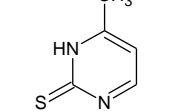

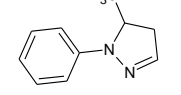
(continued)

92	C19			8.16	4	3	495.582	-8.67	74.58
93	C20			7.4	5	3	538.607	-9.09	108.88
94	C21			7.68	5	2	524.62	-9.11	71.78
95	C22			7.22	4	2	471.512	-9.10	80.4
96	C23			6.91	5	3	511.537	-9.64	104.79
97	C24			6.92	5	3	527.604	-10.87	119.81
98	C25			9.05	4	2	561.641	-10.32	78.93

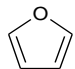
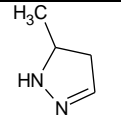

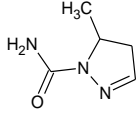
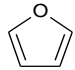
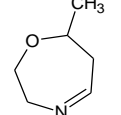
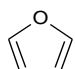
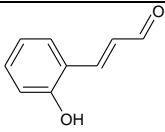
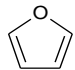
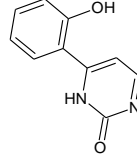
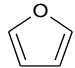
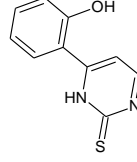
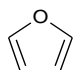
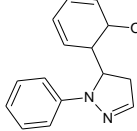
(continued)

99	C26			6.87	4	3	485.543	-8.42	87.72
100	C27			6.11	3	5	528.57	-8.85	122.02
101	C28			6.40	2	5	514.58	-8.86	84.92
102	C29			9.14	2	4	507.59	-10.48	67.26
103	C30			8.84	3	5	547.61	-10.39	91.65
104	C31			8.85	3	5	563.68	-11.63	106.67
105	C32			10.98	2	4	597.72	-11.07	65.79

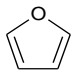
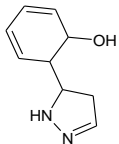

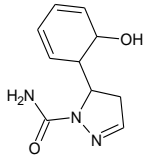

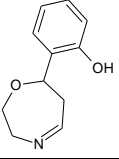

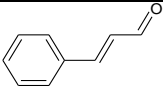

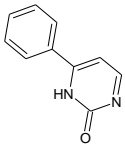

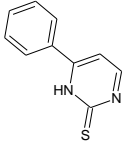
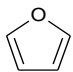
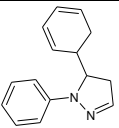
(continued)

106	C33			8.8	3	4	521.62	-9.17	74.58
107	C34			8.04	3	5	564.64	-9.60	108.88
108	C35			8.33	2	5	550.66	-9.62	71.78
109	D(IX)			4.26	2	4	357.36	-6.64	80.4
110	D1			4.91	2	4	383.40	-7.46	80.4
111	D2			4.6	3	5	423.43	-7.69	104.79
112	D3			4.62	3	5	439.50	-8.92	119.81
113	D4			6.96	2	4	473.53	-8.69	78.93

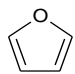
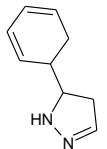
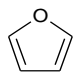
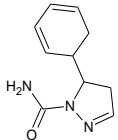
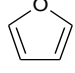
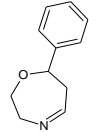
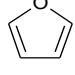
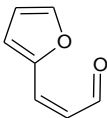
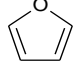
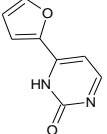
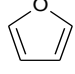
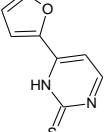

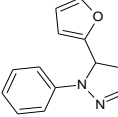
(continued)

114	D5			4.78	3	4	397.43	-6.79	87.72
115	D6			4.02	3	5	440.46	-7.22	122.02
116	D7			4.31	2	5	426.47	-7.23	84.92
117	D8			6.26	3	5	461.47	-8.55	100.63
118	D9			5.95	4	6	501.50	-9.09	125.02
119	D10			5.97	4	6	517.57	-10.32	140.04
120	D11			4.1	3	5	551.60	-9.76	99.16

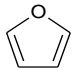
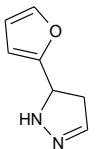

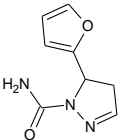
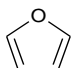
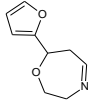
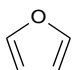
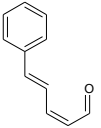

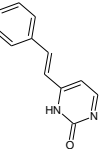

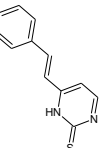
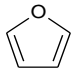
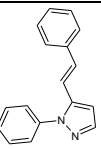
(continued)

121	D12			5.92	4	5	475.50	-7.87	107.95
122	D13			5.16	4	6	518.53	-8.29	142.25
123	D14			4.44	3	6	504.54	-8.31	105.15
124	D15			6.57	2	4	445.47	-8.91	80.4
125	D16			6.26	3	5	485.50	-9.45	104.79
126	D17			6.28	3	5	501.57	-10.68	119.81
127	D18			4.41	2	4	535.60	-10.13	78.93

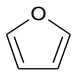
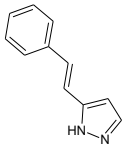

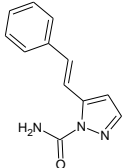

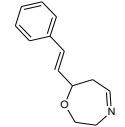
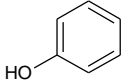
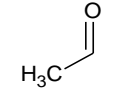
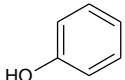
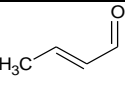
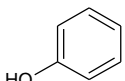
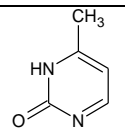
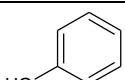
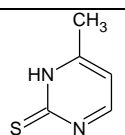
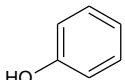
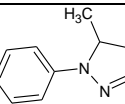
(continued)

128	D19			6.23	3	4	459.50	-8.23	87.72
129	D20			5.47	3	5	502.53	-8.66	122.02
130	D21			5.75	2	5	488.54	-8.67	84.92
131	D22(X)			6.57	2	4	445.47	-9.09	80.4
132	D23(XI)			6.26	3	5	485.50	-9.63	104.79
133	D24(XII)			6.28	3	5	498.57	-10.87	119.81
134	D25(XIII)			4.41	2	4	535.60	-10.31	78.93

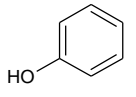
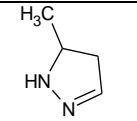
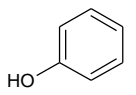
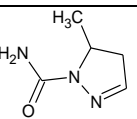
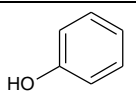
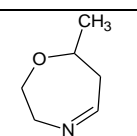
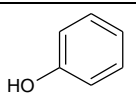
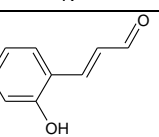
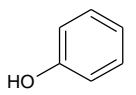
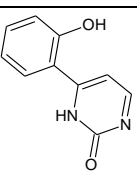
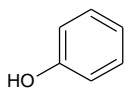
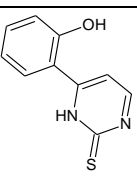
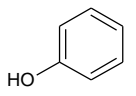
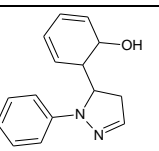
(continued)

135	D26(XIV)			6.23	3	4	459.50	-8.41	87.72
136	D27(XV)			5.47	3	5	499.53	-8.84	122.02
137	D28(XVI)			5.75	2	5	488.54	-8.86	84.92
138	D29			7.22	2	4	471.51	-10.04	80.4
139	D30			4.91	3	5	511.54	-9.95	104.79
140	D31			4.92	3	5	527.60	-11.19	119.81
141	D32			9.05	2	4	561.64	-10.63	78.93

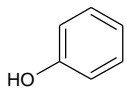
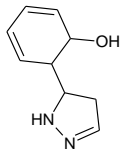
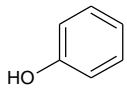
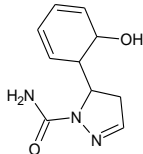
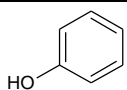
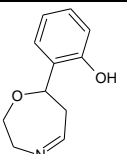
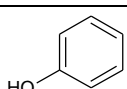
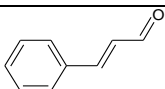
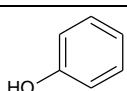
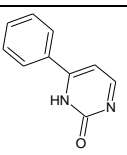
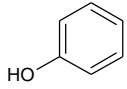
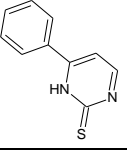
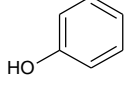
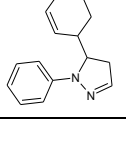
(continued)

142	D33			6.87	3	4	485.54	-8.73	87.72
143	D34			6.11	3	5	528.57	-9.16	122.02
144	D35			4.4	2	5	514.58	-9.18	84.92
145	E			5.24	3	5	383.40	-6.71	87.49
146	E1			5.88	3	5	409.44	-7.53	87.49
147	E2			5.57	4	6	449.47	-7.76	111.88
148	E3			5.59	4	6	465.53	-8.99	126.9
149	E4			7.93	3	5	499.57	-8.76	86.02

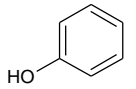
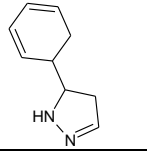
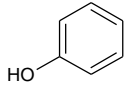
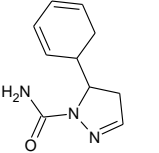
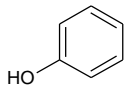
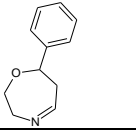
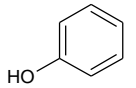
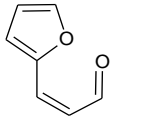
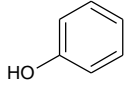
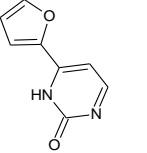
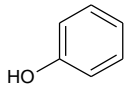
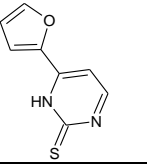
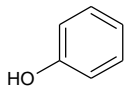
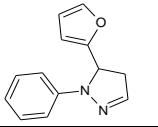
(continued)

150	E5			5.76	4	5	423.47	-6.86	94.81
151	E6			4.99	4	6	466.50	-7.29	129.11
152	E7			5.28	3	6	452.51	-7.30	92.01
153	E8			7.24	4	6	487.51	-8.62	107.72
154	E9			6.93	5	7	527.54	-9.16	132.11
155	E10			6.94	5	7	543.60	-10.39	147.13
156	E11			9.07	4	6	577.64	-9.84	106.25

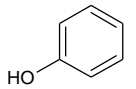
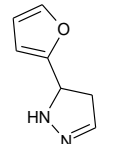
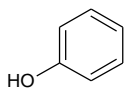
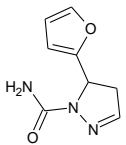
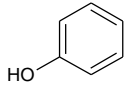
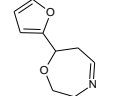
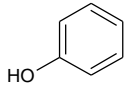
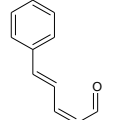
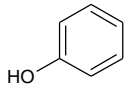
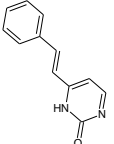
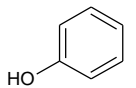
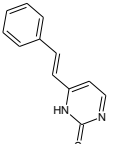
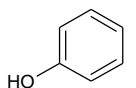
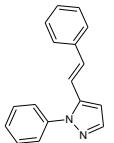
(continued)

157	E12			6.89	5	6	501.54	-7.94	115.04
158	E13			6.13	5	7	544.57	-8.36	149.34
159	E14			6.42	4	7	530.58	-8.38	112.24
160	E15			7.55	3	5	471.51	-8.98	87.49
161	E16			7.24	4	6	511.54	-9.52	111.88
162	E17			7.25	4	6	527.60	-10.75	126.9
163	E18			9.38	3	5	561.64	-10.20	86.02

(continued)

164	E19			7.2	4	5	485.54	-8.30	94.81
165	E20			6.44	4	6	528.57	-8.73	129.11
166	E21			6.73	3	6	514.58	-8.74	92.01
167	E22			6.26	3	5	461.47	-8.73	100.63
168	E23			6.26	3	5	485.50	-9.63	104.79
169	E24			6.28	3	5	501.57	-10.87	119.81
170	E25			8.1	3	5	551.60	-9.95	99.16

(continued)

171	E26			5.92	4	5	475.50	-8.05	107.95
172	E27			5.16	4	6	518.53	-8.48	142.25
173	E28			5.44	3	6	504.54	-8.49	105.15
174	E29			8.19	3	5	497.55	-10.11	87.49
175	E30			7.88	4	6	537.58	-10.02	111.88
176	E31			7.9	4	6	553.64	-11.26	126.9
177	E32			10.03	3	5	587.68	-10.70	86.02

(continued)

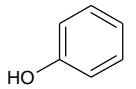
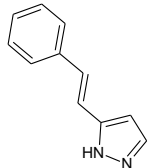
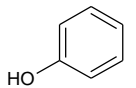
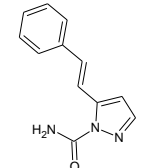
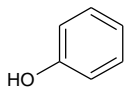
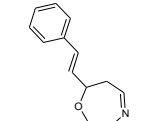
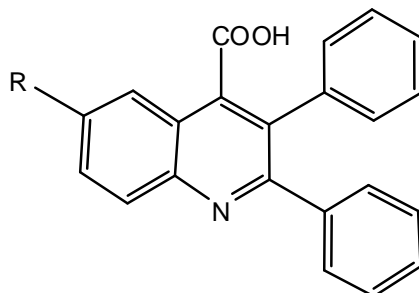
178	E33			7.85	4	5	511.58	-8.80	94.81
179	E34			7.09	4	6	554.61	-9.23	129.11
180	E35			7.37	3	6	540.62	-9.25	92.01

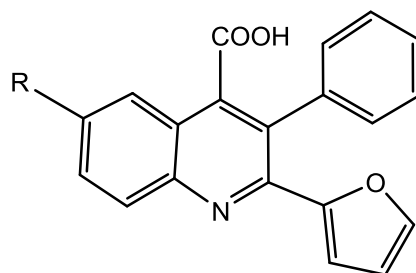
Table 2.7: Chemical names of the prepared quinoline derivatives

Table (2.7.1): Chemical names of 2, 3-diphenylquinoline-4-carboxylic acid derivatives



Comp.No	R	Chemical name
I		6-acetyl-2,3-diphenylquinoline-4-carboxylic acid
II		6-cinnamoyl-2,3-diphenylquinoline-4-carboxylic acid
III		6-(2-oxo-6-phenyl-1,2-dihydropyrimidin-4-yl)-2,3-diphenylquinoline-4-carboxylic acid
IV		2,3-diphenyl-6-(6-phenyl-2-thioxo-1,2-dihydropyrimidin-4-yl)quinoline-4-carboxylic acid
V		6-(1,5-diphenyl-4,5-dihydro-1H-pyrazol-3-yl)-2,3-diphenylquinoline-4-carboxylic acid
VI		2,3-diphenyl-6-(5-phenyl-4,5-dihydro-1H-pyrazol-3-yl)quinoline-4-carboxylic acid
VII		6-(1-carbamoyl-5-phenyl-4,5-dihydro-1H-pyrazol-3-yl)-2,3-diphenylquinoline-4-carboxylic acid
VIII		2,3-diphenyl-6-(7-phenyl-2,3,6,7-tetrahydro-1,4-oxazepin-5-yl)quinoline-4-carboxylic acid

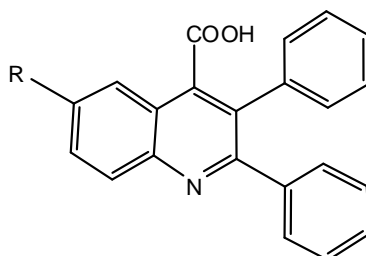
Table (2.7.2): Chemical names of 2 (furan-2-yl), 3-phenylquinoline-4-carboxylic acid derivatives



Comp.No	R	Chemical name
IX		6-acetyl-2-(furan-2-yl)-3-phenylquinoline-4-carboxylic acid
X		(E)-2-(furan-2-yl)-6-(3-(furan-2-yl)acryloyl)-3-phenylquinoline-4-carboxylic acid
XI		2-(furan-2-yl)-6-(6-(furan-2-yl)-2-oxo-1,2-dihydropyrimidin-4-yl)-3-phenylquinoline-4-carboxylic acid
XII		2-(furan-2-yl)-6-(6-(furan-2-yl)-2-thioxo-1,2-dihydropyrimidin-4-yl)-3-phenylquinoline-4-carboxylic acid
XIII		2-(furan-2-yl)-6-(5-(furan-2-yl)-1-phenyl-4,5-dihydro-1H-pyrazol-3-yl)-3-phenylquinoline-4-carboxylic acid
XIV		2-(furan-2-yl)-6-(5-(furan-2-yl)-4,5-dihydro-1H-pyrazol-3-yl)-3-phenylquinoline-4-carboxylic acid
XV		6-(1-carbamoyl-5-(furan-2-yl)-4,5-dihydro-1H-pyrazol-3-yl)-2-(furan-2-yl)-3-phenylquinoline-4-carboxylic acid
XVI		2-(furan-2-yl)-6-(7-(furan-2-yl)-2,3,6,7-tetrahydro-1,4-oxazepin-5-yl)-3-phenylquinoline-4-carboxylic acid

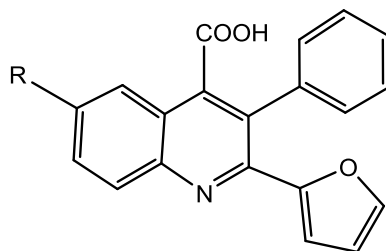
Table (2.8): Reaction conditions of the prepared compounds

Table 2.8.1: Reaction conditions of the prepared 2, 3-diphenylquinoline-4-carboxylic acid derivatives



Comp. No	R	Reaction Temp C°	Time H	Yield %	Yield gram	Color	m.p C°
I		Reflux temperature	3	93.25	2.91	off-white	210-212
II		Room temp	24	85,91	1.22	Pale yellow	110-112
III		Reflux temperature	4	70	0.43	yellow	175-177
IV		Reflux temperature	4	68.33	0.41	yellow	165-167
V		Reflux temperature	3	70	0.42	yellow	119-121
VI		Reflux temperature	3	65	0.39	Pale yellow	128-131
VII		Reflux temperature	3	66.66	0.40	Pale yellow	120-123
VIII		Reflux temperature	4	66.7	0.41	Pale yellow	139-141

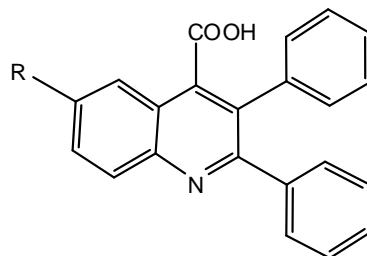
Table 2.8.2: Reaction conditions of the prepared 2 (furan-2-yl), 3-phenylquinoline-4-carboxylic acid derivatives



Comp. No	R	Reaction Temp C°	Time H	Yield %	Yield gram	Color	m.p C°
IX		Reflux temperature	3	81.7	2.40	Beige	143-145
X		Room temp	24	78.0	1.56	Beige	148-150
XI		Reflux temperature	4	71.66	0.43	Brown	145-147
XII		Reflux temperature	4	66.66	0.40	Brown	150-152
XIII		Reflux temperature	3	65	0.39	Pale yellow	147-151
XIV		Reflux temperature	3	68.33	0.41	Beige	167-169
XV		Reflux temperature	3	63.88	0.38	Beige	155-157
XVI		Reflux temperature	4	66.66	0.40	Pale yellow	225-227

Table (2.9): Infra - red spectral data (IR) of the prepared compounds

Table (2.9.1): Infra - red spectral data (IR) of the prepared 2, 3-diphenylquinoline-4-carboxylic acid derivatives



Comp. No	R	C=N	C=O St.vib	C=C St.vib	C-N St.vib	N-H St.vib	C-O St.vib	other
I		-	1678.52(ketone) 1667.51(carboxyl)	1600.60	-	-	-	3246.8 St.vib (O-H) 3089.99 St.vib (C-H ring)
II		-	1682.41(ketone) 1657.42(carboxyl)	1578.2	-	-	-	3060.81 st And 3045.6 st (C-H of α,β -unsaturated ketone)
III		-	1692.41(carboxyl) 1672.75(C=O amid)	1600.68	1375.67	3015.15sp2	-	3089.59 st (C-H of pyrimidinone ring)

(continued)

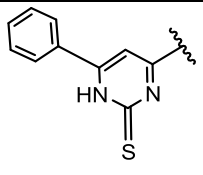
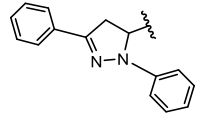
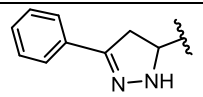
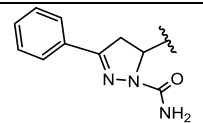
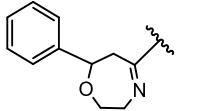
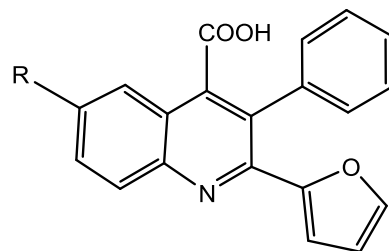
IV		1425.71	1672.51	1600.61	1323.48	3210.32	1566.94	1367.49 St.vib (C=S)
V		1513.12	1698.21	1600.9	-	-	-	2957.52 St.vib (C-H sp ³ of pyrazoline ring)
VI		1518.71	1678.70	1601.74	1369.60	3046.97		2957.52 St.vib (C-H sp ³ of pyrazoline ring)
VII		1517.99	1672.61(carboxyl) 1619.22(C=O amid)	1600.35	1367.63	3100.5 3098.71	-	2952.43 St.vib C-H pyrazoline ring
VIII		1506.93	1681.96	1600.94	1366.63	-	1216.45 (oxazepin)	3262.23 St.vib O-H 2911.25 St.vib C-H oxazepin ring

Table (2.9.2): Infra - red spectral data (IR) of the prepared 2 (furan-2-yl), 3-phenylquinoline-4-carboxylic acid derivatives



Comp. No	R	C=N	C=O St.vib	C=C St.vib	C-N St.vib	N-H St.vib	C-O St.vib	other
IX		-	1674.61(ketone) 1663.51(carboxyl)	1598.60	-	-	1274.21 Furan ring	3242.81 St.vib (O-H) 3144.21St.vib (C-H ring)
X		-	1672.56(ketone) 1660.42(carboxyl)	1600.61	-	-	1274.61 Furan ring	3060.81 st And 3045.6 st (C-H of α,β -unsaturated ketone)
XI		-	1692.41(carboxyl) 1672.75(C=O amid)	1600.51	1375.60	3285.15	1280.13 Furan ring	3089.89 st (C-H of pyrimidinone ring)

(continued)

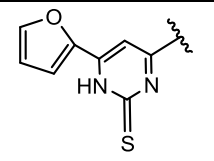
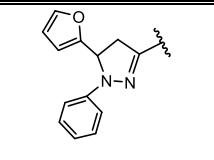
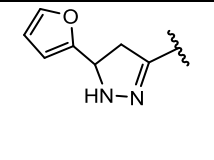
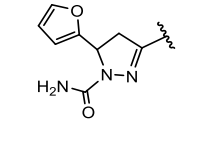
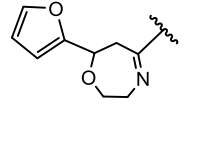
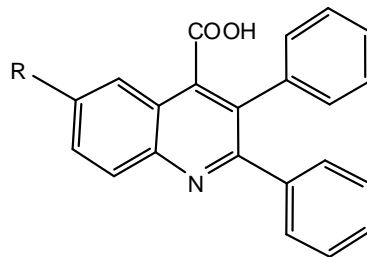
XII		-	1674.78	1600.80	1323.48	3265.32	1285.8 Furan ring	1365.81 St.vib (C=S)
XIII		1525.78	1670.85	1598.36	-	-	1268.85 Furan ring	2805.15 St.vib (C-H sp2 of pyrazoline ring)
XIV		1515.01	1674.75	1598.74	1216.75	3275.1	1268.75 Furan ring	2925.79 St.vib (C-H sp2 of pyrazoline ring)
XV		1540.99	1702.81(carboxyl) 1689.26(C=O amid)	1603.79	1367.63	3360.4 3400.11	1267.88 Furan ring	2950.70 St.vib (C-H sp2 of pyrazoline ring)
XVI		1514.30	1691.27	1597.65	1361.77	-	1275.27 Furan ring 1230.81 (oxazepin)	3386.75 St.vib O-H 2912.60 St.vib C-H sp2 of oxazepin ring

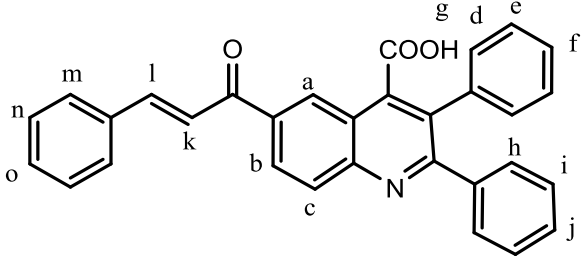
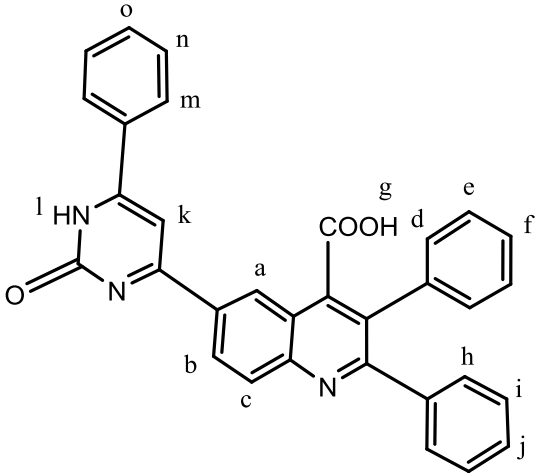
Table 2.10: ^1H Nuclear magnetic resonance (^1H NMR) data of the prepared compounds

Table (2.10.1): ^1H Nuclear magnetic resonance (^1H NMR) of the prepared 2, 3-diphenylquinoline-4-carboxylic acid derivatives

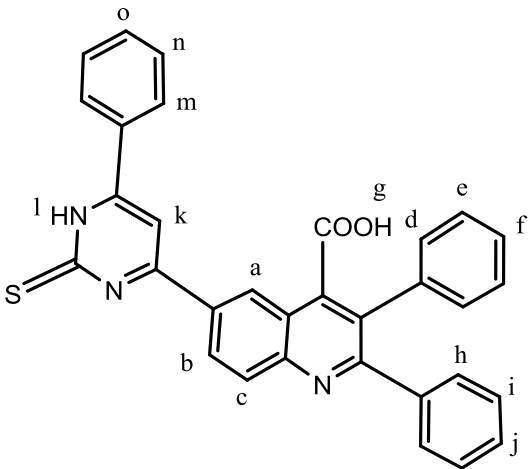
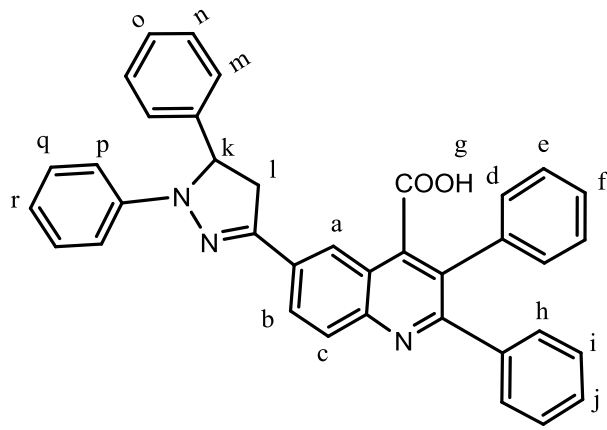


Comp. No	Structure and number of signal	signal	Chemical shift ppm
I		a	9.45 (s, 1H, CH quinoline ring)
		b	8.42 (d, 1H, CH quinoline ring)
		c	8.22 (d, 1H, CH quinoline ring)
		d	7.90 (d, 2H, H-Ar)
		e	7.22 (t, 2H, H-Ar)
		f, h, i, j	7.68- 7.16(m , 8H, H-Ar)
		k	2.55 (s, 3H, CH ₃)

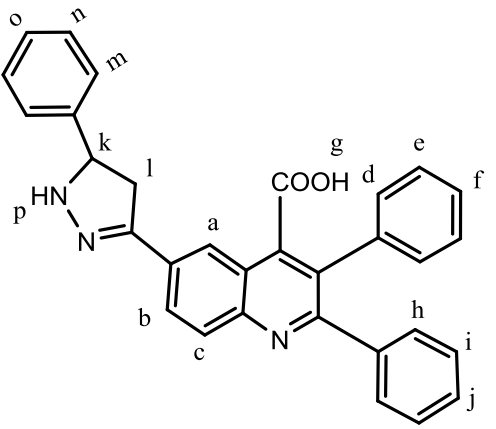
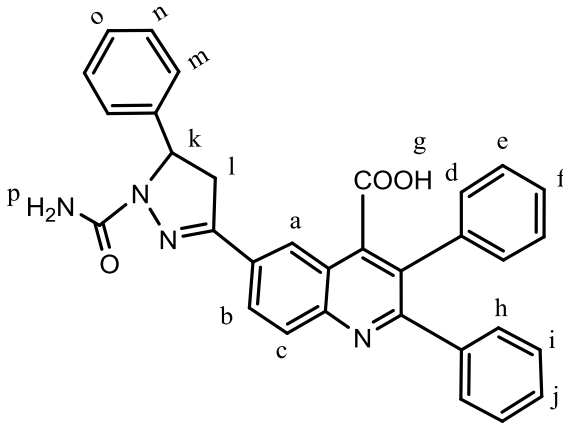
(continued)

II		a	9.72 (s, 1H, CH quinoline ring)
		b	8.51 (d, 1H, CH quinoline ring)
		c	8.18 (d, 1H, CH quinoline ring)
		d	7.63 (d, 2H, H-Ar)
		e, f, h, i, j, m, n, o	7.93-6.71 (m, 13H, H-Ar)
		k	7.40(d , 1H, H-C=)
		l	7.28 (d, 1H, H-C=)
III		a	9.83 (s , 1H, CH quinoline ring)
		b	9.23 (d, 1H, CH quinoline ring)
		c	8.45 (d, 1H, CH quinoline ring)
		d, e, f, h, i, j, m, n, o	8.09 (m, 15H, H-Ar)
		k	5.73(s , 1H, CH)
		l	10.02 (s, 1H, NH)

(continued)

IV		a	9.24 (s, 1H, CH quinoline ring)
		b	9.02 (d, 1H, CH quinoline ring)
		c	8.05 (d, 1H, CH quinoline ring)
		d	7.84-7.83 (d, 2H, H-Ar)
		h	7.79 (d, 2H, H-Ar)
		i	7.68-7.61 (m, 2H, H-Ar)
		e, f, j, n, m, o	7.77-7.29 (m, 7H, H-Ar)
		k	5.96 (s, 1H, CH)
		l	10.68 (s, 1H, NH)
V		a	9.61 (s, 1H, CH quinoline ring)
		b	8.43 (d, 1H, CH quinoline ring)
		c	8.22 (d, 1H, CH quinoline ring)
		h	8.08 (d, 2H, H-Ar)
		d, e, f, i, j, o, p, q, r	7.99-7.13 (m, 14H, H-Ar)
		m	8.02-8.01 (d, 2H, H-Ar)
		n	7.23-7.21 (d, 2H, H-Ar)
		k	4.99-5.02 (dd, 1H _(X) -CH)
		l	3.71-3.75 (dd, 1H _(A) , CH ₂ , dd, 1H _(B) , CH ₂)

(continued)

VI		a	9.88 (s , 1H, CH quinoline ring)
		b	8.58 (d, 1H, CH quinoline ring)
		c	8.31 (d, 1H, CH quinoline ring)
		h	8.13-8.12 (d, 2H, H-Ar)
		d,e, f, i, j,m, n, o	7.78-7.21 (m, 13H, H-Ar)
		p	10.03 (s, 1H, -NH)
		k	4.93-4.95 (dd, 1H _(X) -CH)
		l	3.70-3.73 (dd, 1H _(A) , CH ₂ , dd, 1H _(B) , CH ₂)
VII		a	9.50 (s , 1H, CH quinoline ring)
		b	8.47 (d, 1H, CH quinoline ring)
		c	8.22 (d, 1H, CH quinoline ring)
		h	7.94-7.93 (d, 2H, H-Ar)
		d,e, f, i, j,m, n, o	7.72-7.10 (m, 13H, H-Ar)
		p	6.01 (s, 1H, C-NH ₂)
		k	4.93 - 4.98 (dd, 1H _(X) -CH)
		l	3.70-3.74 (dd, 1H _(A) , CH ₂ , dd, 1H _(B) , CH ₂)

(continued)

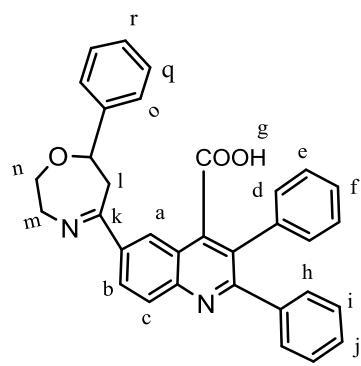
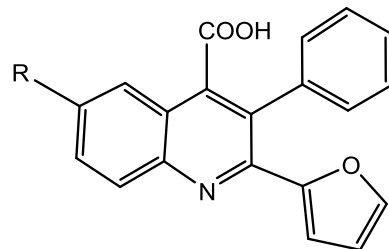
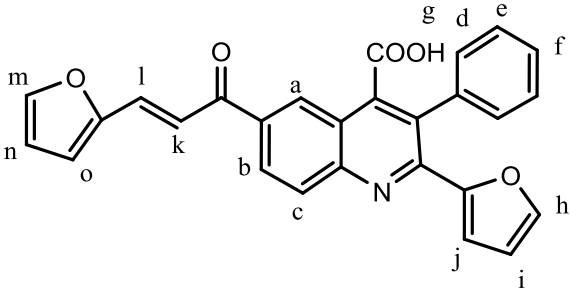
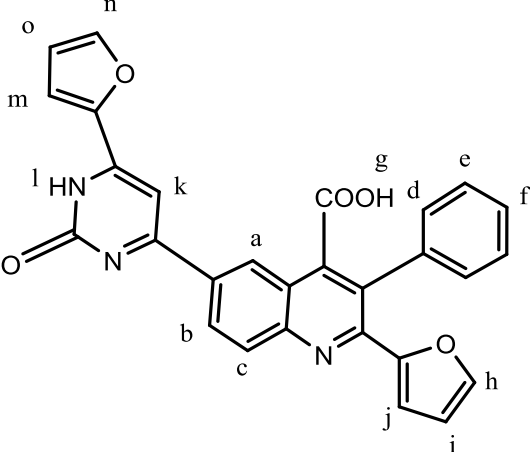
VIII		a	9.95 (s , 1H, CH quinoline ring)
		b	8.54 (d, 1H, CH quinoline ring)
		c	8.22 (d, 1H, CH quinoline ring)
		d	7.74-7.73 (d, 2H, H-Ar)
		h	7.98-7.97 (d, 2H, H-Ar)
		i	7.68-7.66(t, 2H, H-Ar)
		j	7.68-7.66(t, 1H, H-Ar)
		e, f, ,o, p, q, r	7.50 - 7.16 (m, 7H, H-Ar)
		k	4.90 - 4.93 (dd, 1H _(X) -CH)
		l	3.34 - 3.39 (dd, 1H _(A) , CH ₂ , dd, 1H _(B) , CH ₂)
		m, n	3.61 (t, 2H,-CH ₂), 3.78 (t, 2H,-CH ₂)

Table (2.10.2): ^1H Nuclear magnetic resonance ($^1\text{HNMR}$) of the 2 (furan-2-yl), 3-phenylquinoline-4-carboxylic acid derivatives

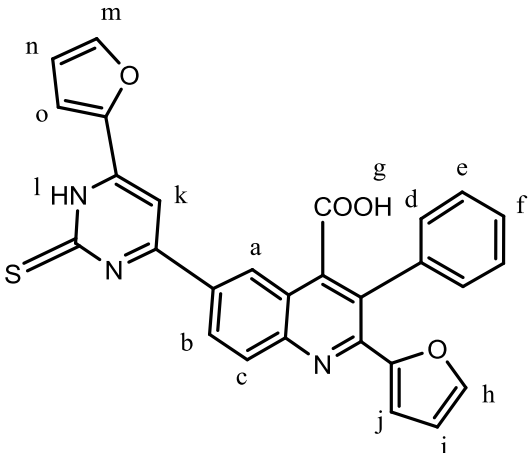
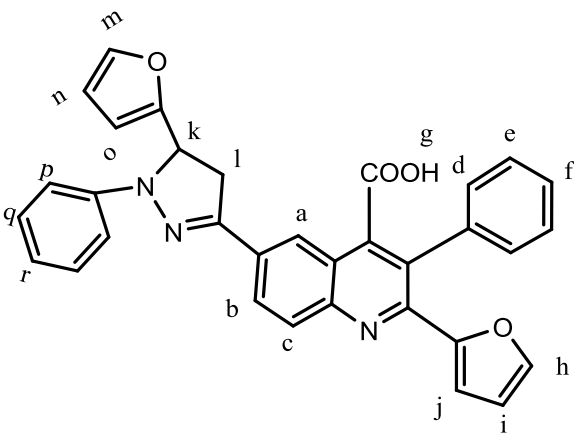


Comp. No	Structure and number of signal	signal	Chemical shift ppm
I		a	9.72 (s , 1H, CH quinoline ring)
		b	8.42 (d, 1H, CH quinoline ring)
		c	8.22 (d, 1H, CH quinoline ring)
		d	8.01 (d, H, H-phenyl)
		h	8.12 (d, 1H, H-furyl)
		j	8.08 (d, 1H, H-furyl)
		e, f, i,	7.36-7.24 (m , 4H, H-Ar)
k	2.55 (s, 3H, CH ₃)		

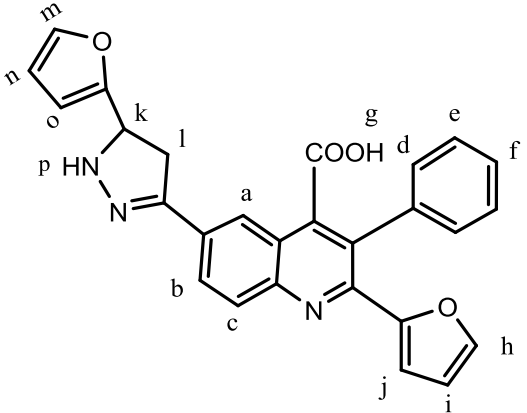
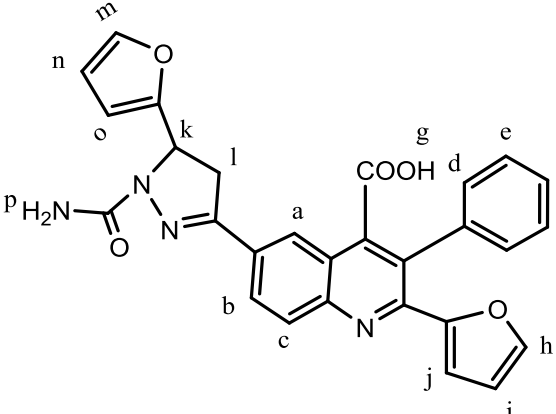
(continued)

II	 <p>Chemical structure of compound II, a quinoline derivative. The quinoline ring is substituted with a phenyl group (protons d, e, f), a furfuryl group (protons g, h, i, j), and a propenoic acid side chain (protons k, l, m, n, o). The quinoline ring protons are labeled a, b, and c.</p>	a	9.66 (s , 1H, CH quinoline ring)
		b	8.12 (d, 1H, CH quinoline ring)
		c	8.10 (d, 1H, CH quinoline ring)
		d	7.70 (d, 2H, H-phenyl)
		e, f, h, i, j, m, n, o	7.36-7.24 (m, 9H, H-Ar)
		k	7.96(d , 1H, H-C=)
		l	7.67 (d, 1H, H-C=)
III	 <p>Chemical structure of compound III, a quinoline derivative. The quinoline ring is substituted with a phenyl group (protons d, e, f), a furfuryl group (protons g, h, i, j), and a propenoic acid side chain (protons k, l, m, n, o). The quinoline ring protons are labeled a, b, and c.</p>	a	9.97 (s , 1H, CH quinoline ring)
		b	8.12 (d, 1H, CH quinoline ring)
		c	8.10 (d, 1H, CH quinoline ring)
		d, e, f, h, i, j, m, n,o	7.75-6.17 (m, 10H, H-Ar)
		k	6.17 (s , 1H, CH)
		l	10.02 (s, 1H, NH)

(continued)

IV		<p>a 9.92 (s , 1H, CH quinoline ring)</p> <p>b 8.09 (d, 1H, CH quinoline ring)</p> <p>c 8.12 (d, 1H, CH quinoline ring)</p> <p>d 8.09 (d, 1H, H-furyl)</p> <p>h 7.71 (d, 2H, H-phenyl)</p> <p>e, f,i, j, n,m, o 7.58-7.29 (m, 8H, H-Ar)</p> <p>k 6.17 (s , 1H, CH)</p> <p>l 9.92 (s, 1H, NH)</p>	
V		<p>a 9.61 (s , 1H, CH quinoline ring)</p> <p>b 8.01 (d, 1H, CH quinoline ring)</p> <p>c 8.04 (d, 1H, CH quinoline ring)</p> <p>h 8.12-8.08 (d, 2H, H-furyl)</p> <p>d,e, f, j,m, p, q, r 7.99-7.13 (m, 14H, H-Ar)</p> <p>i 6.68 (t, 1H, H-furyl)</p> <p>o 6.62 (d, 1H, H-furyl)</p> <p>k 4.09 - 4.19 (dd, 1H_(X)-CH)</p> <p>l 3.63-3.68 (dd, 1H_(A), CH₂, dd, 1H_(B), CH₂)</p>	

(continued)

VI		a	9.95 (s , 1H, CH quinoline ring)
		b	8.77 (d, 1H, CH quinoline ring)
		c	8.08 (d, 1H, CH quinoline ring)
		h	7.96 (d, H, H-furyl)
		m	7.70 (d, H, H-furyl)
		o	6.21 (d, 1H, H-furyl)
		d,e, f, i, j, n,	7.50-7.10 (m, 8H, H-Ar)
		k	4.11 - 4.15 (dd, 1H _(X) -CH)
		l	3.65-3.70 (dd, 1H _(A) , CH ₂ , dd, 1H _(B) , CH ₂)
VII		a	9.61 (s , 1H, CH quinoline ring)
		b	8.10 (d, 1H, CH quinoline ring)
		c	8.06 (d, 1H, CH quinoline ring)
		h	7.93 (d, 1H, H-furyl)
		m	7.76 (d, H, H-furyl)
		o	6.67 (d, 1H, H-furyl)
		d,e, f, i, j, n,	7.60-7.10 (m, 13H, H-Ar)
		p	6.01 (s, 1H, C-NH ₂)
		k	4.10 - 4.15 (dd, 1H _(X) -CH)
		l	3.67-3.70 (dd, 1H _(A) , CH ₂ , dd, 1H _(B) , CH ₂)

(continued)

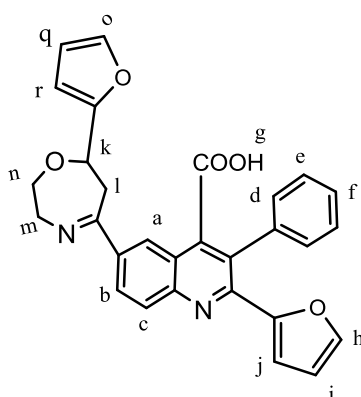
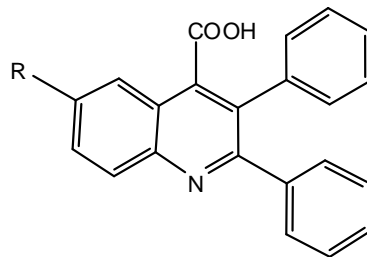
VIII		a	9.61 (s , 1H, CH quinoline ring)
		b	8.08 (d, 1H, CH quinoline ring)
		c	8.03 (d, 1H, CH quinoline ring)
		h	7.96(d, 2H, H-furyl)
		o	7.94 (d, 1H, H-furyl)
		d,e, f, i, j,r, p, q	7.81-7.25 (m, 13H, H-Ar)
		k	4.98-5.01 (dd, 1H _(X) -CH)
		l	3.25 - 3.35 (dd, 1H _(A) , CH ₂ , dd, 1H _(B) , CH ₂)
		n,m	3.64 (t, 2H,-CH ₂), 3.83 (t, 2H,-CH ₂)

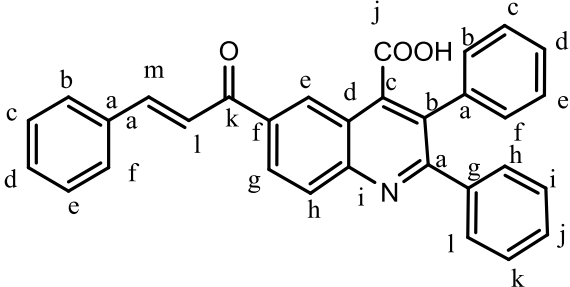
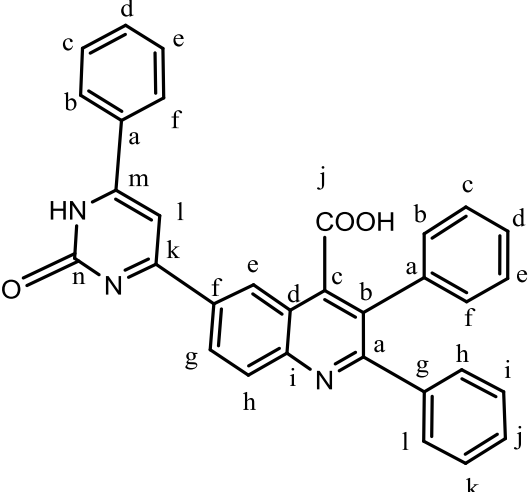
Table 2.11: ^{13}C Nuclear magnetic resonance ($^{13}\text{CNMR}$) data of the prepared compounds

Table (2.11.1): ^{13}C Nuclear magnetic resonance ($^{13}\text{CNMR}$) of the prepared 2, 3-diphenylquinoline-4-carboxylic acid derivatives

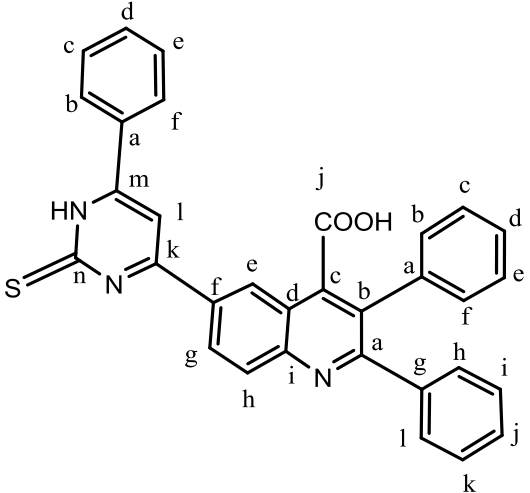
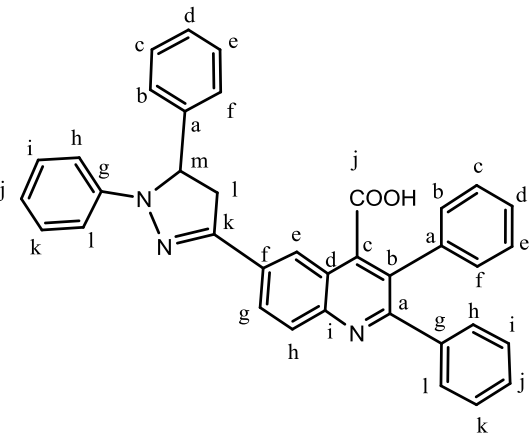


Comp. No	Structure and number of signal	signal	Chemical shift ppm
I		b	133.46 (C,quinoline)
		c	135.78 (C,quinoline)
		g	122.3 (CH,quinoline)
		j	166.50 (C, carboxylic acid group)
		l	26.45 (C, methyl group)
		a,b,c,d,e,f,g,h i,j,k,h	127.70-129.78(1CH, Quinoline,12CH,H-Ar)
		k	196.98(C, carbonyl group)

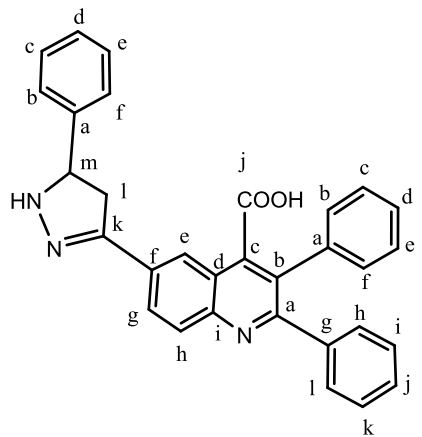
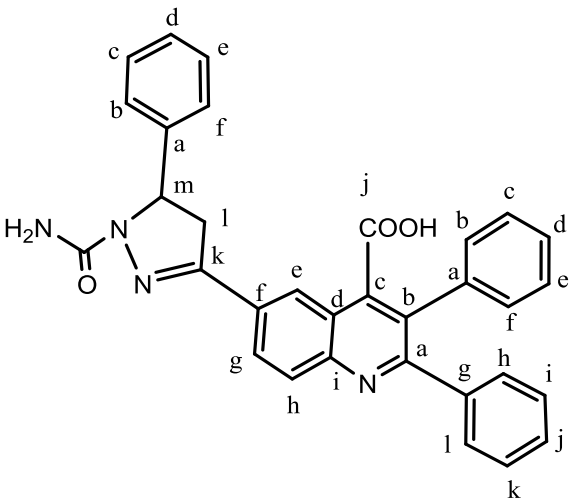
(continued)

II		a	135.90 (C,phenyl)
		b	133.46 (C,quinoline)
		c	135.78 (C,quinoline)
		j	166.50 (C, carboxylic acid group)
		k	189.14(C, carbonyl group)
		l	121.14 (C, ethylene group)
		m	144.48 (C, ethylene group)
		a,b,c,d,e,f, a,b,c,d,e,f,g, h,I,kl,d,e,g	127.30-129.20(2CH,1C, Quinoline,12 CH, H-Ar)
III		c	133.46 (C,quinoline)
		d	123.26 (C,quinoline)
		e	144.74 (C,quinoline)
		f	127.70 (C,quinoline)
		j	166.50 (C, carboxylic acid group)
		a,b,c,d,e,f, a,b,c,d,e,f,g, h,I,J,k,l,h,g	127.50-130.20(2CH,1C, Quinoline,18 CH, H-Ar)

(continued)

IV		b	133.33 (C,quinoline)
		c	133.44 (C,quinoline)
		d	123.26 (C,quinoline)
		e	142.47 (C,quinoline)
		f	126.93 (C,quinoline)
		j	166.50 (C, carboxylic acid group)
		m	174.86(C, pyrimidinone group)
		n	197.17(C, pyrimidinone group)
a,b,c,d,e,f, a,b,c,d,e,f,g, h,I,J,k,l,h,g	127.50-130.20(2CH,1C, Quinoline,18 CH, H-Ar)		
V		b	135.75 (C,phenyl)
		c	133.44 (C,quinoline)
		d	123.26 (C,quinoline)
		j	166.50 (C, carboxylic acid group)
		i	166.50 (CH, pyrazoline ring)
		a,b,c,d,e,f, a,b,c,d,e,f,g, h,I,J,k,l,h,g	127.50-130.20(2CH,1C, Quinoline,24 CH, H-Ar)

(continued)

VI		b	132.67 (C,quinoline)
		c	135.88 (C,quinoline)
		d	123.07 (C,quinoline)
		j	166.17 (C, carboxylic acid group)
		l	41.23 (CH ₂ , pyrazoline ring)
		m	63.61 (CH, pyrazoline ring)
		a,b,c,d,e,f, a,b,c,d,e,f,g, h,I,J,k,l,h,g	127.02-130.97(2CH,1C, Quinoline,18 CH, H-Ar)
VII		b	133.71 (C,quinoline)
		c	134.88 (C,quinoline)
		d	123.07 (C,quinoline)
		l	41.15 (CH ₂ , pyrazoline ring)
		m	63.26 (CH, pyrazoline ring)
		a,b,c,d,e,f, a,b,c,d,e,f,g, h,I,J,k,l,h,g	127.01-130.91(2CH,1C, Quinoline,18 CH, H-Ar)

(continued)

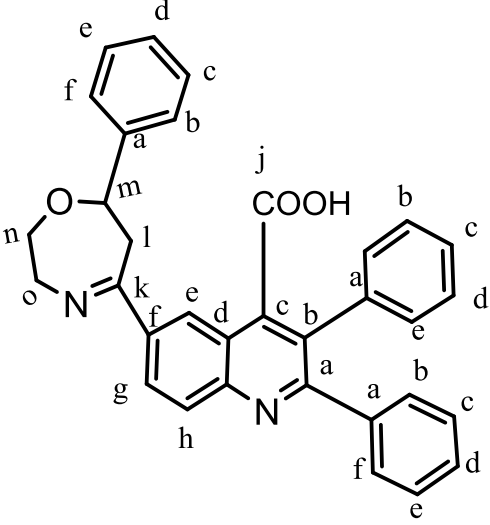
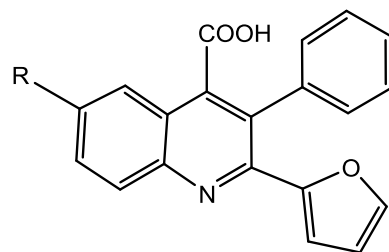
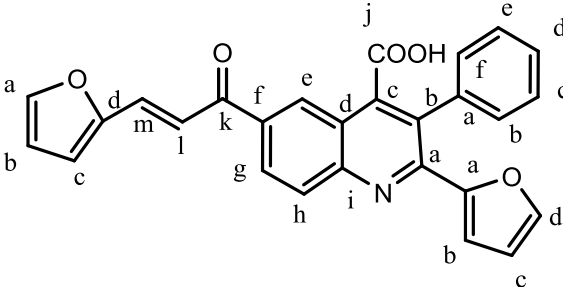
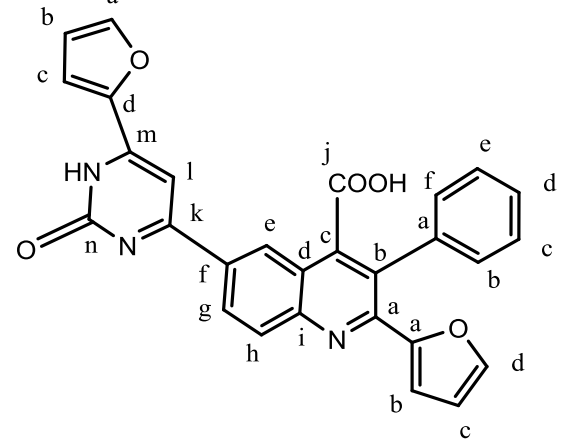
VIII		c	134.46 (C,quinoline)
		d	123.10 (C,quinoline)
		l	30.26 (C, CH ₂)
		n	63.34 (C, CH)
		j	166.20 (C, carboxylic acid group)
		a,b,c,d,e,f, a,b,c,d,e,f,g, h,I,J,k,l,h,g	127.71-130.57(2CH,1C, Quinoline,18 CH, H-Ar)

Table (2.11.2): ^{13}C Nuclear magnetic resonance (^{13}C NMR) of the 2 (furan-2-yl), 3-phenylquinoline-4-carboxylic acid derivatives

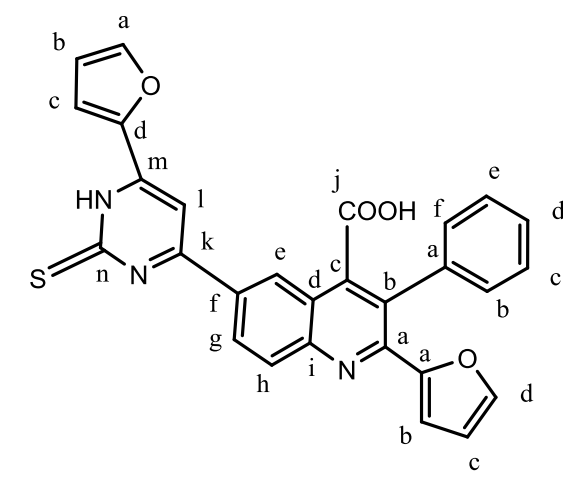
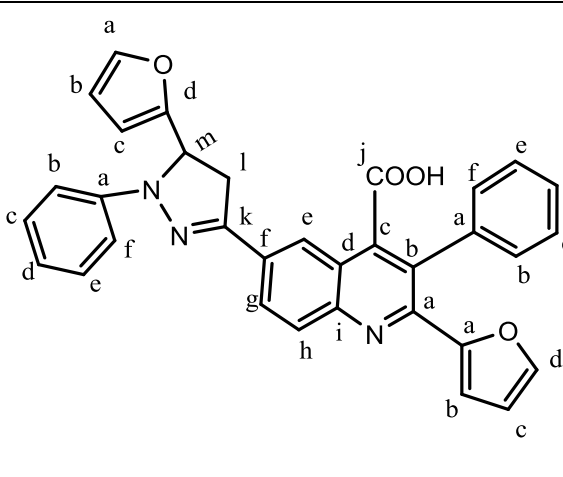


Comp. No	Structure and number of signal	signal	Chemical shift ppm
I		b	133.53 (C,quinoline)
		g	125.6 (CH,quinoline)
		j	166.50 (C, carboxylic acid group)
		l	26.75 (C, methyl group)
		k	196.98(C, carbonyl group)
		a,b,c,d,e,f, a,b,c,d, a,b,c,d g,h	110.19-133.53(2CH,1C, Quinoline,10 CH, H-Ar)

(continued)

II		a	142.90 (CH,furyl ring)
		b	133.46 (C,quinoline)
		d	141.57 (CH,furyl ring)
		i	148.54 (C,quinoline)
		k	197.08(C, carbonyl group)
		l	127.31 (C, ethylene group)
		m	120.52 (C, ethylene group)
		a,b,c,d,e,f, a,b,c,d, a,b,c,d g,h	110.18-133.55(2CH,1C, Quinoline,14 CH, H-Ar)
III		a	142.90 (CH,furyl ring)
		b	133.55 (C,quinoline)
		d	141.69 (CH,furyl ring)
		i	148.54 (C,quinoline)
		m	141.20 (C, pyrimidinone ring)
		a,b,c,d,e,f, a,b,c,d, a,b,c,d g,h	110.18-133.55(2CH,1C, Quinoline,14 CH, H-Ar)

(continued)

IV		a	142.90 (CH,furyl ring)
		b	133.55 (C,quinoline)
		d	141.73 (CH,furyl ring)
		i	148.55 (C,quinoline)
		l	105.52 (C, pyrimidinone ring)
		a,b,c,d,e,f, a,b,c,d, a,b,c,d g,h	110.19-130.65(2CH,1C, Quinoline,14 CH, H-Ar)
V		a	142.81 (CH,furyl ring)
		b	134.63 (C,quinoline)
		d	143.21 (CH,furyl ring)
		i	148.01 (C,quinoline)
		l	39.98 (CH ₂ , pyrazoline ring)
		m	62.87 (CH, pyrazoline ring)
		a,b,c,d,e,f, a,b,c,d,e,f, a,b,c,d, a,b,c,d g,h	110.47-130.21(2CH,1C, Quinoline,20 CH, H-Ar)

(continued)

VI		l	30.95 (CH ₂ , pyrazoline ring)
VII		a b d i l m a,b,c,d,e,f, a,b,c,d, a,b,c,d g,h	142.93 (CH,furyl ring) 131.22 (C,quinoline) 141.22 (CH,furyl ring) 148.52 (C,quinoline) 36.03 (CH ₂ , pyrazoline ring) 56.76 (CH, pyrazoline ring) 106.07-130.61(2CH,1C, Quinoline,14 CH, H-Ar)

(continued)

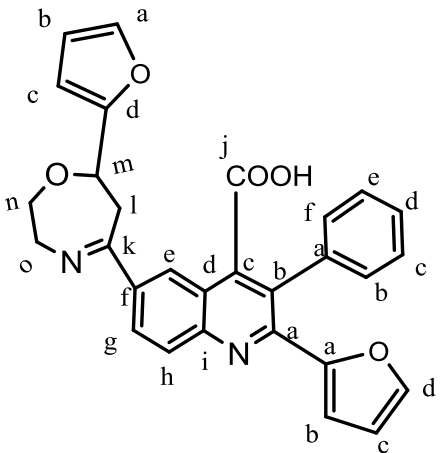
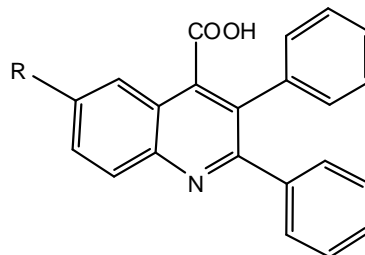
VIII		a	142.93 (CH,furyl ring)
		b	134.11 (C,quinoline)
		d	141.22 (CH,furyl ring)
		i	146.59 (C,quinoline)
		l	30.96 (C, CH ₂)
		m	45.44 (C, CH)
		n	56.76 (C, CH ₂)
a,b,c,d,e,f, a,b,c,d, a,b,c,d g,h	106.07-131.22(2CH,1C, Quinoline,14 CH, H-Ar)		

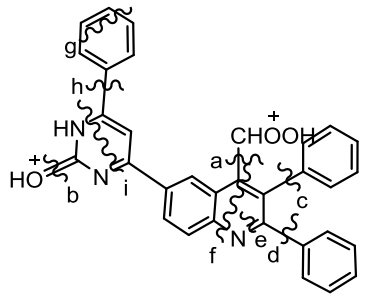
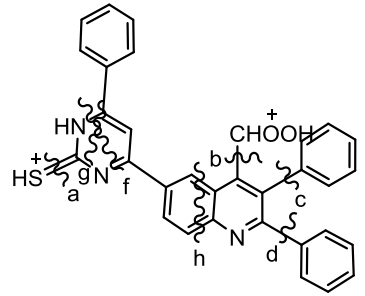
Table 2.12: Gas chromatography- mass spectroscopy (GCMS) data of the prepared compounds

Table (2.12.1): Liquid chromatography- mass spectroscopy (GCMS) 2, 3-diphenylquinoline-4-carboxylic acid derivatives

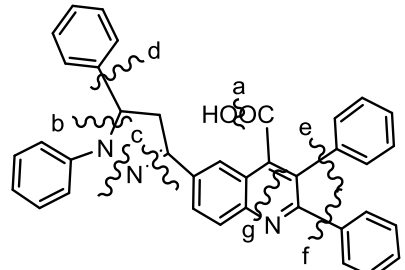
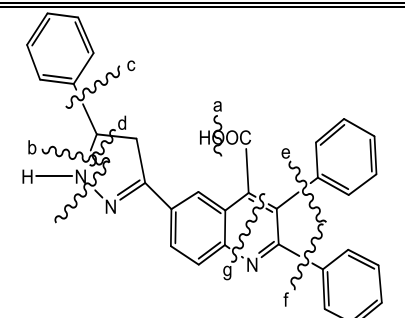
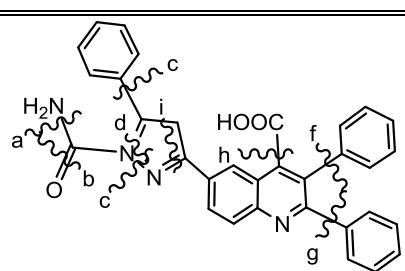


Comp .No	Structure of compound	Retention time min	M.wt Calculated	M ⁺ m/s	Mass Spectral Fragmentation	
					path of Fragment lost	Peak obtained m/s
I		0.1-0.2	367.40	367.4392	$a+b = [M^+ - (C_2H_3O + Ph)]^+ m/s$	248.1108
					$a+b+c = [M^+ - (C_2H_3O + Ph + COOH)]^+ m/s$	205.0810
					$d = [M^+ - (2 Ph + C_3N + COOH)]^+ m/s$	124.0515
					$e = [M^+ - (2 Ph + C_5N + COOH)]^+ m/s$ (Base peak)	97.0734
II		0.1	455.51	455.52	$a = [M^+ - H_2O]^+ m/s$ (Base peak)	437.1802
					$a+b = [M^+ - (C_7H_7 + H_2O)]^+ m/s$	362.3149
					$c = [M^+ - 2 Ph]^+ m/s$	303.1102
					$c+d = [M^+ - (2 Ph + COOH)]^+ m/s$	256.2547
					$e = [M^+ - (2 Ph + COOH + quin)]^+ m/s$	119.0812

(continued)

III		0.1	495.54	497.54 [M ⁺ +2]	a = [M ⁺ - COO ⁺ H ₂] ⁺ m/s	453.1538
					a+b=[M ⁺ - (H ₂ O ⁺ + COO ⁺ H ₂) ⁺ m/s	437.1803
					i+c=[M ⁺ - (H ⁺ NCON ⁺ H + ph)] ⁺ m/s	364.4280
					a+b+c=[M ⁺ - (H ₂ O ⁺ + COO ⁺ H ₂ + ph)] ⁺ m/s	362.31555
					a+i=[M ⁺ - (COO ⁺ H ₂ + H ⁺ NCON ⁺ H)] ⁺ m/s	318.2902
					a+b+c=[M ⁺ - (H ₂ O ⁺ + COO ⁺ H ₂ + 2ph)] ⁺ m/s	287.0726
					a+b+c+d+e=[M ⁺ - (H ₂ O ⁺ + COO ⁺ H ₂ + 2ph + N)] ⁺ m/s	274.2651
					a+b+c+d+g=[M ⁺ - (H ₂ O ⁺ + COO ⁺ H ₂ + 2ph + H ⁺ CC ⁺ H)] ⁺ m/s	264.1044
					a+b+f=[M ⁺ - (H ₂ O ⁺ + COO ⁺ H ₂ + 2 ph ⁺ CCN ⁺ H)] ⁺ m/s (Base peak)	248.1110
					g+f=[M ⁺ - (H ⁺ CC ⁺ H + 2 ph ⁺ CCN ⁺ H)] ⁺ m/s	219.0705
					f+h+i = [M ⁺ - (2 ph ⁺ CCN ⁺ H + ph + H ⁺ NCON ⁺ H)] ⁺ m/s	133.0926
IV		0.1-0.9	511.60	513.609 [M ⁺ +2]	a = [M ⁺ - (H ₂ S)] ⁺ m/s	513.609
					g=[M ⁺ - H ₂ SCN ⁺ H] ⁺ m/s	453.1528
					a+b= [M ⁺ - (H ₂ S ⁺ + COO ⁺ H ₂)] ⁺ m/s	437.1793
					b+g=[M ⁺ - (COO ⁺ H ₂ + H ₂ SCN ⁺ H)] ⁺ m/s	408.0863
					b+f=[M ⁺ - (COO ⁺ H ₂ + H ⁺ NCSN ⁺ H)] ⁺ m/s	364.4280
					a+b+c=[M ⁺ - (H ₂ S ⁺ + COO ⁺ H ₂ + ph)] ⁺ m/s	362.3145
					a+b+c+d=[M ⁺ - (H ₂ S ⁺ + COO ⁺ H ₂ + 2ph)] ⁺ m/s	318.2902
					h=[M ⁺ - (C ₄ H ₃ ⁺ + C ₄ HN ₂ S ⁺ + ph)] ⁺ m/s	274.2644
b+c+d+f=[M ⁺ - (H ₂ S ⁺ + COO ⁺ H ₂ + 2ph)] ⁺ m/s	248.1101					

(continued)

V		0.2	545.64	545.15	$a = [M^{+} - H_2O]^{+}m/s$	528.6429
					$a+b = [M^{+} - (H_2O+NH)]^{+}m/s$	515.1705
					$a+c = [M^{+} - (H_2O + PhNH)]^{+}m/s$	437.1430
					$a+c+d = [M^{+} - (H_2O + PhNH + Ph)]^{+}m/s$	360.2829
					$a+b+c+d = [M^{+} - (H_2O + PhNH + NH + Ph)]^{+}m/s$	274.2426
					$a+b+c+d+e+f = [M^{+} - (H_2O + PhNH + PhNH + 2Ph)]^{+}m/s$	197.6307
					$g = [M^{+} - (C_2N + 2Ph)]^{+}m/s$	357.2754
VI		0.2	469.54	469.53	$a = [M^{+} - H_2O]^{+}m/s$	452.5314
					$b = [M^{+} - NH]^{+}m/s$	456.2347
					$a+b = [M^{+} - (H_2O+NH)]^{+}m/s$	437.1435
					$a+b+c = [M^{+} - (H_2O+NH+Ph)]^{+}m/s$	360.2829
					$b+c = [M^{+} - (NH+Ph)]^{+}m/s$	300.2560
					$a+d+f = [M^{+} - (H_2O+PhCNH+Ph)]^{+}m/s$	274.2430
					$g = [M^{+} - (C_3COOH+2Ph)]^{+}m/s$	236.0916
VII		0.2	512.57	512.53	$a = [M^{+} - H_2O]^{+}m/s$	498.1105
					$b = [M^{+} - NH]^{+}m/s$	496.0745
					$b = [M^{+} - NH_2CONH]^{+}m/s$	453.1159
					$d+e = [M^{+} - (NH_2CONH+Ph)]^{+}m/s$	362.2858
					$f+g+h = [M^{+} - (2Ph+COOH)]^{+}m/s$	317.3722
					$i+f = [M^{+} - (NH_2CONHCPh + Ph)]^{+}m/s$	274.2432

(continued)

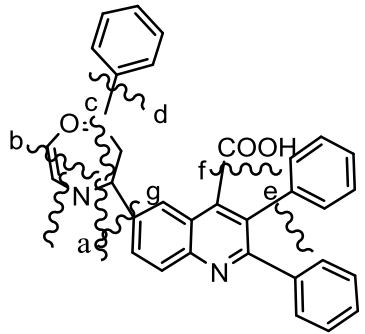
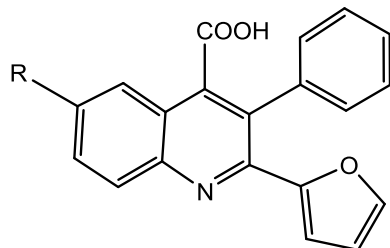
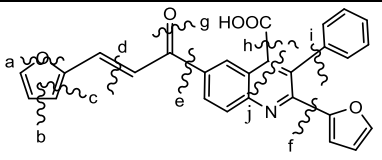
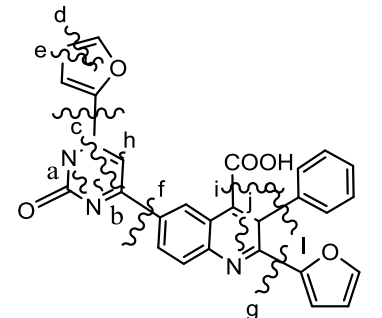
VIII		498.58	498.07 500.12 [M ⁺ +2]	a = [M ⁺ - H ₂ O] ⁺ m/s	482.5768
				b = [M ⁺ - C ₂ H ₂ O] ⁺ m/s	453.1155
				c = [M ⁺ - NC ₂ H ₂ O] ⁺ m/s	438.5120
				c+f = [M ⁺ - (NC ₂ H ₂ O+COOH)] ⁺ m/s	359.5134
				c+d = [M ⁺ - (NC ₂ H ₂ O+Ph)] ⁺ m/s	362.2854
				c+d+f = [M ⁺ - (NC ₂ H ₂ O+Ph+COOH)] ⁺ m/s	318.2641
				c+d+e+f = [M ⁺ - (NC ₂ H ₂ O+2Ph+COOH)] ⁺ m/s	274.2429
				c+d = [M ⁺ - (NC ₂ H ₃ O+Ph+ Ph)] ⁺ m/s	249.2300

Table (2.12.2): Gas chromatography- mass spectroscopy (GCMS) of prepared 2 (furan-2-yl), 3-phenylquinoline-4-carboxylic acid derivatives

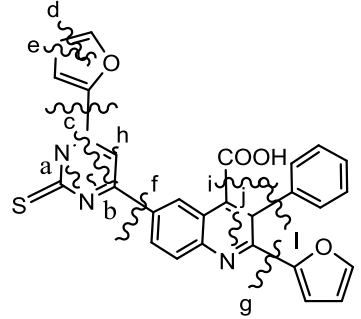
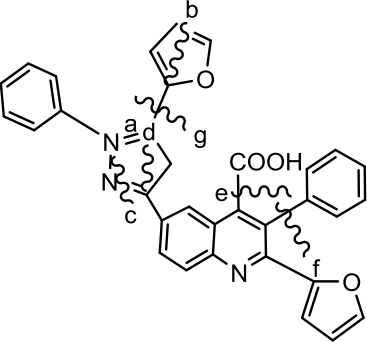


Comp. No	Structure of compound	Retention time min	M.wt Calculate d	M ⁺ m/s	Mass Spectral Fragmentation	
					path of Fragment lost	Peak obtained m/s
IX		0.2-0.9	357.37	357.34	a = [M ⁺ - H ₂ O] ⁺ m/s	340.1216
					b = [M ⁺ - CH ₃ CO] ⁺ m/s	318.2896
					c = [M ⁺ - furyl ring] ⁺ m/s	293.0684
					a+c = [M ⁺ - (H ₂ O+furyl ring)] ⁺ m/s	274.2646
					b+d = [M ⁺ - (CH ₃ CO+COOH)] ⁺ m/s	270.0755
					b+c = [M ⁺ - (CH ₃ CO+furyl ring)] ⁺ m/s	249.1106
					e = [M ⁺ - (CH ₃ COPh)] ⁺ m/s	242.1089
					c+f = [M ⁺ - (furyl ring+Ph)] ⁺ m/s	214.0785
					e+d = [M ⁺ - (CH ₃ COPh+COOH)] ⁺ m/s	197.0524
					b+g = [M ⁺ - (CH ₃ CO+furyl ringC'NHCPH)] ⁺ m/s	136.0707

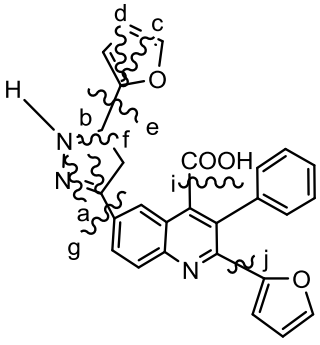
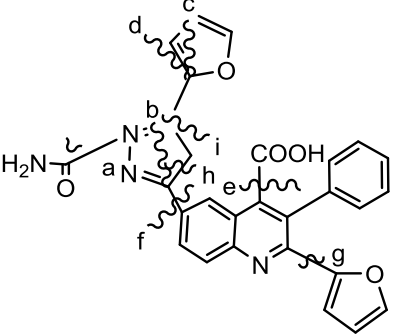
(continued)

X		0.1-0.9	435.44	437.17	$a = [M^{+} - H_2O]^{+}m/s$ $b = [M^{+} - CHCHO]^{+}m/s$ $c = [M^{+} - CHCHCHO]^{+}m/s$ $d = [M^{+} - (furyl\ ringCH)]^{+}m/s$ $e = [M^{+} - (furyl\ ringCHCH_3CO)]^{+}m/s$ $d+f+g = [M^{+} - (furyl\ ringCH +furyl\ ring +H_2O)]^{+}m/s$ $e+h = [M^{+} - (furyl\ ringCHCH_3CO + COOH)]^{+}m/s$ $e+f = [M^{+} - (furyl\ ringCHCH_3C'O +furyl\ ring)]^{+}m/s$ $d+c+f = [M^{+} - (furyl\ ringC'H + furyl\ ring+Ph)]^{+}m/s$ $e+j = [M^{+} - (furyl\ ringCHCH_3CO + furyl\ ringC'NHCPh)]^{+}m/s$	415.1983 393.0665 382.0928 360.1114 318.2898 274.2647 270.0755 248.1108 214.0786 136.0707
XI		0.1-0.9	475.46	477.41 [M ⁺ +2]	$a = [M^{+} - CO]^{+}m/s$ $b = [M^{+} - HN'C'O]^{+}m/s$ $c = [M^{+} - HN'CON'H]^{+}m/s$ $c+d = [M^{+} - (HN'CON'H+CHO)]^{+}m/s$ $c+e = [M^{+} - (HN'CON'H+CHCHO)]^{+}m/s$ $f = [M^{+} - (furyl\ ring+pyrimidenone\ ring)]^{+}m/s$ $c+g+h = [M^{+} - (HN'CON'H+furyl\ ring+furyl\ ringCH)]^{+}m/s$ $f+i = [M^{+} - ((furyl\ ring+pyrimidenone\ ring) + COOH)]^{+}m/s$ $f+g = [M^{+} - ((furyl\ ring+pyrimidenone\ ring)+furyl\ ring)]^{+}m/s$ $k+c+g+l = [M^{+} - (furyl\ ring + HN'CON'H+furyl\ ring + Ph)]^{+}m/s$ $f+j = [M^{+} - ((furyl\ ring+pyrimidenone\ ring) + furyl\ ringC'NHCPh)]^{+}m/s$	453.1534 437.1801 421.4500 398.0669 382.0931 318.2900 274.2649 270.0754 248.1108 214.0786 136.0709

(continued)

XII		0.1-0.9	491.52	493.61 [M ⁺ +2]	$a = [M^{++} - CS]^{+}m/s$ $b = [M^{++} - HN'CS]^{+}m/s$ $c = [M^{++} - HN'CSN'H]^{+}m/s$ $c+d = [M^{++} - (HN'CSN'H+CHO')]^{+}m/s$ $c+e = [M^{++} - (HN'CSN'H+CHCHO')]^{+}m/s$ $f = [M^{++} - (furyl\ ring+pyrimidenthione\ ring)]^{+}m/s$ $c+g+h = [M^{++} - (HN'CSN'H+furyl\ ring+furyl\ ringCH')]^{+}m/s$ $f+i = [M^{++} - ((furyl\ ring+pyrimidenthione\ ring) + 'COOH)]^{+}m/s$ $f+g = [M^{++} - ((furyl\ ring+pyrimidenthione\ ring)+furyl\ ring)]^{+}m/s$ $k+c+g+l = [M^{++} - (furyl\ ring+ HN'CSN'H+furyl\ ring+ Ph')]^{+}m/s$ $f+j = [M^{++} - ((furyl\ ring+pyrimidenthione\ ring) + furyl\ ringC'NHCPH)]^{+}m/s$	453.1531 437.1796 418.1256 398.0661 382.0926 318.2896 274.2646 270.0754 248.1106 209.0492 136.0452
XIII		0.1-0.2	525.56	525.54 527.54 [M ⁺ +2]	$a = [M^{++} - 'NH]^{+}m/s$ $b = [M^{++} - 'CHO']^{+}m/s$ $c = [M^{++} - 'NHPh]^{+}m/s$ $d = [M^{++} - 'NH'NHPh]^{+}m/s$ $b + d = [M^{++} - ('CHO' + 'NH'NHPh)]^{+}m/s$ $d + e + f = [M^{++} - ('NH'NHPh + 'COOH + 'Ph)]^{+}m/s$ $d + f + g = [M^{++} - ('NH'NHPh + 'Ph + furyl\ ring)]^{+}m/s$	512.4438 486.1252 437.1435 421.4500 393.1423 303.1096 279.3000

(continued)

XIV		0.0-0.1	449.47	451.11 [M ⁺ +2]	a = [M ⁺ - NH] ⁺ m/s	437.4700
					b = [M ⁺ - (NH NH)] ⁺ m/s	425.1121
					b+c = [M ⁺ - (NH NH + CHO)] ⁺ m/s	398.1435
					b+d = [M ⁺ - (NH NH + CHCHO)] ⁺ m/s	384.0405
					b+e = [M ⁺ - (NH NH + furyl ring)] ⁺ m/s	362.0610
					b+f = [M ⁺ - (NH NH + furyl ring CH)] ⁺ m/s	344.3900
					g = [M ⁺ - (pyrazole ring + furyl ring)] ⁺ m/s	318.3400
					b + i+j = [M ⁺ - (NH NH + COOH + furyl ring)] ⁺ m/s	306.0888
					b+f+j = [M ⁺ - (NH NH + furyl ring CH + furyl ring)] ⁺ m/s	274.2428
b+f+i+j = [M ⁺ - (NH NH + furyl ring CH + COOH + furyl ring)] ⁺ m/s	226.2700					
XV		0.1	492.49	492.07 494.06 [M ⁺ +2]	a = [M ⁺ - NH ₂ CO] ⁺ m/s	449.4700
					b = [M ⁺ - (NH NCONH ₂)] ⁺ m/s	422.0885
					b+c = [M ⁺ - (NH NCONH ₂ + CHCHO)] ⁺ m/s	384.0405
					b+e = [M ⁺ - (NH NCONH ₂ + CHCHCHO)] ⁺ m/s	360.2831
					f = [M ⁺ - (pyrazole ring + furyl ring)] ⁺ m/s	318.3400
					b + e+g = [M ⁺ - (NH NCONH ₂ + COOH + furyl ring)] ⁺ m/s	306.0888
					b+i+g = [M ⁺ - (NH NCONH ₂ + furyl ring CH + furyl ring)] ⁺ m/s	274.2428
b+h+e+g = [M ⁺ - (NH NCONH ₂ + furyl ring CH CH + COOH + furyl ring)] ⁺ m/s	214.0623					

(continued)

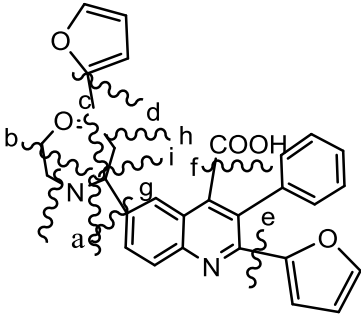
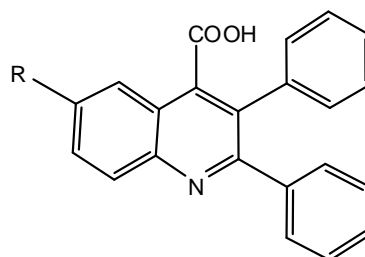
XVI		0.1-0.2	474.47	478.51	$a = [M^{++} - H_2O]^{+}m/s$	456.4900
				480.11	$b = [M^{++} - C_2H_2O]^{+}m/s$	437.1439
				$[M^{++}]$	$c = [M^{++} - NC_2H_2O]^{+}m/s$	421.4500
					$c+f = [M^{++} - (NC_2H_2O + COOH)]^{+}m/s$	360.2830
					$g = [M^{++} - (oxazepin\ ring + furyl\ ring)]^{+}m/s$	318.2854
					$c+h+e = [M^{++} - (NC_2H_2O + furyl\ ring\ 'CH + furyl\ ring\ ')]^{+}m/s$	274.2428
					$c+i+f+e = [M^{++} - (NC_2H_2O + furyl\ ring\ 'CH\ 'CH + COOH + furyl\ ring\ ')]^{+}m/s$	214.0623

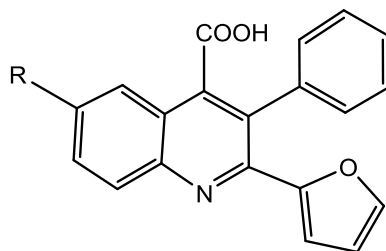
Table 2.13 Thin layer chromatography (TLC) data of the prepared compounds:

Table 2.13.1 thin layer chromatography (TLC) data of the prepared 2, 3-diphenylquinoline-4-carboxylic acid derivatives



Comp.No	R	Solvent system	R _f value
I		Chloroform9.8: 0.2.methanol	0.16
II		Chloroform9.8: 0.2.methanol	0.47
III		Chloroform9.8: 0.2.methanol	0.29
IV		Chloroform9.8: 0.2.methanol	0.26
V		Chloroform9.8: 0.2.methanol	0.32
VI		Chloroform9.8: 0.2.methanol	0.30
VII		Chloroform9.8: 0.2.methanol	0.47
VIII		Chloroform9.8: 0.2.methanol	0.43

Table 2.13.2: Thin layer chromatography (TLC) data of the prepared 2 (furan-2-yl), 3-phenylquinoline-4-carboxylic acid derivatives



Comp.No	R	Solvent system	R _f value
IX		Chloroform9.8: 0.2.methanol	0.47
X		Chloroform9.8: 0.2.methanol	0.33
XI		Chloroform9.8: 0.2.methanol	0.55
XII		Chloroform9.8: 0.2.methanol	0.49
XIII		Chloroform9.8: 0.2.methanol	0.56
XIV		Chloroform9.8: 0.2.methanol	0.17
XV		Chloroform9.8: 0.2.methanol	0.25
XVI		Chloroform9.8: 0.2.methanol	0.42

Table 2.14: Binding energy, bond interaction and Amino acid interaction of quinoline derivatives data set

No.	compd	Binding energy (S) (KJ/mol)	Number of bond interacted	Amino acid interaction	Interaction group	Bonds length
1	brequinar validation	-35.31	2 polar bonds	Arg 136	C=O of carboxylic acid OH of carboxylic acid	2.92 2.98
2	brequinar	-35.06	2 polar bonds	Arg 136	C=O of carboxylic acid OH of carboxylic acid	2.34 2.16
3	L1	-32.66	2 polar bonds	Arg 136	C=O of carboxylic acid OH of carboxylic acid	2.90 2.79
4	L2	-30.90	2 polar bonds	Arg 136	C=O of carboxylic acid OH of carboxylic acid	3.08 2.81
5	L3	-31.08	2 polar bonds	Arg 136	C=O of carboxylic acid OH of carboxylic acid	3.09 2.90
6	L4 ^T	-33.49	2 polar bonds	Arg 136	C=O of carboxylic acid OH of carboxylic acid	3.08 2.81
7	L11 ^T	-33.45	2 polar bonds	Arg 136	C=O of carboxylic acid OH of carboxylic acid	3.04 2.94
8	L12	-33.97	2 polar bonds	Arg 136	C=O of carboxylic acid OH of carboxylic acid	2.93 2.91
9	L16	-34,15	2 polar bonds	Arg 136	C=O of carboxylic acid OH of carboxylic acid	2.97 2.77
10	L18	-33.75	2 polar bonds	Arg 136	C=O of carboxylic acid OH of carboxylic acid	2.94 2.91
11	L22	-30.73	2 polar bonds	Arg 136	C=O of carboxylic acid OH of carboxylic acid	2.99 2.94
12	L24	-32.84	2 polar bonds	Arg 136	C=O of carboxylic acid OH of carboxylic acid	2.92 2.88
13	L26 ^T	-32.59	2 polar bonds	Arg 136	C=O of carboxylic acid OH of carboxylic acid	2.93 2.91

(continued)

14	L29	-26.42	2 polar bonds	Arg 136	C=O of carboxylic acid OH of carboxylic acid	3.08 2.75
15	L30	-35.81	1 polar bonds	Arg 136	Phenyl group	-
16	L31	-34.19	2 polar bonds	Arg 136	C=O of carboxylic acid OH of carboxylic acid	2.94 2.76
17	L32	-34.78	2 polar bonds	Arg 136	C=O of carboxylic acid OH of carboxylic acid	2.91 2.90
18	L33 ^T	-34.26	2 polar bonds	Arg 136	C=O of carboxylic acid OH of carboxylic acid	2.93 2.91
19	L34	-34.71	2 polar bonds	Arg 136	C=O of carboxylic acid OH of carboxylic acid	2.91 2.89
20	L35	-33.33	2 polar bonds	Arg 136	C=O of carboxylic acid OH of carboxylic acid	2.94 2.92
21	L36	-33.98	2 polar bonds	Arg 136	C=O of carboxylic acid OH of carboxylic acid	2.90 2.92
22	L39	-34.98	2 polar bonds	Arg 136	C=O of carboxylic acid OH of carboxylic acid	2.96 2.79
23	L40 ^T	-34.32	2 polar bonds	Arg 136	C=O of carboxylic acid OH of carboxylic acid	2.92 2.80
24	L42	-37.48	2 polar bonds	Arg 136	C=O of carboxylic acid OH of carboxylic acid	2.91 2.89
25	L43	-36.85	2 polar bonds	Arg 136	C=O of carboxylic acid OH of carboxylic acid	2.89 2.79
26	L44	-29.32	2 polar bonds	Arg 136 Phe 62	C=O of carboxylic acid OH of carboxylic acid Pi interaction	2.84 2.81 -

Table 2.15: Binding energy, Amino acid interacted, Type interaction and Bonds length for synthesized compounds with portion (iuuo) pocket as inhibition of human dihydroorotate dehydrogenase enzyme (DHODH)

No	compound	Energy bonds (S)	Amino acid interaction	Interaction group	Type of interaction	Bonds length
*	brequinar	-35.31	Arg138	O – carboxylic acid O=C carboxylic acid	Hydrogen bound Hydrogen bound	2.92 2.98
1	I	-1.33	-	-	-	-
2	II	11.61	-	-	-	-
3	III	-13.54	Ser305 Ser305 Asn145 Lys100	H – carboxylic acid O=C carboxylic acid O=C carboxylic acid phenyl	Hydrogen bound Hydrogen bound Hydrogen bound Pi interaction	3.64 2.72 2.41 -
4	IV	-2.38	Tys357 His56 Arg 138	O=C carboxylic acid Phenyl Phenyl	Hydrogen bound Pi interaction Pi interaction	- - -
5	V	21.95	-	-	-	-
6	VI	15.69	-	-	-	-
7	VII	11.93	-	-	-	-
8	VIII	21.07	Tys357	phenyl	Pi interaction	-
9	IX	-5.67	-	-	-	-
10	X	-3.17	Tyr356	H – carboxylic acid	Hydrogen bound	2.31

(continued)

11	XI	-0.07	Tyr356	H-amide	Hydrogen bound	3.01
12	XII	-	-	-	-	-
13	XIII	13.09	-	-	-	-
14	XIV	-13.29	Pro52	H-N-pyrazoline	Hydrogen bound	3.04
				Furyl	Pi interaction	-
15	XV	-0.03	Tyr356	H-amino	Hydrogen bound	3.71
16	XVI	-4.21	Ser305	H – O-carboxylic acid	Hydrogen bound	3.63
			Ser305	O=C carboxylic acid	Hydrogen bound	2.67
			Asn145	O=C carboxylic acid	Hydrogen bound	2.33
			Lys100	phenyl	Pi interaction	-

Table 2.16: Binding energy, Amino acid interacted, Type interaction and Bonds length for docking a new designed compounds with portion (iuuo) pocket as inhibition of human dihydroorotate dehydrogenase (DHODH)

No	compound	Energy bonds (S)	Amino acid interaction	Interaction group	Type of interaction	Bonds length
*	brequinar	-35.31	Arg 138	O – carboxylic acid O=C carboxylic acid	Hydrogen bound Hydrogen bound	2.92 2.98
1	A11	-17.62	Ala55	H – carboxylic acid	Hydrogen bound	2.74
2	A25	-13.33	Ala55	H – carboxylic acid	Hydrogen bound	2.17
3	A29	-18.91	Tyr 357	O=C carbonayl	Hydrogen bound	2.85
4	A32	0.93	-	-	-	-
5	A33	-23.06	-	-	-	-
6	B1	-8.55	-	-	-	-
7	B2	-9.78	Tys35	H – carboxylic acid	Hydrogen bound	2.70
8	B4	0.645	-	-	-	-
9	B8	2.54	Tys357	phenyl	Pi interaction	-
10	B11	28.24	-	-	-	-
11	B12	11.38	Tys357	O=C carboxylic acid H-o-phenyl	Hydrogen bound Pi interaction	2.79 -
12	B25	17.81	-	-	-	-
13	B29	-16.95	-	-	-	-
14	B32	38.17	-	-	-	-
15	B33	-22.19	-	-	-	-

(continued)

16	B34	-12.23	-	-	-	-
17	B35	8.95	His56	phenyl	Pi interaction	-
18	C	14.74	Arg136	H – carboxylic acid phenyl	Hydrogen bound Pi interaction	2.04 -
19	C4	31.91	-	-	-	-
20	C5	-3.89	-	-	-	-
21	C9	7.45	His56	H – carboxylic acid	Hydrogen bound	1.91
22	C11	-12.61	Arg136 Gin87 Arg136	H – carboxylic acid o-phenyl phenyl	Hydrogen bound Hydrogen bound Pi interaction	1.86 1.93 -
23	C12	-14.02	-	-	-	-
24	C13	22.44	Thr63	H-amino	Hydrogen bound	2.19
25	C15	1.62	Tyr356	phenyl	Pi interaction	-
26	C17	-1.95	-	-	-	-
27	C18	12.82	-	-	-	-
28	C19	8.01	-	-	-	-
29	C21	-5.57	-	-	-	-
30	C22	-10.05	-	-	-	-
31	C25	28.69	-	-	-	-
32	C26	-15.83	-	-	-	-

(continued)

33	C27	-10.68	Lle360 Thr63 Arg136	H – carboxylic acid H-amino phenyl	Hydrogen bound Hydrogen bound Pi interaction	2.23 2.39 -
34	C28	13.75	-	-	-	-
35	C29	-14.96	-	-	-	-
36	C30	-4.23	Tyr365	phenyl	Pi interaction	-
37	C31	21.56	Tyr365	phenyl	Pi interaction	-
38	C32	4.46	Tyr38	O=C carboxylic acid	Pi interaction	2.59
39	C33	-11.93	-	-	-	-
40	C34	-13.54	-	-	-	-
41	C35	18.64	-	-	-	-
42	D4	1.03	-	-	-	-
43	D11	39.87	Arg138 His56	Phenyl phenyl	Pi interaction Pi interaction	- -
44	D15	-11.66	-	-	-	-
45	D16	-13.01	Ser305 Asn145 Asn145 Lys100	H – carboxylic acid O=C carboxylic acid O=C carboxylic acid phenyl	Hydrogen bound Hydrogen bound Hydrogen bound Pi interaction	3.64 2.69 2.33 -

(continued)

46	D18	35.85	Arg136	phenyl	Pi interaction	-
47	D19	-8.66	-	-	-	-
48	D20	-15.07	Tyr356	O=C carboxylic acid H-amino	Hydrogen bound Pi interaction	2.08 3.71
49	D21	13.88	Tyr356	phenyl	Pi interaction	-
50	D29	-12.28	Tyr356	phenyl	Pi interaction	-
51	D32	18.99	-	-	-	-
52	D33	-21.6	-	-	-	-
53	E4	13.79	-	-	-	-
54	E10	-5.35	His56 Ala59 Thr63	H-o-phenyl H-o-phenyl H-o-phenyl	Hydrogen bound Hydrogen bound Hydrogen bound	1.80 2.57 1.96
55	E11	46.48	Arg136	phenyl	Pi interaction	-
56	E12	-20.10	-	-	-	-
57	E13	-7.92	Arg136 Ala55 Thr63	O=C amide O=C carboxylic acid H-o-phenyl	Hydrogen bound Hydrogen bound Hydrogen bound	2.06 2.74 2.19
58	E14	24.77	His56 Thr63	H-o-phenyl H-o-phenyl	Hydrogen bound Hydrogen bound	2.45 1.97
59	E15	-20.05	-	-	-	-

(continued)

60	E17	13.33	-	-	-	-
61	E18	18.18	-	-	-	-
62	E19	-2.52	-	-	-	-
63	E20	30.07	-	-	-	-
64	E21	-8.47	-	-	-	-
65	E25	31.15	Tyr63	H-o-phenyl	Hydrogen bound	1.82
66	E29	-17.92	Tyr38	H-o-phenyl	Hydrogen bound	2.58
67	E32	-5.89	-	-	-	-
68	E33	-21.71	-	-	-	-
69	E34	-9.84	-	-	-	-
70	E35	6.03	Tyr38	H-o-phenyl	Hydrogen bound	1.84
			Tyr38	phenyl	Pi interaction	-

CHAPTER THREE

Discussion

3.DISCUSSION

3.1 QSAR Study

The set of selected compounds reported by Das *et al.* (Das *et al.*, 2013) was used to QSAR study. Only 25 compounds have were selected from three combine set according to which that compounds have F, Br, and H atom in position R, and also phenyl, alkyl and heterocycle group in position R¹. Structure of compound with substitution of R and R¹ position and their biological activity as inhibit *in vitro* VSV replication in MDCK epithelial cells were reported.

These compounds were evaluated for their ability to inhibit VSV replication in MDCK epithelial cells in terms of half maximal effective concentration (EC₅₀) values. For the purpose of modeling study, all 25 derivatives were divided into training and test sets. Out of the 25 derivatives, fifth compounds were placed in the test set for the validation of derived models. The biological activities of 25 compounds transformation to pEC₅₀ (Table 2.1). After 8 descriptors were selected (logPo/w, MR, AM1-Hf, AM1-dipole, ASA-P, Chi0, density and AM1-P) (Table 2.2).

Where:

LogPo/w (Octanol/Water Partition Coefficient) is defined as the ratio of the concentration of a chemical in n-octanol and water at equilibrium at a specified temperature. LogP used in drug discovery processes to estimate the solubility, membrane permeability, and bioavailability of compounds (Ogata *et al.*, 2018).

MR (Molar refractivity) is a measure of the total polarizability of a mole of a substance and is dependent on the temperature, the index of refraction, and the pressure (Shukla *et al.*, 2012).

HF (Heat of formation) is defined as the amount of heat absorbed or evolved at 25° C and at one atmosphere pressure when one mole of a compound is formed from its constituent elements, each substance being in its normal physical state (gas, liquid, or solid) (Bettely, 2018).

Dipole (dipole moment) is a measurement of the separation of two opposite electrical charges. In chemistry, dipole moments are applied to the distribution of electrons between two bonded atoms. The existence of a dipole moment is the difference between polar and nonpolar bonds. Molecules with a net dipole moment are polar molecules (Williems, 1993).

ASA-P (Total polar surface area) is defined as the sum of surface contributions of polar atoms (usually oxygens, nitrogens and attached hydrogens) in a molecule, has been shown to correlate well with drug transport properties, such as intestinal absorption, or blood-brain barrier penetration (Ertl *et al.*, 2000).

Chi₀ (Atomic connectivity index order zero) is practical graph-based topological index, introduced by Randić a quarter of a century ago and developed by Kier and Hall, that made possible a description of structure that is simple and demonstratively valuable in predictive power. Simply Chi₀ is the number of non-hydrogen atoms bonded in particular atom and with limited exception (Kier and Hall, 2002).

Density (the volumetric mass density) of a substance is its mass per unit volume. Is a steric parameter and parameter, is related with the bulk and size of the substituents (Mohring & Coville, 1992).

IP (ionization potential) is the energy necessary to remove an electron from the neutral atom (Kalil, 2003).

To study the correlation between the selected descriptors and pEC₅₀ was established. The value of the correlation coefficient for each pair of selected descriptors was examined. The greatest value of the correlation coefficient (0.859) is that belonging to the pair of descriptors logP_{o/w} and AM1-dipol.

The models obtained for the prediction of inhibitory concentration of 4- quinoline carboxylic acid derivatives, using 25 compounds, with highest significant models in four descriptors are given below:

$$pEC_{50} = 0.111305 - 0.56687AM1.dipole + 1.12247logP + 0.00702AM1.HF + 0.00732ASA.P$$

(model ¹)

$$pEC_{50} = 1.38478 - 0.49189AM1.dipole + 0.85383logP + 0.00642AM1.HF + 0.09659Chi_0$$

(model ²)

$$pEC_{50} = -4.38843 - 0.51373AM1.dipole + 1.01001logP + 0.00616AM1.HF + 0.09659 AM1.IP$$

(model ³)

The 4 relevant descriptors (variables) in Equations (1, 2 and 3) of 25 compound (n training =20 and n test set = 5) could explain 91.3%, 90.4% and 89.7% of the variance (adjusted coefficient of variation) of the inhibitory concentration. The difference between r² and q² of three models were be <0.1. These differences were less than 0.3, signifying the robustness of the models. While Equations were applied for prediction of test set

compounds, the predictive r^2_{pred} values for the test set were found to be $<r^2$. The values of all the statistical parameters, being within the acceptable limit, reflect the internal and external predictive potential of the developed models (Mitra *et al.*, 2012) (Table 2.4).

The highest significant models in three and two descriptors are given also below:

$$\text{pEC}_{50} = 2.43728 - 0.49571\text{AM1.dipole} + 1.01033\log\text{P} + 0.00731\text{AM1.HF} \text{ (model } ^4\text{)}$$

$$\text{pEC}_{50} = 2.00731 - 0.42239\text{AM1.dipole} + 0.95099\log\text{P} \text{ (model } ^5\text{)}$$

The 3 and 2 relevant descriptors (variables) in models (4 and 5) showed Criteria Model signifying the robustness of the two models.

The plot showing goodness of fit between observed and calculated activities for the training and test set compounds is given in Figure 3.1-3.3 for the best model (model ¹).

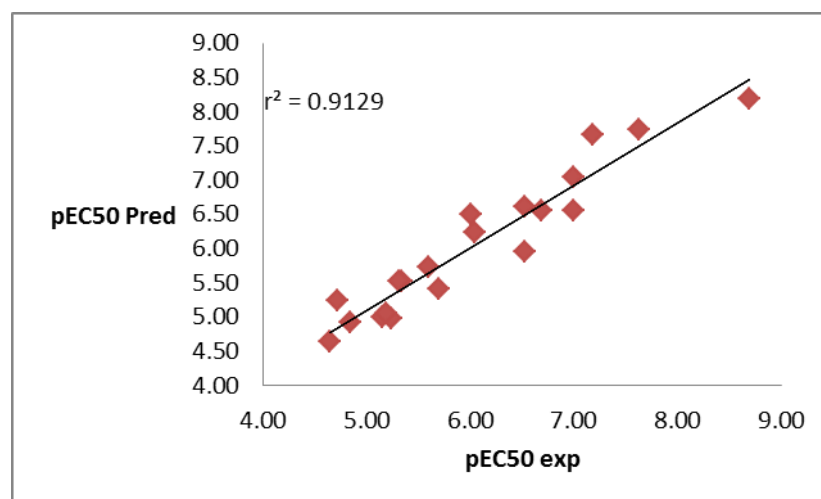


Fig 3.1: Plot of predicted training set versus experimental pEC₅₀ values for (model ¹).

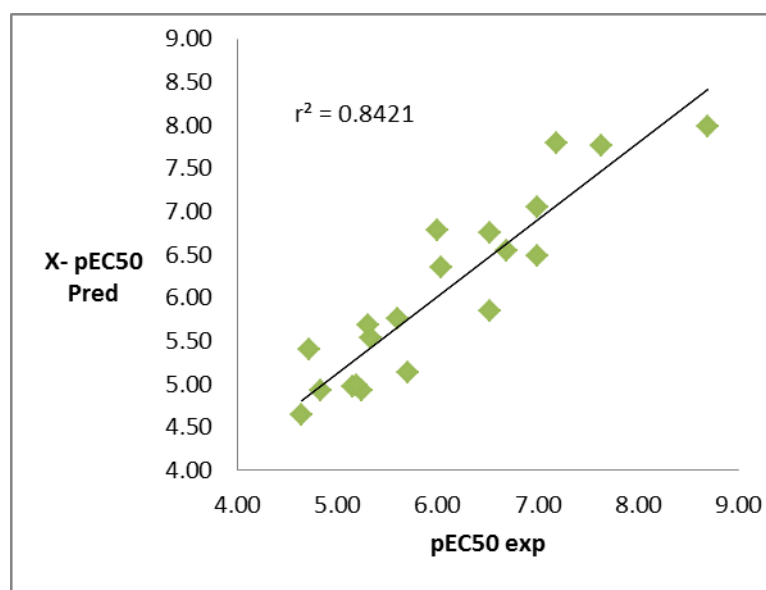


Fig 3.2: Plot of cross validation prediction versus experimental pEC₅₀ values for (model ¹).

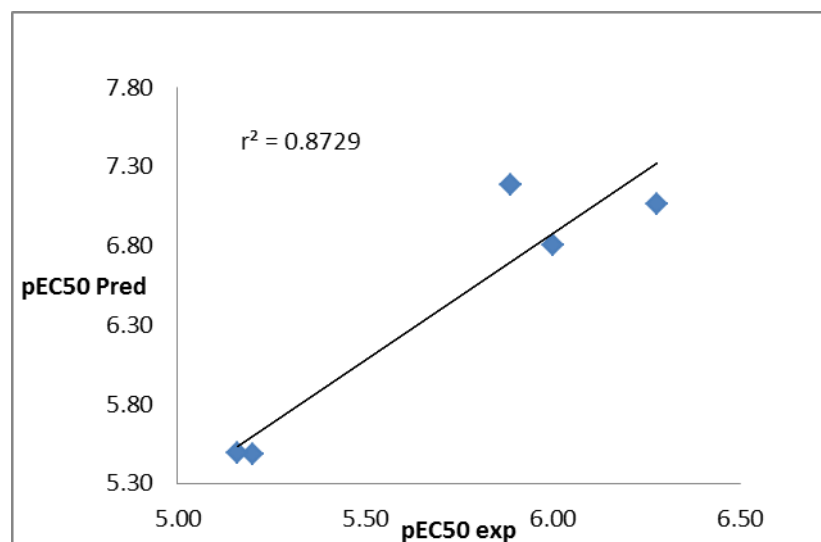


Fig 3.3: Plot of predicted test set versus experimental pEC₅₀ values for (model ¹).

The 180 quinoline derivatives were designed as new compounds of quinoline-4-carboxylic acids, and their descriptors were calculated. The model ¹ obtained from data was set used to predicted biological activity of a new quinoline compounds.

The biological activity predicted in the term of pEC₅₀ for designed new compounds showed good value mostly with derivative containing exactly pyrazoline ring that has 1-phenyl pyrazoline showing higher value. The pEC₅₀ higher values of designed new compounds were summarized in 13 compounds as their highest values (14.2 for compound C32, 13.71 for compound C18, 13.03 for compound C11, 12.9 for compound E32, 12.62 for compound B32, 11.95 for compound E18, 11.89 for compound C25, 11.51 for compound B33, 11.51 for compound C19, 11.11 for compound D25, 11.6 for compound D32, 10.55 for compound A32, 10.38 for compound B32 and 10.36 for compound B4) and pEC₅₀ higher values of synthesized were summarized in 2 compounds (11.36 for compound B18(v) and 11.28 for compound D18(v)). While the brequinar compound reference as inhibitor to human dihydroorotate dehydrogenase (DHODH) showed experimental pEC₅₀ value equal 6.52 which means that designed new derivatives have higher pEC₅₀ values of biological activity than brequinar (Table 2.5).

3.2 ADMET Study

Physicochemical properties were related to pharmacokinetic (PK) in term ADMET descriptors (absorption, distribution, metabolism, excretion and toxicity) of new designed quinoline -4-carboxylic acids derivatives and reference. The virtual screening results indicate that all the active derivatives followed Lipinski's "Rule of Five" for drug likeness properties compliance. The compound's hydrophilicity was measured through LogP value. Low hydrophilicity and therefore high LogP values might cause poor absorption or

permeation. It has been shown for compounds to have a reasonable probability of being well absorbed when their LogP value must not be >5. The virtual screening study for drug likeness mostly compounds A1-35 were within acceptable limits while other compounds showed higher log P. MW of 500 or less for good adoption. Some compounds showed higher MW indicating to low solubility.

All compounds having five or fewer hydrogen bond donor sites and 10 or fewer hydrogen bond acceptor sites (N and O atoms). Showed acceptable hydrogen bond donor and acceptor.

Typically, a low solubility goes along with a bad absorption, and therefore the general aim is to avoid poorly soluble compounds.

The LogS of a compound significantly affected its absorption and distribution characteristics. The calculated LogS values of studied active compounds were within acceptable limits, LogS should be more than -5.7 values.

Topological polar surface area (TPSA) allows prediction of transport properties of drug candidates in the intestines and blood–brain barrier crossing. The low score of TPSA suggested that this molecule preferentially acts as hydrophobic in nature and can easily transport through the blood brain barrier. Generally, it has been seen that passively absorbed molecules with a $PSA > 140 \text{ \AA}^2$ (less than 140 \AA^2 or equal to 140 \AA^2) are thought to have low oral bioavailability. Anew design compounds showed acceptable value of TPSA .

The metabolism of most drugs that takes place in the liver is associated with large and hydrophobic compounds. Higher lipophilicity of compounds leads to increased metabolism and poor absorption, along with an increased probability of binding to undesired hydrophobic macromolecules, thereby increasing the potential for toxicity (Mathew *et al.*, 2016) (Table 2.6).

3.3 Docking Study:

Vesicular stomatitis virus (VSV) is an enveloped, nonsegmented, negative-stranded RNA virus and the prototype member of the family Rhabdoviridae (Hong *et al.*, 2005) and its membrane glycoprotein G (VSVG) are often used as models to study endocytosis) and secretory traffic. For the same reasons, VSVG is often used for pseudo typing of retroviral vectors for gene delivery (Arakaki *et al.*, 2008).

The dihydroorotate dehydrogenase (DHODH) is the fourth enzyme in the de novo pyrimidine nucleosides biosynthetic pathway (Schröder *et al.*, 2005). Pyrimidine nucleotides play a critical role in cellular metabolism serving as activated precursors of

RNA and DNA, CDPdiacylglycerol phosphoglyceride for the assembly of cell membranes and UDP-sugars for protein glycosylation and glycogen synthesis (Evans *et al.*, 2004).

Therefore (DHODH) is considered as a key enzyme in biosynthesis pathway in most prokaryotic and eukaryotic cells (Ohishi *et al.*, 2018). The therapeutic potential of inhibiting de novo pyrimidine biosynthesis at the dihydroorotate dehydrogenase (DHODH) catalyzed step is revealed by the antiproliferative agents leflunomide and brequinar (Palmer *et al.*, 2009).

To develop a deeper insight into the molecular mechanism of 4- quinoline carboxylic acid derivatives as human dihydroorotate dehydrogenase (DHODH) inhibitor comprising the compounds : brequinar (reference), L12, L32, L42, L43 and L44 were simulated computationally to the active sites of human (DHODH) protein (PDB code: 1UUO).

Figure (3.4) shows structure of human (DHODH) protein (1UUO) that was imported from PDB. Human (DHODH) protein consisted of active site as shown in Figure 3.5.

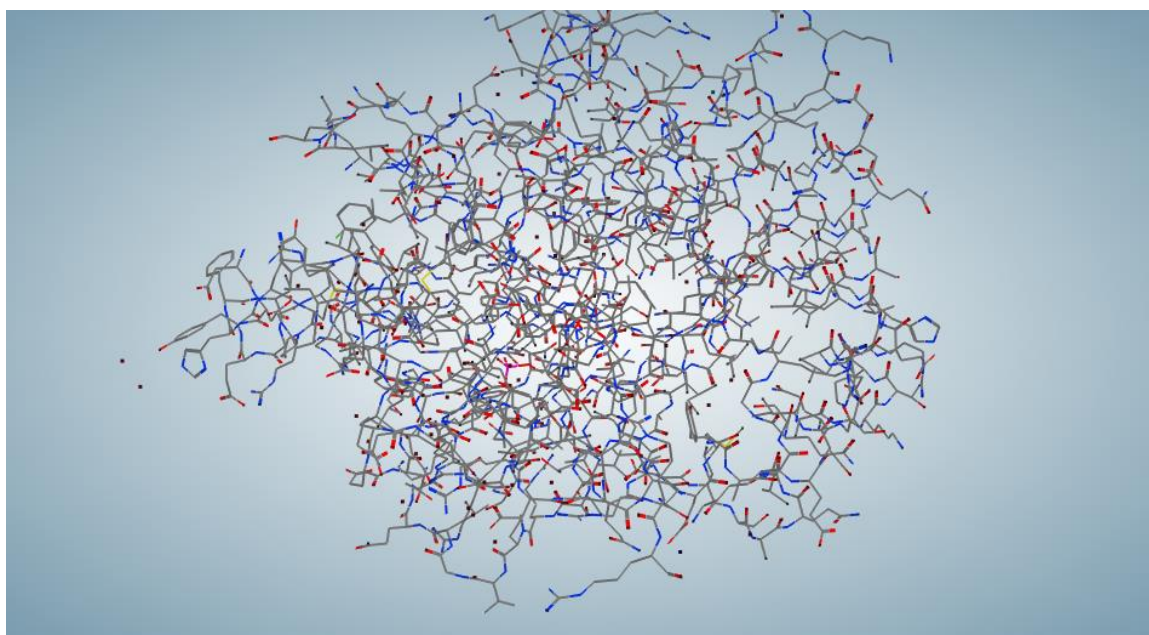


Figure 3.4: Structure of human (DHODH) protein (PDB code: 1UUO).

Silico molecular docking results, produced the different docking conformations based on binding energy. The variants with the minimal energy of the enzyme–inhibitor complex were selected for studies of binding mode. Preferred docked conformations of most of the ligands have formed one cluster inside the active (Arif *et al.*, 2017).

All the docked conformations for each compound were analyzed and it was found that the most favorable docking poses with maximum number of interactions were those which were ranked the highest, based on the minimal binding energy computed as a negative value by the software.

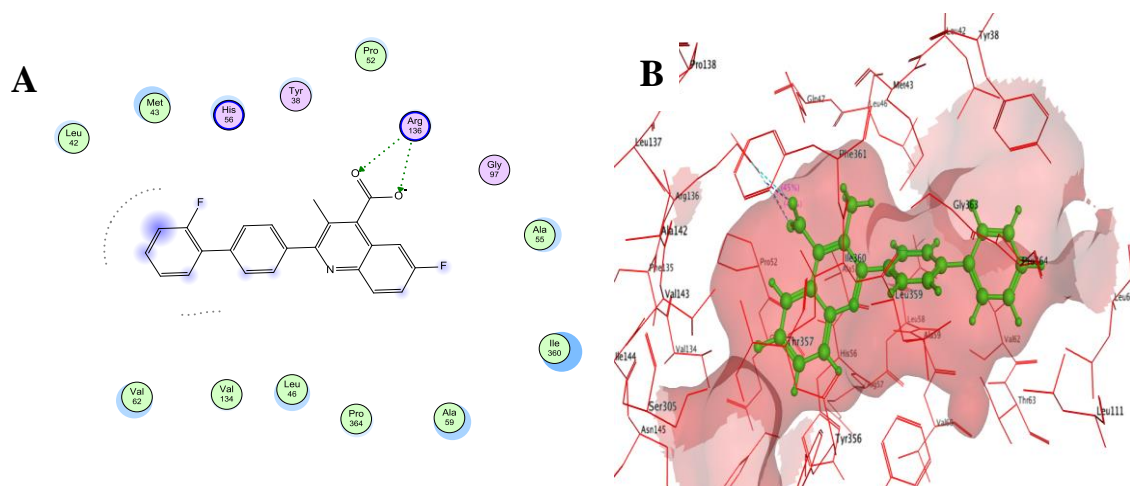


Fig 3.5: (a) active sites of human (DHODH) protein with brequinar ligand.
 (b) Ligand interaction with protein.

The most favorable docking poses of the 25 docked conformations of data set for each compound were analyzed to investigate further the interactions of the docked conformations within the active sites.

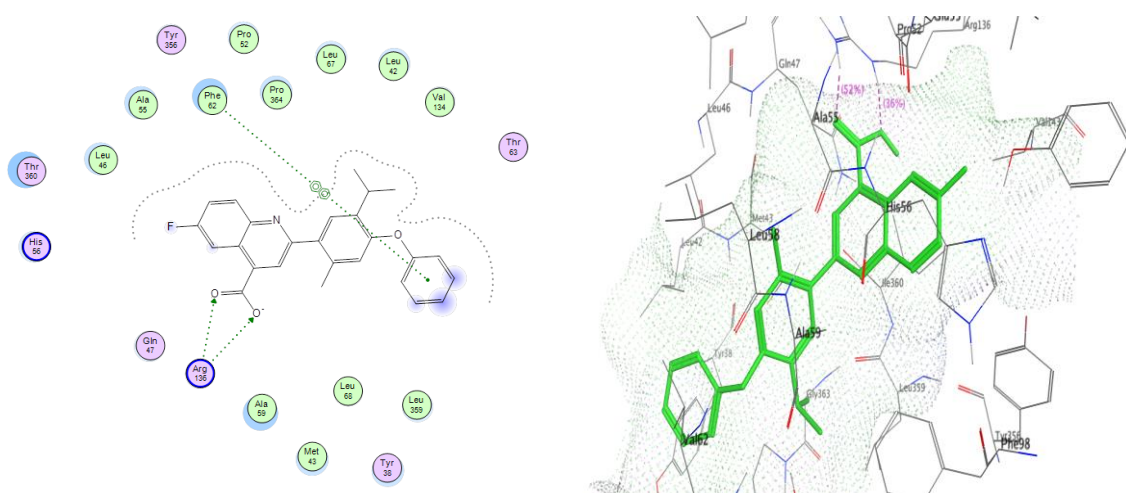


Fig 3.6: 2D and 3D models of biochemical interactions of compound L44 with DHODH enzyme: ● polar ● greasy ⊕ +arene-cation

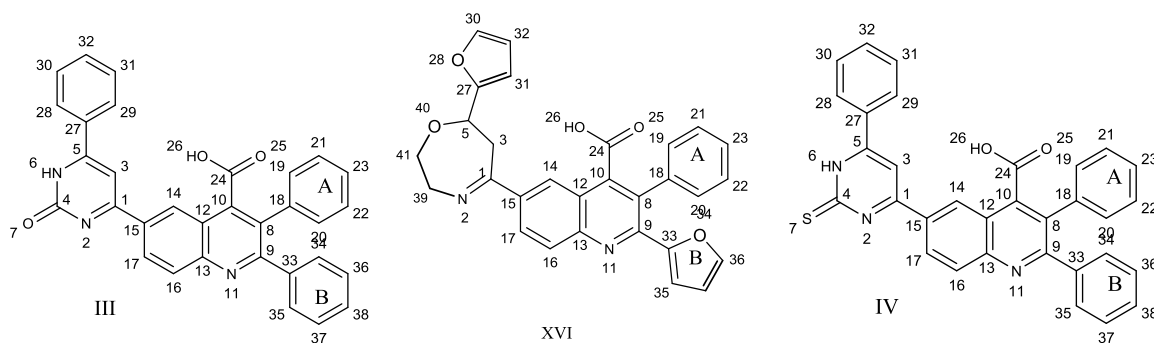
The active sites consisting of hydrophilic amino acids (His56, Tyr38, Arg136 and Gly 97) and the hydrophobic portions were constructed (Ala55, Ile360, Pro364, Ala59, Val134, Val62, Leu42, Met43 and Pro52).

All the ligands showed strong polar interactions with Arg136 by two oxygen atoms in carboxylic group as hydrophilic interaction.

Strong hydrogen bonding interactions of ligands with Arg136 showed bond distances in the range from 2.77 to 3.09 Å. Noted that the binding free energies (S) in Escore-1 (London dG) for 25 ligands were in the different ranges from -26.42 to -37.48 kcal/mol.

Although compound L44 showed higher biological activity than others showed, it had lower binding free energy "S" (-29.32 kcal/mol). The Pi-interaction between phenyl ring in compound L44 and phenyl ring in Phe62 beside to two hydrogen bonding interactions mentioned above, might explain the higher experimental activity ($EC_{50} = 0.002 \mu\text{M}$) of compound L44 than experimental activity of stranded brequinar ($EC_{50} = 0.03 \mu\text{M}$) with docking score (-32.16 kcal/mol) as shown in Figure 3.6 and table 2.14.

The docking study of synthesized quinoline derivatives listed in Table 2.15. Compounds I-XVI showed low docking score range from -0.03 to -13.54 kcal/mol compared with brequinar (-32.16 kcal/mol). The seven compounds failed to show interaction with the amino acid in the docking study. The best docking interactions between ligands and amino acid was assigned to compounds IV and VIII. Two Compounds forming the same interactions, 3 H- bonds and one pi- interaction.



Two H- bonds interactions between H26 and O25 of carboxylic acid with hydrogen and oxygen of hydroxyl group were shown in Ser305. Third H- bond interactions between O25 of carboxylic acid with hydrogen of hydroxyl group was shown in Asn145. The length bond of 3 H- bonds in compound III was at 3.64, 2.72 and 2.31 and length bond in compound XVI was at 3.63, 2.67 and 2.33 Å, respectively. Pi- interaction between phenyl ring B in III and furyl ring B in compound XVI with amino group was in Lys100 (Figures 3.7 and 3.8.

Although lower binding free energy "S" of both Compounds III (-13.54 kcal/mol) and XVI (-4.21 kcal/mol) was observed, higher interactions were shown similar to compound L44. thus Compounds III and XVI were expected to show experimentally higher biological activity.

Compound IV showed one H- bonds interaction between O25 of carboxylic acid with hydrogen amino group in Tyr357 and two pi interactions between phenyl ring A with nitrogen atom in Arg136 and phenyl ring B with phenyl ring in His 65.

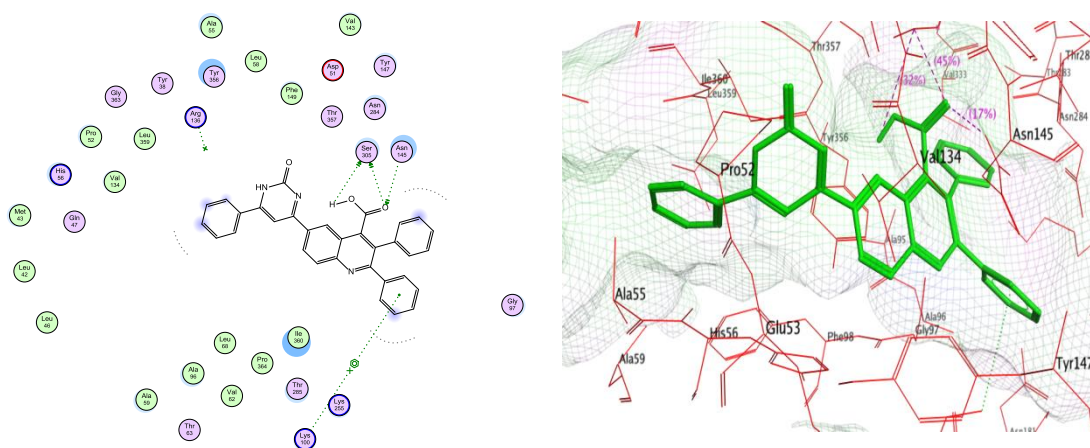


Fig 3.7: 2D and 3D models of biochemical interactions of compound III with DHODH enzyme: ● polar ● greasy ⊕ +arene-cation

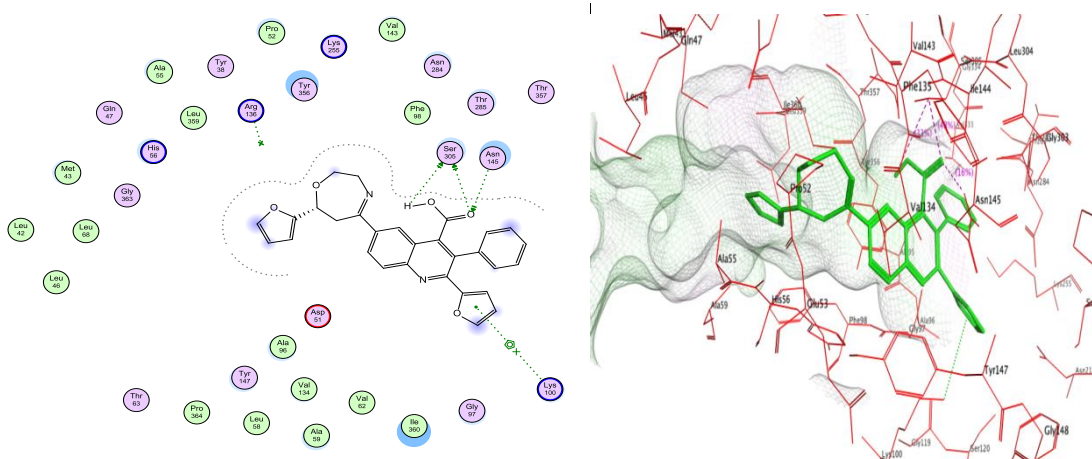


Fig 3.8: 2D and 3D models of biochemical interactions of compound XVI with DHODH enzyme: ● polar ● greasy ⊕ +arene-cation

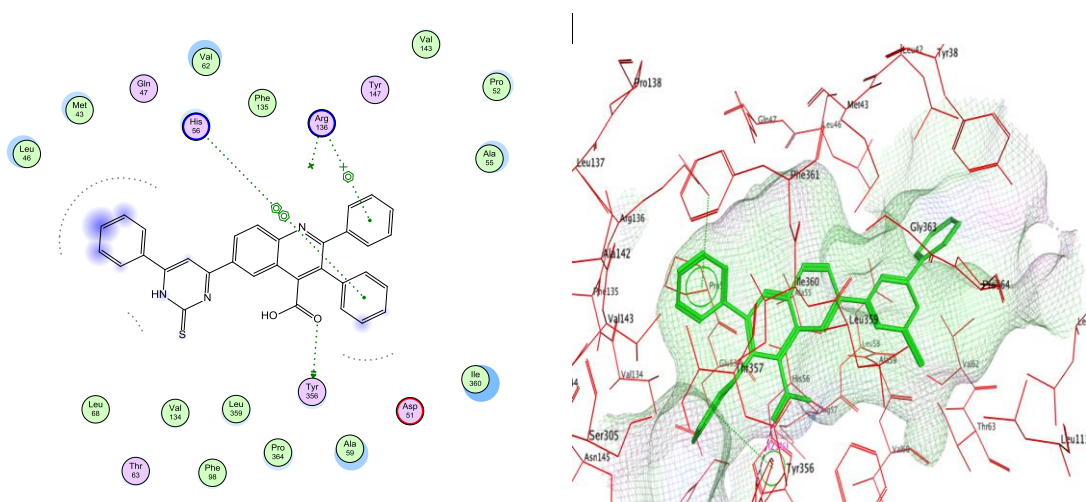


Fig 3.9: 2D and 3D models of biochemical interactions of compound IV with DHODH enzyme: ● polar ● greasy ⊕ +arene-cation

And other synthesized compounds showed interactions of one H- bonds or pi-interactions see Fig (3.10).

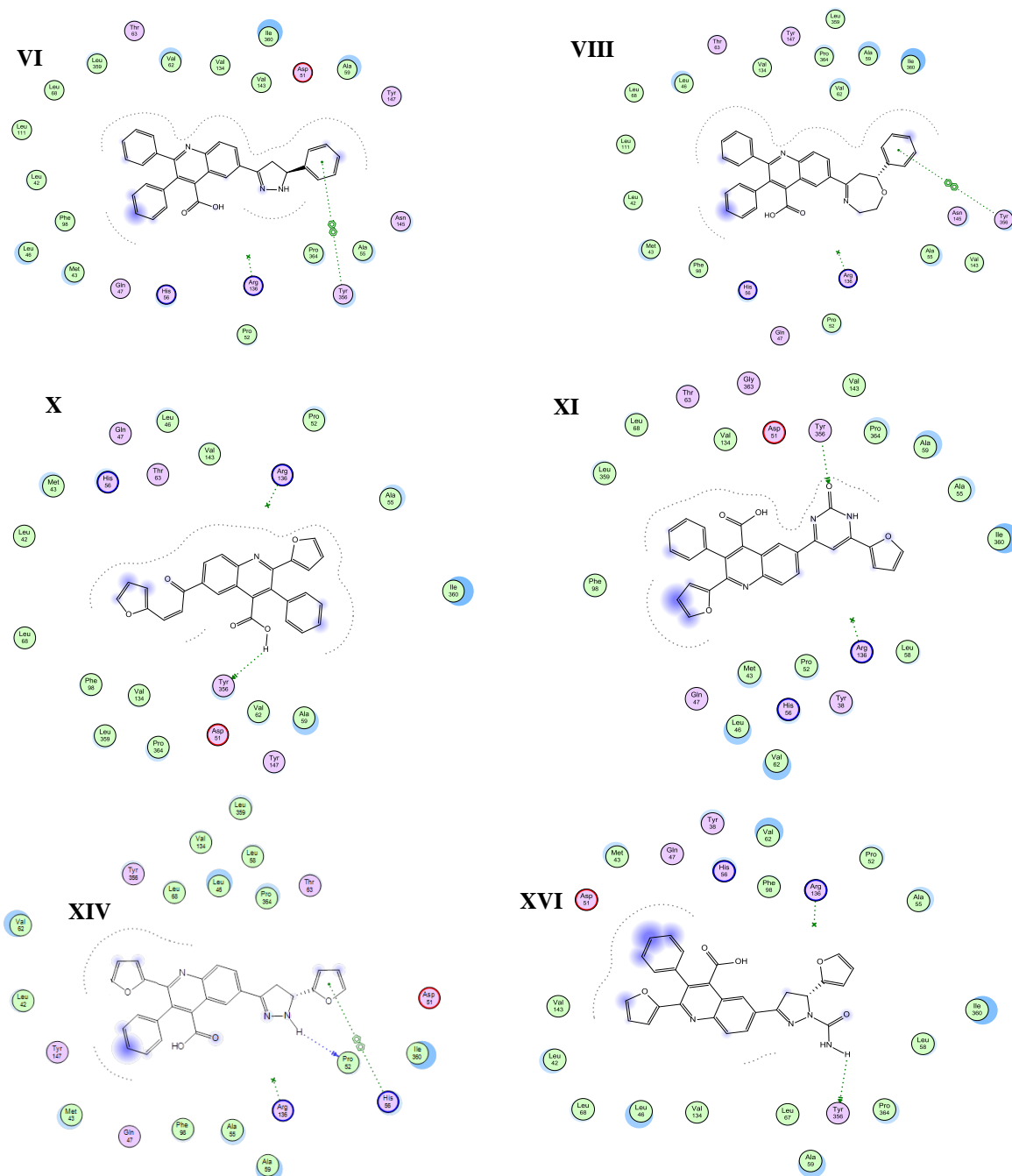
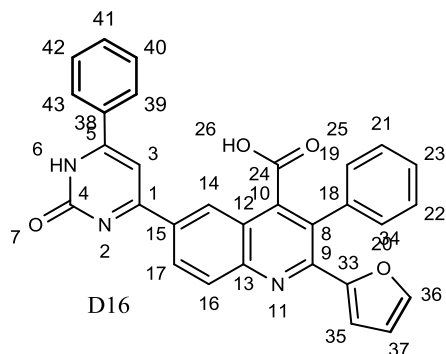


Fig 3.10: 2D models of biochemical interactions of other synthesized compounds with DHODH enzyme: ● polar ● greasy ⊕ arene-cation

From 180 new designed derivatives 70 derivatives were selected with higher predicted pEC₅₀ value to docking in human (DHODH) protein (PDB code: 1UUO). From 70 docked compounds, 26 compounds interacted with lower binding free energies (S) compared to berquinar. But these compounds showed higher interactions than berquinar. There are five compounds (D16, C11, C27, E10 and E13) showed higher interactions.



The binding free energy (ΔG) of Compound D16 is -13.009 kcal/mol and D16 forming 3 H-bond interactions and one pi- interaction.

Two H-bonds between H26 and O25 of carboxylic acid with hydrogen and oxygen of hydroxyl group were in Ser305. Third H-bond interaction between O25 of carboxylic acid with hydrogen of hydroxyl group was in Asn145. The length bond of 3 H-bonds at 3.64, 2.69 and 2.33 Å, respectively. While the Pi- interaction between furfuryl ring and amino group was in Lys100.

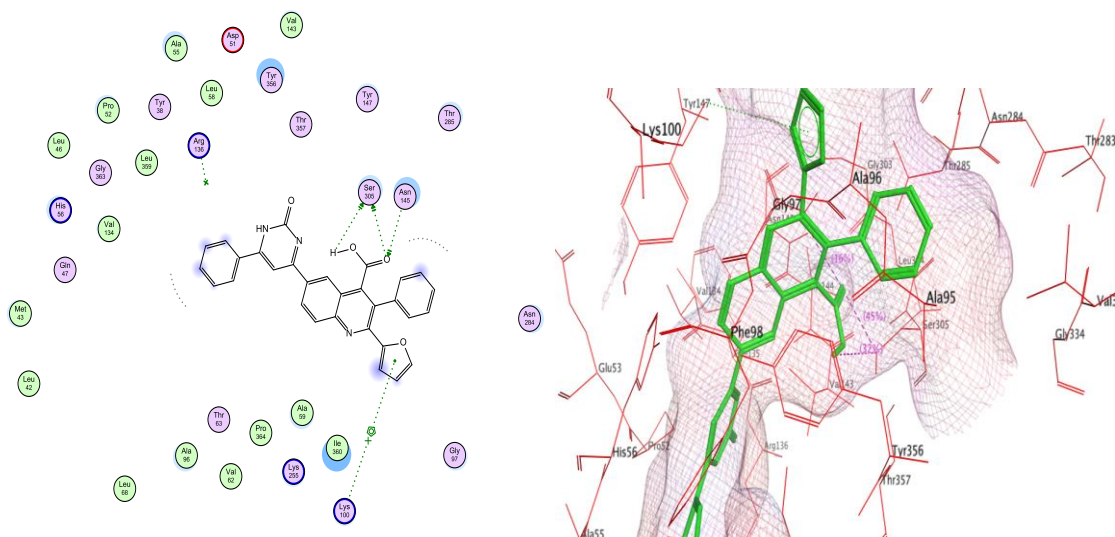
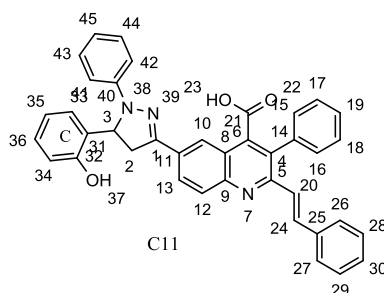


Fig 3.11: 2D and 3D models of biochemical interactions of compound D16 with DHODH enzyme: ● polar ● greasy ⊕ +arene-cation



The binding free energy (ΔG) of Compound C11 was -12.61 kcal/mol and showed 2 H-bonds interactions and one pi- interaction. Two H-bonds interactions were between H37 and O37 of hydroxyl in phenol group acid with oxygen of Ile36 and hydrogen of Gln47

with length 1.86 and 1.93 respectively. While the Pi-interaction between phenol ring C and methaniminum group in Arg136 (Figure 3.12).

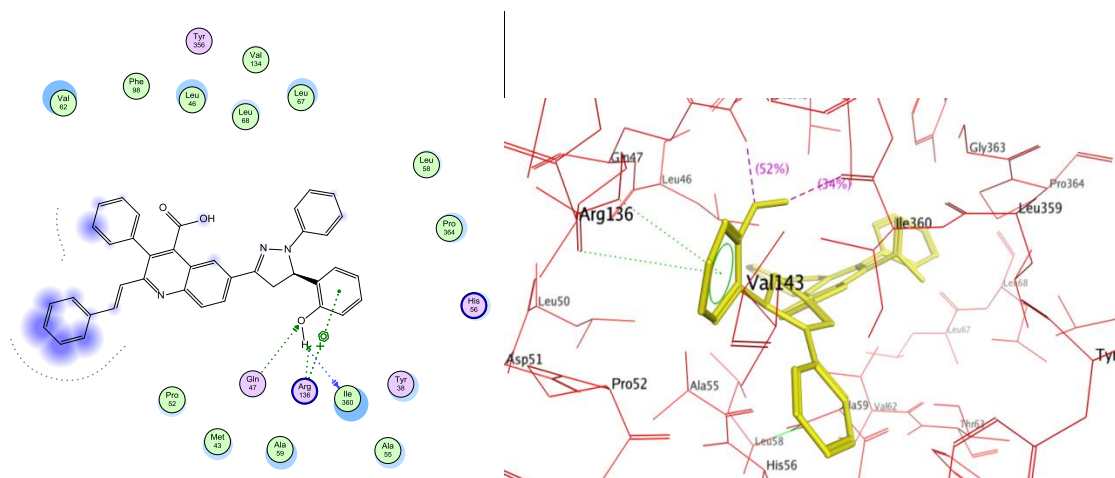
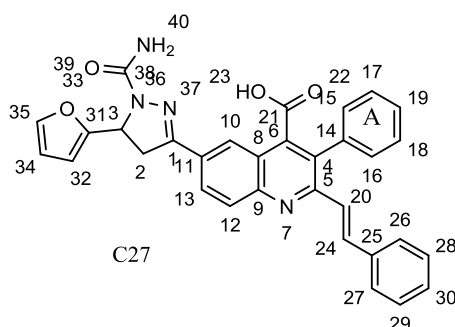


Fig 3.12: 2D and 3D models biochemical interactions of compound C11 with DHODH enzyme: ● polar ● greasy ● greasy ⊕ + arene-cation ⋯ → sidechain acceptor

Compound C27 had -10.68 Kcal/mol binding free energies (S) and three interactions, two H-bond interactions and pi- interaction.



Two H- bonds were between H23 in carboxylic acid and H40 in amino group with oxygen in Ile360 and Oxygen in Thr63 with length 2.23 and 2.39 Å, respectively. While the Pi-interaction between phenyl ring A and amino group was in Arg136.

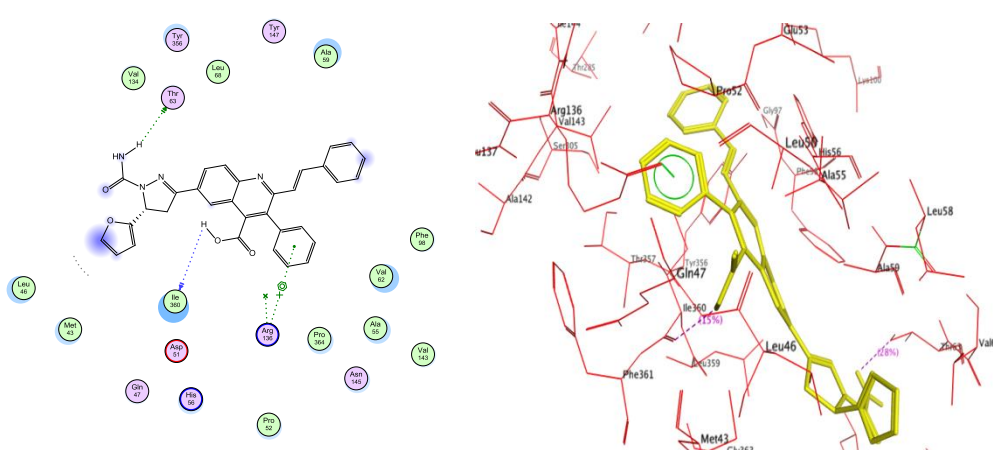
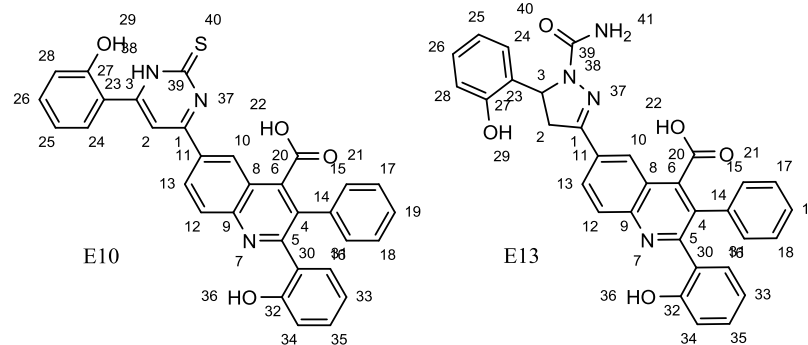


Fig 3.13: 2D and 3D models biochemical interactions of compound C27 with DHODH enzyme: ● polar ● greasy ● greasy ⊕ + arene-cation ⋯ → sidechain acceptor



Compound E10 showed binding free energies (S) -5.35 Kcal/mol and 3H-bond interactions between H29 in hydroxyl of phenol ring and N atom in His56, while two bond between H36 in phenol ring with oxygen atom in were shown Thr63 and Ala59. The length bonds at 1.80 , 2.57 and 1.97 Å, respectively.

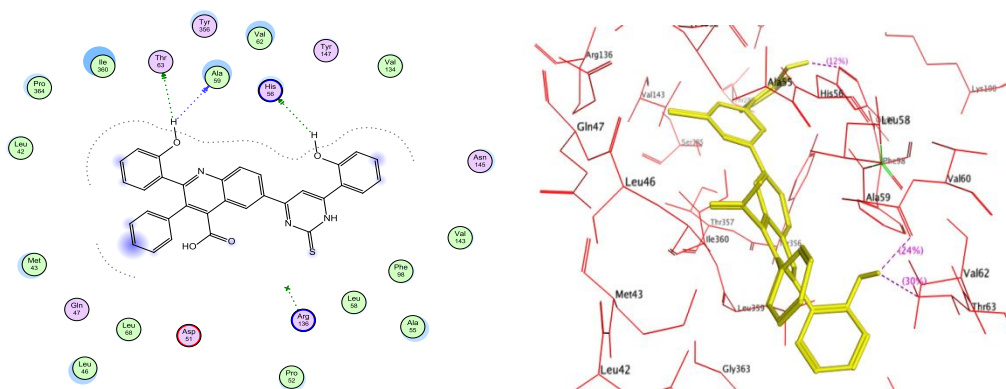


Fig 3.14: 2D and 3D models biochemical interactions of compound E10 with DHODH enzyme: ● polar ● greasy ● greasy ⊕ arene-cation ⋯ sidechain acceptor

Compound E13 showed binding free energies (S) -7.92 Kcal/mol and 3H-bond interactions between O40 in amide group with H atom in Arg136, while other two bond interactions between O21 in carboxyl group with hydrogen atom in Thr63 and H29 in phenol ring with O atom in hydroxyl group in Ala56. The length bonds at 2.06 , 2.74 and 2.19 Å, respectively.

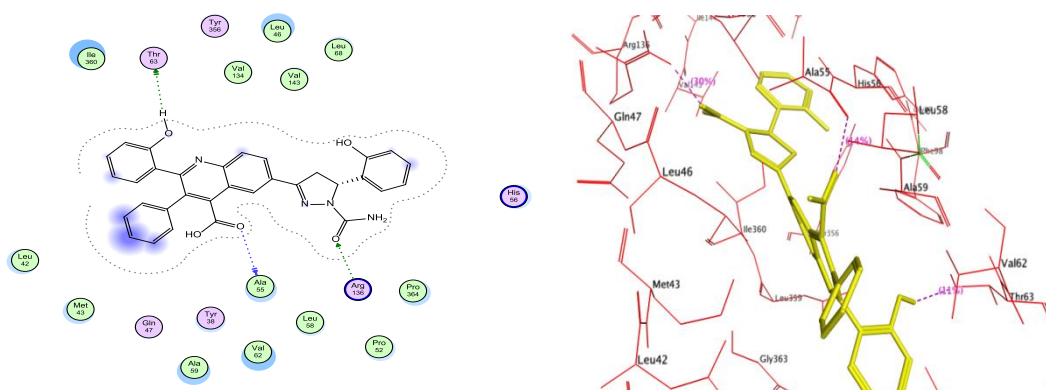


Fig 3.15: 2D and 3D models biochemical interactions of compound E13 with DHODH enzyme: ● polar ● greasy ● greasy ⊕ arene-cation ⋯ sidechain acceptor

Compounds (B12, C, D20, E14 and E35) showed two interactions with an amino acid by H-bond interactions, pi-interactions or both. While compounds (A11, A25, A29, B2, B8, B35, C13, C15, C30, C31, C32, D18, D21, E11, E25 and E29) showed one interaction by H-bond interaction or pi-interaction. All of the figures 2D models of these listed compounds were shown in the appendix.

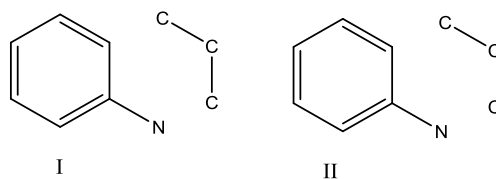
In a further look to the interactions and binding free energies (ΔG) score results of docking studies compared to values of pEC_{50} of QSAR studies, we can observe that more active compounds III, XVI, C11, C17, E10 and E14 (EC_{50} = 9.28, 8.53, 13.03, 8.15 and 8.87 respectively). The inconsistency between some of the results of docking and QSAR studies may be due to some factors such as bulky substituents will decrease the inhibitory activity these compounds.

3.4 Synthetic design

Retrosynthetic analysis is a technique widely-used by organic chemists to design synthetic routes to “target” molecules, where the target is recursively transformed into simpler precursor molecules until commercially available “starting” molecules are identified (Corey *et al.*, 1995).

The starting product structural of quinoline in this study has been synthesized by Doebner-Millar reaction which is a condensation reaction between phenyl pyruvic acid, primary aryl amines and aryl aldehydes to form 2,3-diphenyl/2-(furan-2-yl)-3-phenylquinoline-4-carboxylic Acid. The corresponding α,β -unsaturated carbonyl derivatives are obtained in aldol condensation of the substituted 2,3-diphenyl/2-(furan-2-yl)-3-phenylquinoline-4-carboxylic Acid derivatives and the substituted aryl aldehydes (Mahgoub *et al.*, 2014). Then treatment of α,β -unsaturated carbonyl derivatives with urea derivative, hydrazine derivatives and monoethanolamine in boiling ethanol gives Pyrimidinone /thiones (Dinakaran *et al.*, 2012), pyrazoline (Joshi *et al.*, 2012), and oxazepines (Bharuch *et al.*, 2000) compounds. The structure of the above mentioned compounds was confirmed by IR, NMR and MS spectral data.

The present work generally depended on the appropriate retrosynthetic analysis, through the disconnection or the functional group interchange (FGI) and functional group removal strategies. The retrosynthetic analysis of quinoline derivatives exemplified two important overall strategies by which the heterocyclic ring can be constructed, as indicated by I and II (Saeed *et al.*, 2011):



The strategy (I) an important method for quinoline and many of its derivatives by which a carbon skeleton of three atoms was allowed to be condensed with a primary aromatic amine.

The retrosynthetic analysis for the quinoline-4-carboxylic acid revealed, aniline, pyruvic acid and benzaldehyde as a precursors or synthetic equivalents for the reaction.

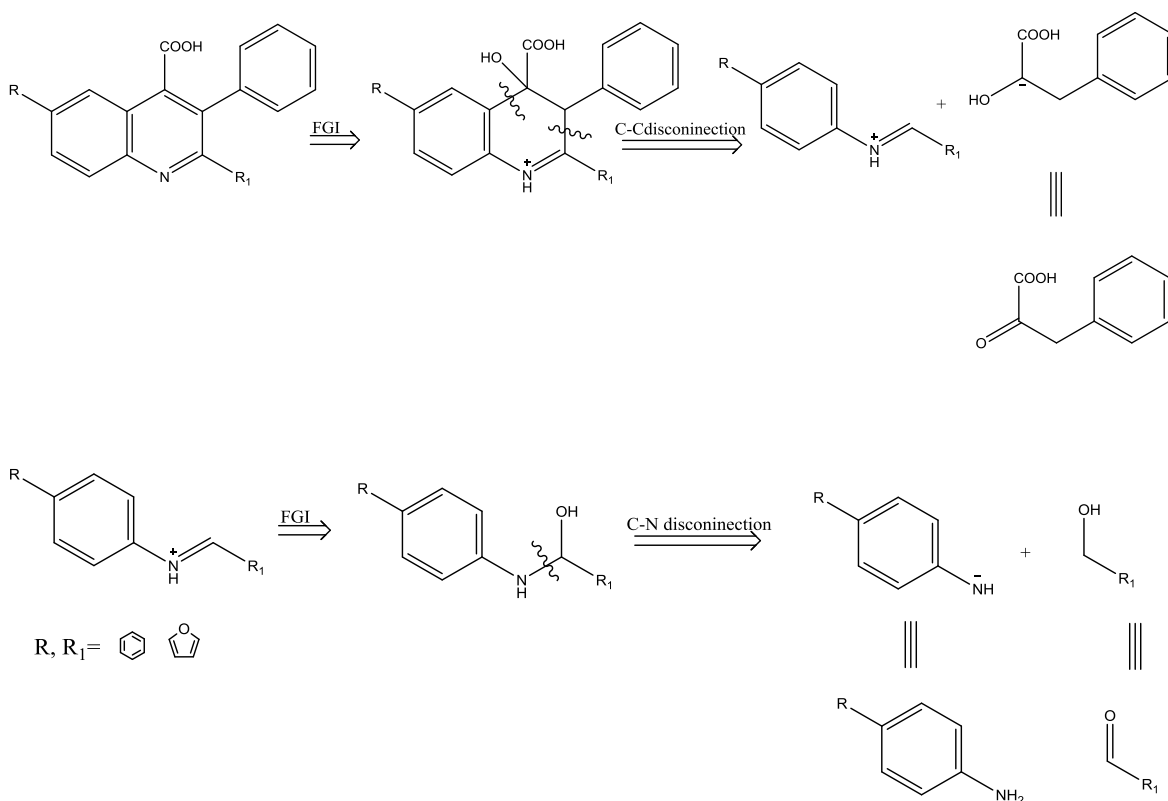


Fig 3.16: Retrosynthetic analysis of 2,3-diphenyl/2-(furan-2-yl)-3-phenyl quinoline-4-carboxylic acid derivatives

The synthesis of α,β -unsaturated carbonyl derivatives and their heterocyclic compounds (pyrimidinone/thione, pyrazoline, oxazepines) derivatives presented in this work were designed according to the following retrosynthetic analysis through the disconnection approach.

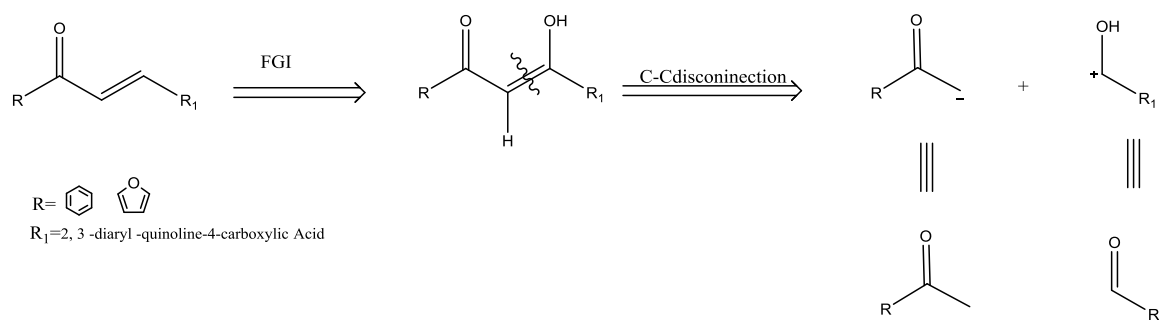


Fig.3.17: Retrosynthetic analysis of α,β -unsaturated carbonyl derivatives

Pyrimidinone/thione is heterocyclic with two heteroatoms; it is useful to look for recognizable fragment containing both; the ring of pyrimidinone/thione can be disconnected to urea/thiourea and suitable electrophilic fragment.

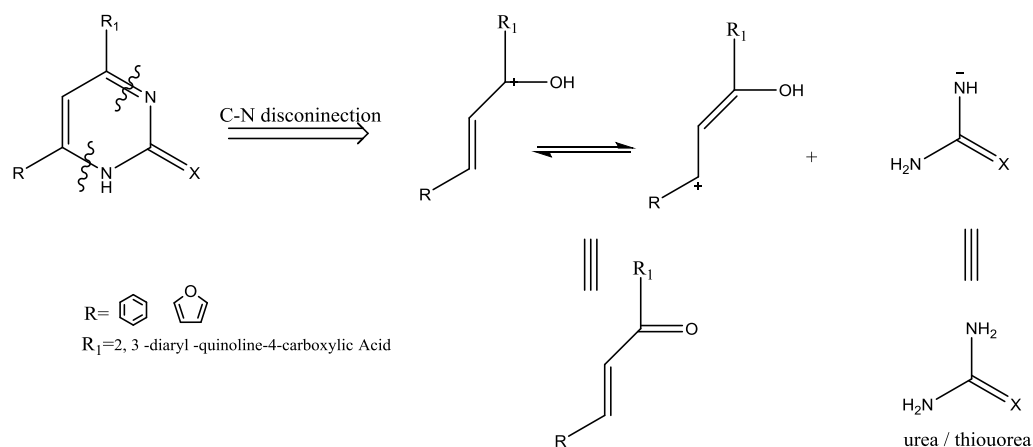


Fig.3.18: Retrosynthetic analysis of pyrimidinone/thione derivatives

The retrosynthesis pathway of pyrazoline derivatives synthesis is shown in (Figure 3.19).

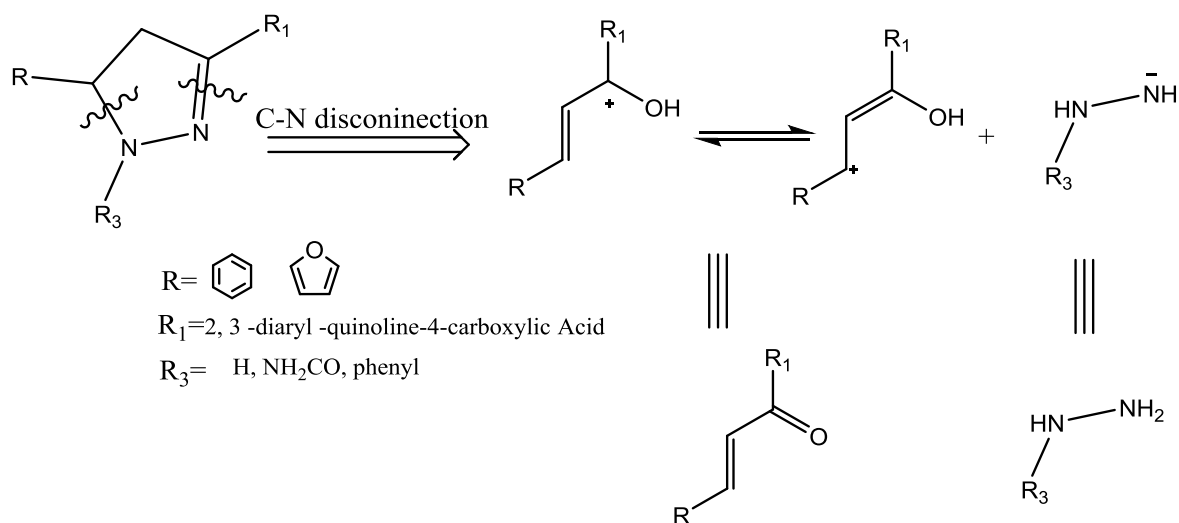


Fig.3.19: Retrosynthetic analysis of pyrazoline derivatives

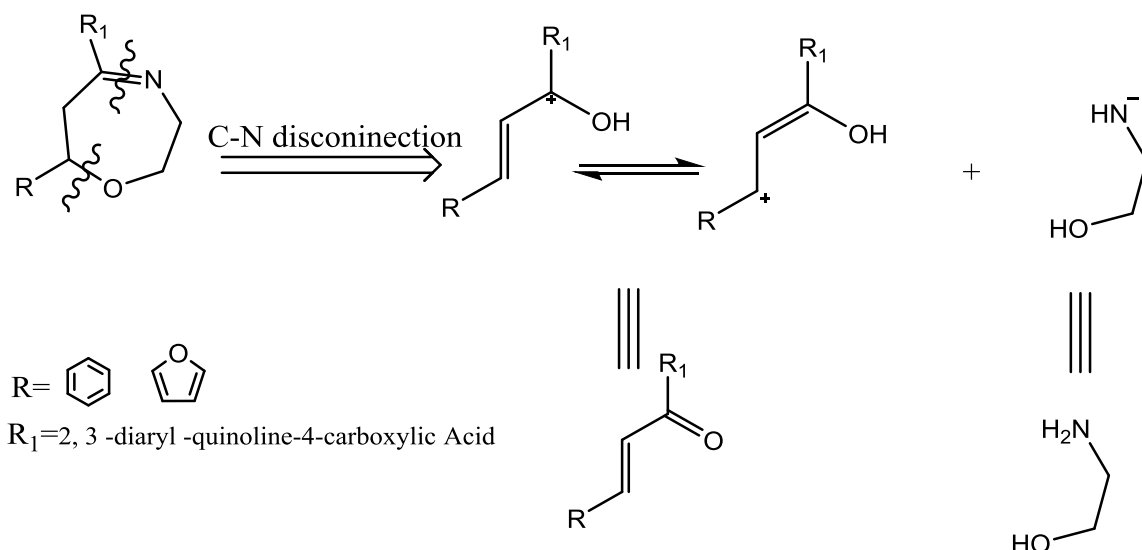


Fig.3.20: Retrosynthetic analysis of oxazepine derivatives

3.5 Reaction mechanism of quinoline derivatives

The quinoline-4-carboxylic acid derivatives were prepared by the Doebner-Millar reaction, through the condensation of amine acetophenone with phenylpyruvic acid and aromatic aldehydes; mechanism of this reaction involves attack of the nucleophilic NH₂ group in aromatic amines on the electrophilic carbonyl carbon in aromatic aldehyde, followed by condensation reaction; the condensation product, attacked by phenylpyruvic acid, subsequent intramolecular condensation and oxidation, leads to the target molecule.

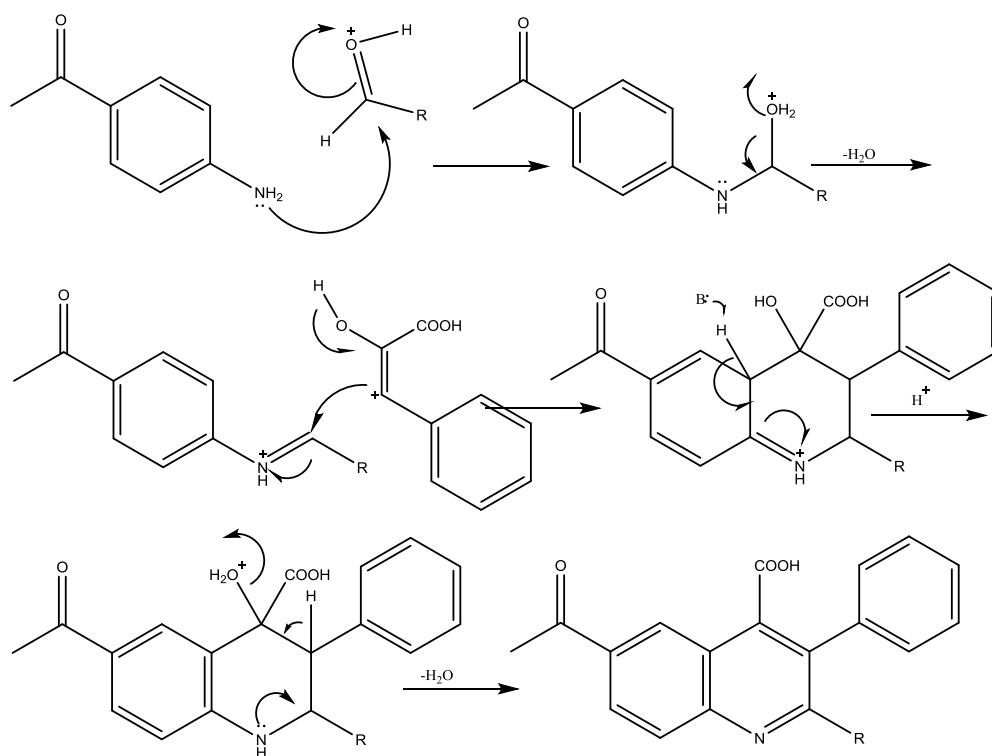


Fig.3.21 Synthesis mechanism of quinolones derivatives

3.6 α,β -unsaturated carbonyl derivatives from Claisen-Schmidt condensation

The preparation of α,β -unsaturated carbonyl derivatives by Claisen-Schmidt condensation was carried out in basic media, involving nucleophilic addition of carbanion derived from the keto group attached to quinoline ring, to carbonyl carbon of the aromatic aldehydes. Dehydration of hydroxyl ketones forms α,β -unsaturated carbonyl derivatives.

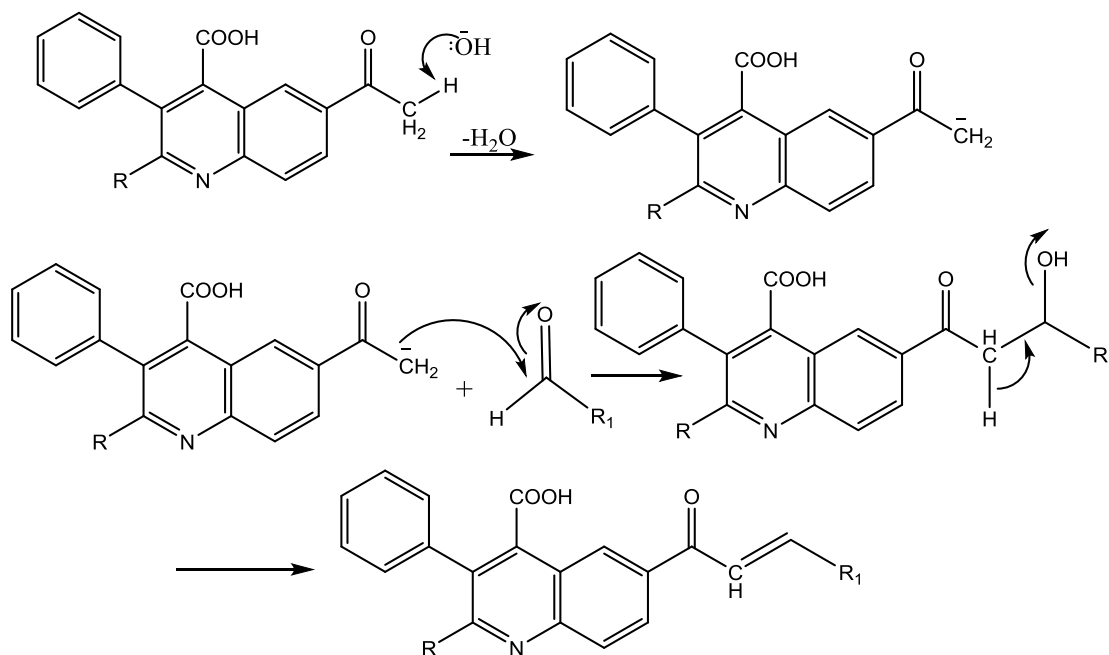


Fig.3.22: Synthesis mechanism of α,β -unsaturated carbonyl derivatives

3.7 Reaction mechanism of pyrimidinone/thione derivatives

The pyrimidinone/thione derivatives investigated in this work were all prepared by the cyclization reaction of some synthesized α,β -unsaturated carbonyl compounds, with urea or thiourea in the presence of basic catalyst using ethanol (95%) as solvent.

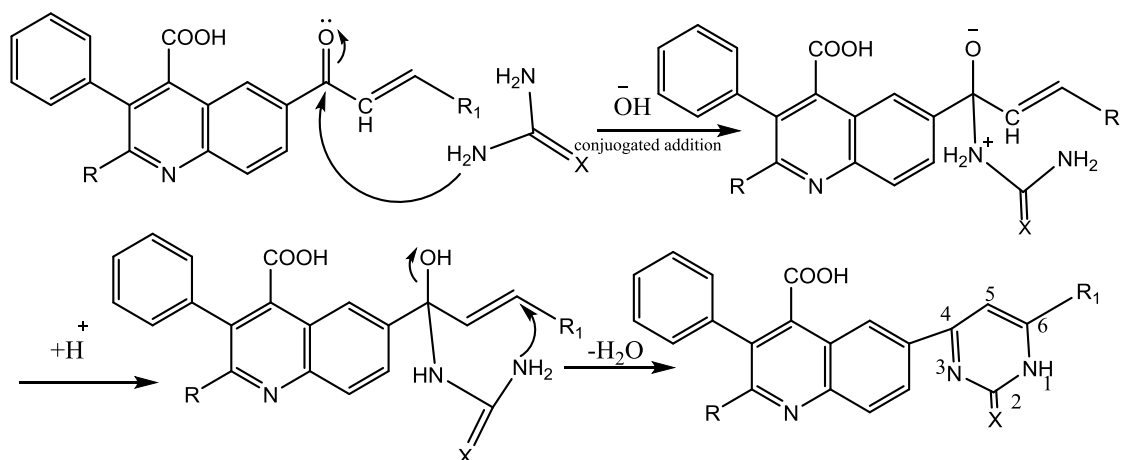


Fig.3.23: Synthesis mechanism of the pyrimidinone/thione derivatives

3.8 Reaction mechanism of pyrazolines derivatives

The pyrazoline derivatives were synthesized by the cyclization reaction of some synthesized α,β -unsaturated carbonyl compounds and thiosemicarbazide in the presence of sodium hydroxide and ethanol with refluxing for about 2 hours (Shekarchi *et al.*, 2008).

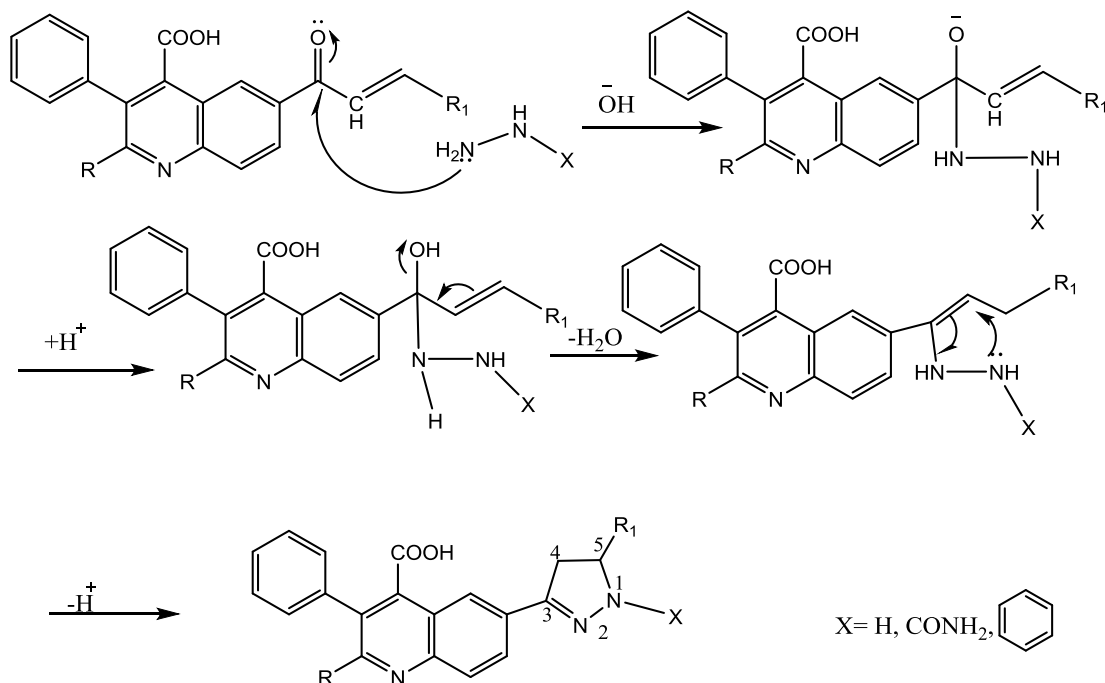


Fig.3.24: Synthesis mechanism of the pyrazoline derivatives

3.9 Reaction mechanism of oxazepine derivatives

The prepared oxazepine derivatives in this study, were prepared by cyclization reaction of α,β -unsaturated carbonyl derivatives with monoethanolamine in ethanol.

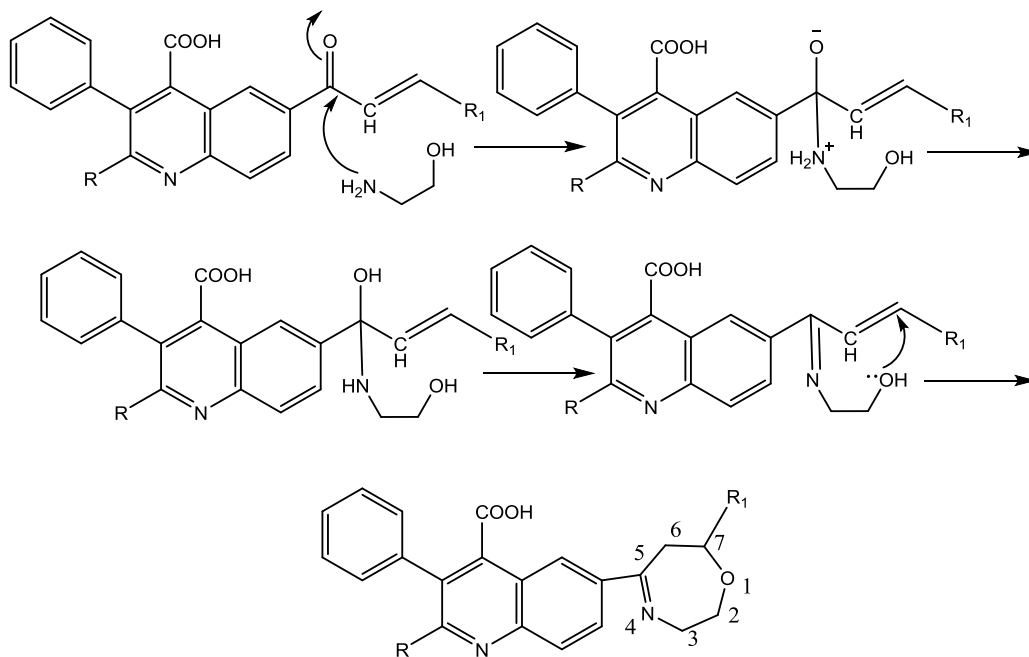


Fig.3.25 Synthesis mechanism of the oxazepine derivatives

3.10 Spectral characterization

The structure of the above mentioned compounds was confirmed by IR, NMR and MS spectral data.

The formations of quinoline acid I and IX were confirmed by the peak at (≈ 3250) cm^{-1} in IR spectrum which is due to the OH stretching of carboxylic acid. A band at (≈ 1670) cm^{-1} is due to C=O stretch of the acid group and other band for C=O in acetyl group at (≈ 1680) cm^{-1} . The ^1H NMR spectra of compounds I and IX show doublet signals at δ (8.33 and ≈ 8.41) ppm and singlet at δ (9.45-9.66) ppm is due to quinoline-3H proton. The mass spectrum of compounds I and IX shows a molecular ion peak at M^+ , which is in agreement with the molecular formula.

The IR spectra of all α,β -unsaturated carbonyl derivatives II and X show characteristic peaks of particular carbonyl functional groups of enones in the region of (1672-1682) cm^{-1} , and (3060-3049) cm^{-1} stretching vibration for H-C bond of $C\alpha=C\pi$. The ^1H NMR spectra of II and X show characteristic signals for α , β -protons at δ (7.22 - 7.99) ppm; this refers to the effect of resonance of the phenyl rings that bonded to β -carbon atom. The ^{13}C NMR spectra assignment of carbon atoms presented in α,β -unsaturated carbonyl derivatives moiety show the characteristic peak related to the β -C atom around δ (≈ 131.25 -134.84) ppm which is more deshielded than that of α -C atom approximately at δ (119.99-121.69) ppm. Mass spectra of II and X, show the M^+ consistent with their molecular formula.

The structure of the pyrimidinone and pyrimidinthiones was characterized by IR spectra showing the disappearance of two absorption bands but appearance of new absorption bands for NH, C=O and C=S groups around (3265.32-3015.15) cm^{-1} , 1672.75 cm^{-1} , 1365.81 cm^{-1} , respectively. ^1H NMR spectra of compounds III (Fig.B.3), IV (Fig.B.4), IX (Fig.B.9) and XI (Fig.B.3) show singlet signal at δ 5.73ppm due to the proton of C5-pyrimidinone. Also, singlet broad signal one proton of NH group appears at δ 10.02 ppm. Further, ^{13}C NMR spectra exhibit confirmatory signals of the carbonyl carbon C1, C3, and the methyl carbon C4 around δ 166.94, 157.13, and 110.19 ppm respectively. Mass spectra exhibit molecular ion peak [$M^{++} 2$], appearing at different intensities, confirmed the exact mass or molecular weights of the examined compounds III, IV, IX and XI.

In the IR spectra of pyrazoline derivatives V, VI, VII, XIII, XIV and XVI show strong band at (1590-1550) cm^{-1} for C=N stretching vibration. In addition to the appearance of above bands, the most important evidence for the formation of 2-pyrazoline is the disappearance of carbonyl group special band for the α,β -unsaturated carbonyls moiety at (1660 - 1657) cm^{-1} . The ^1H NMR spectra of pyrazolines show characteristic signals

corresponding to the protons of C4 and C5 of 2-pyrazoline ring and appearance of three doublet to doublet (dd) signals for each compound approximately at δ (3.63-5.05) ppm. The ABX type spin system pattern of proton appeared as a doublet of doublets owing to vicinal coupling with the two magnetically non-equivalent protons (HA and HB) of methylene at position 4 and methine proton (HX) at position 5 in pyrazoline ring. The ^{13}C -NMR spectra of pyrazolines, show three signals belongs to (C3, C4 and C5) for pyrazoline carbons approximately at, δ (151.25-154.04, 41.27-39.98 and 63.31-66.58) ppm. Mass spectra of pyrazolines, show the M^+ consistent with their molecular formula of pyrazoline derivatives.

The IR spectra of 1,4-oxazepines VIII and XVI show typical peaks at (≈ 1505 - 1509) cm^{-1} for C=N stretching vibration and at (≈ 1216 - 1227) cm^{-1} for ethers. These peaks confirmed us that 1,4-oxazepines rings were formed. ^1H NMR spectra of compounds VIII and XVI show similar effects on the chemical shifts of the pyrazoline protons signal of three doublet to doublet (dd) signals approximately at δ (≈ 3.25 - 5.01) ppm for each compound owing to the ABX spin pattern of two protons of methylene at position 6 and methine proton at position 7 in 1,4-oxazepine ring. The characteristic two triplet signals at (≈ 3.61 - 3.63 and 3.73 - 3.83) ppm for each methylene protons in position 2 and 3 in 1,4-oxazepines ring. The ^{13}C NMR spectra of 1,4-oxazepines showed the signal for C2, C3 and C6 of the seven-membered ring appears in the range of δ (58.71, 45.44 and 30.96) ppm, respectively. Mass spectra of VIII and XVI show peak [$\text{M}^+ + 2$] and M^+ , these were consistent with product structures.

4. CONCLUSION AND RECOMMENDATIONS

The following points could be concluded from this work:

- The derived QSAR models had provided rationales to explain of quinoline-4-carboxylic acid derivatives inhibitory activity to VSV replication, according to descriptors (logPo/w, MR, AM1-HF, AM1-dipol, ASA-P, Chi₀, density and AM1-P).
- The models predicted showed that reactivity of quinoline-4-carboxylic acid derivatives were determined by log P and dipole moment.
- PLS analysis has also confirmed that the suggested models had acceptable predictability. All the compounds were within the applicability domain of the proposed models and were evaluated correctly.
- The QSAR models were not only predictable within the same series of compounds but also valid for other chemical classes.
- Docking study of new designed quinoline-4-carboxylic acid derivatives showed lower energy compared to reference barquinar, while their some compounds showed more interactions compared to barquinar.
- Some of new derivatives were expected to show experimentally higher biological activity.
- Further studies of new designed quinoline-4-carboxylic acid compounds could be docked with other proteins for efficiency with an enzyme or microbes.
- The 2D models of quinoline-4-carboxylic acid derivatives showed that the main residues in the active pocket of human DHODH are hydrophobic.
- New designed quinoline-4-carboxylic acid compounds mostly showed high molecular weight, indicating that some new derivatives are hard to dissolve in water, less to be extracted, more metabolisms and distribution in body, and also when we consider their having higher log P also.
- This study showed that newly substituted quinolin-4-carboxylic acid derivatives could easily be synthesized by Doebner-Millar reaction and then condensed by Claisen-Schmidt condensation to yield α,β -unsaturated carbonyl derivatives which could be cyclized by different agents to form various heterocyclic derivatives (pyrimidinone\thion, pyrazolines, oxazepines, pyrazoles, oxazoles, isoxazoles..et) with good yield.

- The purity and identities of products were elucidated through thin layer chromatography (TLC), melting point and spectroscopic data (IR, ¹H NMR, ¹³C NMR, GC-Mass).
- Docking is correlated strongly with QSAR results.
- QSAR, docking and Synthesis results of this work could be useful for other chemists working on the field of predicted biological activity as dihydroorotate dehydrogenase (DHODH) enzyme inhibitor, designed or newly heterocycles quinoline synthesis.

CHAPTER FOUR

References

4. REFERENCES

- ☒ Aghera, V.K.; Patel, J.P.; and Parsania, P. H.; (2008). Synthesis, spectral and microbial studies of some novel quinoline derivatives via Vilsmeier–Haack reagent. *Arkivoc.*: 2008 (xii), 195-204.
- ☒ Ahsan, M. J.; Yadav, R.; and Jadav, S. S.; (2015). Synthesis anticancer activity and molecular docking studies of newer quinoline analogues. *1st International Electronic Conference on Medicinal Chemistry.*: 2, (27), 1-17.
- ☒ Ali, I.A.; (2008). Convenient syntheses of new quinoline nucleosides bearing amino acid esters. *Arkivoc.*: 2008 (xvii), 77-89.
- ☒ Arakaki, T. L.; Buckner, F. S.; Gillespie, J. R.; Malmquist, N. A.; Phillips, M. A.; Kalyuzhniy, O.; and Hol, W. G.; (2008). Characterization of Trypanosoma brucei dihydroorotate dehydrogenase as a possible drug target; structural, kinetic and RNAi studies. *Molecular microbiology.*: 68 (1), 37-50.
- ☒ Arif, M.; Jabeen, F., Saeed, A.; Qureshi, I. Z.; and Mushtaq, N.; (2017). a new class of potential antidiabetic acetohydrazides: synthesis, in vivo antidiabetic activity and molecular docking studies. *Bangladesh Journal of Pharmacology*, 12(3), 319-332.
- ☒ Battley, E. H.; (2003). Absorbed heat and heat of formation of dried microbial biomass studies on the thermodynamics of microbial growth. *Journal of Thermal Analysis and Calorimetry.*: 74(3), 709-721.
- ☒ Benfenati, E.; (2008). "Practical Aspects of Computational Chemistry", Springer.: ch8, p 186.
- ☒ Bharun, P.B.; and Naik, H. B.; (2000). Synthesis and antibacterial activity of some chalcone and 1,4-oxazepine derivatives. *Sin journal of chemistry.*: 1(2), 318-320.
- ☒ Corey, E. J.; and Wipke, W. T.; (1969). Computer-assisted design of complex organic syntheses. *Science*, 166(3902), 178-192.
- ☒ Chen, Y. L.; Chen, I. L.; Lu, C.M.; Tzeng, C. C.; Tsao, L. T.; and Wang, J. P.; (2004). Synthesis and anti-inflammatory evaluation of 4-anilino-furo [2,3-b] quinoline and 4-phenoxy-furo[2,3-b] quinoline derivatives. *Bioorganic & Medicinal Chemistry.*: 12, 387–392.
- ☒ Cherkasov, A.; (2005). Inductive QSAR Descriptors. Distinguishing Compounds with Antibacterial Activity by Artificial Neural Networks. *International Journal of Molecular Sciences.*: 6, 63-86.

- ☒ Choudhary, M.; Pilania, P.; and Sharma, B. K.; (2015). QSAR rationales for the 5-HT_{2A} receptor antagonistic activity of 2-Alkyl-4-aryl-Pyrimidine fused heterocycles. *Research Journal of Pharmaceutical Biological and Chemical Sciences.*: 6(2), 326-338.
- ☒ Chaudhur, M. K.; and Hussain, S.; (2006). An efficient synthesis of quinolines under solvent - free conditions. *Journal of Chemistry science.*:118, 199-202.
- ☒ Das, P.; Deng, X.; Zhang, L.; Roth, M. G.; Fontoura, B. M.; Phillips, M. A.; and De Brabander, J. K.; (2013). SAR-based optimization of a 4-quinoline carboxylic acid analogue with potent antiviral activity. *ACS medicinal chemistry letters.*: 4(6), 517-521.
- ☒ Dinakaran, V. S.; Jacob, D.; and Mathew, J. E.; (2012). Synthesis and biological evaluation of novel pyrimidine-2 (1H)-ones/thiones as potent anti-inflammatory and anticancer agents. *Medicinal chemistry research.*: 21(11), 3598-3606.
- ☒ Dudek, A. Z.; Arodz, T.; and Galvez, J.; (2006). Computational Methods in Developing Quantitative Structure-Activity Relationships (QSAR). *Combinatorial Chemistry & High Throughput Screening.*: 9. 3. 213-228.
- ☒ El-Agrody, A. M.; and El-Agrody, A. M.; (2011). Synthesis of certain novel 4H pyrano [3,2-h] quinoline derivative. *Arkivoc*: 2011(xi), 134-46.
- ☒ Ertl, P.; Rohde, B.; & Selzer, P.; (2000). Fast calculation of molecular polar surface area as a sum of fragment-based contributions and its application to the prediction of drug transport properties. *Journal of medicinal chemistry.*: 43(20), 3714-3717.
- ☒ Evans, D. R.; and Guy, H. I.; (2004). Mammalian pyrimidine biosynthesis: fresh insights into an ancient pathway. *Journal of Biological Chemistry.*: 279(32), 33035-33038.
- ☒ Fujita, T.; Iwasa, J.; and Hansch, C; (1964). A new substituent constant, π , derived from partition coefficients. *Journal of the American Chemical Society.*: 86(23), 5175-5180.
- ☒ Ferreira, L. G; Santos, R. N; Oliva, G.; and Andricopulo, A. D.; (2015). Molecular Docking and Structure-Based Drug Design Strategies. *Molecules.*: 20(7), 1420-3049, 13384-13421.
- ☒ Gao, W.; Liu, J.; Jiang, y.; and Li, Y.; (2011). First synthesis of 2-(benzofuran-2-yl) - 6, 7- methylene dioxyquinoline-3-carboxylic acid derivatives.: *Beilstein journal of organic chemistry*: 7, 210-217.

- ☒ Gasteiger, J.; (2016). Chemoinformatics: Achievements and Challenges, a Personal View. *Molecules.*: 21, 151, 1-15.
- ☒ Ginelle, A. Ramann.; and Bryan J. C.; (2015). Quinoline synthesis by improved Skraup – Doebner–Von Miller reactions utilizing acrolein diethyl acetal. *Tetrahedron Letters.*: 56 6436–6439.
- ☒ Gozalbes, R.; Doucet, J. P.; and Derouin, F.; (2002). Application of topological descriptors in QSAR and drug design: history and new trends. *Current Drug Targets-Infectious Disorders.*: 2(1), 93-102.
- ☒ Hong, S. K.; Jung, Y. T.; Park, S. W.; and Paik, S. Y.; (2005). Inducible Vesicular Stomatitis Virus (VSV) L Cell Line for Packaging of Recombinant VSV. *Virus genes.*: 31(2), 195-201.
- ☒ Ivanciuc, O.; Ivanciuc, T.; and Cabrol-Bass, D.:(2002). QSAR for dihydrofolate reductase inhibitors with molecular graph structural descriptors. *Journal of Molecular Structure .*: 582, 39-51.
- ☒ Jean, C. B.; Shen, G.; Norton, P. P.; and John, D. W.; (2009). Survey of Solvents for the Conrad – Limpach Synthesis of 4-Hydroxyquinolines. *Synthetic Communications.*: 39(9), 1563–1569.
- ☒ Jhanwar, B.; Sharma, V.; Singla, R. K.; and Shrivastava, B.:(2011). QSAR - Hansch Analysis and Related Approaches in Drug Design. *Pharmacologyonline.*: 1, 306-344.
- ☒ Joseph, P. M.; (2008). Quinoline, quinazoline and acridone alkaloids. *The Royal Society of Chemistry.*: 25(7), 166–187.
- ☒ Khalil, N.; (2003). Quantum chemical approach of corrosion inhibition. *Electrochimica Acta.*: 48(18), 2635-2640.
- ☒ Kannappan, N.; Reddy, B. S.; Sen, S.; Nagarajan, R.; and Dashpute, S.:(2009). Synthesis and chemical characterization of quinoline imine derivatives. *Journal of Applied Chemical Research.*: 34(9), 58-69.
- ☒ Kapetanovic, I. M.; (2009). computer-aided drug discovery and development (cadd) in silico-chemico-biological approach. *Chem Biol Interact.*: 171(2), 165–176.
- ☒ Katritzky, A. R., Lobanov, V. S., & Karelson, M. (1995). QSPR: the correlation and quantitative prediction of chemical and physical properties from structure. *Chemical Society Reviews.*: 24(4), 279-287.

- ☒ Kier, L. B.; and Hall, L. H.; (2002). The meaning of molecular connectivity: A bimolecular accessibility model. *Croatica chemica acta.*: 75(2), 371-382.
- ☒ Kouznetsov, V. V.; Rojas Ruíz, S. V.; Vargas Méndez, L. Y.; and Gupta, M. P.; (2012). Simple C-2-substituted quinolines and their anticancer activity. *Letters in Drug Design & Discovery.*: 9, 680-686.
- ☒ Kore, P. P.; Mutha, M. M.; Antre, R. V.; Oswal, R. J.; and Kshirsagar, S. S.; (2012). Computer-Aided Drug Design An Innovative Tool for Modeling. *Open Journal of Medicinal Chemistry.*: 2, 139-148.
- ☒ Kumar, A.; Srivastava, K.; Kumar, S. R.; Puri, S. K.; and Chauhan, P. S.;(2010).Synthesis of new 4-aminoquinolines and quinoline acridine hybrids as antimalarial agents. *Bioorganic Medical Chemistry Letter.*: 20(10), 7059-7063.
- ☒ Kutter, E.; and Hansch, C.; (1969). Steric parameters in drug design. Monoamine oxidase inhibitors and antihistamines. *Journal of medicinal chemistry.*: 12(4), 647-652.
- ☒ Nqoro, X.; Tobeka, N.; and Aderibigbe, B.; (2017). Quinoline-based hybrid compounds with antimalarial activity. *Molecules.*: 22 (12), 2268-2280.
- ☒ Ogata, K.; Hatakeyama, M.; and Nakamura, S.; (2018). Effect of Atomic Charges on Octanol–Water Partition Coefficient Using Alchemical Free Energy Calculation. *Molecules.*: 23(2), 1-15.
- ☒ Leo, A.; Hansch, C.; and Elkins, D.; (1971). Partition coefficients and their uses. *Chemical reviews*, 71(6), 525-616.
- ☒ Lewars, E.; (2004). *Computational chemistry- Introduction to the theory and applications of molecular and quantum mechanics*. Kluwer Academic Publishers: ch1, p 1-3.
- ☒ Macalino, S. J. Y.; Gosu, V.; Hong, S.; and Cho, S.; (2015). Role of computer-aided drug design in modern drug discovery. *Archives of Pharmacal Research*: 38(7), 1686–1701.
- ☒ Madapa, S.; Tusi, Z.; and Batra, V.; (2008). Advances in the syntheses of quinoline and quinoline-annulated ring systems. *Current Organic Chemistry*: 12(13), 1116-1183.

- ☒ Mahgoub, H.; Hussein, A.; and Saeed, A.; (2014). synthesis of some 2, 3-diaryl-6-isoxazol-4-quinoline-4-carboxylic acid derivatives. *International Journal of Pharmaceutical Sciences and Research.*: 5(11), 5050-5056.
- ☒ Makki, M. T.; Bakhotmah, D. A.; and Abdel-Rahman, R. M.; (2012). highly efficient synthesis of novel fluorine bearing quinoline-4-carboxylic acid and the related compounds as amyolytic agents. *International Journal of Organic Chemistry.*: 2(11), 49-55.
- ☒ Malik, J. K.; Soni, H.; Singhai A. K.; and Pandey,H.;(2013). QSAR - application in drug design. *International Journal of Pharmaceutical Research and Allied Sciences.*: 2(1), 1-13.
- ☒ Mandal, S.; Moudgil, M.; and Mandal, S.; (2009). Rational drug design. *European Journal of Pharmacology.*: 625(1-3) , 90–100
- ☒ Marella,A.; Tanwar, O.; Saha, R.; Ali, R.M.; Srivastava,M.; Akhter,M.; Shaquiquzzaman, M.; and Alam, M. M.; (2013). Quinoline A versatile heterocyclic. *Saudi Pharmaceutical Journal.*: 21(13), 1-12.
- ☒ Mcleese, D. W.; Zitko, V.; and Peterson, M. R; (1979). Structure-lethality relationships for phenols, anilines, and other aromatic compounds in shrimp and clams. *Chemosphere.*; 2, 53-57.
- ☒ Möhring, P. C.; and Coville, N. J.; (1992). Quantification of the influence of steric and electronic parameters on the ethylene polymerisation activity of (CpR)₂ZrCl₂ / ethylaluminumoxane Ziegler—Natta catalysts. *Journal of molecular catalysis.*: 77(1), 41-50.
- ☒ Pattan, S. R.; Ahirrao, G. B.; Pawar, S. S.; Pawar, S. B.; Godge, R. K.; Kapse, G. K.; Bhawar, H. S.; Gharate, U. D.; and Kavade, S.; (2011). a review on quantitative structure activity relationship. *Pharmacologyonline- Newsletter.*: 13(2), 786-806,
- ☒ Massoud, M. A.; El Bialy, S. A.; Bayoumi, W. A.; and El Hussein, W. M.; (2014). Synthesis of new 2- and 3-hydroxyquinoline- 4-carboxylic acid derivatives as potential antioxidants. *Heterocyclic Communications.*: 20(5), 81–88.

- ☒ Mital, A.; Negi, V. S.; and Ramachandran, U.; (2006). Synthesis and antimycobacterial activities of certain trifluoromethyl-aminoquinoline derivatives. *Arkivoc.*: 10, 220-227.
- ☒ Mathew, B.; Suresh, J.; Mathew, G. E.; Haridas, A., Suresh, G.; and Sabreena, P. (2016). Synthesis, ADME studies, toxicity estimation, and exploration of molecular recognition of thiophene based chalcones towards monoamine oxidase-A and B. Beni-Suef. *university journal of basic and applied sciences.*: 5(4), 396-401.
- ☒ Mitra, I.; Saha, A.; and Roy, K.; (2012). Predictive modeling of antioxidant coumarin derivatives using multiple approaches: descriptor-based QSAR, 3D-pharmacophore mapping, and HQSAR. *Scientia pharmaceutica*; 81(1), 57-80.
- ☒ Nantasenamat, C.; Ayudhya, C. I.; Naenna, T.; and Prachayasittikul, V.; (2009). a practical overview of quantitative structure-activity relationship. *excli journal.*: 22(4), 2156, 74-88.
- ☒ Ohishi, T., Inaoka, D. K., Kita, K., & Kawada, M. (2018). Dihydroorotate Dehydrogenase as a Target for the Development of Novel Helicobacter pylori-Specific Antimicrobials. *Chemical and Pharmaceutical Bulletin.*: 66(3), 239-242.
- ☒ Palmer, P. B.; and O'connell, D. G. (2009).; Regression analysis for prediction: understanding the process. *Cardiopulmonary physical therapy journal.*: 20(3), 23.
- ☒ Pandeya, S.N .; and Tyagi, a.; (2011). Synthetic approaches for quinoline and isoquinoline. *International Journal of Pharmacy and Pharmaceutical Sciences.*: 42(3), 53-61.
- ☒ Puzyn, T.; Leszczynski, J.; and Cronin, M. T.:(2010). *Recent Advances in QSAR Studies Methods and Applications*. Springer, 8th ed., ch1.
- ☒ Raevsky, O. A.:(2003). physicochemical descriptors in property based drug design. *Mini Reviews in Medicinal Chemistry.*: 4, 1041-1052.
- ☒ Ramachandran, K. I.; Deepa, G.; and Namboori, K.; (2008)." *Computational chemistry and molecular modeling* ", Springer, ch1, p 1.
- ☒ Saeed, A. E. M.; and Elhadi, S. A.; (2011). Synthesis of some 2-aryl-and 2, 3-diaryl-quinolin-4-carboxylic acid derivatives. *Synthetic Communications.*: 41(10), 1435-1443.

- ☒ Sangshetti, J. N.; Zambare, A. Z.; and Shinde, D.; (2014). Pfitzinger Reaction in Synthesis of Bioactive Compounds A Review. *Mini Reviews in Organic Chemistry*.: 11. 1-27.
- ☒ Schröder, M.; Giermann, N.; and Zrenner, R.; (2005). Functional analysis of the pyrimidine de novo synthesis pathway in solanaceous species. *Plant physiology*.: 138(4), 1926-1938.
- ☒ Selassie, C. D.; (2003). *Burger's Medicinal Chemistry and Drug Discovery*, John Wiley & Sons, Inc.: 6th ed., ch1.
- ☒ Sharma, B. K.; Paliana, P.; & Singh, P.; (2010). QSAR rationales for the 1, 2-diarylcyclopentenes as prostaglandin EP1 receptor antagonists: Potentially useful in the treatment of inflammatory pain. *European Journal of Chemistry*: 1(4), 325-334.
- ☒ Sharma², B. K.; and Srivastava, B.; (2010). Quantitative Structure-Activity Relationship Study on Pyrrolotriazine Derivatives as Met Kinase Inhibitors. *Asian Journal of Chemistry*.: 22(10), 8231-8245.
- ☒ Shekarchi, M.; Pirali-Hamedania, b.L.; Navidpour, L and Adibaand, S.; (2008). Synthesis, Antibacterial and Antifungal Activities of 3-Aryl-5-(pyridin-3-yl)-4,5-dihydropyrazole-1-carbothioamide Derivatives, *Journal of the Iranian Chemical Society*.: 1, 150.
- ☒ Shukla, R. K.; Misra, P.; Sharma, S.; Tomar, N.; and Jain, P. (2012). Refractive index and molar refractivity of benzonitrile, chlorobenzene, benzyl chloride and benzyl alcohol with benzene at T = 298.15, 303.15, 308.15 and 313.15 K. *Journal of the Iranian Chemical Society*.: 9(6), 1033-1043.
- ☒ Selvam, P.; (2012). Synthesis, Anti-mycobacterial and Cytotoxicity Studies of Novel [(Sulphamoylphenyl) amino]methylpiperazinyl fluoroquinolones. *International Journal of Drug Design and Discovery*.: 3, 837-839.
- ☒ Singh, S.; Gupta, A. K.; and Verma, A.; (2013). Molecular Properties and Bioactivity score of the Aloe vera antioxidant compounds – in order to lead finding. *Research Journal of Pharmaceutical, Biological and Chemical Sciences*: 2, 876-881.
- ☒ Sliwoski, G.; Kothiwale, S.; Meiler, J.; and Lowe, E. W.; (2014). Computational Methods in Drug Discovery. *Pharmacological Reviews*.: 66, 334–395.
- ☒ Thangavelu, P.; Cellappa, S.; and Thangavel, S; (2018). Synthesis, evaluation and docking studies of novel formazan derivatives as an enoyl-acp reductase

- Inhibitors. *International Journal of Pharmacy and Pharmaceutical Sciences.*: 10(8), 56-61.
- ☒ Tiwari, B.; Pratapwar, A.; Tapas, A.; Butle, S.; and Vatkar, B; (2010). Synthesis and Antimicrobial Activity of Some Chalcone Derivatives. *International Journal of ChemTech Research.*: 2, (1), 499-503.
 - ☒ Turel ,I.; Sonc. A.; Zupancic1,M.; Sepcic,K.; and Turk,T.:(2000) biological activity of some magnesium (ii) complexes of quinolones. *Journal of Chemistry:* 7,101-104.
 - ☒ Vatsala, J. R.; Yakaiah, E.; Bhavanarushi, .; Bharath, G.; and Gangagnirao, A.; (2014). Design synthesis of novel quinoline-4-carboxylic acid derivatives and their antibacterial activity supported by molecular docking studies .*world journal of pharmacy and pharmaceutical sciences.*: 3, (12), 1612-1634.
 - ☒ Wadher, S. J.; Karande, N. A.; Borkar, D. S.; and Yeole, P. G.; (2009). Synthesis and biological evaluation of schiff basesof cinchophen as antimicrobial agents. *International Journal of ChemTech Research.*: 1, (4), 1297-1302.
 - ☒ Wang¹, G.; and Yang, G.; (2010). Synthesis and antifungal Activity of Some 6H-thiochromeno [4,3-b]quinolines. *International Journal of Chemistry.*: 2,(1), 19-24.
 - ☒ Wang², R., Jiang, J.; Pan, Y.; Cao, H.; & Cui, Y.; (2009). Prediction of impact sensitivity of nitro energetic compounds by neural network based on electrotopological-state indices. *Journal of Hazardous Materials.*: 166(1), 155-186.
 - ☒ Xu, X., Wang, J; and Yao, Q; (2015). Synthesis and quantitative structure–activity relationship (QSAR) analysis of some novel oxadiazolo[3,4-d]pyrimidine nucleosides derivatives as antiviral agents. *Bioorganic & Medicinal Chemistry Letters.*: 25,(2), 241-244.
 - ☒ Williams, J. H.; (1993). The molecular electric quadrupole moment and solid-state architecture. *Accounts of Chemical Research.*: 26(11), 593-598.
 - ☒ Wongrattanakamon, P.; Lee, V. S.; Nimmanpipug, P.; & Jiranusornkul, S.; (2016). 3D-QSAR modelling dataset of bioflavonoids for predicting the potential modulatory effect on P-glycoprotein activity. *Data in Brief.*: 9, 35-42.
 - ☒ Youg, D. C.; (2001)." Computational chemistry", John Wiley & Sons, Inc.: ch1, p 1.
 - ☒ Zhao, Y. L.; Chen, Y. L.; Sheu, J. Y.; Chen, I. L.; Wang, T, C.; and Tzeng, C. C.; (2005). Synthesis and antimycobacterial evaluation of certain fluoroquinolone derivatives. *Bioorganic & Medicinal Chemistry.*: 13, 3921–3926

Appendix A

Infra-red spectroscopy (IR) data of the prepared 2, 3-diphenyl/ 2 (furan-2-yl), 3-phenylquinoline-4-carboxylic acid derivatives:

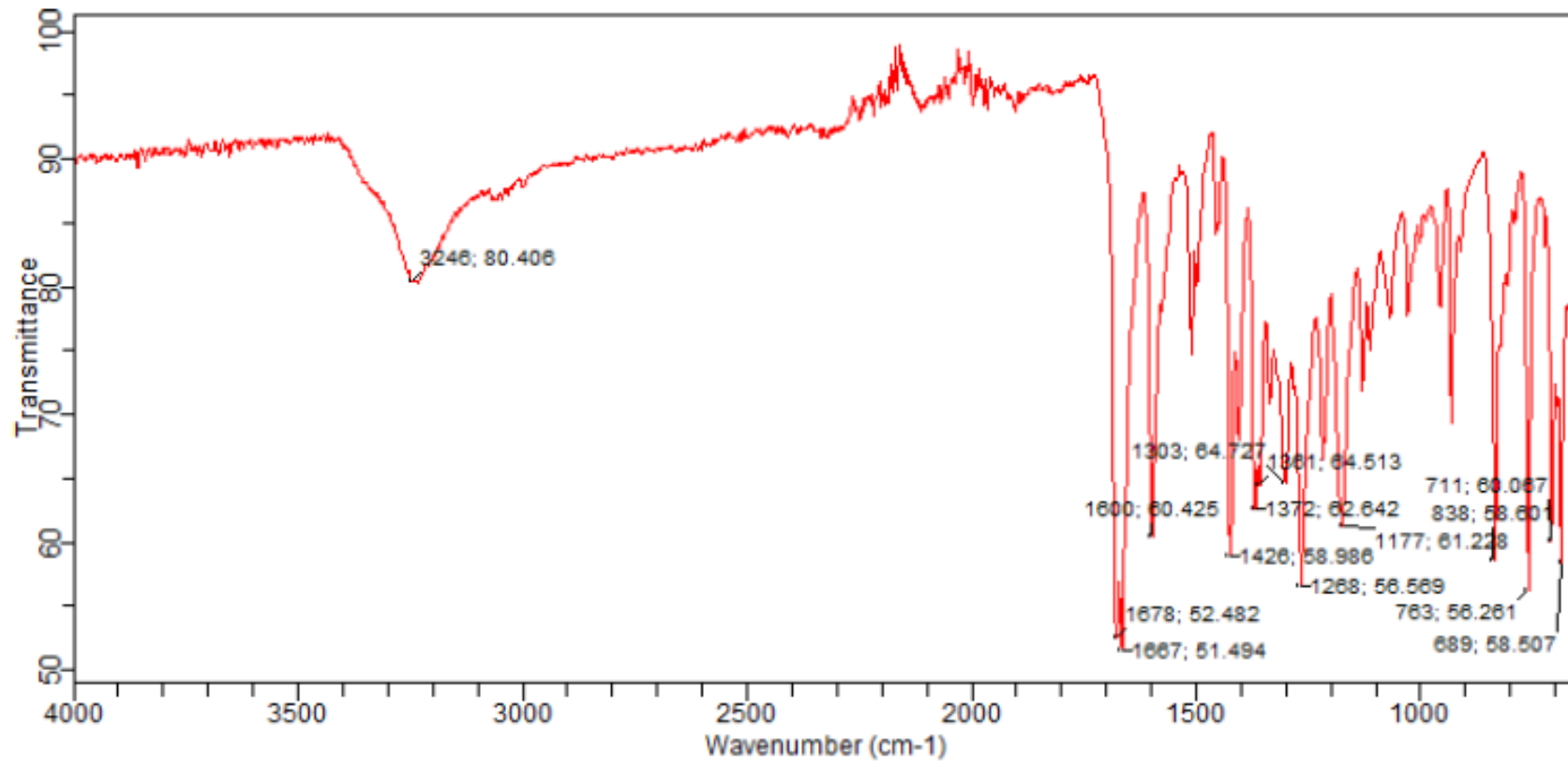


Fig A. 1: IR spectrum of 6-acetyl-2,3-diphenylquinoline-4-carboxylic acid (**I**).

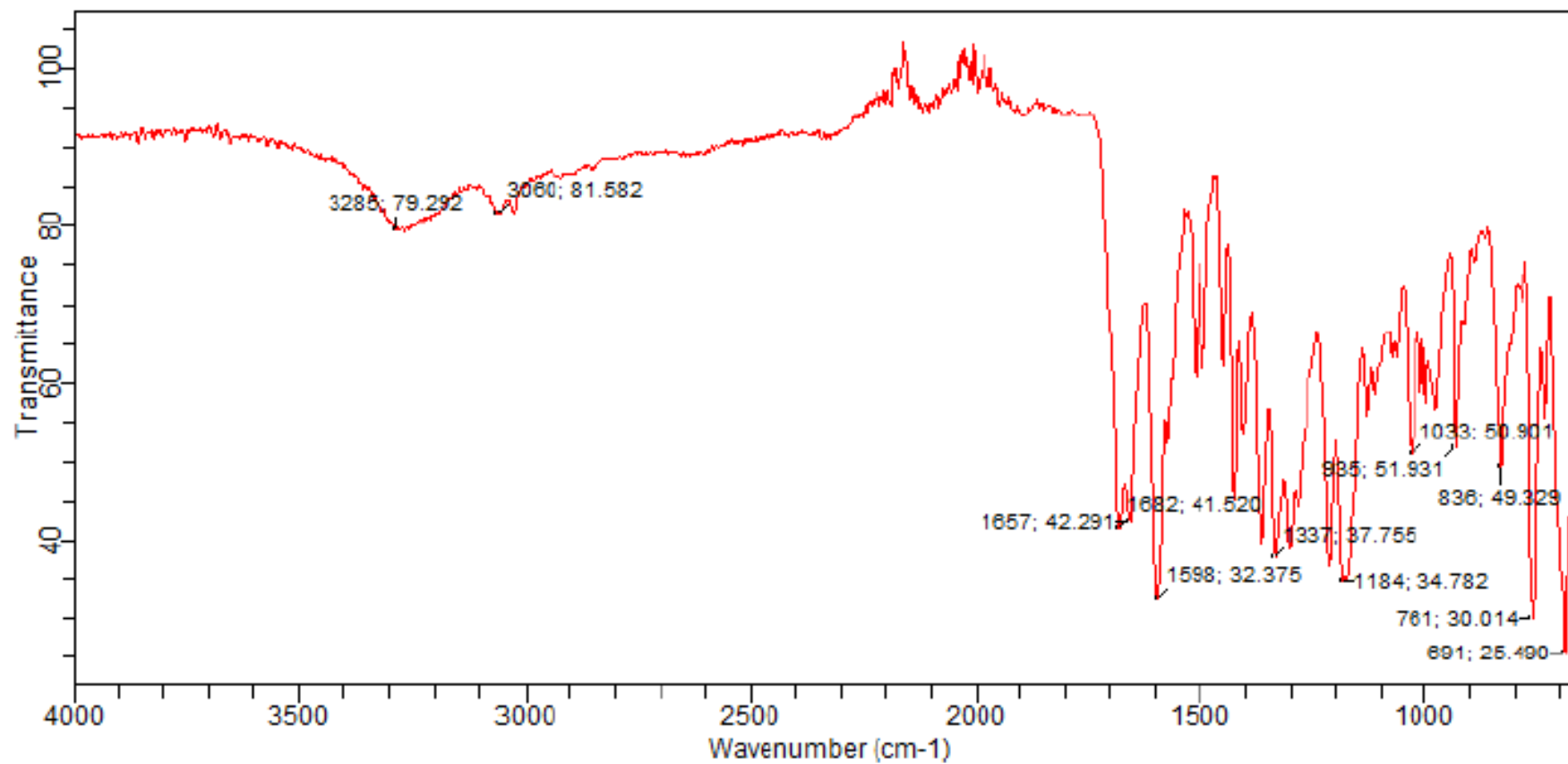


Fig A. 2: IR spectrum of 6-cinnamoyl-2,3-diphenylquinoline-4-carboxylic acid (II).

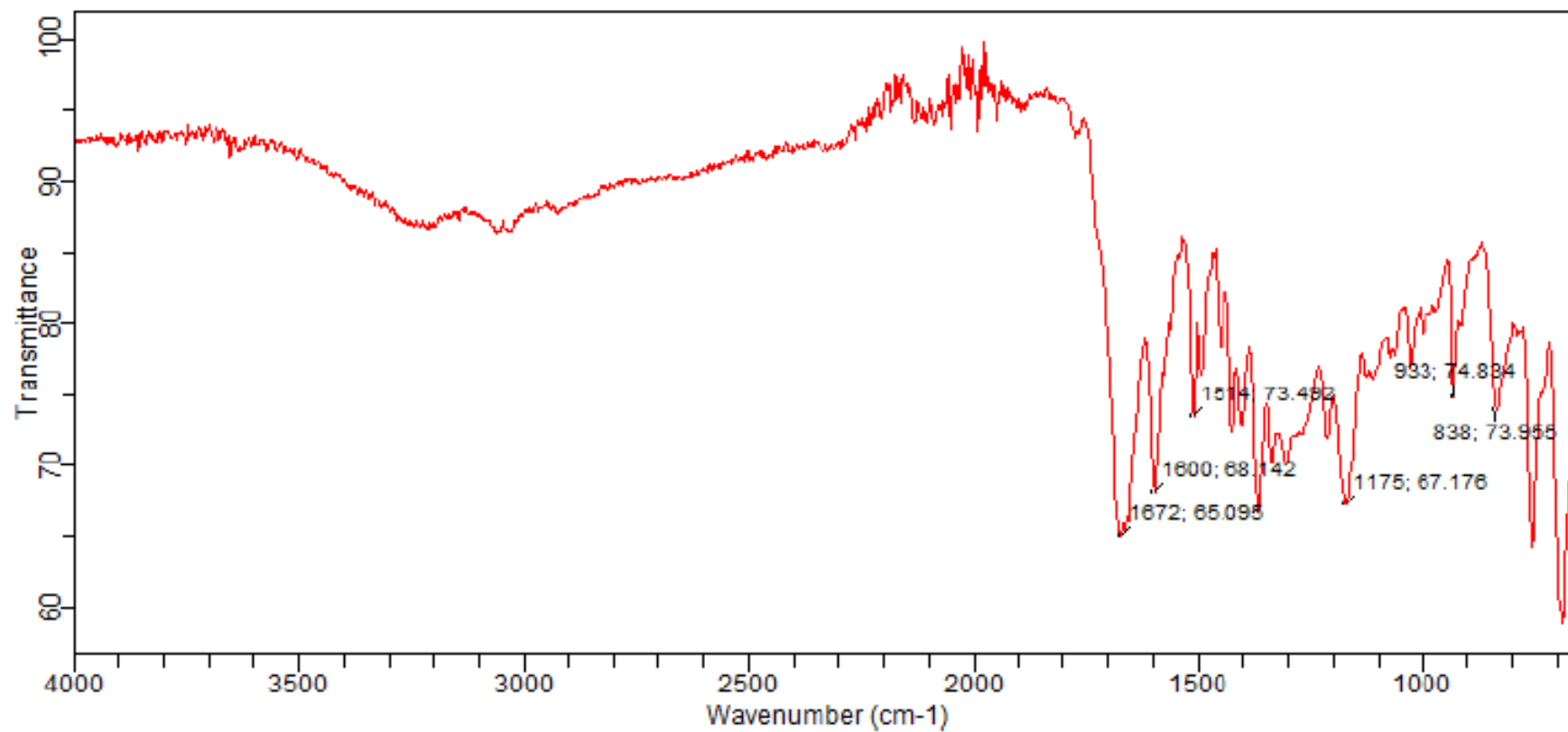


Fig A. 3: IR spectrum of 6-(2-oxo-6-phenyl-1,2-dihydropyrimidin-4-yl)-quinoline-4-carboxylic acid (III).

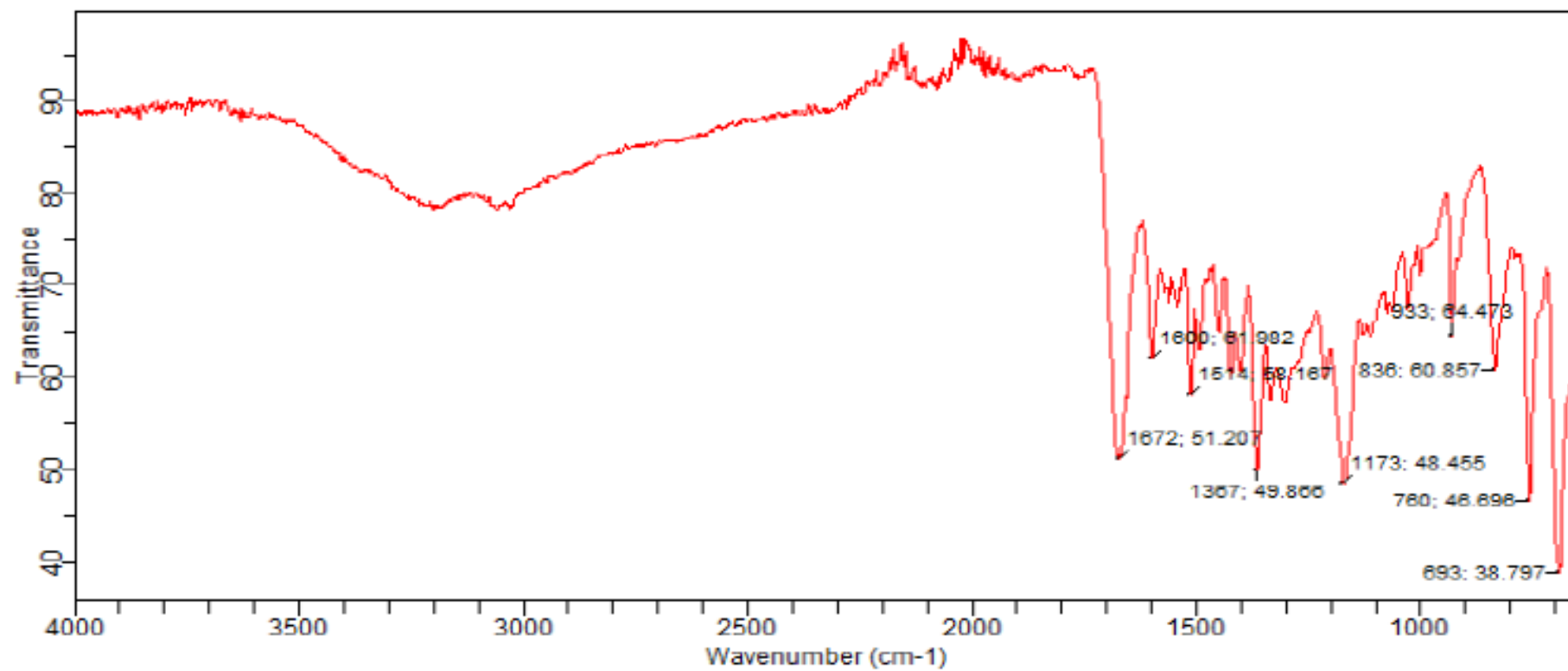


Fig A. 4: IR spectrum of 2,3-diphenyl-6-(6-phenyl-2-thioxo-1,2-dihydropyrimidin-4-yl)quinoline-4-carboxylic acid (**IV**).

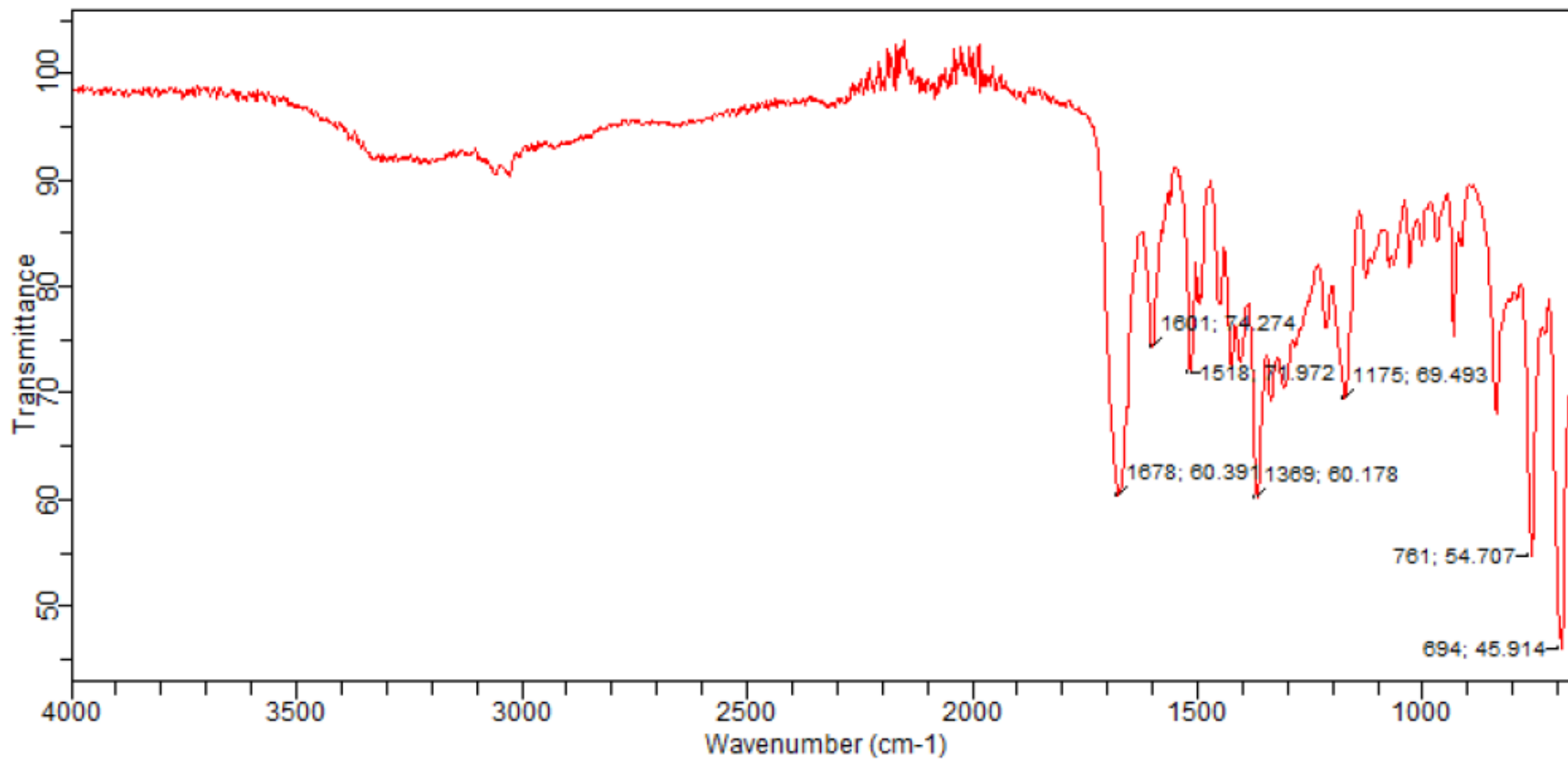


Fig A. 5: IR spectrum 2,3-diphenyl-6-(5-phenyl-4,5-dihydro-1H-pyrazol-3-yl)quinoline-4-carboxylic acid (VI).

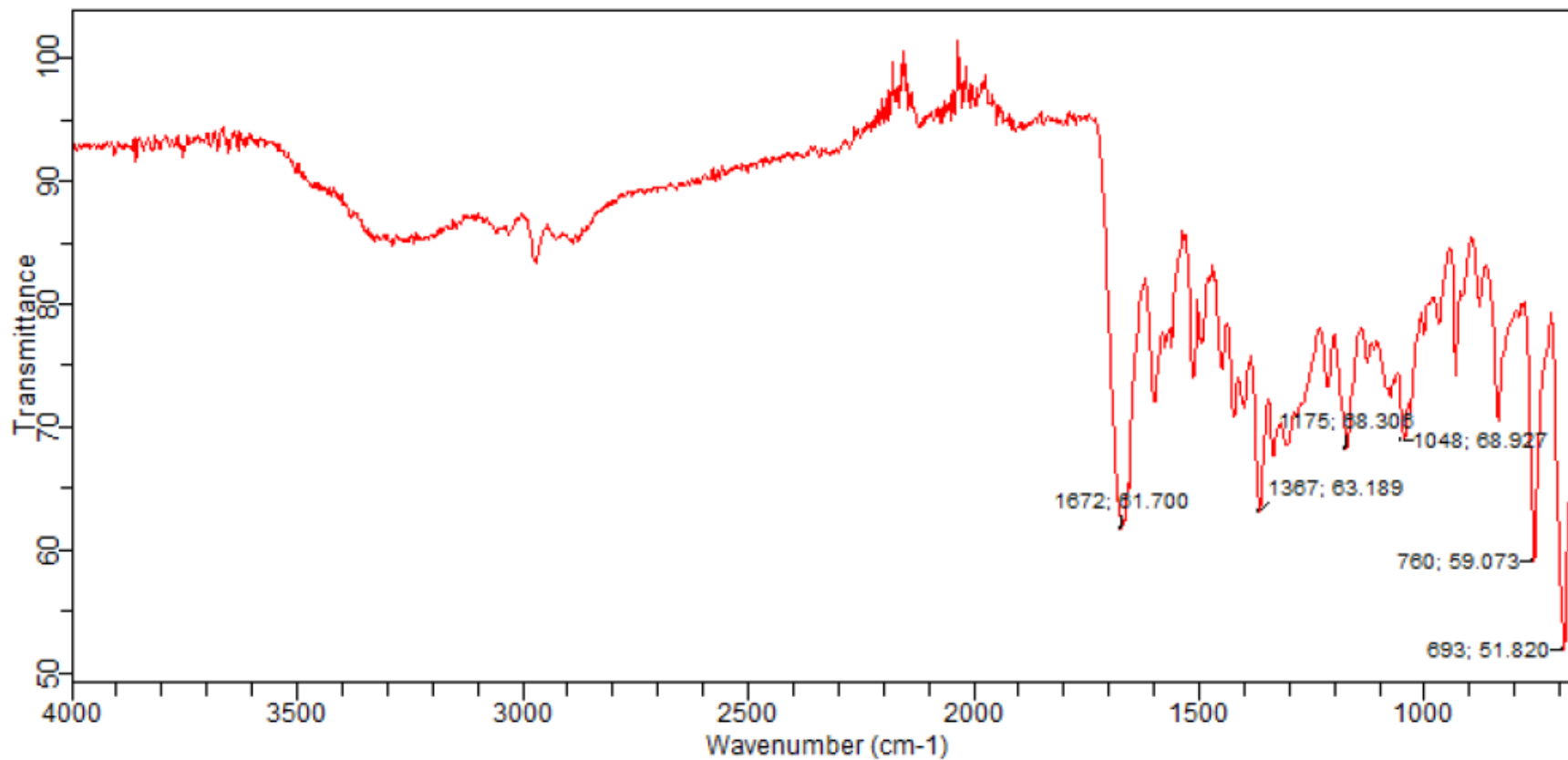


Fig A. 6: IR spectrum of 6-(1-carbamoyl-5-phenyl-4,5-dihydro-1H-pyrazol-3-yl)-2,3-diphenylquinoline-4-carboxylic acid (**VII**).

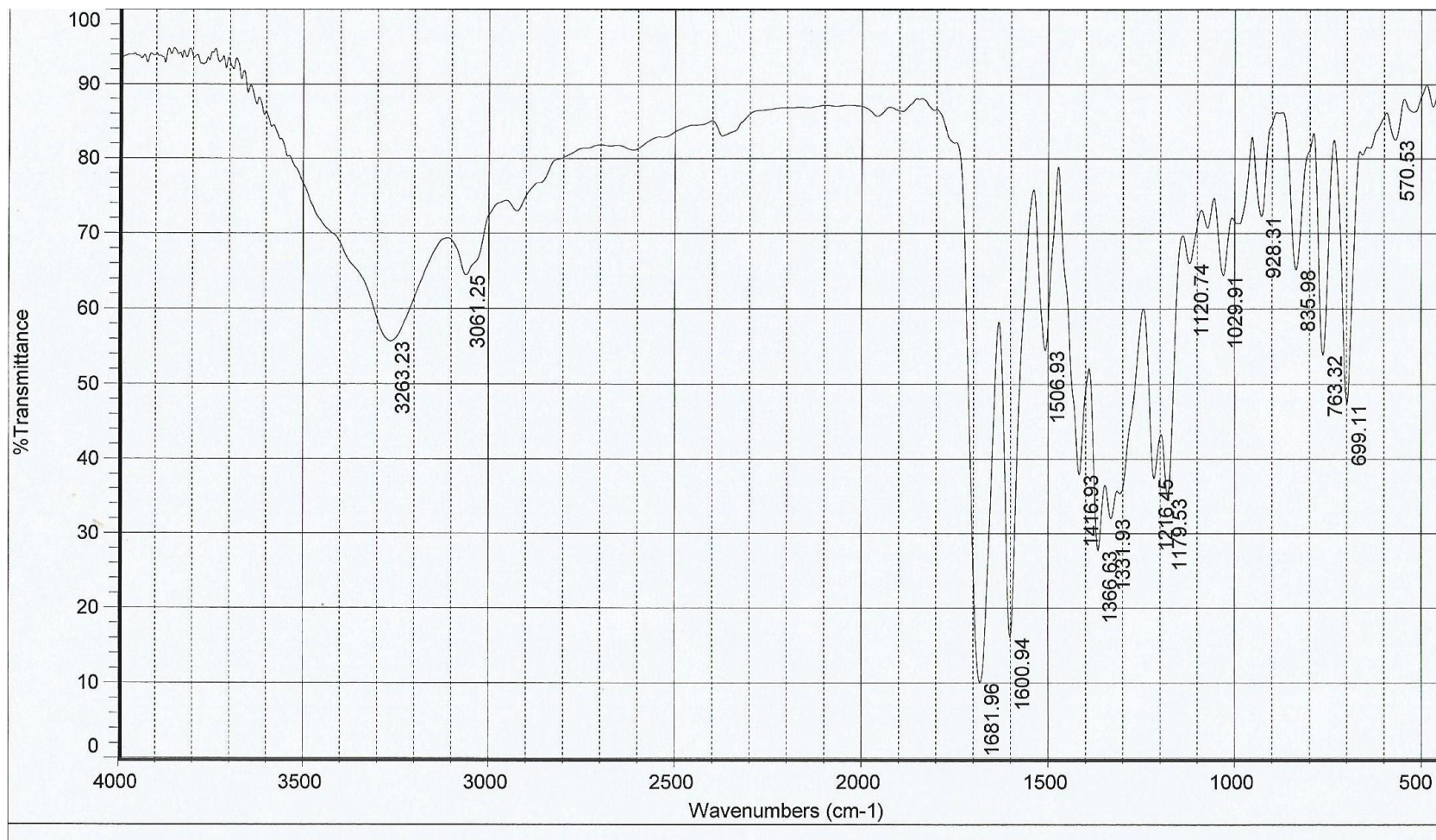


Fig A. 7: IR spectrum of 2,3-diphenyl-6-(7-phenyl-2,3,6,7-tetrahydro-1,4-oxazepin-5-yl)quinoline-4-carboxylic acid (**VIII**).

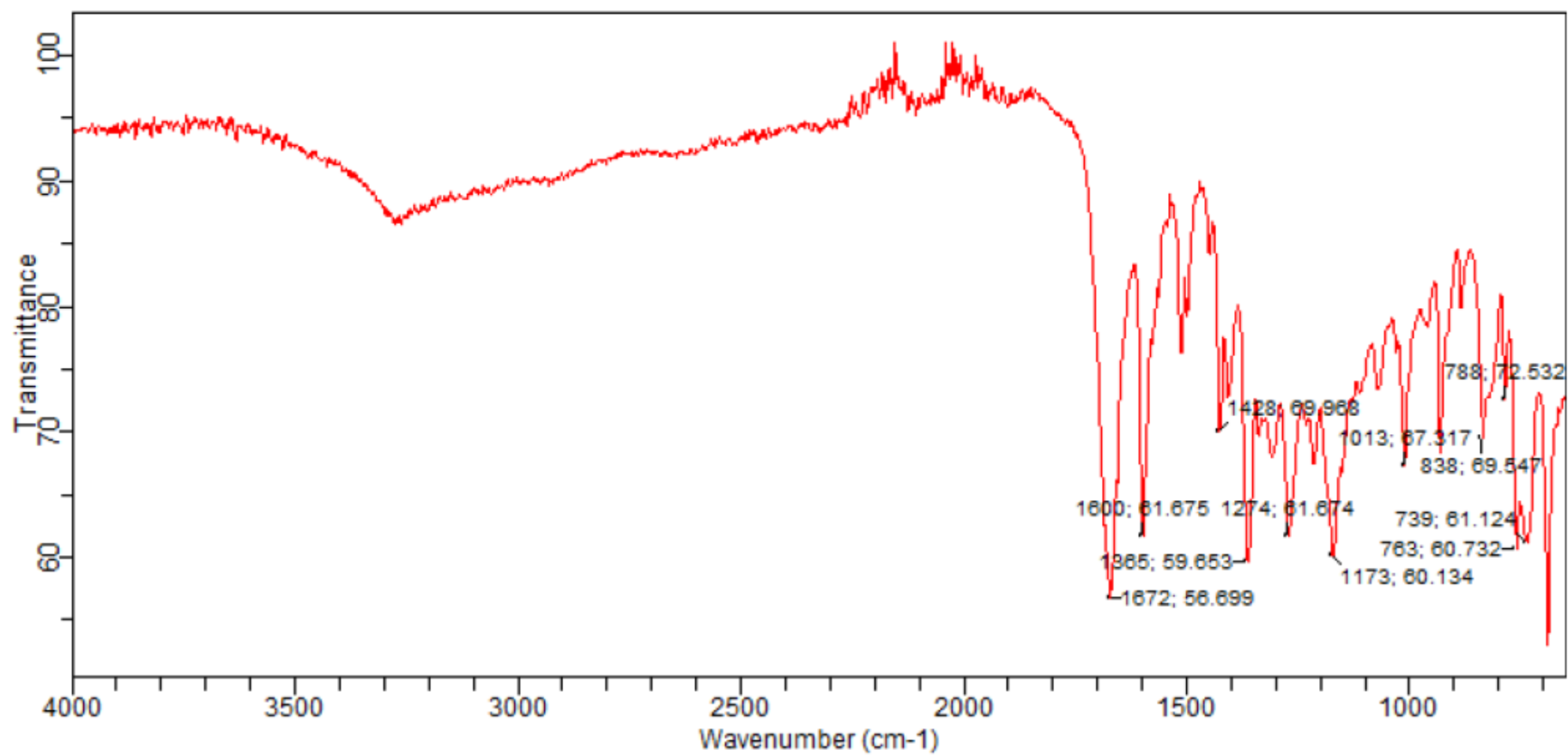


Fig A. 8: IR spectrum of 6-acetyl-2-(furan-2-yl)-3-phenylquinoline-4-carboxylic acid (**X**).

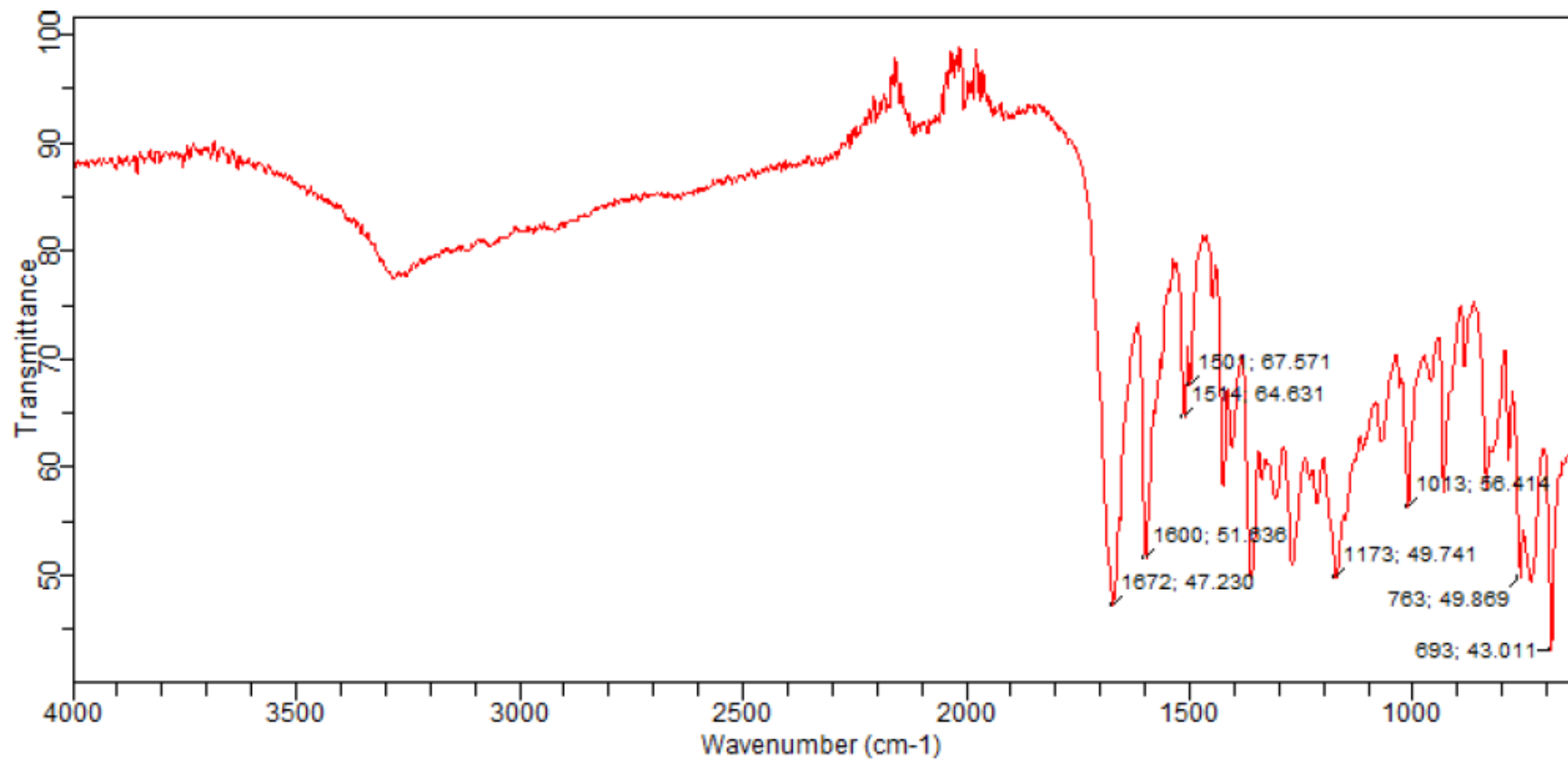


Fig A. 9: IR spectrum of 2-(furan-2-yl)-6-(6-(furan-2-yl)-2-oxo-1,2-dihydropyrimidin-4-yl)-3-phenylquinoline-4-carboxylic acid (**XI**).

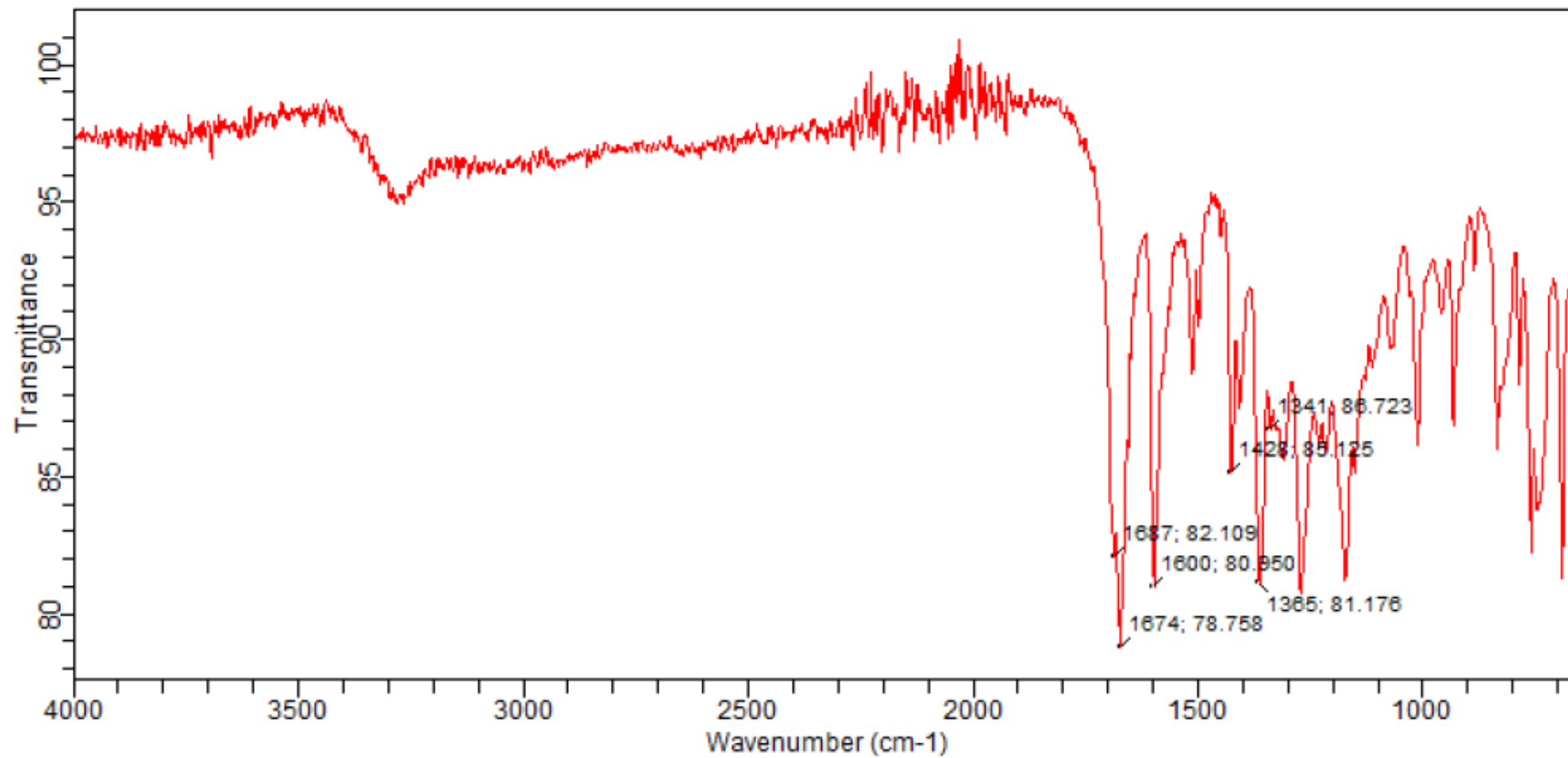


Fig A. 10: IR spectrum of 2-(furan-2-yl)-6-(6-(furan-2-yl)-2-thioxo-1,2-dihydropyrimidin-4-yl)-3-phenylquinoline-4-carboxylic acid (**XII**).

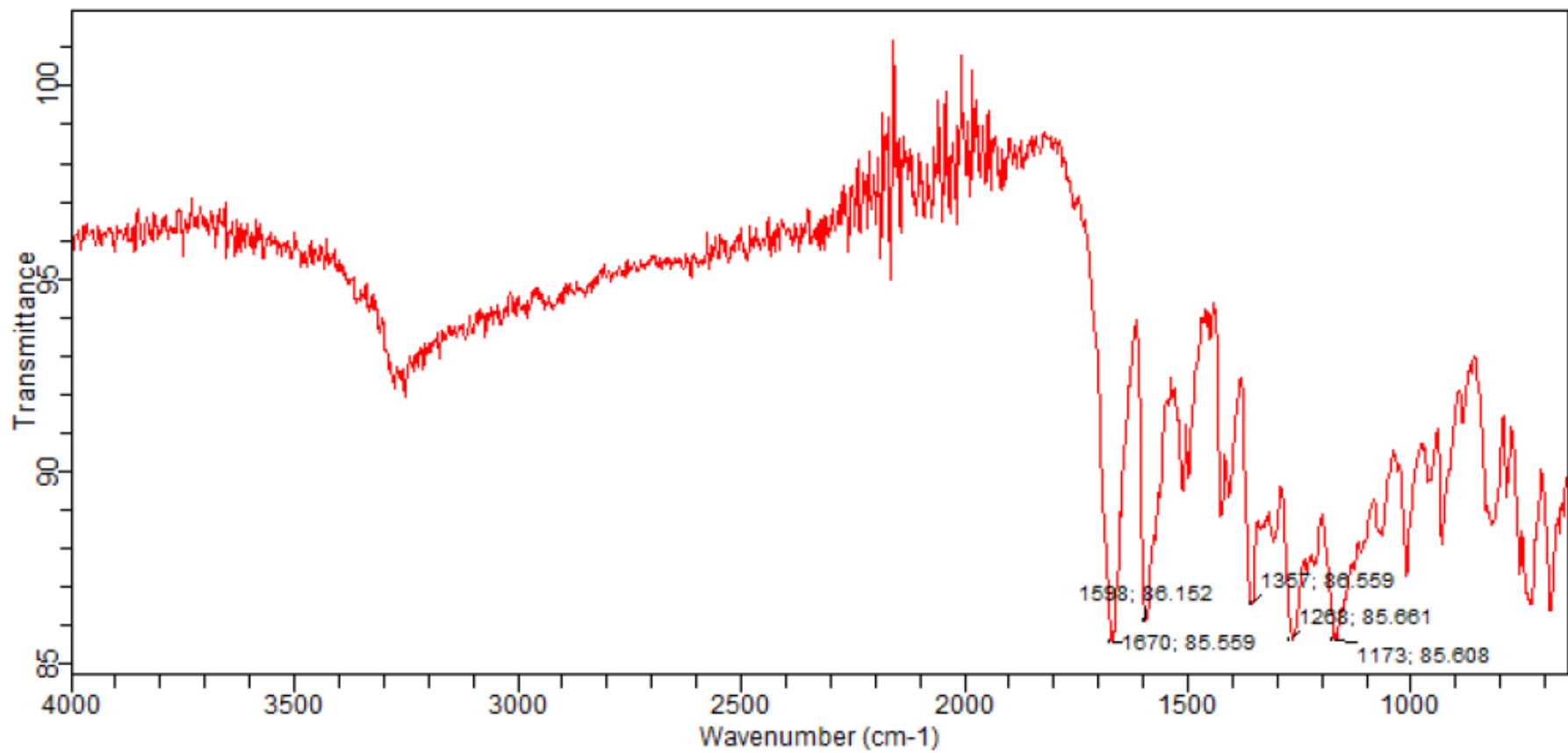


Fig A. 11: IR spectrum of 2-(furan-2-yl)-6-(5-(furan-2-yl)-1-phenyl-4,5-dihydro-1H-pyrazol-3-yl)-3-phenylquinoline-4-carboxylic acid (**XIII**).

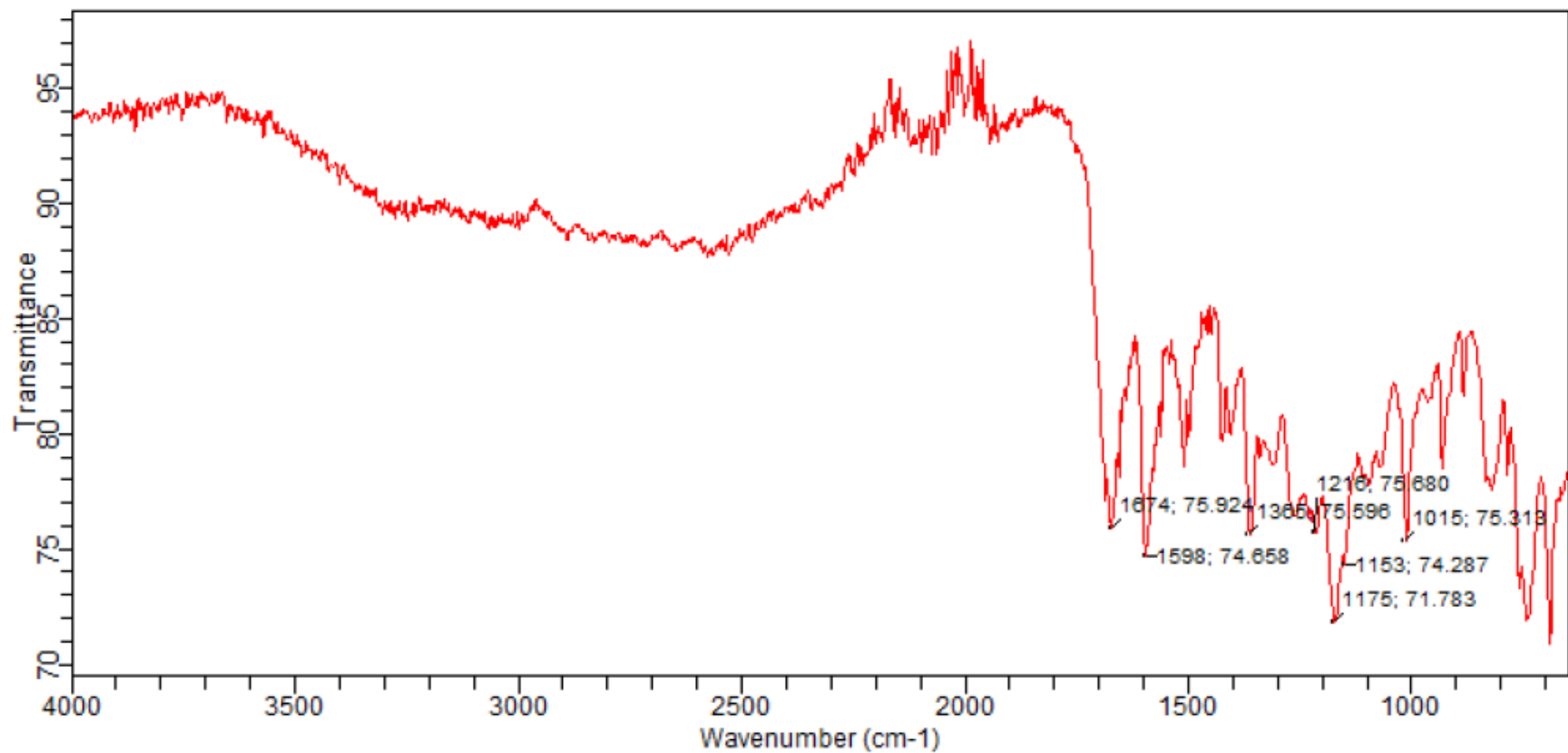


Fig A. 12: IR spectrum of 6-(1-carbamoyl-5-(furan-2-yl)-4,5-dihydro-1H-pyrazol-3-yl)-2-(furan-2-yl)-3-phenylquinoline-4-carboxylic acid (**XIV**).

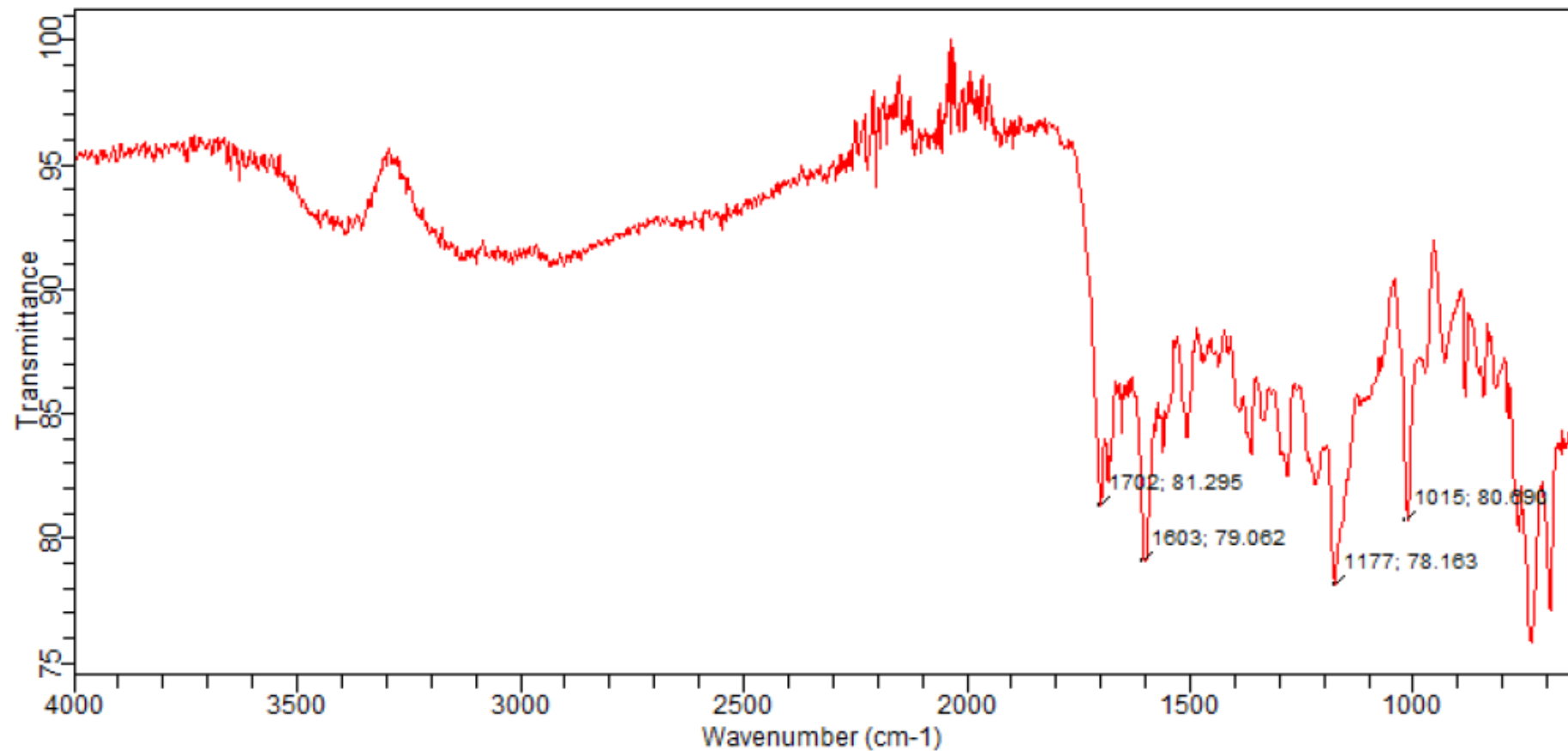


Fig A. 13: IR spectrum spectrum of 6-(1-carbamoyl-5-(furan-2-yl)-4,5-dihydro-1H-pyrazol-3-yl)-2-(furan-2-yl)-3-phenylquinoline-4-carboxylic acid (XV).

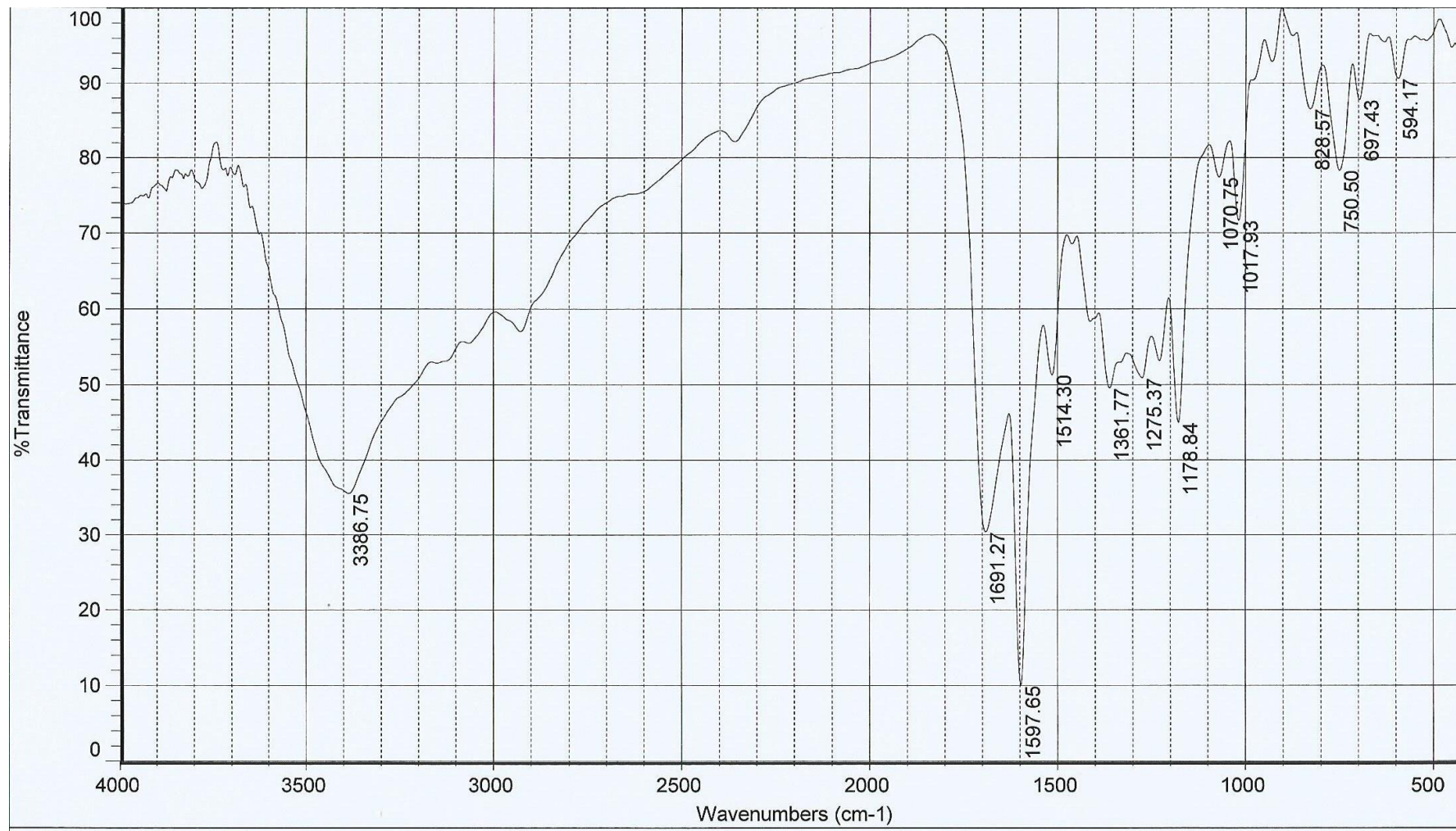


Fig A. 14: IR spectrum of 2-(furan-2-yl)-6-(7-(furan-2-yl)-2,3,6,7-tetrahydro-1,4-oxazepin-5-yl)-3-phenylquinoline-4-carboxylic acid (XVI).

Appendix B

^1H Nuclear magnetic resonance (^1H NMR) spectrum of the prepared 2, 3-diphenyl/ 2 (furan-2-yl), 3-phenylquinoline-4-carboxylic acid derivatives:

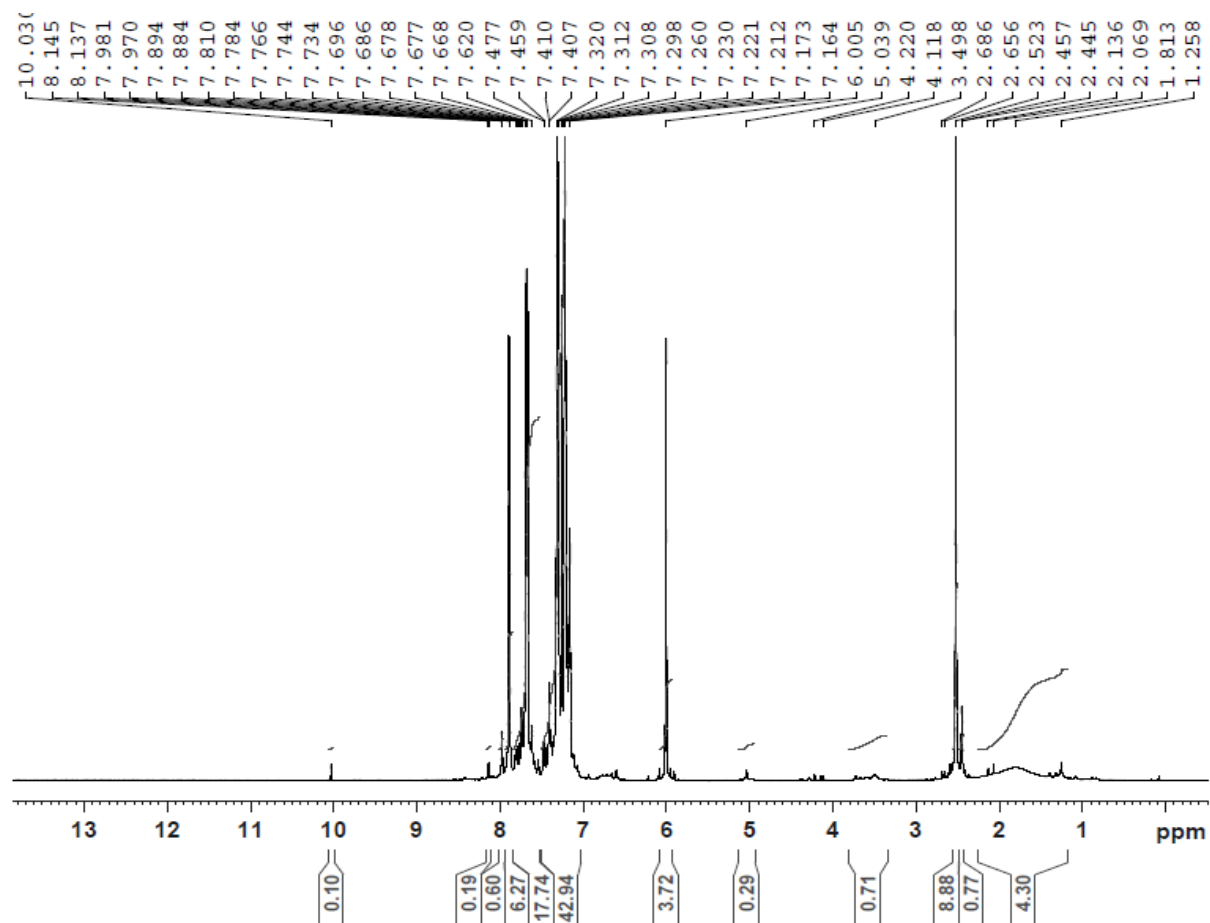


Fig B.1: ^1H NMR spectrum of 6-acetyl-2,3-diphenylquinoline-4-carboxylic acid (I).

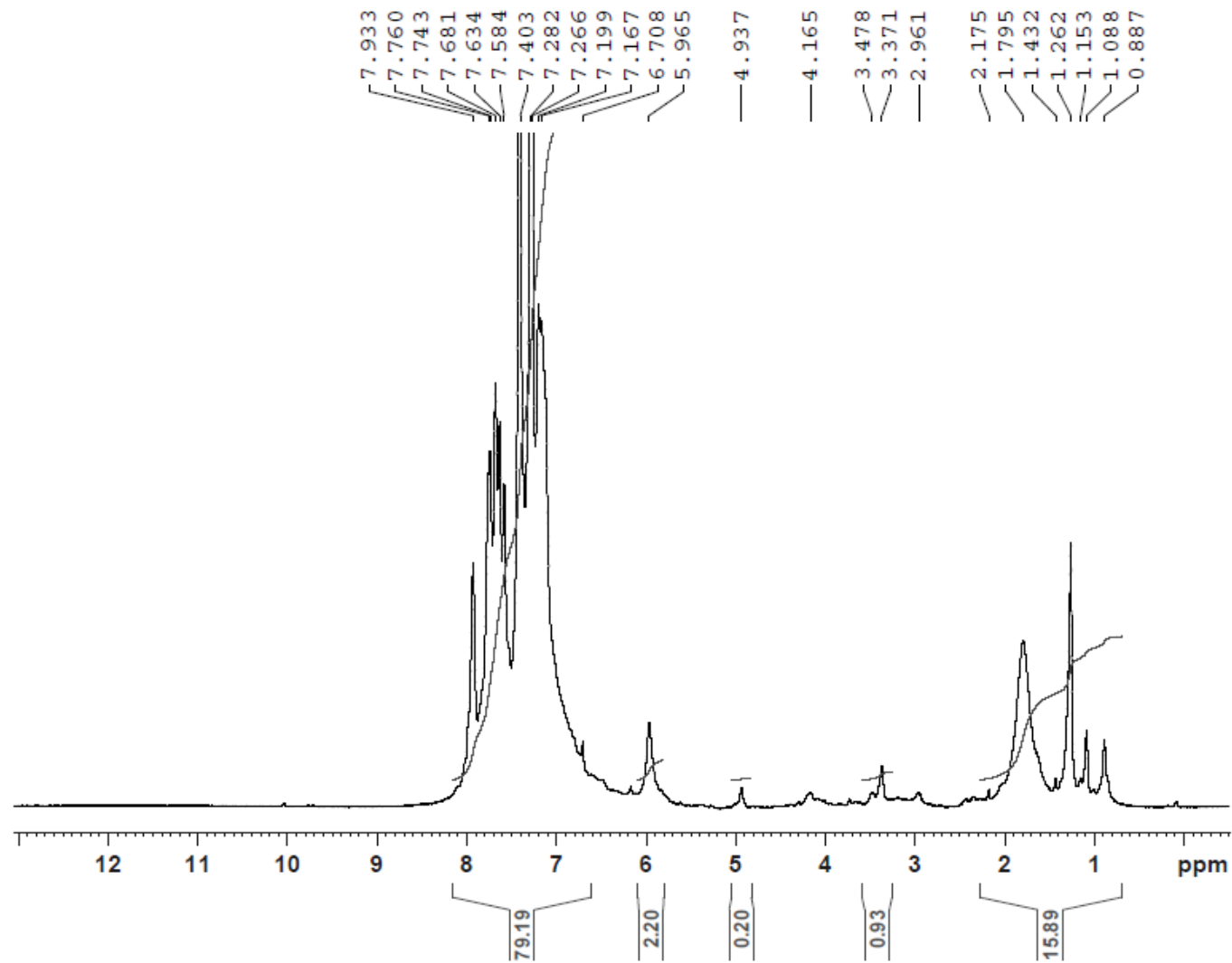


Fig B. 2: ^1H NMR spectrum of 6-cinnamoyl-2,3-diphenylquinoline-4-carboxylic acid (**II**).

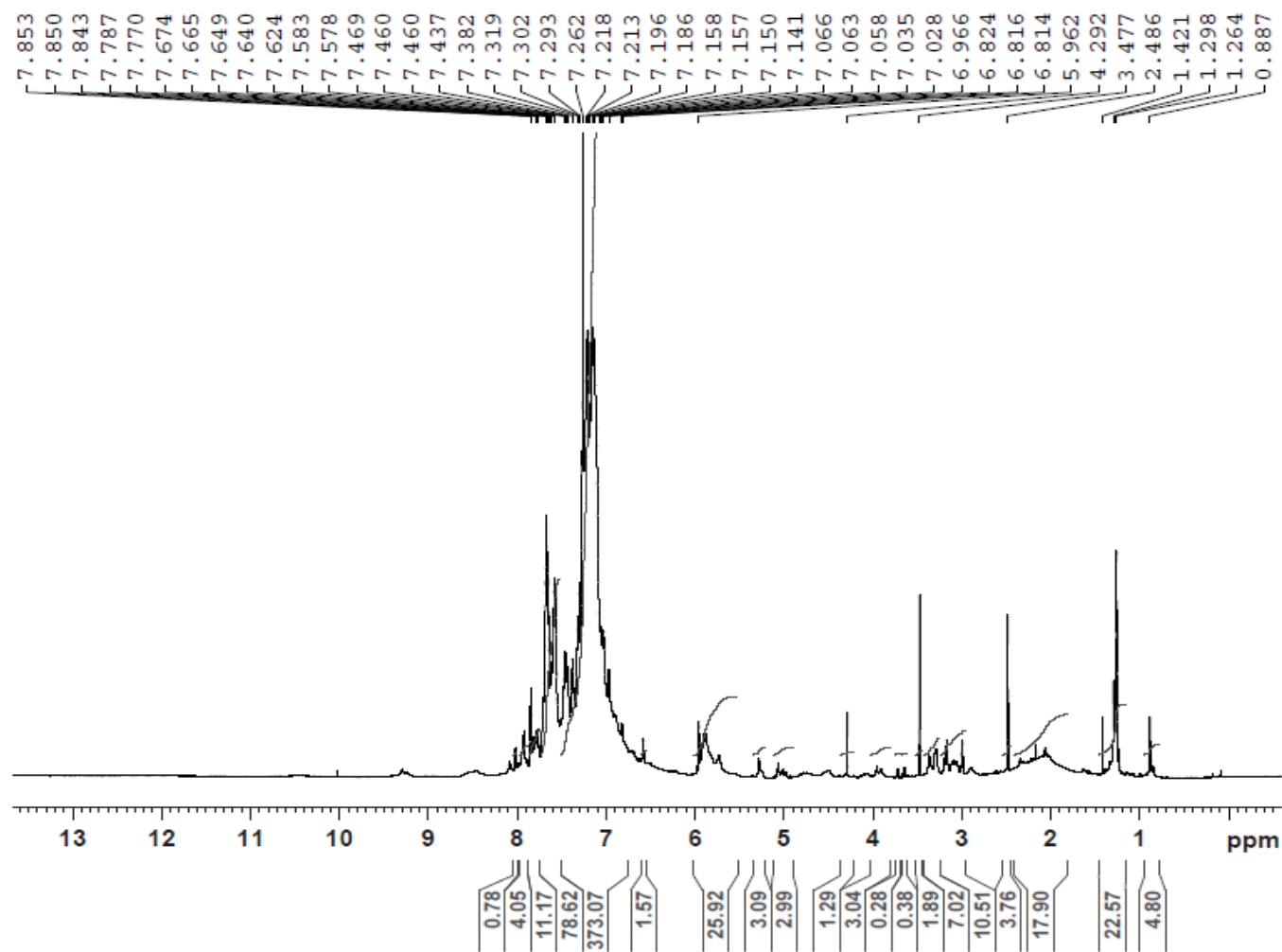


Fig B. 3: ^1H NMR spectrum of 6-(2-oxo-6-phenyl-1,2-dihydropyrimidin-4-yl)-quinoline-4-carboxylic acid

(III).

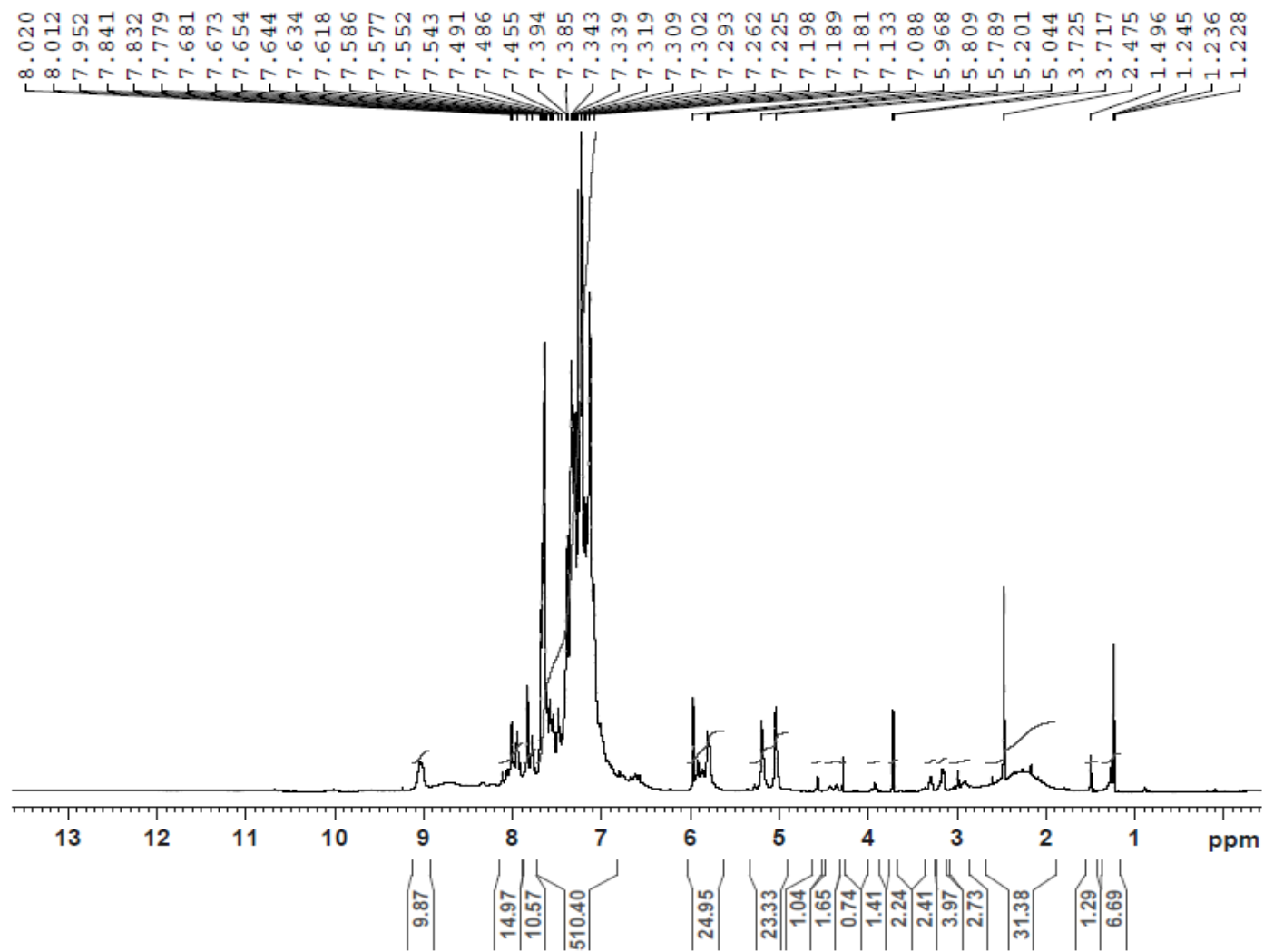


Fig B. 4: ^1H NMR 2,3-diphenyl-6-(6-phenyl-2-thioxo-1,2-dihydropyrimidin-4-yl)quinoline-4-carboxylic acid (**IV**).

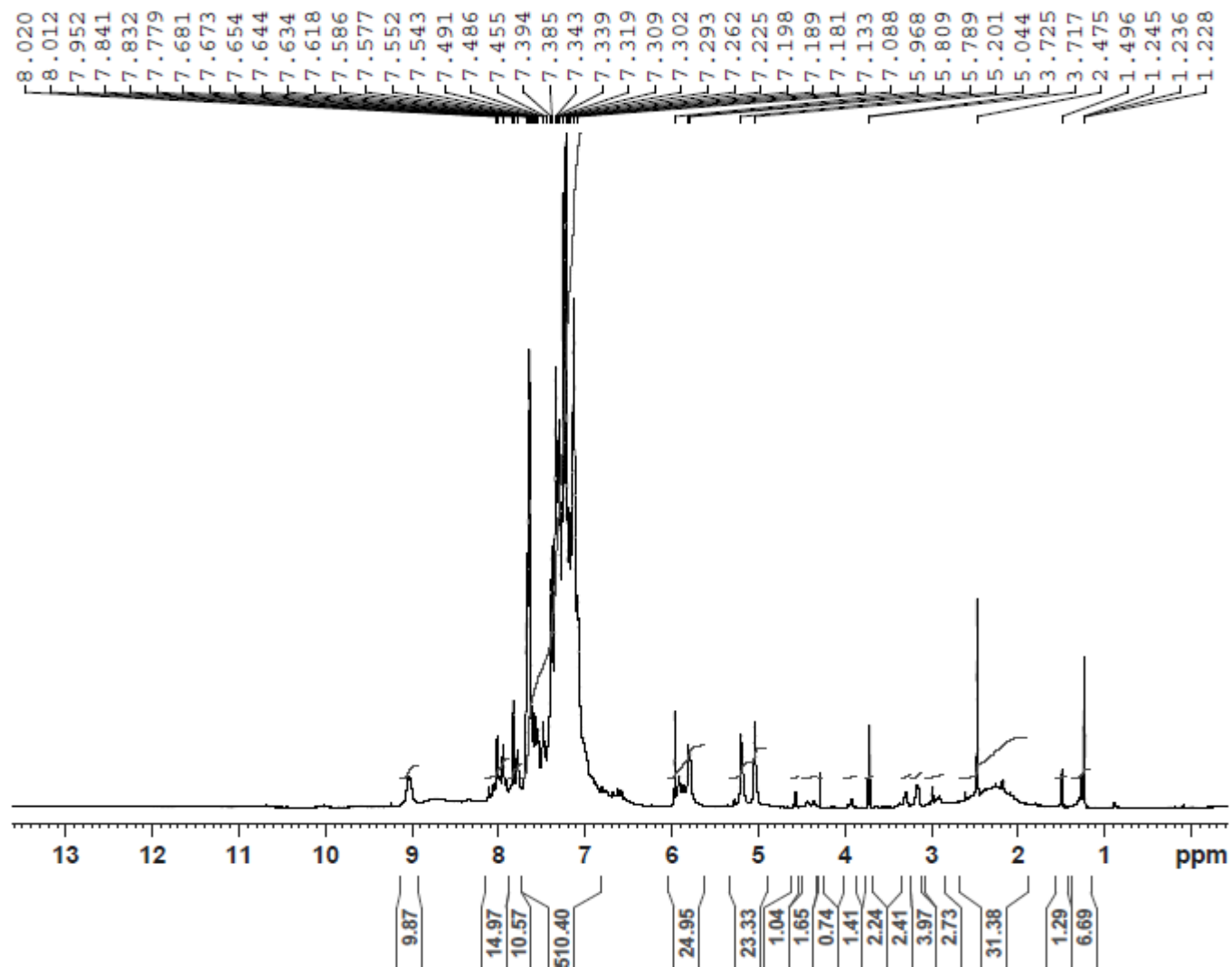


Fig B. 5: ¹H NMR of 6-(1,5-diphenyl-4,5-dihydro-1H-pyrazol-3-yl)-2,3-diphenylquinoline-4-carboxylic acid (V).

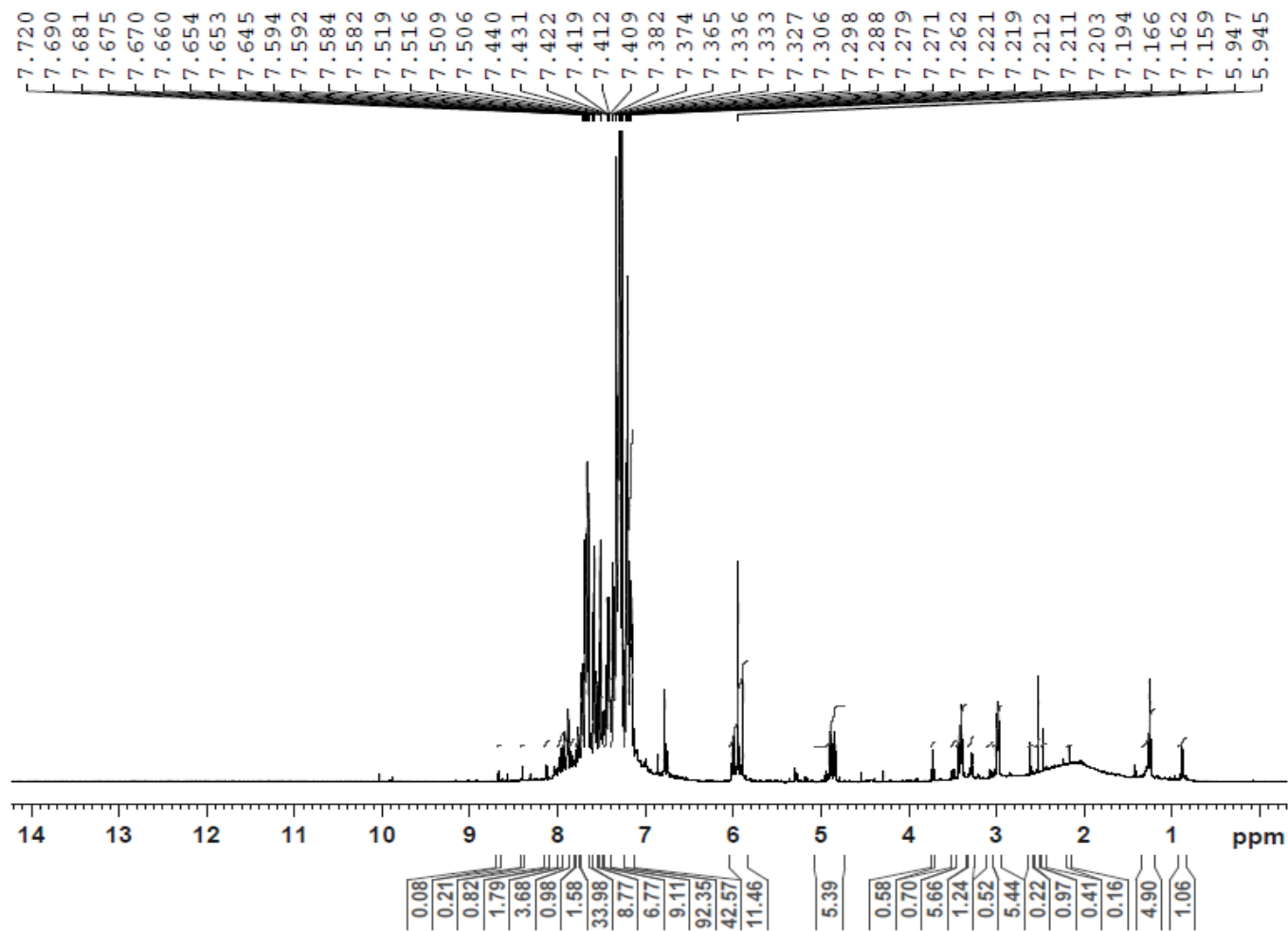


Fig B. 6: ^1H NMR 2,3-diphenyl-6-(5-phenyl-4,5-dihydro-1H-pyrazol-3-yl)quinoline-4-carboxylic acid (**VI**).

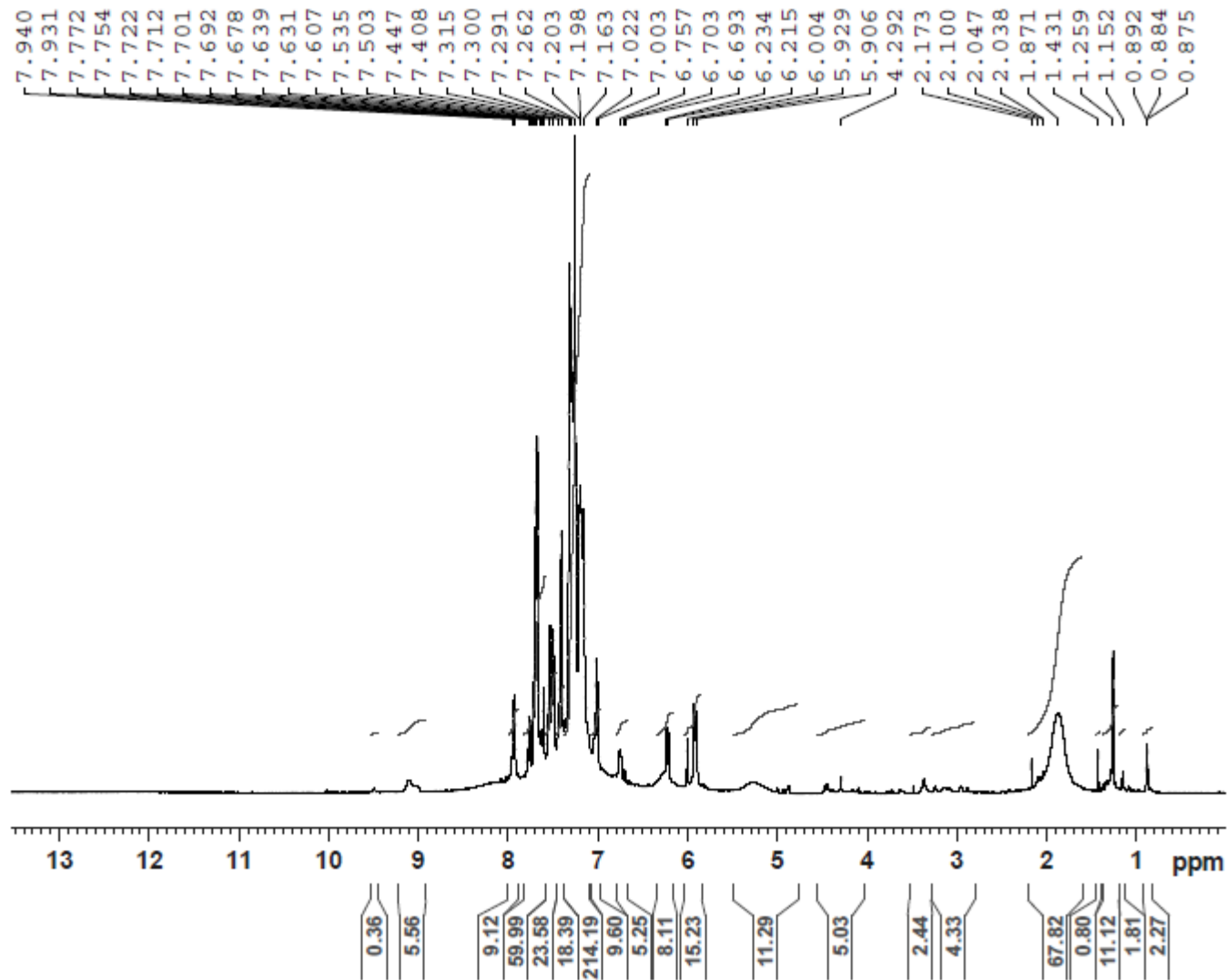


Fig B. 7: ¹H NMR 2,3-diphenyl-6-(5-phenyl-4,5-dihydro-1H-pyrazol-3-yl)quinoline-4-carboxylic acid (VII).

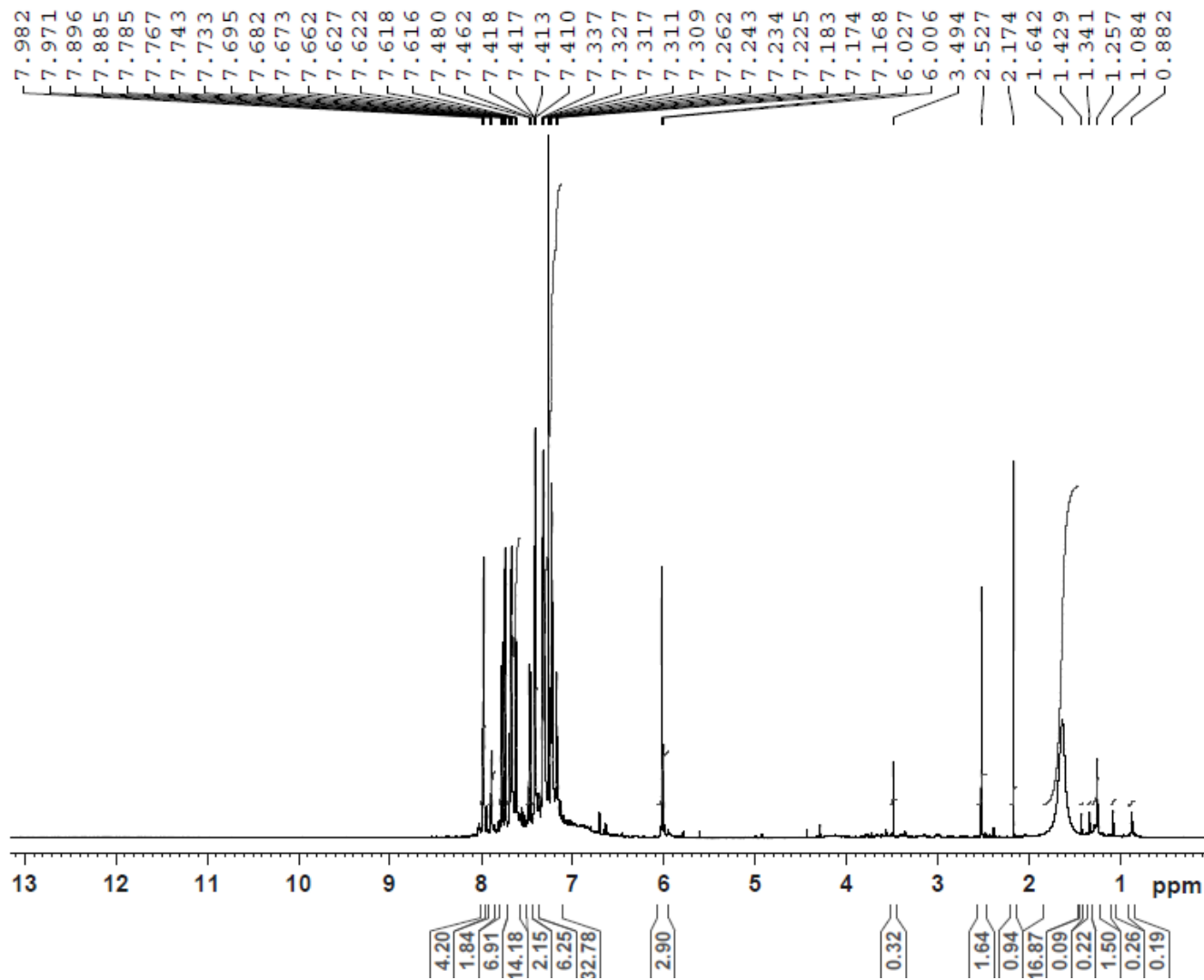


Fig B. 8: ¹H NMR 2,3-diphenyl-6-(7-phenyl-2,3,6,7-tetrahydro-1,4-oxazepin-5-yl)quinoline-4-carboxylic acid (VIII).

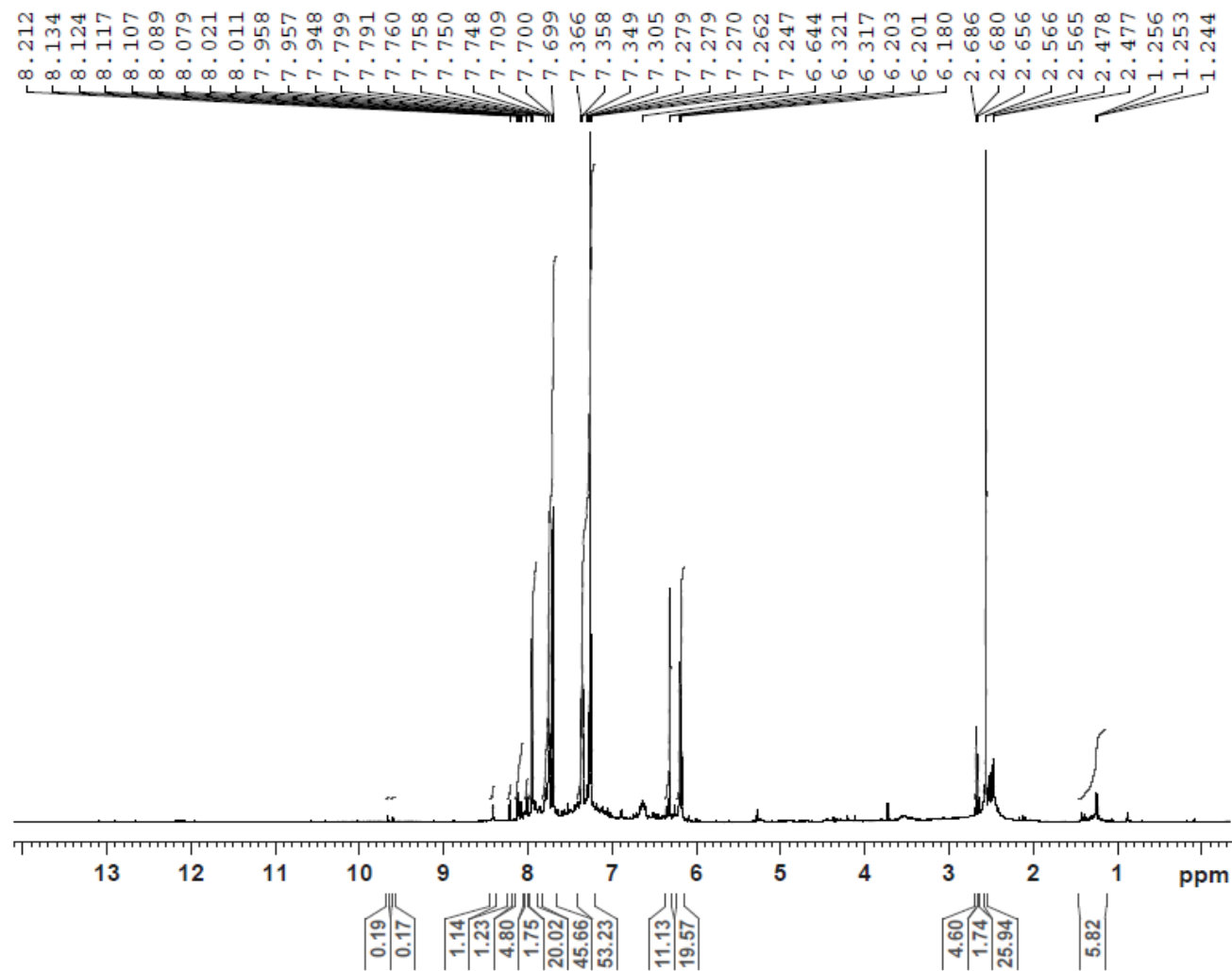


Fig B. 9: ^1H NMR of 6-acetyl-2-(furan-2-yl)-3-phenylquinoline-4-carboxylic acid (**IX**).

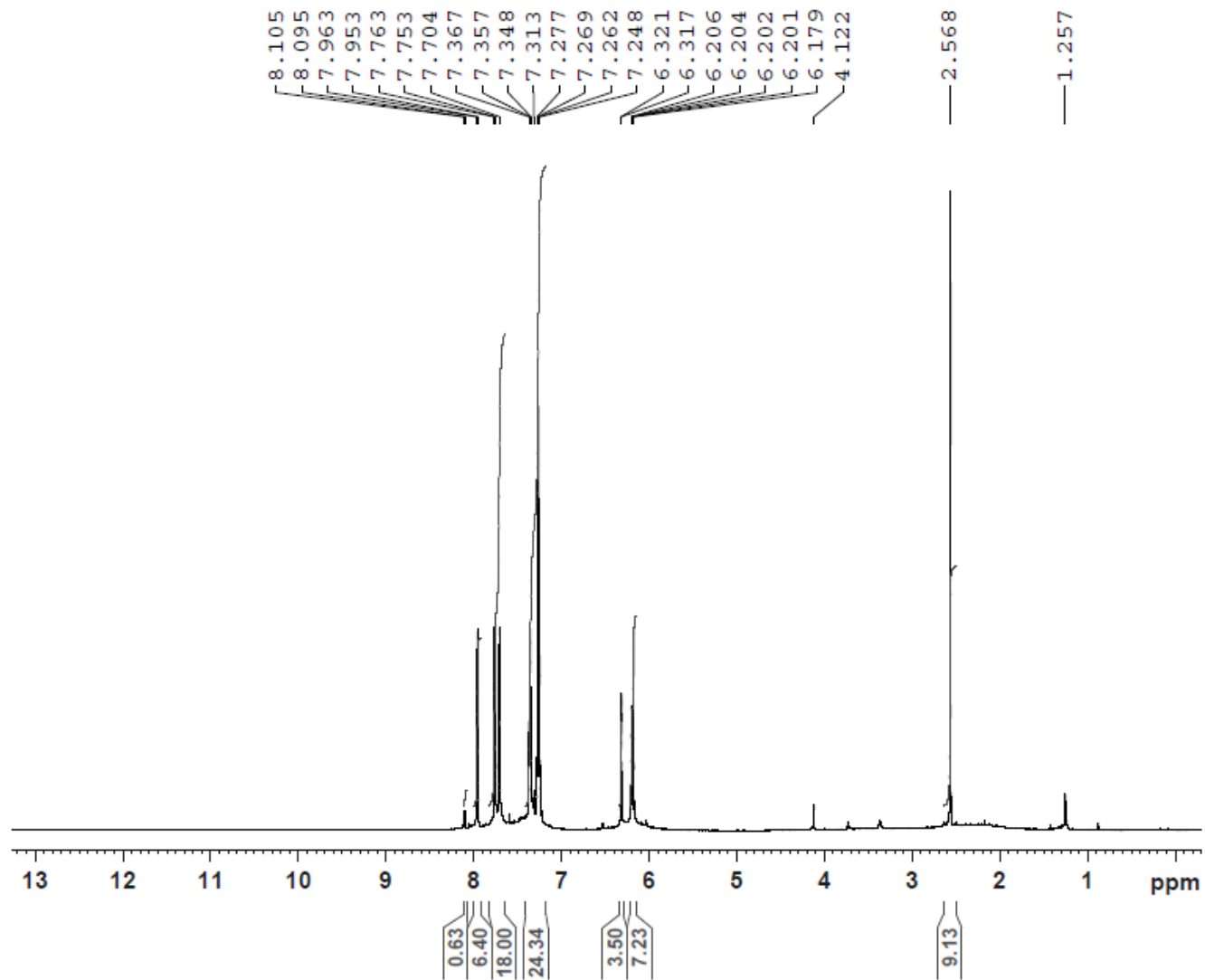


Fig B. 10: ¹H NMR of (E)-2-(furan-2-yl)-6-(3-(furan-2-yl)acryloyl)-3-phenylquinoline-4-carboxylic acid (**X**).

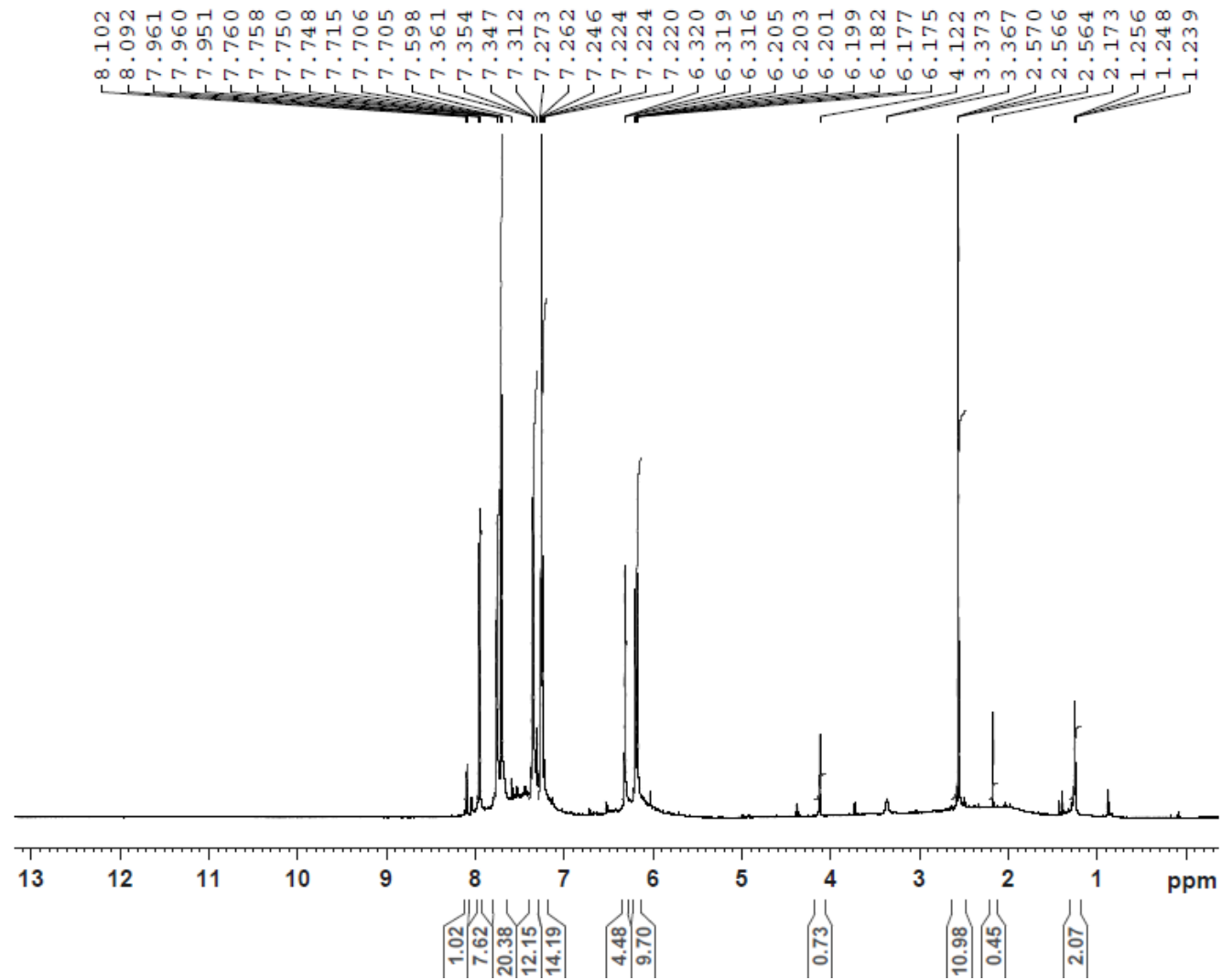


Fig B. 11: ^1H NMR of 2-(furan-2-yl)-6-(6-(furan-2-yl)-2-oxo-1,2-dihydropyrimidin-4-yl)-3-phenylquinoline-4-carboxylic acid (**XI**)

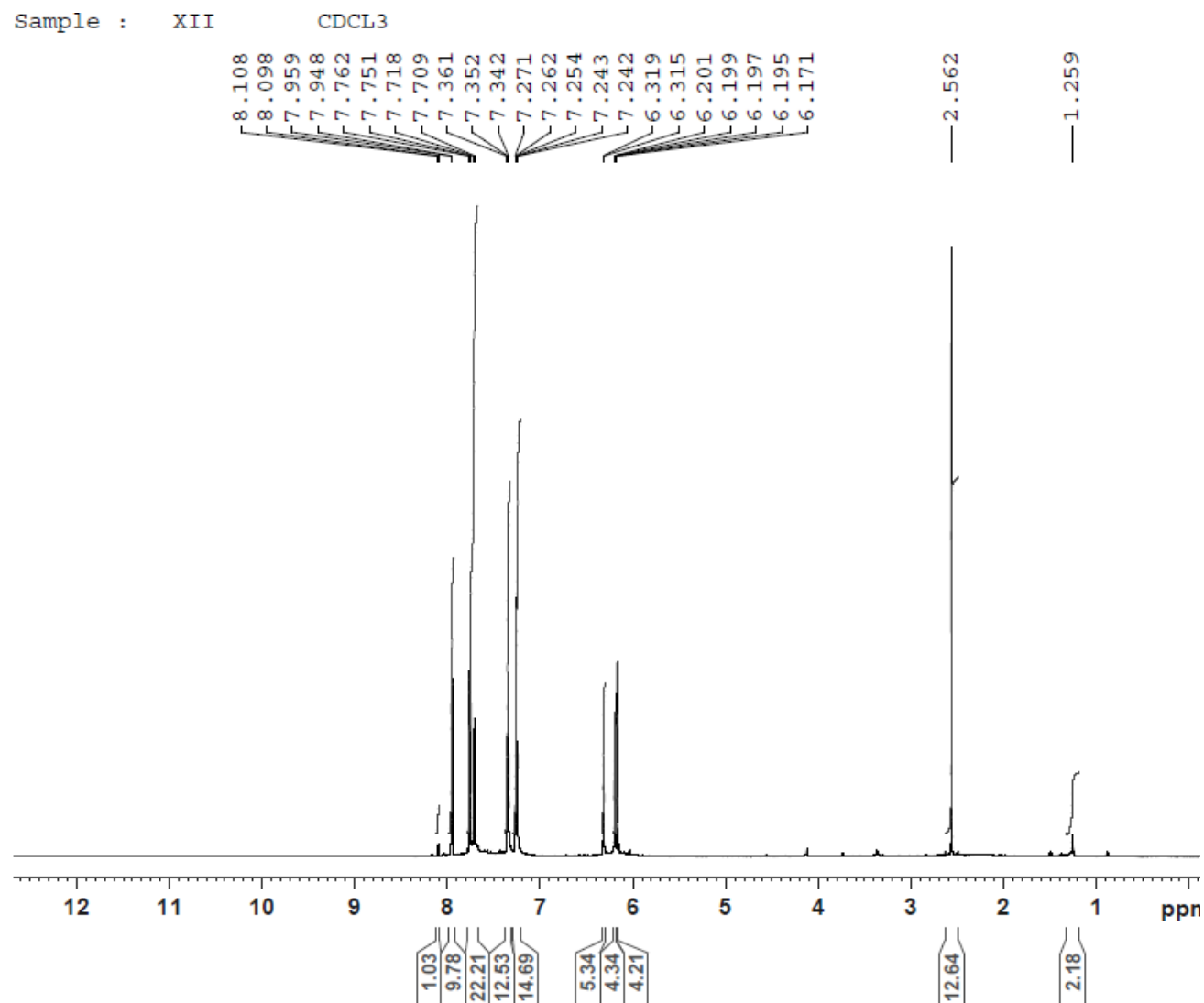


Fig B. 12: ¹HNMR of 2-(furan-2-yl)-6-(5-(furan-2-yl)-1-phenyl-4,5-dihydro-1H-pyrazol-3-yl)-3-phenylquinoline-4-carboxylic acid (**XII**).

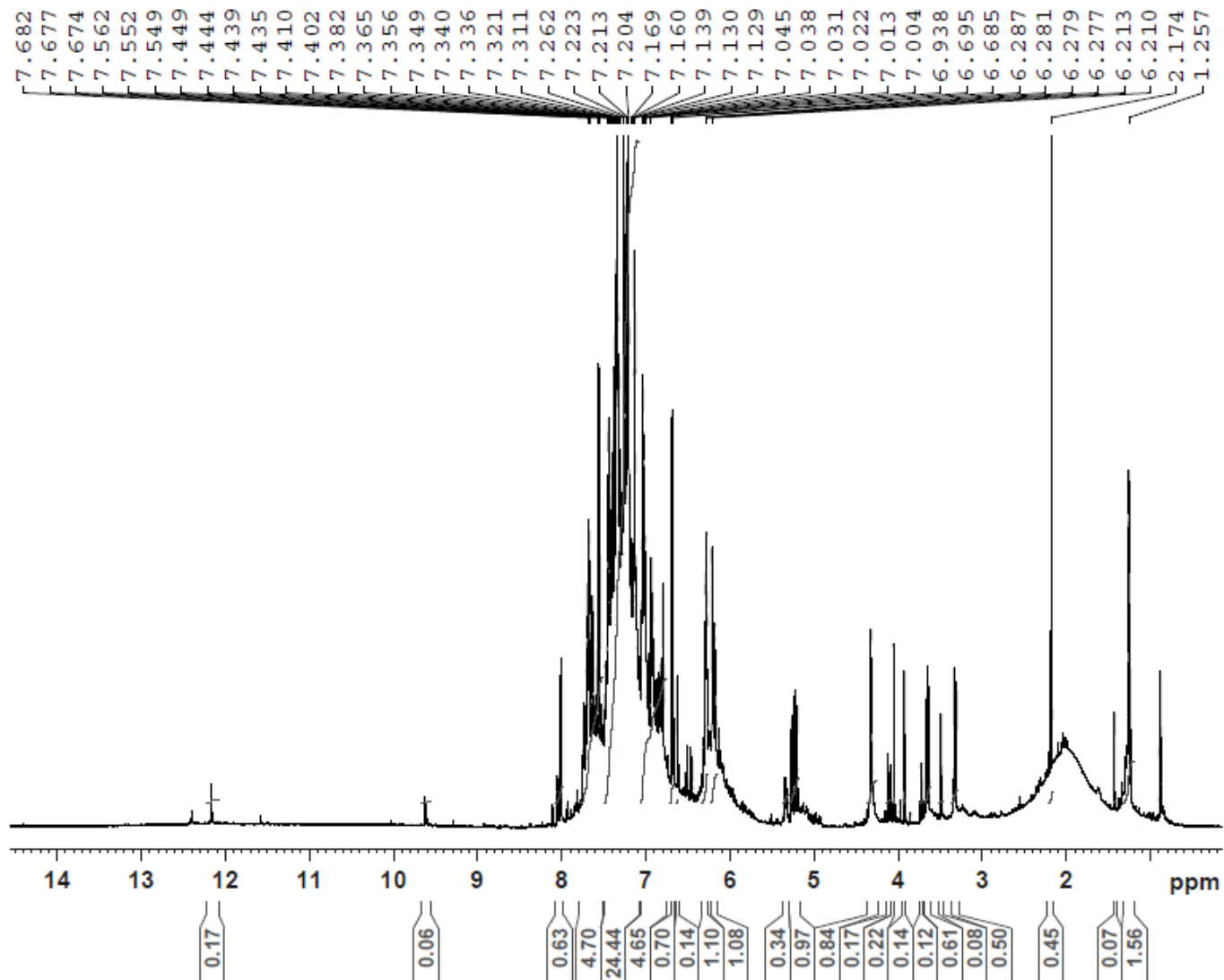


Fig B. 13: ¹H NMR of 2-(furan-2-yl)-6-(5-(furan-2-yl)-1-phenyl-4,5-dihydro-1H-pyrazol-3-yl)-3-phenylquinoline-4-carboxylic acid (**XIII**).

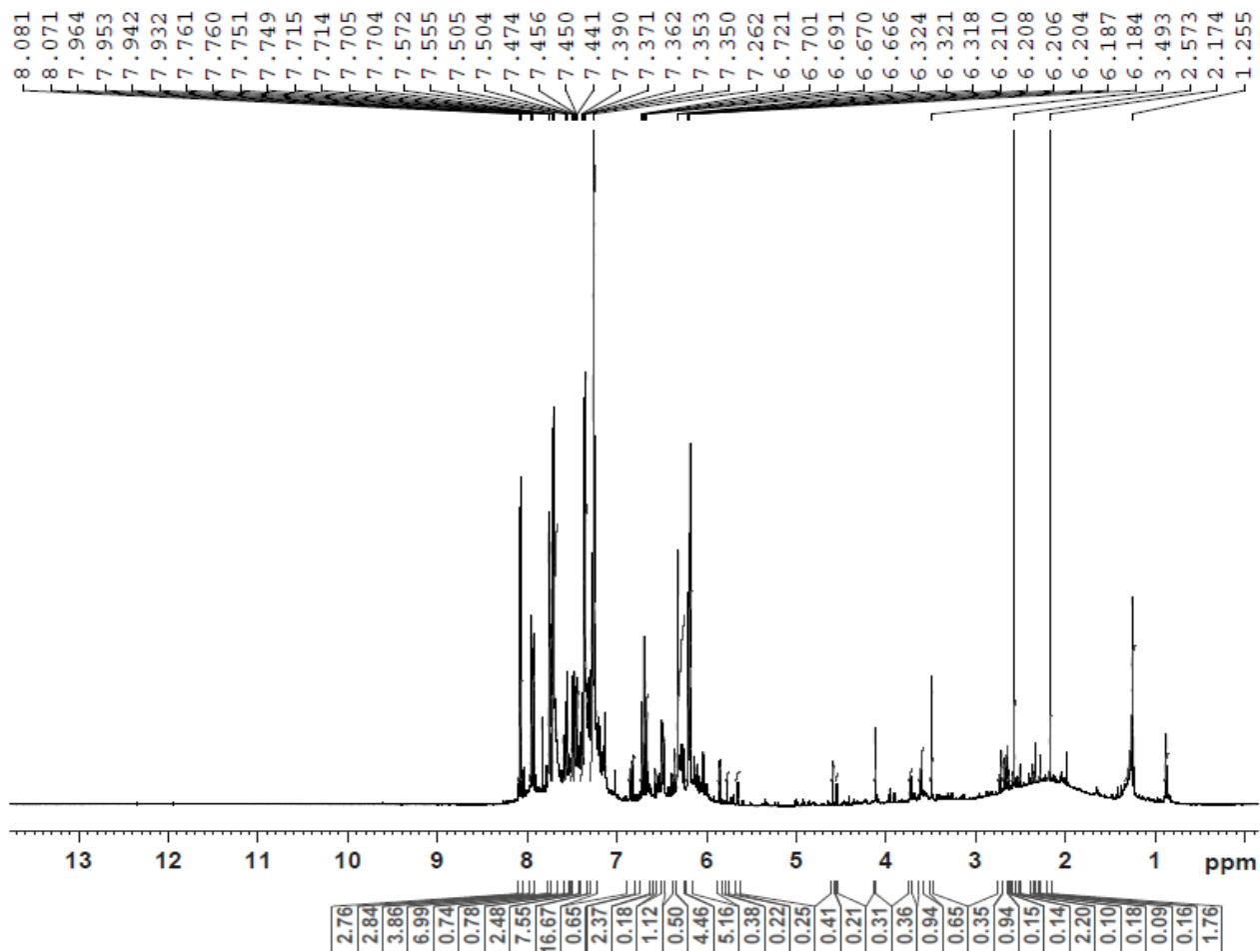


Fig B. 14: ¹H NMR of 6-(1-carbamoyl-5-(furan-2-yl)-4,5-dihydro-1H-pyrazol-3-yl)-2-(furan-2-yl)-3-phenylquinoline-4-carboxylic acid (XIV).

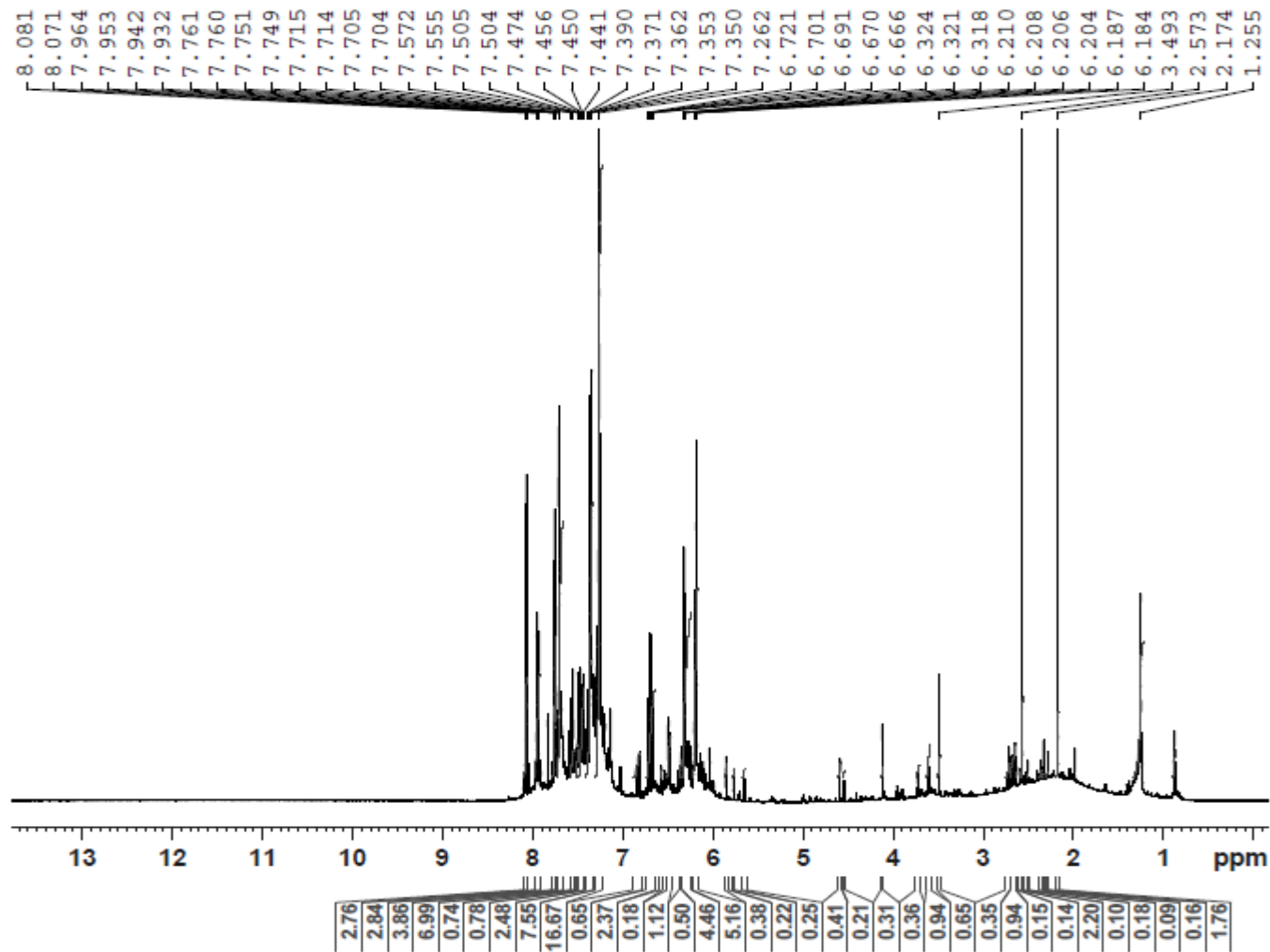


Fig B. 15: ^1H NMR of 6-(1-carbamoyl-5-(furan-2-yl)-4,5-dihydro-1H-pyrazol-3-yl)-2-(furan-2-yl)-3-phenylquinoline-4-carboxylic acid (**XV**).

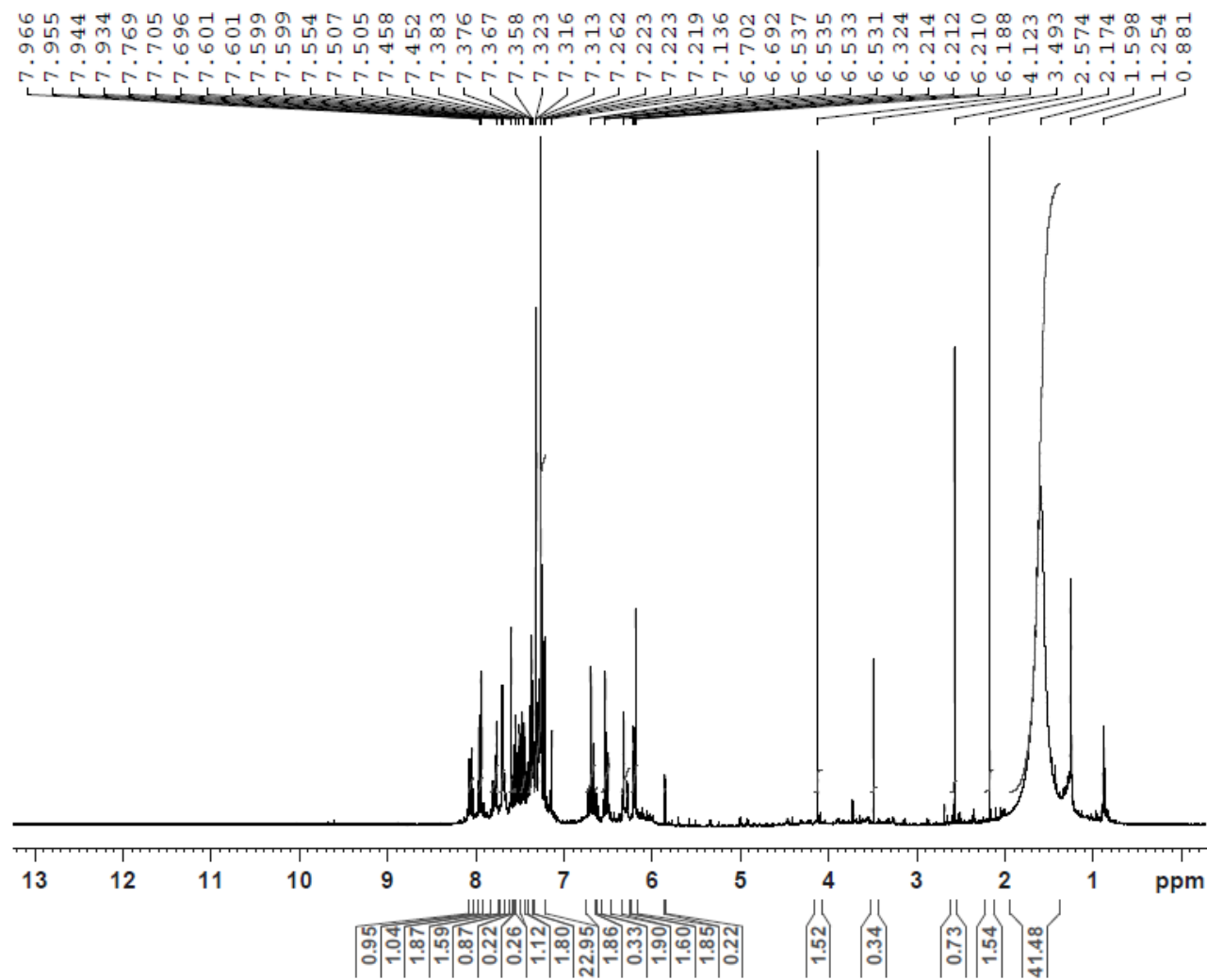


Fig B. 16: ¹H NMR of 2-(furan-2-yl)-6-(7-(furan-2-yl)-2,3,6,7-tetrahydro-1,4-oxazepin-5-yl)-3-phenylquinoline-4-carboxylic acid (XVI).

Appendix C

^{13}C Nuclear magnetic resonance (^{13}C NMR) spectrum of the prepared 2, 3-diphenyl/ 2 (furan-2-yl), 3-phenylquinoline-4-carboxylic acid derivatives:

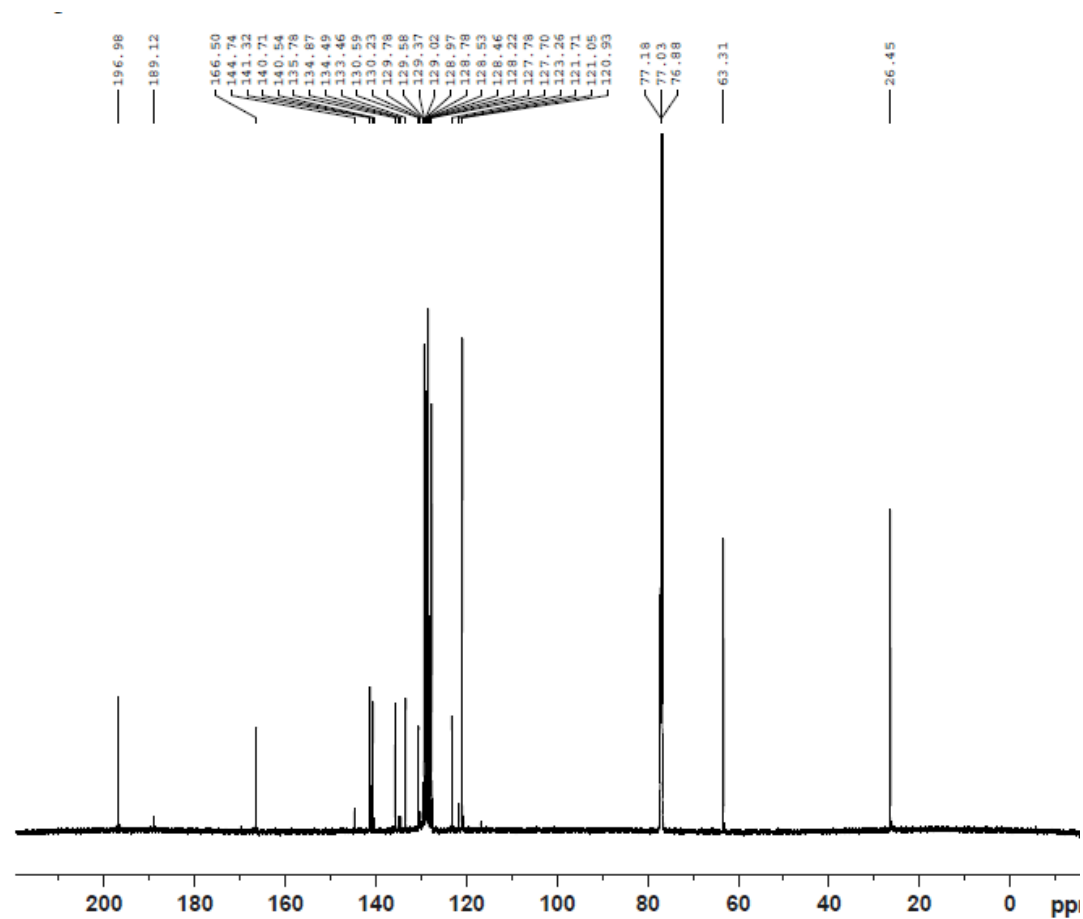


Fig C.1: ^{13}C NMR spectrum of 6-acetyl-2,3-diphenylquinoline-4-carboxylic acid (**I**).

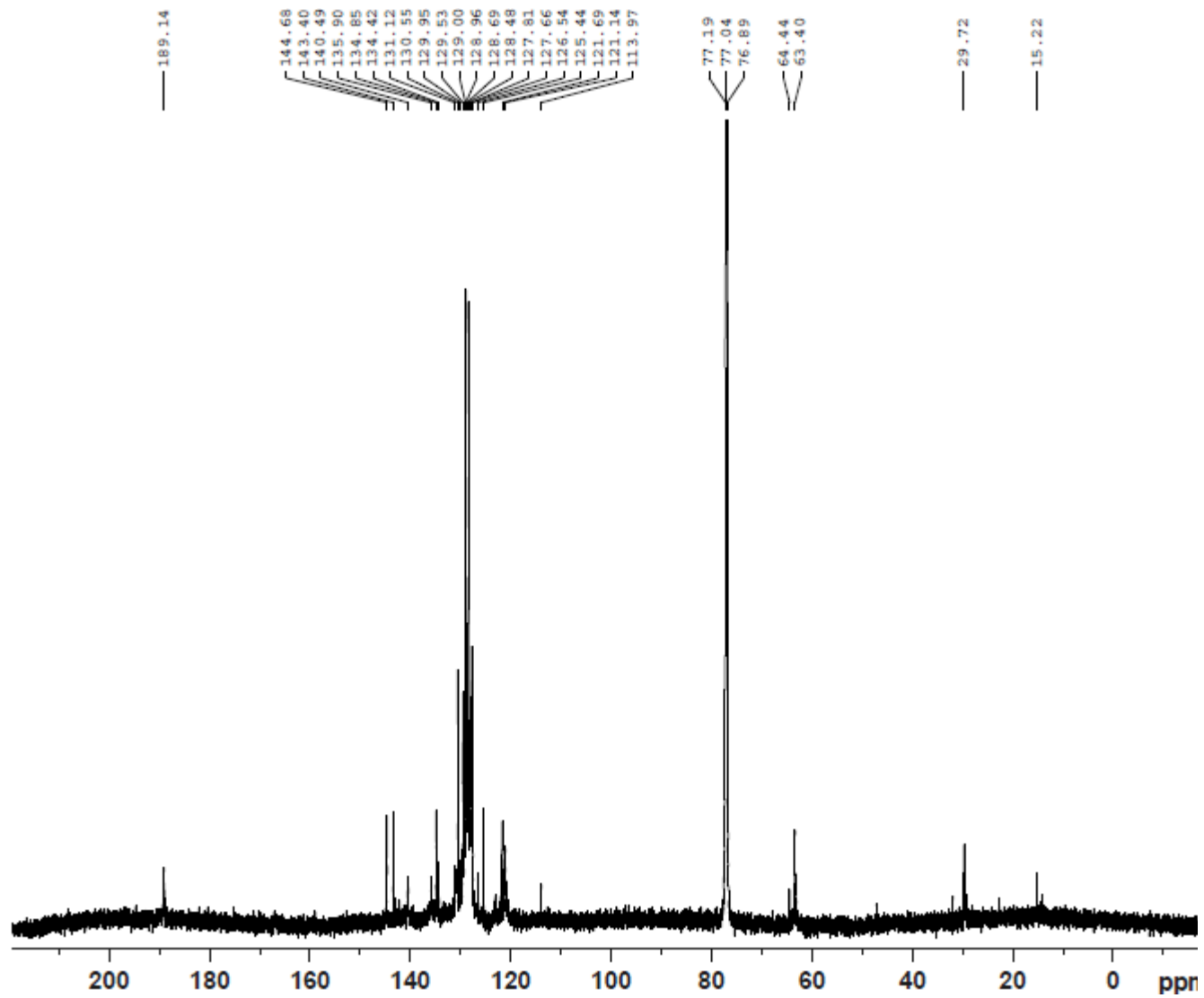


Fig C.2: ^{13}C NMR spectrum of 6-cinnamoyl-2,3-diphenylquinoline-4-carboxylic acid (**II**).

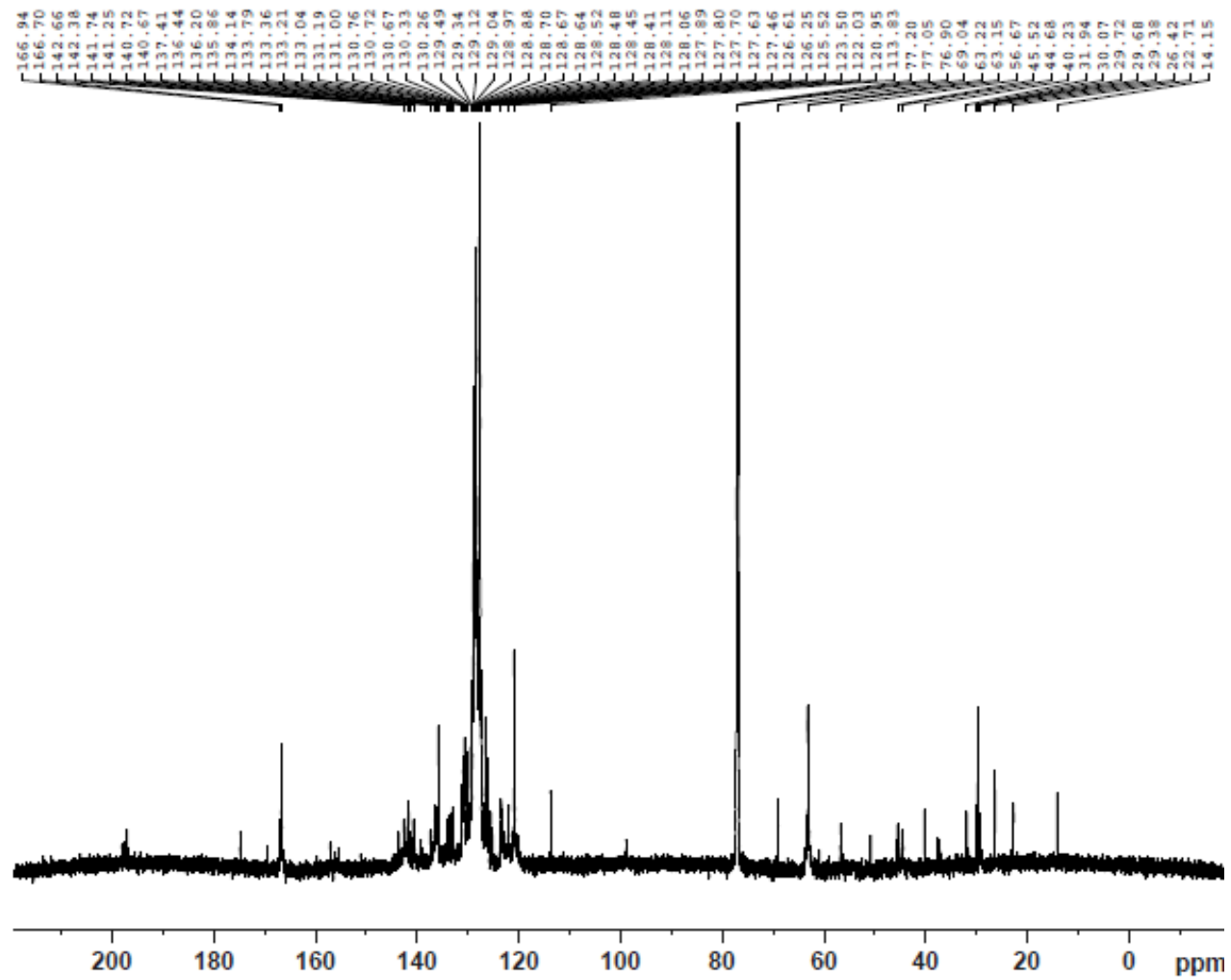


Fig C.3: ^{13}C NMR spectrum of 6-(2-oxo-6-phenyl-1,2-dihydropyrimidin-4-yl)-2,3-diphenylquinoline-4-carboxylic acid (**III**).

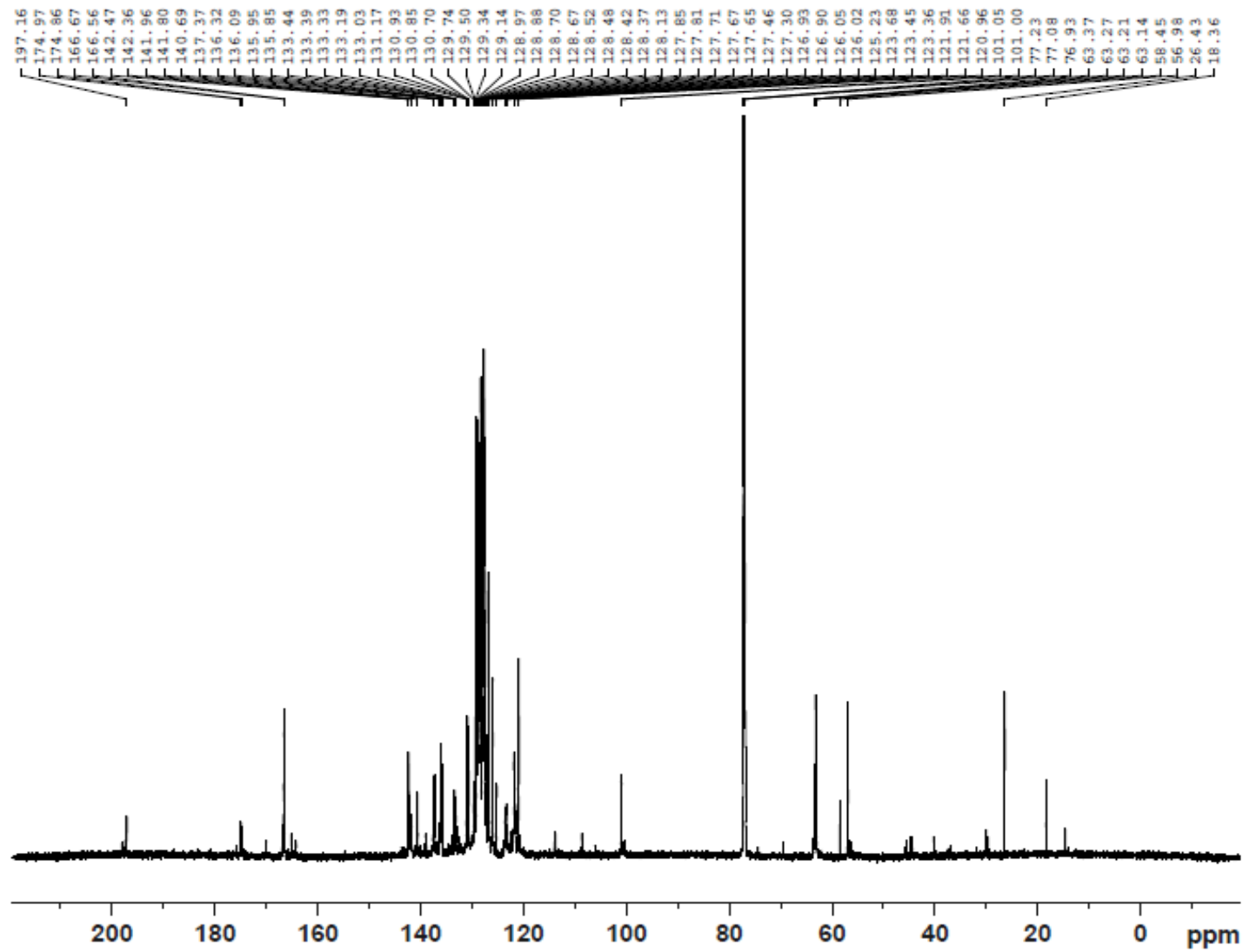


Fig C.4: ^{13}C NMR spectrum of 2,3-diphenyl-6-(6-phenyl-2-thioxo-1,2-dihydropyrimidin-4-yl)quinoline-4-carboxylic acid (**IV**).

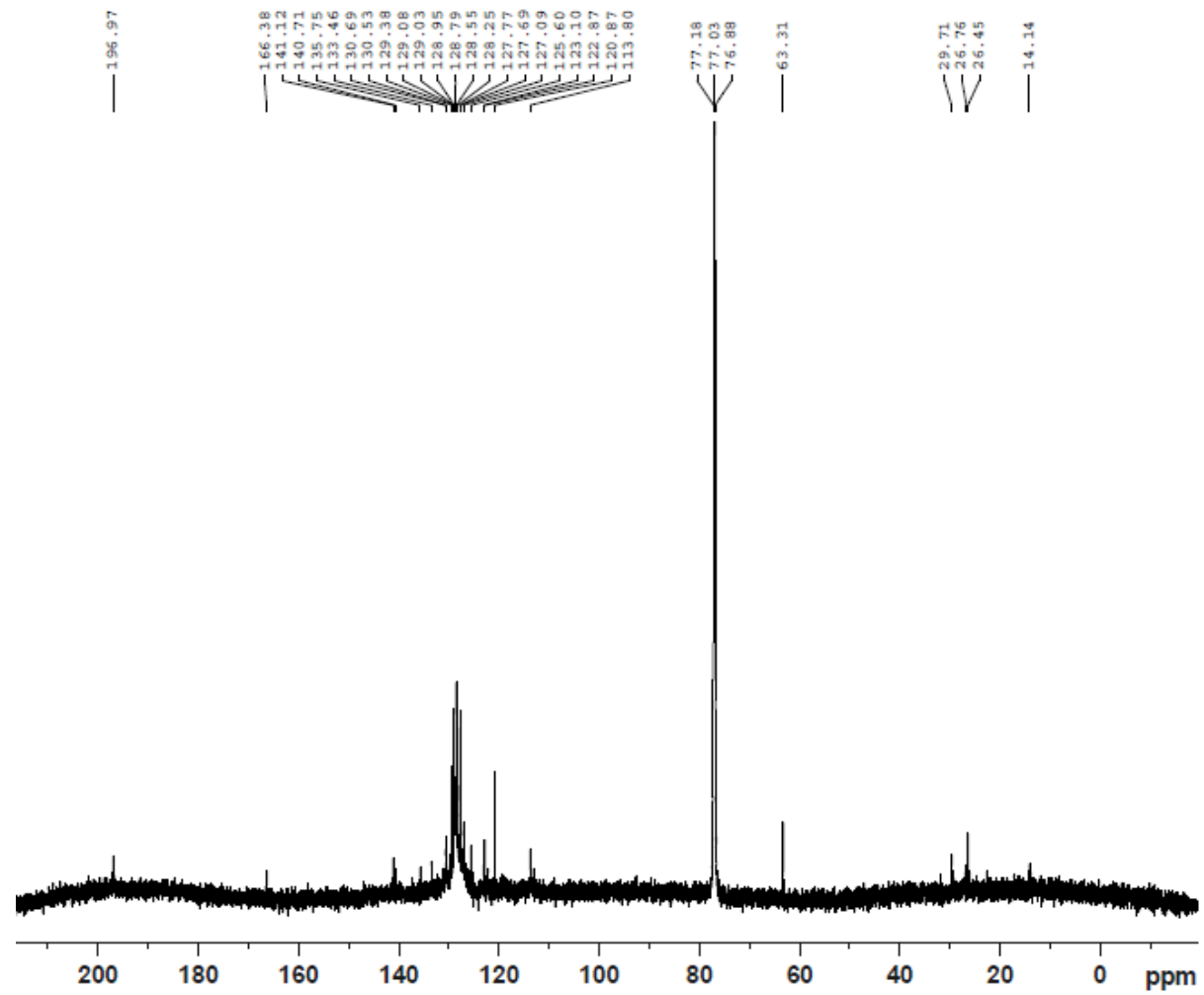


Fig C.5: ^{13}C NMR spectrum of 6-(1,5-diphenyl-4,5-dihydro-1H-pyrazol-3-yl)-2,3-diphenylquinoline-4-carboxylic acid (V).

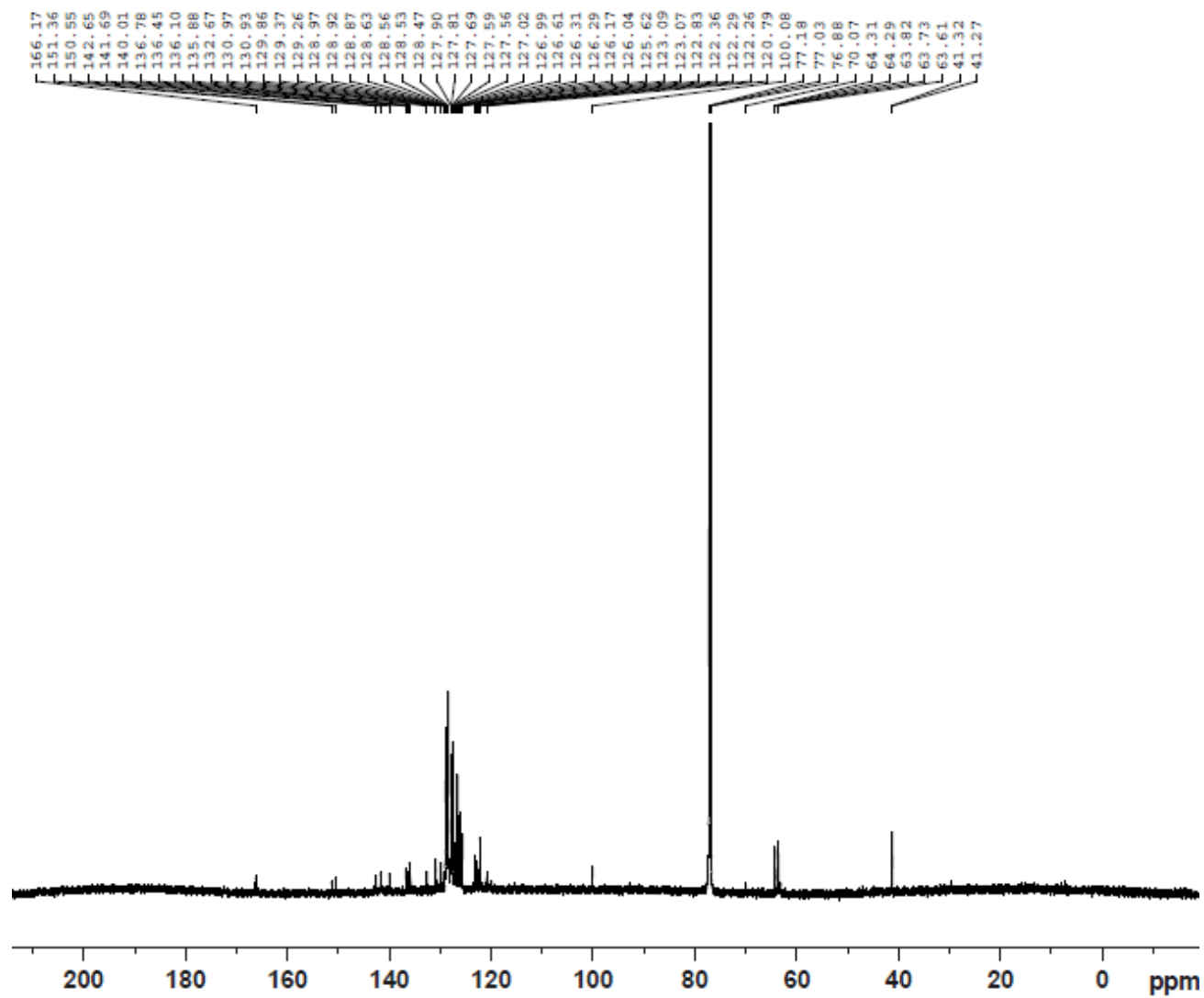


Fig C.6: ^{13}C NMR spectrum of 2,3-diphenyl-6-(5-phenyl-4,5-dihydro-1H-pyrazol-3-yl)quinoline-4-carboxylic acid (VI)

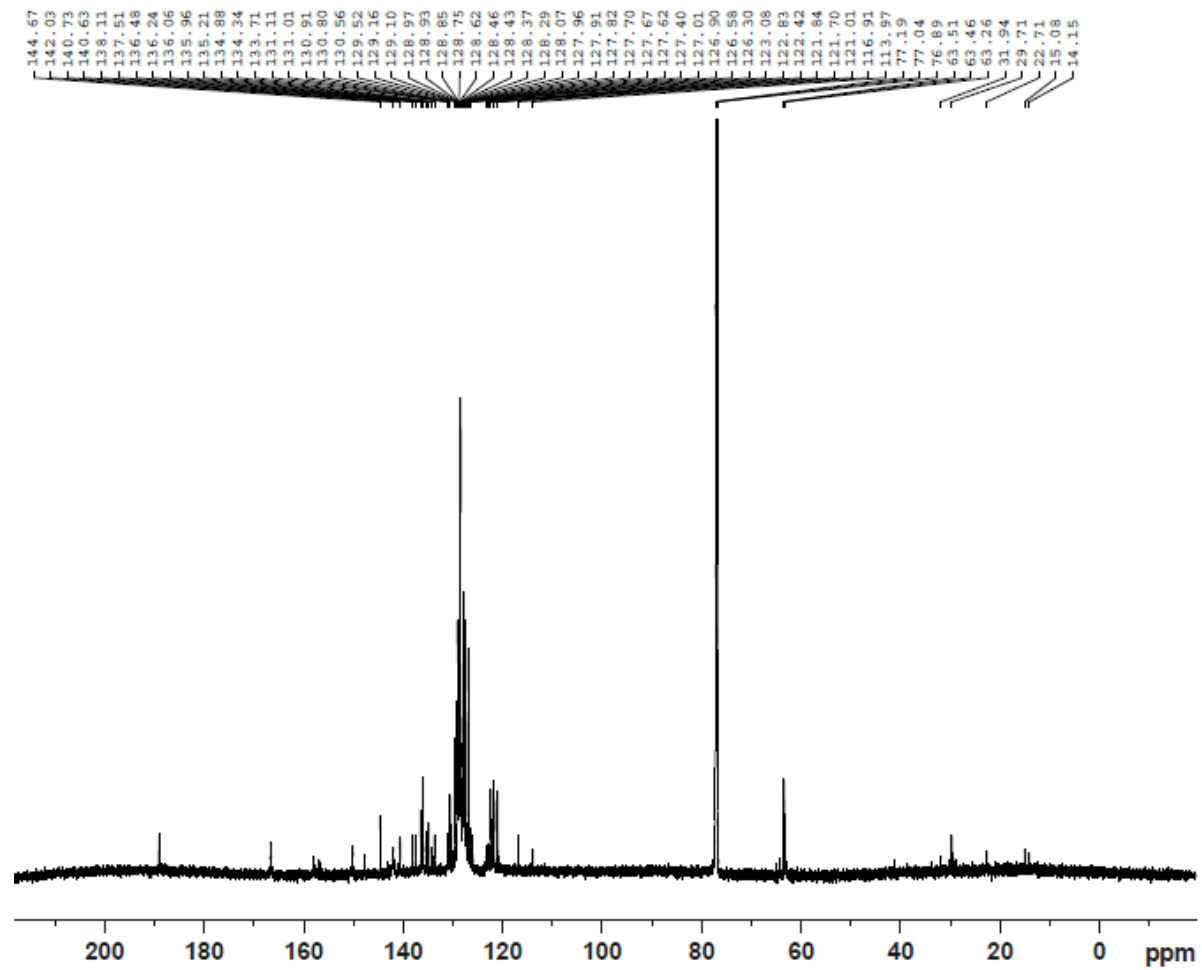


Fig C.7: ^{13}C NMR spectrum of 6-(1-carbamoyl-5-phenyl-4,5-dihydro-1H-pyrazol-3-yl)-2,3-diphenylquinoline-4-carboxylic acid (**VII**)

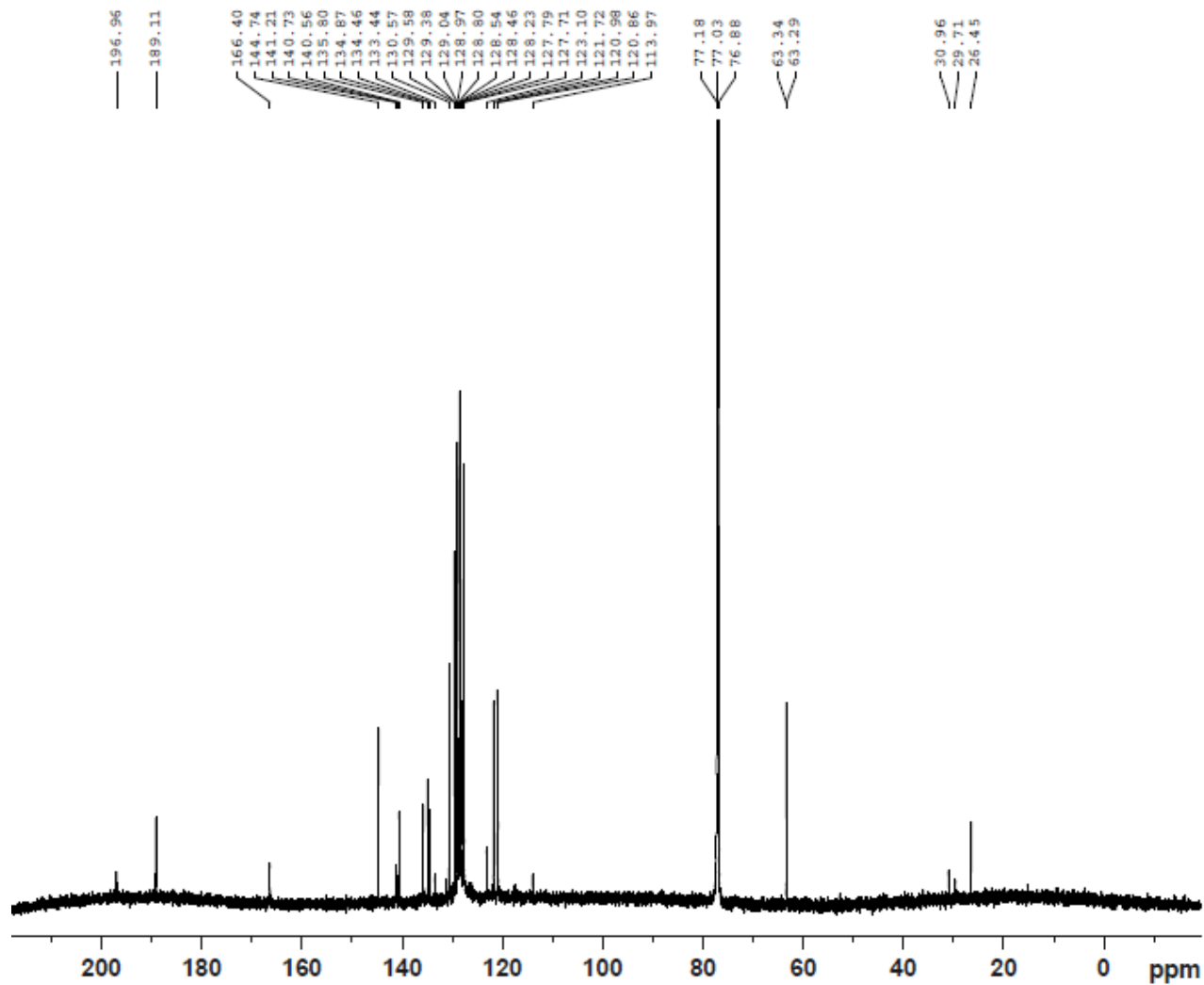


Fig C.8: ^{13}C NMR spectrum of 2,3-diphenyl-6-(7-phenyl-2,3,6,7-tetrahydro-1,4-oxazepin-5-yl)quinoline-4-carboxylic acid (**VIII**)

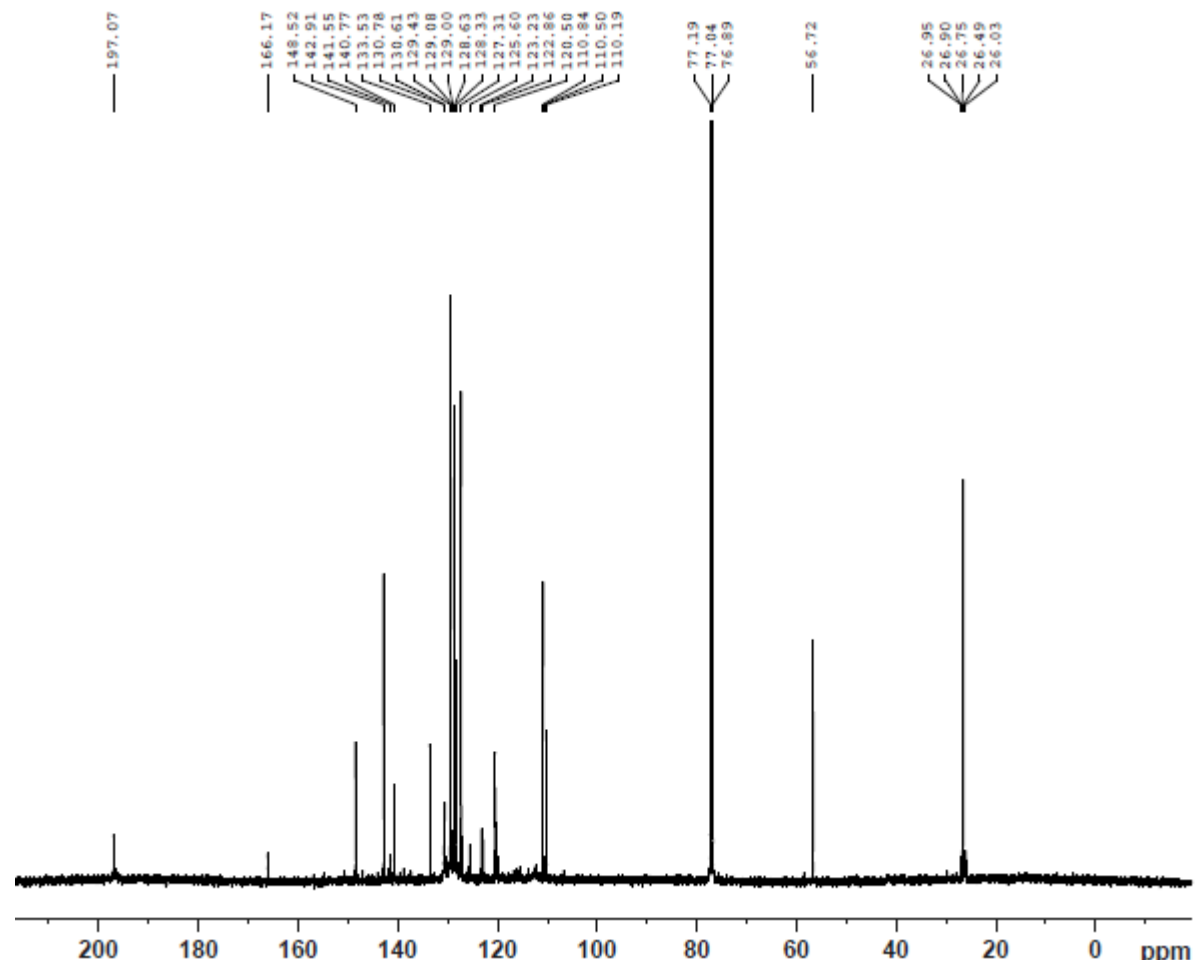


Fig C.9: ^{13}C NMR spectrum of 6-acetyl-2-(furan-2-yl)-3-phenylquinoline-4-carboxylic acid (**IX**).

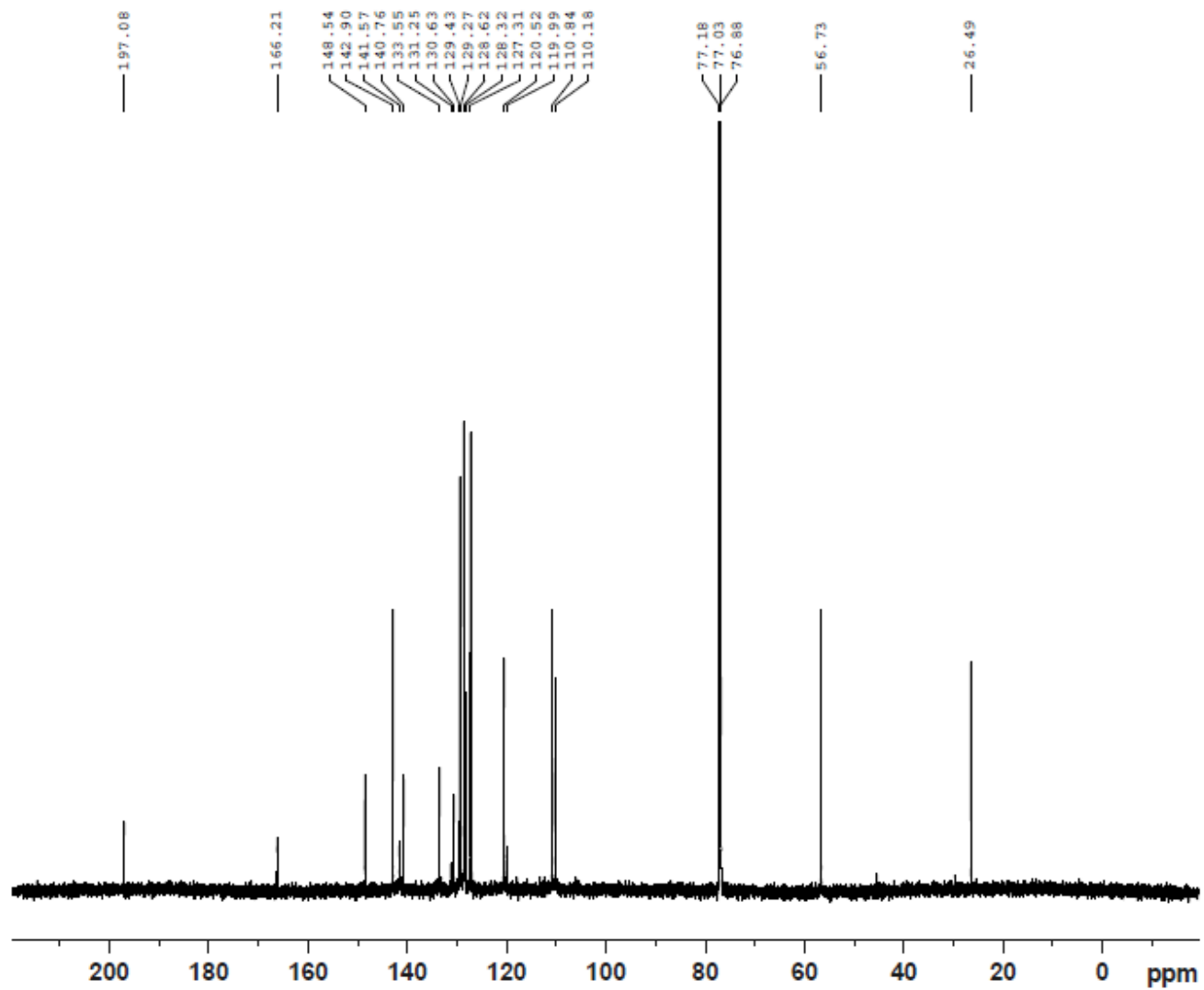


Fig C.10: ^{13}C NMR spectrum of (E)-2-(furan-2-yl)-6-(3-(furan-2-yl)acryloyl)-3-phenylquinoline-4-carboxylic acid (**X**).

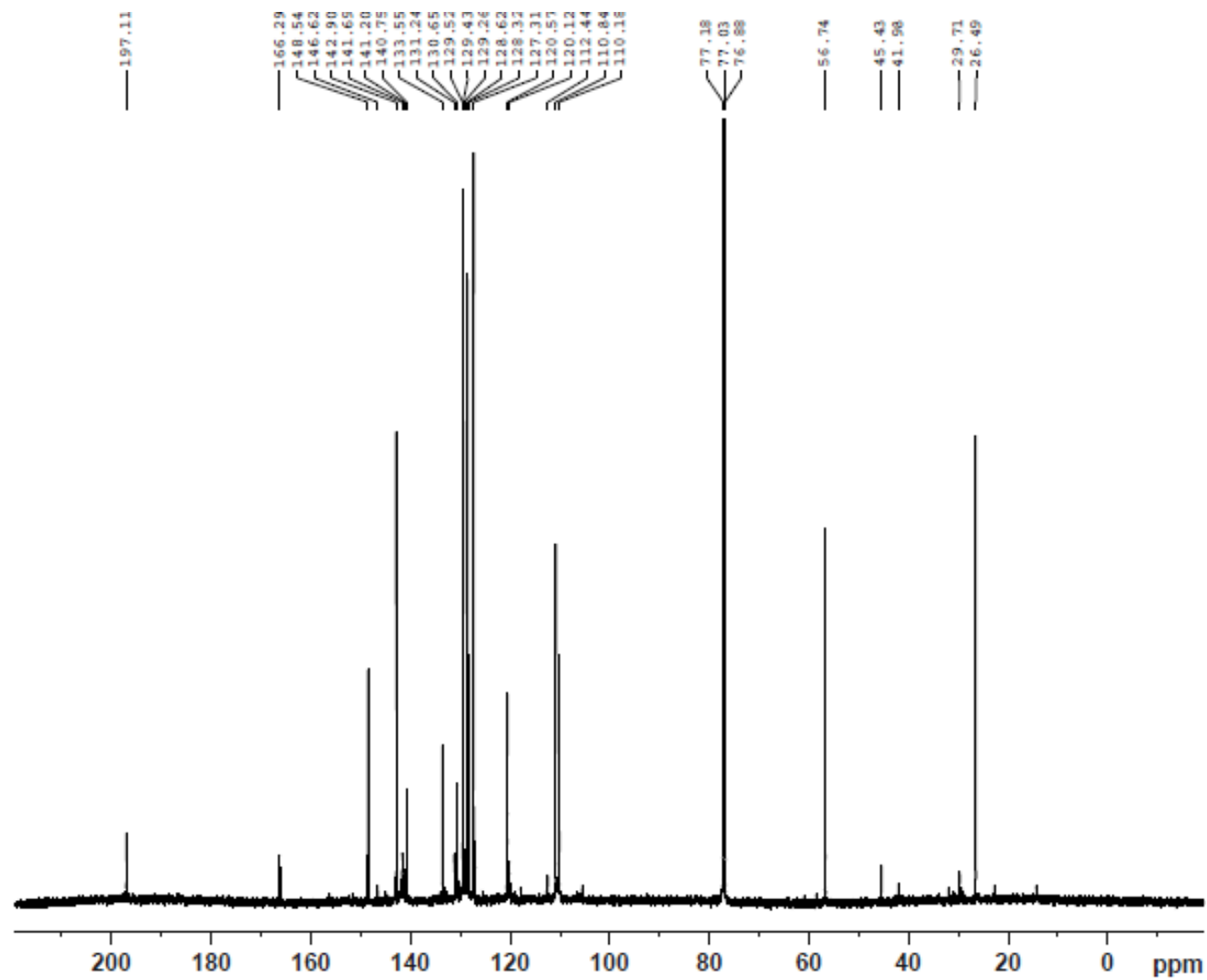


Fig C.11: ^{13}C NMR spectrum of 2-(furan-2-yl)-6-(6-(furan-2-yl)-2-oxo-1,2-dihydropyrimidin-4-yl)-3-phenylquinoline-4-carboxylic acid (**XI**).

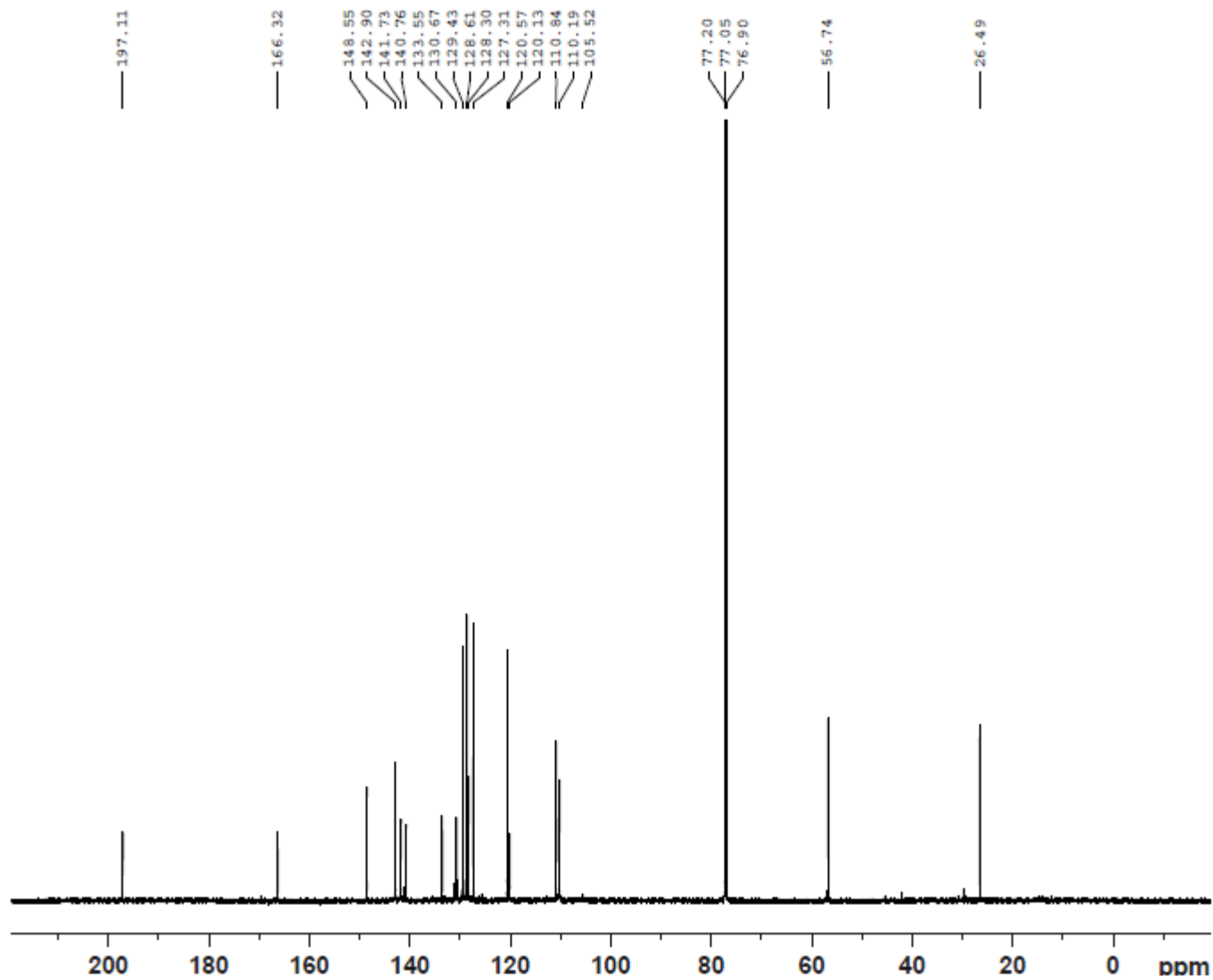


Fig C.12: ^{13}C NMR spectrum of 2-(furan-2-yl)-6-(6-(furan-2-yl)-2-thioxo-1,2-dihydropyrimidin-4-yl)-3-phenylquinoline-4-carboxylic acid (**XII**).

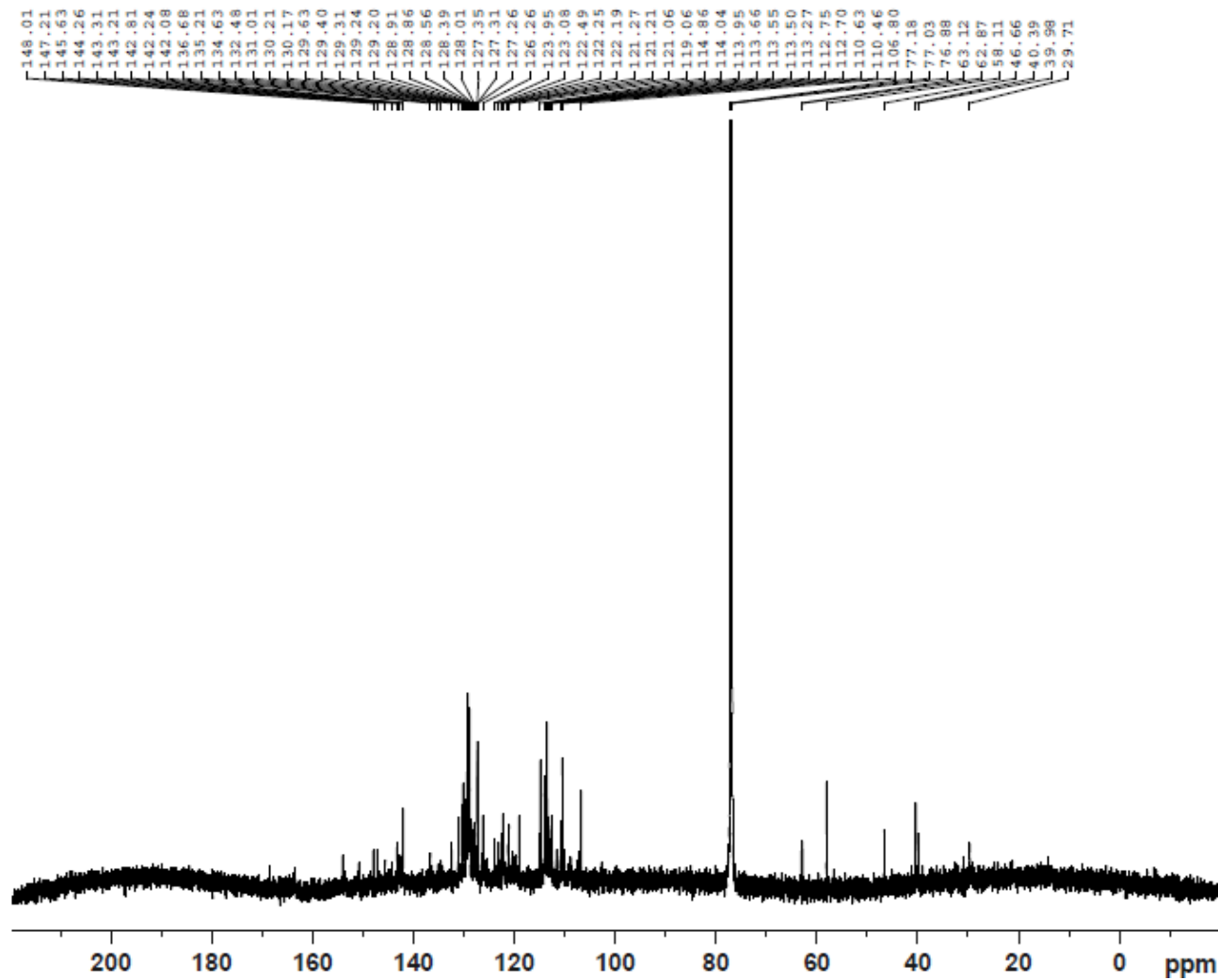


Fig C.13: ^{13}C NMR spectrum of 2-(furan-2-yl)-6-(5-(furan-2-yl)-1-phenyl-4,5-dihydro-1H-pyrazol-3-yl)-3-phenylquinoline-4-carboxylic acid (**XIII**).

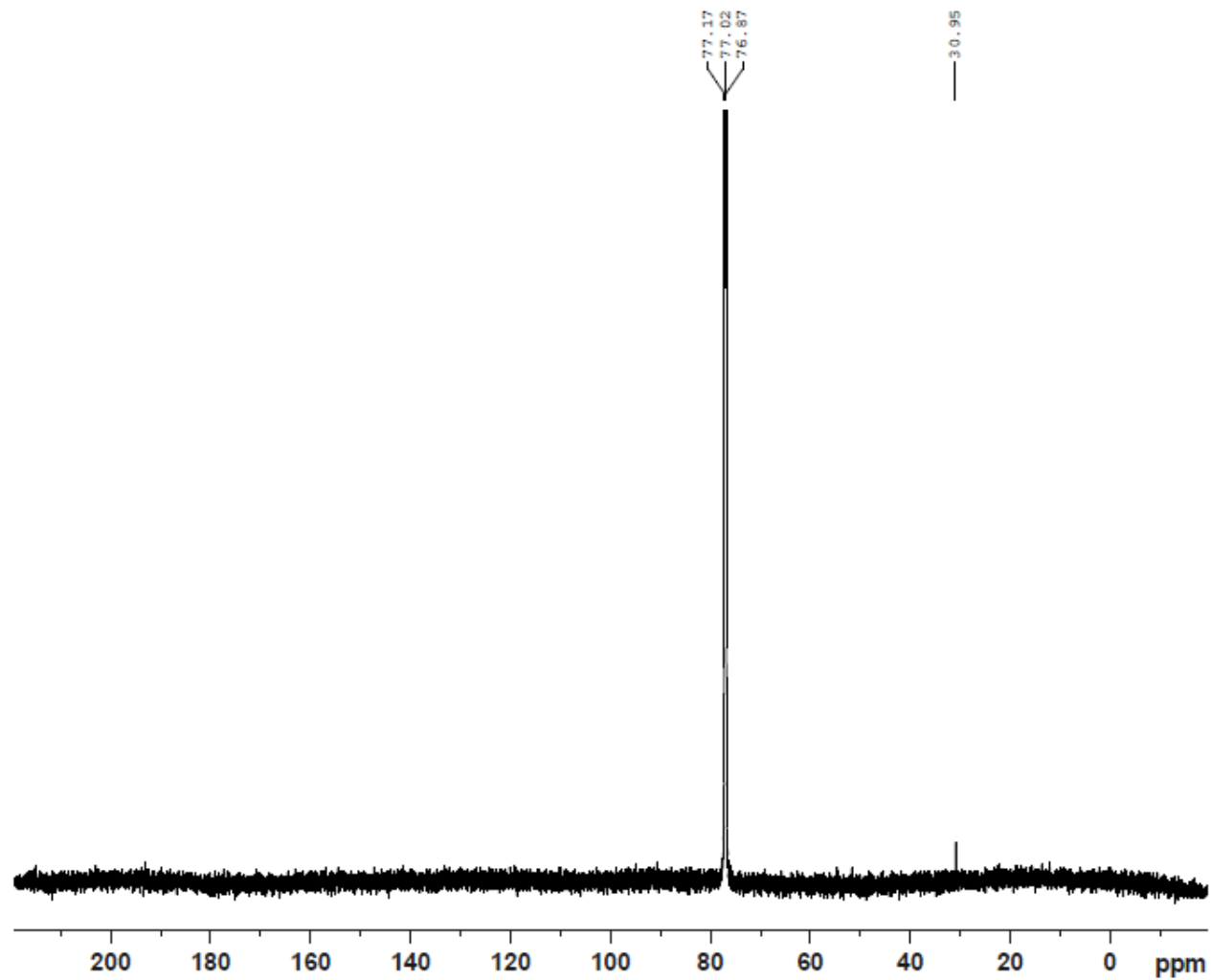


Fig C.14: ^{13}C NMR spectrum of 2-(furan-2-yl)-6-(5-(furan-2-yl)-4,5-dihydro-1H-pyrazol-3-yl)-3-phenylquinoline-4-carboxylic acid (**XIV**).

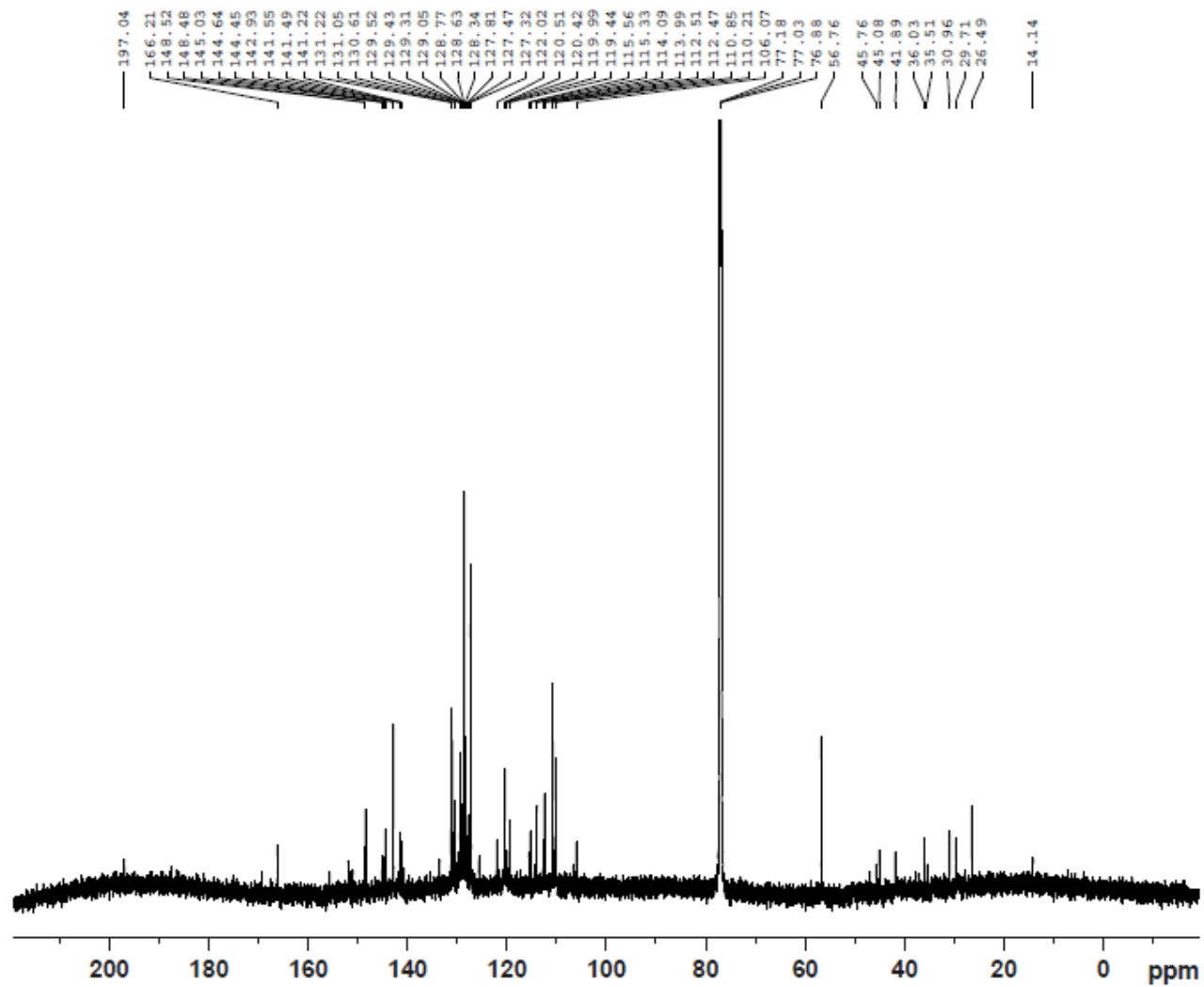


Fig C.15: ^{13}C NMR spectrum of 6-(1-carbamoyl-5-(furan-2-yl)-4,5-dihydro-1H-pyrazol-3-yl)-2-(furan-2-yl)-3-phenylquinoline-4-carboxylic acid (XV).

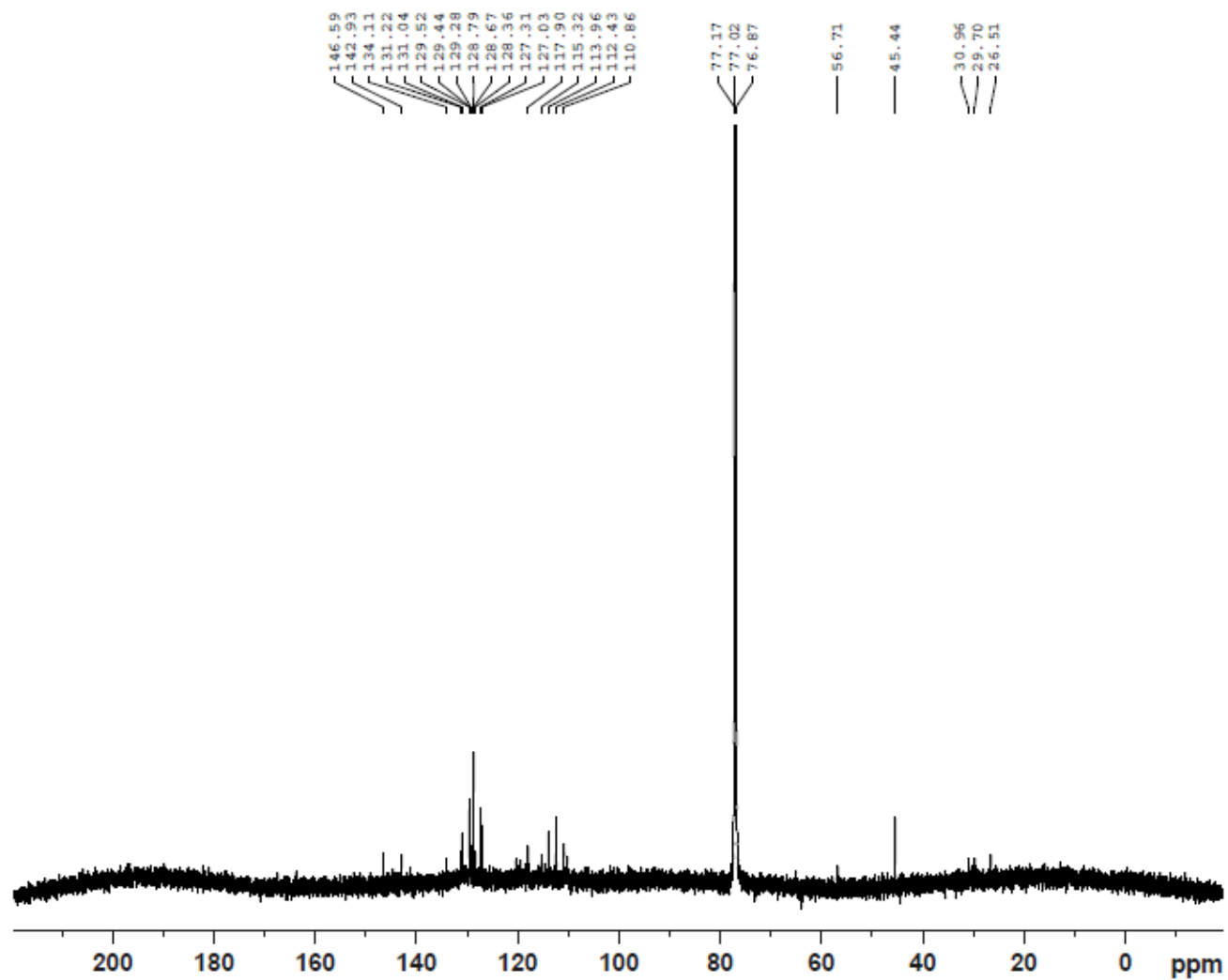


Fig C.16: ^{13}C NMR spectrum of 2-(furan-2-yl)-6-(7-(furan-2-yl)-2,3,6,7-tetrahydro-1,4-oxazepin-5-yl)-3-phenylquinoline-4-carboxylic acid (XVI).

Appendix D

Gas chromatography- mass spectroscopy (GCMS) spectrum of 2, 3-diphenyl/ 2 (furan-2-yl), 3-phenylquinoline-4-carboxylic acid derivatives

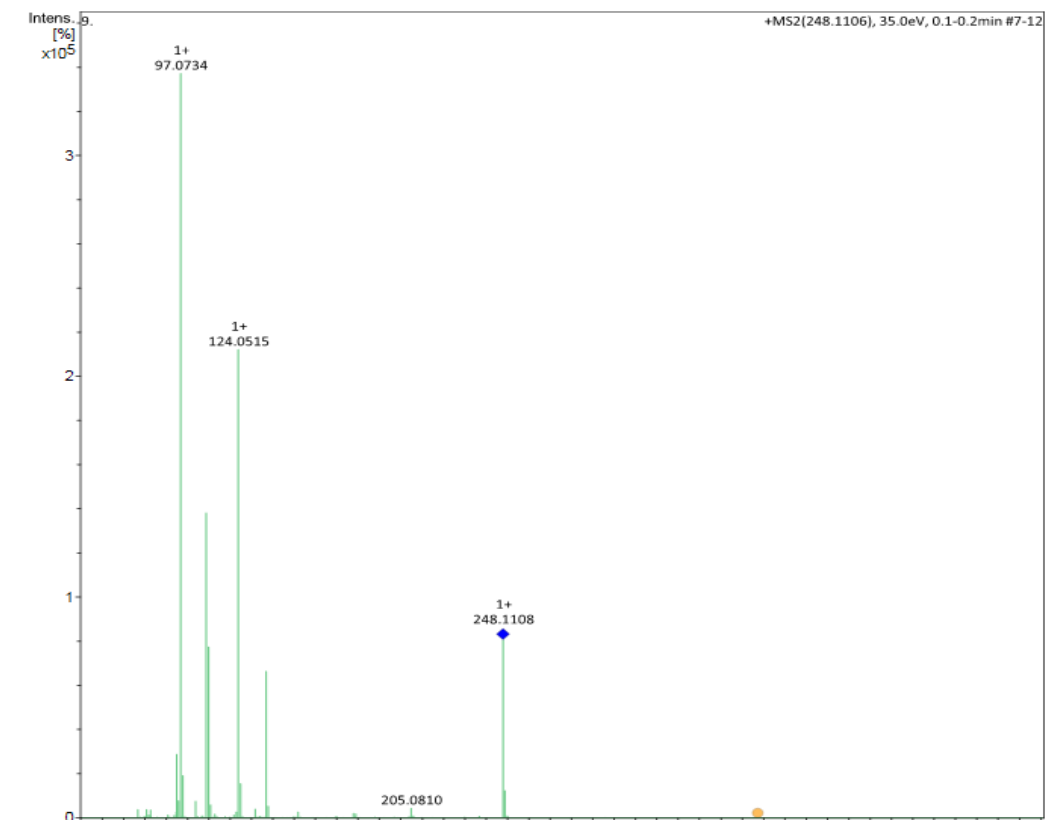


Fig D. 1: GC-MS of 6-acetyl-2,3-diphenylquinoline-4-carboxylic acid (**I**).

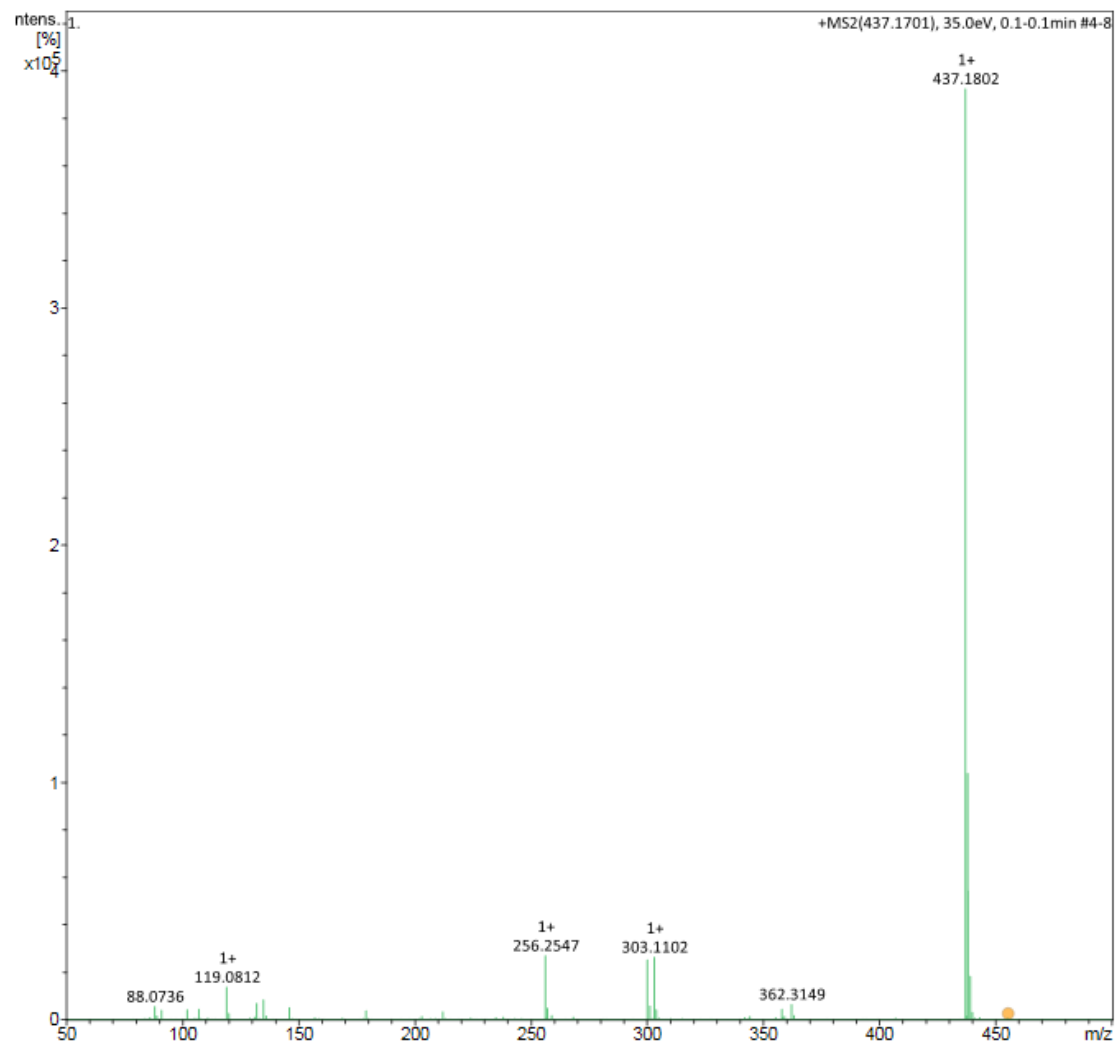


Fig D. 2: GC-MS of 6-cinnamoyl-2,3-diphenylquinoline-4-carboxylic acid (**II**).

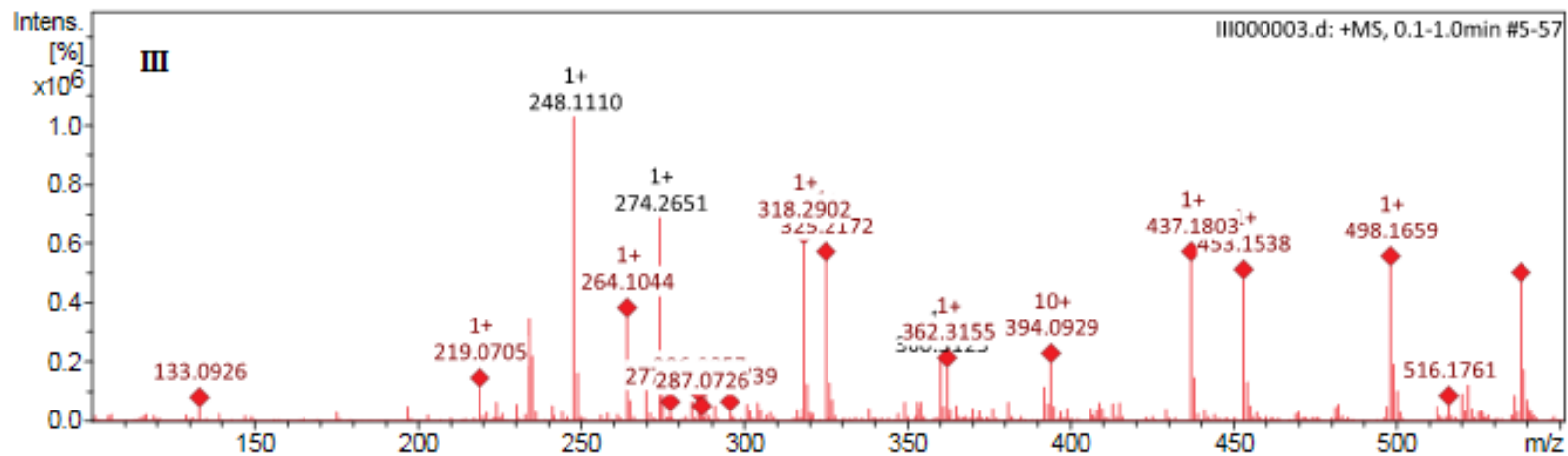


Fig D. 3: GC-MS of 6-(2-oxo-6-phenyl-1,2-dihydropyrimidin-4-yl)-2,3-diphenylquinoline-4-carboxylic acid (**III**).

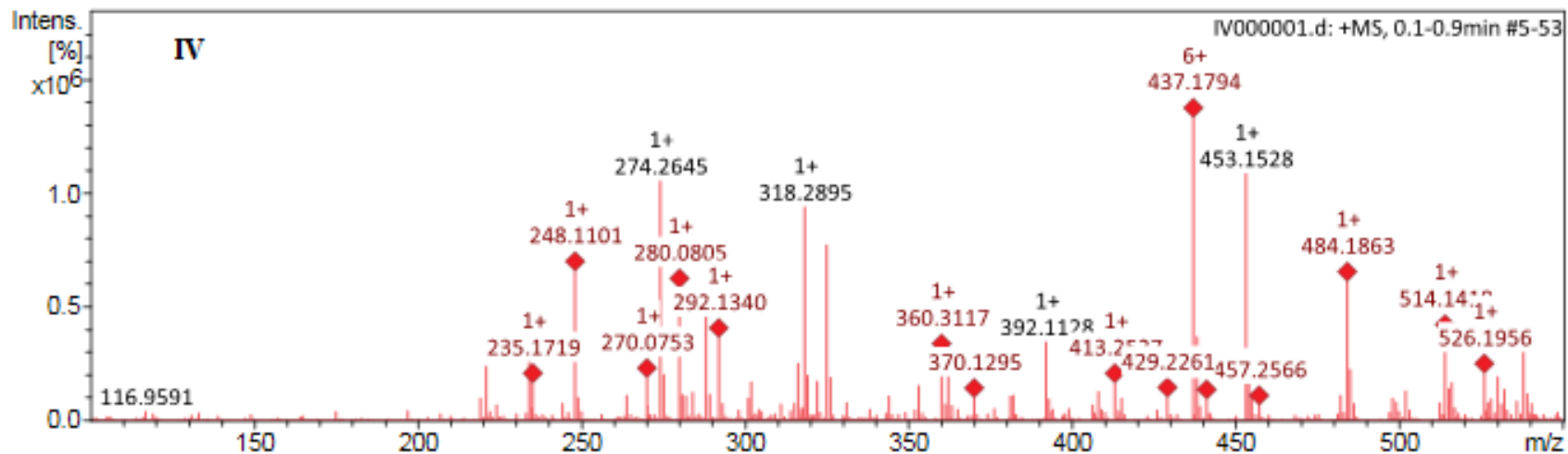


Fig D. 4: GC-MS of 2,3-diphenyl-6-(6-phenyl-2-thioxo-1,2-dihydropyrimidin-4-yl)quinoline-4-carboxylic acid (**IV**).

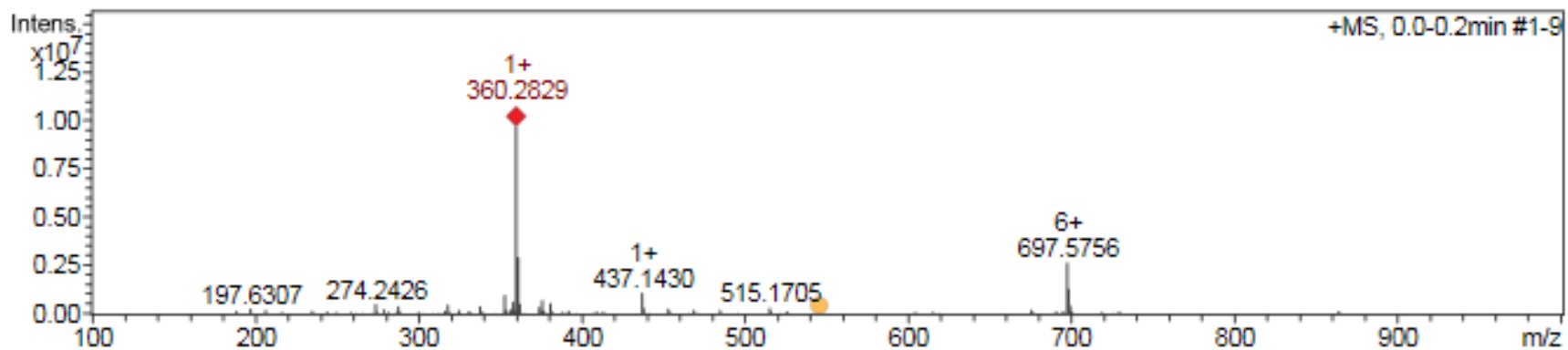


Fig D. 5: GC-MS of 6-(1,5-diphenyl-4,5-dihydro-1H-pyrazol-3-yl)-2,3-diphenylquinoline-4-carboxylic acid (V).

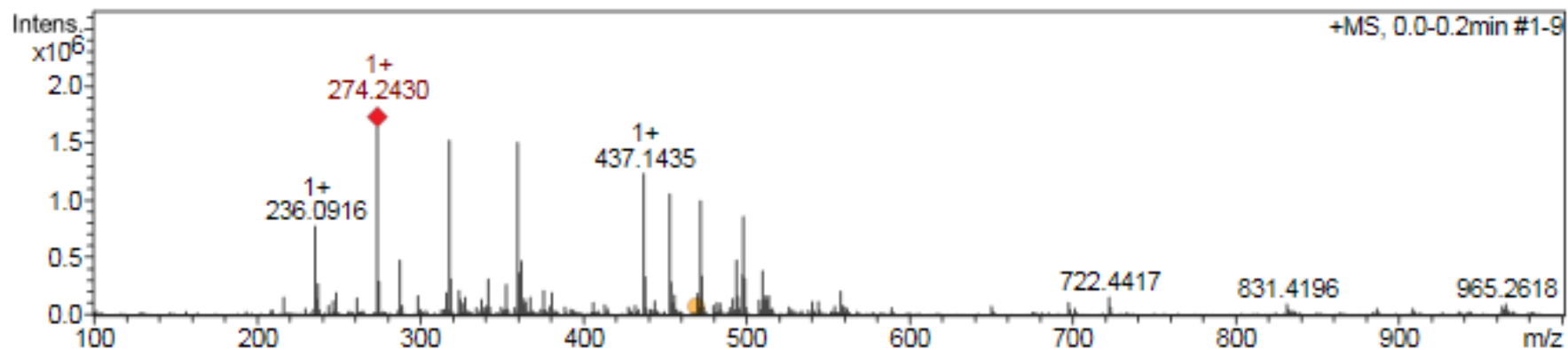


Fig D. 6: GC-MS of 2,3-diphenyl-6-(5-phenyl-4,5-dihydro-1H-pyrazol-3-yl)quinoline-4-carboxylic acid (VI).

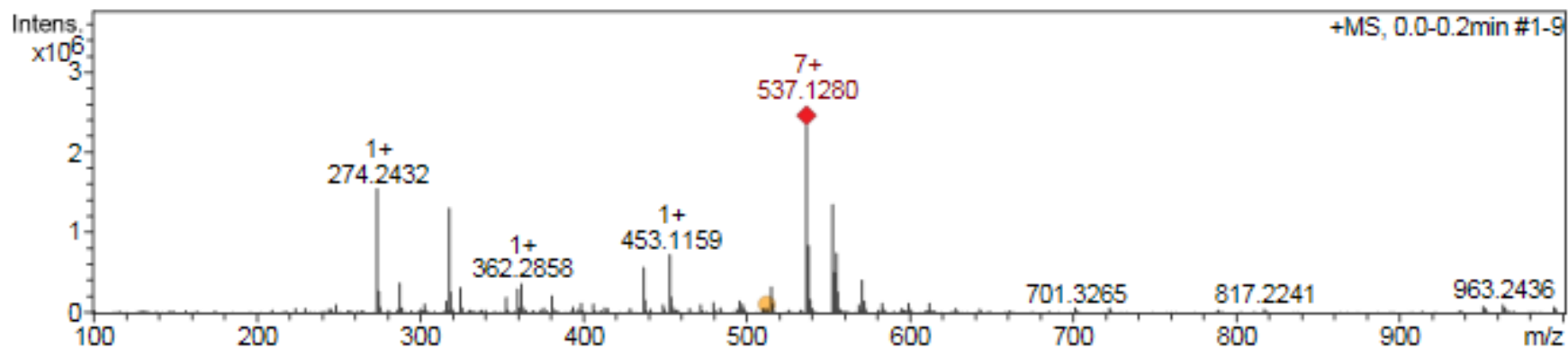


Fig D. 7: GC-MS of 6-(1-carbamoyl-5-phenyl-4,5-dihydro-1H-pyrazol-3-yl)-2,3-diphenylquinoline-4-carboxylic acid (VII).

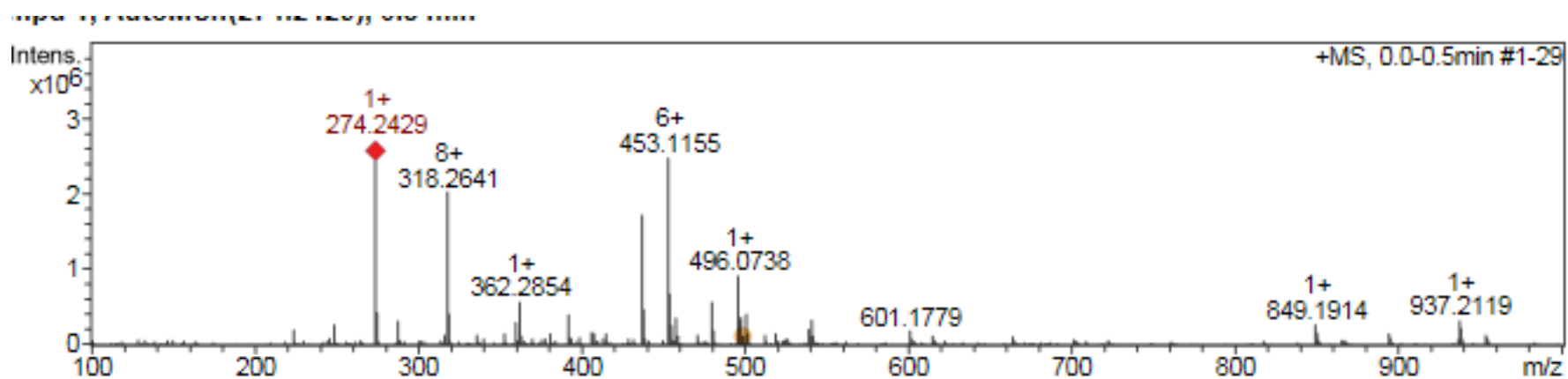


Fig D.8: GC-MS of 2,3-diphenyl-6-(7-phenyl-2,3,6,7-tetrahydro-1,4-oxazepin-5-yl)quinoline-4-carboxylic acid (VIII).

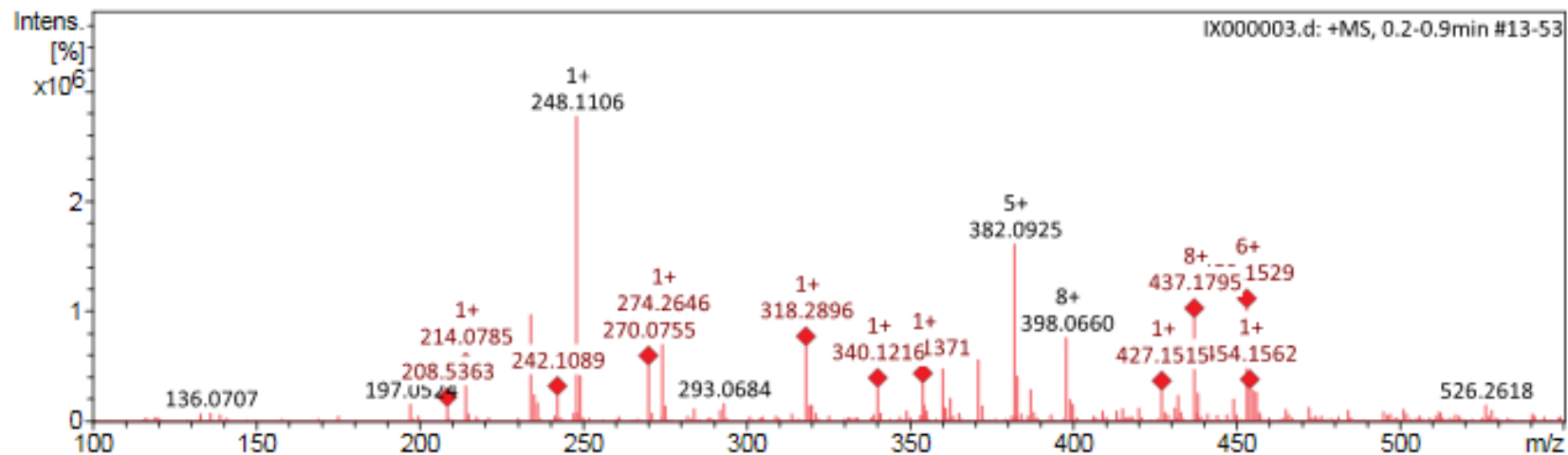


Fig D.9: GC-MS of 6-acetyl-2-(furan-2-yl)-3-phenylquinoline-4-carboxylic acid (**IX**).

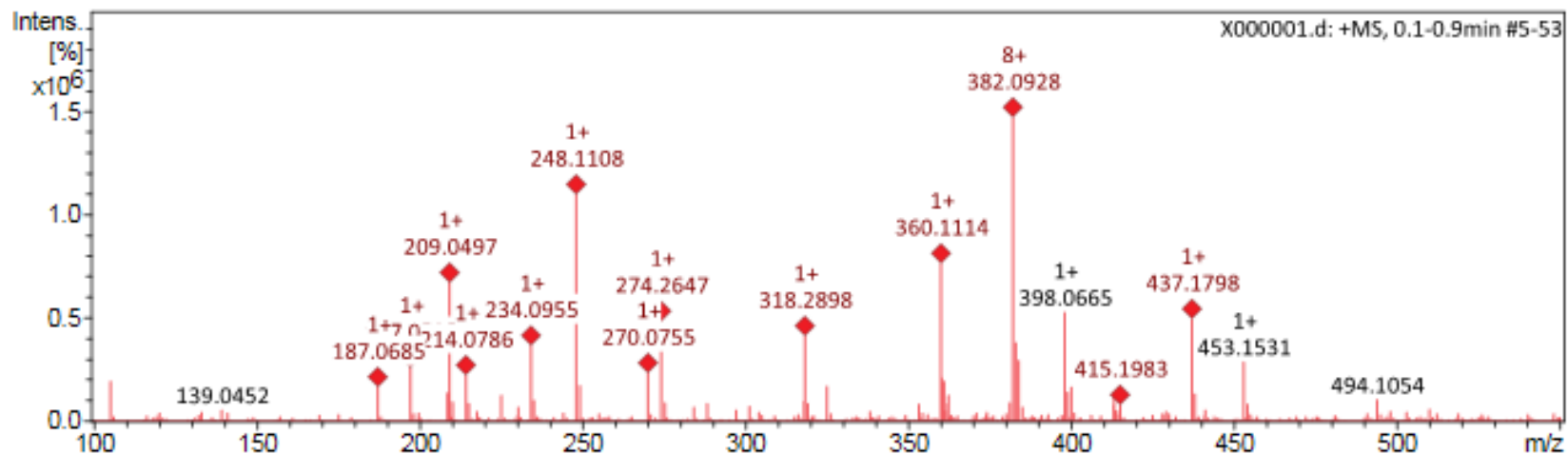


Fig D.10: GC-MS of (E)-2-(furan-2-yl)-6-(3-(furan-2-yl)acryloyl)-3-phenylquinoline-4-carboxylic acid (**X**).

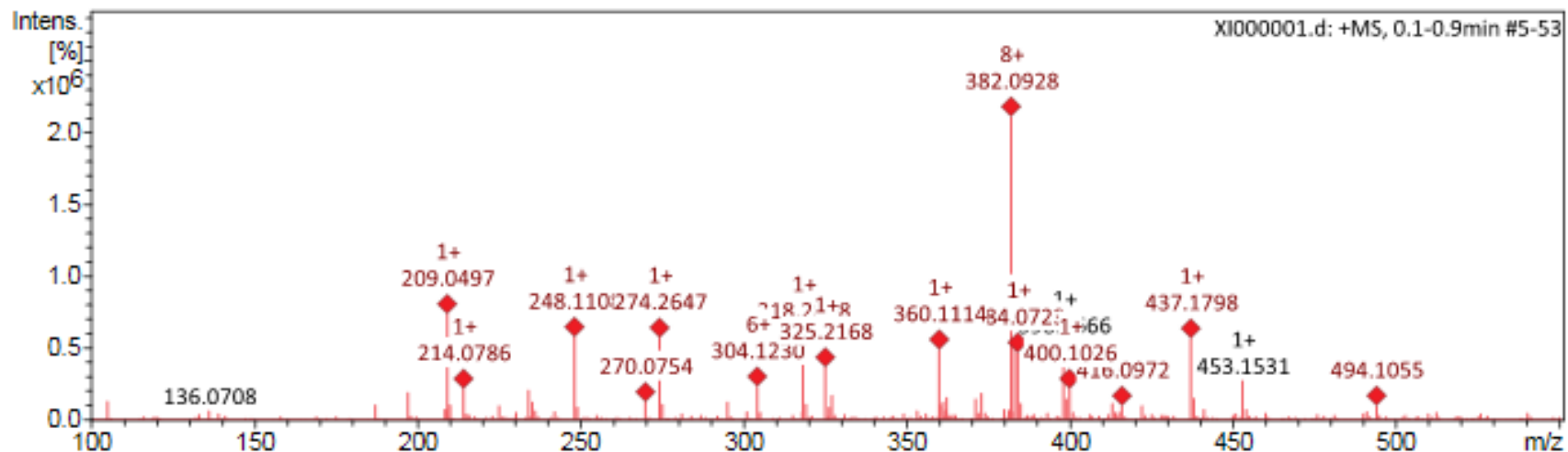


Fig D.11: GC-MS of 2-(furan-2-yl)-6-(6-(furan-2-yl)-2-oxo-1,2-dihydropyrimidin-4-yl)-3-phenylquinoline-4-carboxylic acid (XI).

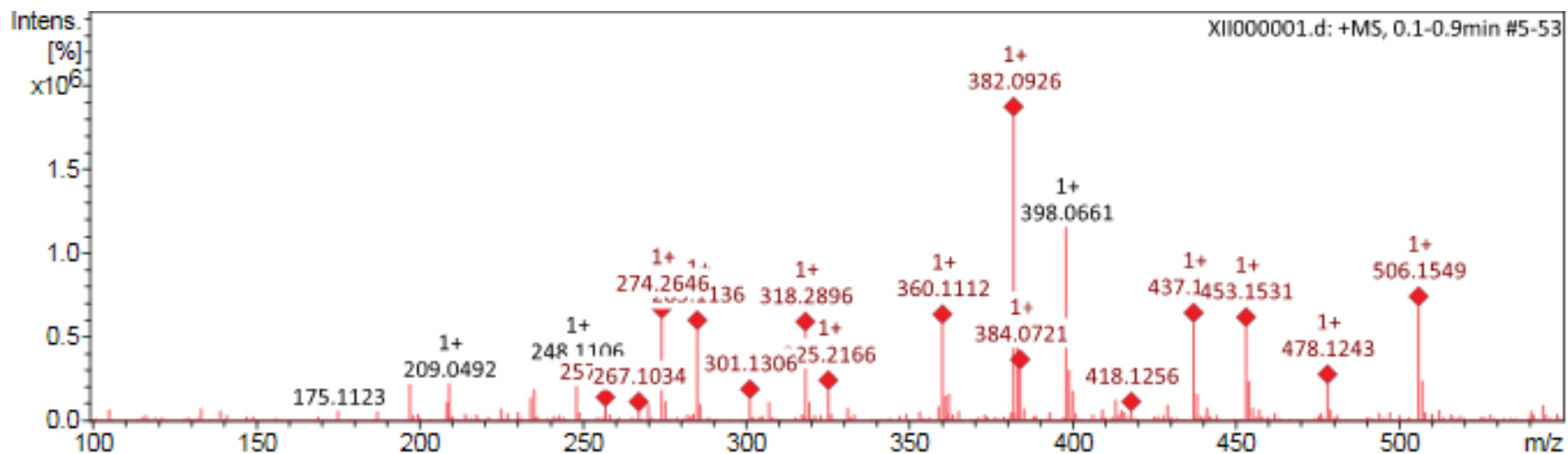


Fig D.12: GC-MS of 2-(furan-2-yl)-6-(6-(furan-2-yl)-2-thioxo-1,2-dihydropyrimidin-4-yl)-3-phenylquinoline-4-carboxylic acid (XII).

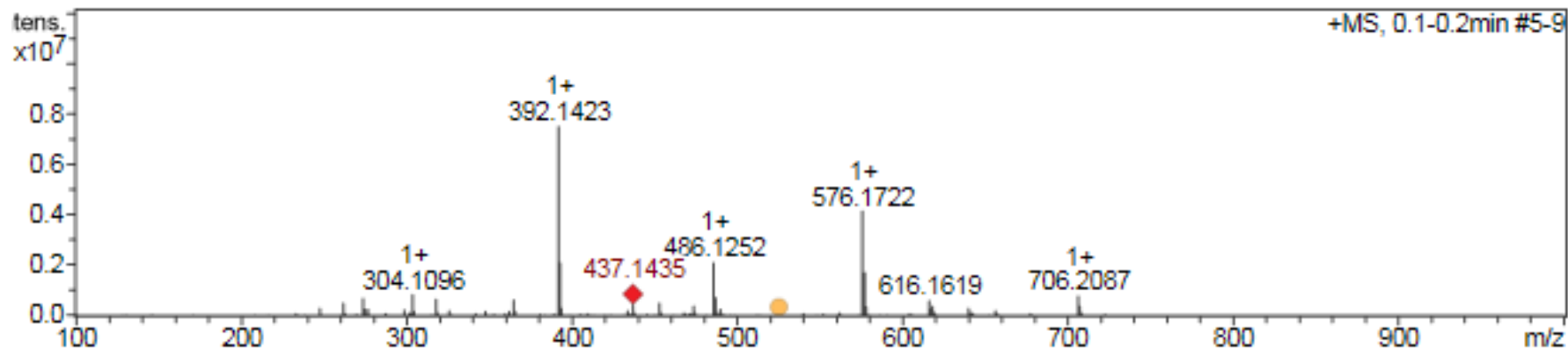


Fig D.13: GC-MS of 2-(furan-2-yl)-6-(5-(furan-2-yl)-1-phenyl-4,5-dihydro-1H-pyrazol-3-yl)-3-phenylquinoline-4-carboxylic acid (XIII).

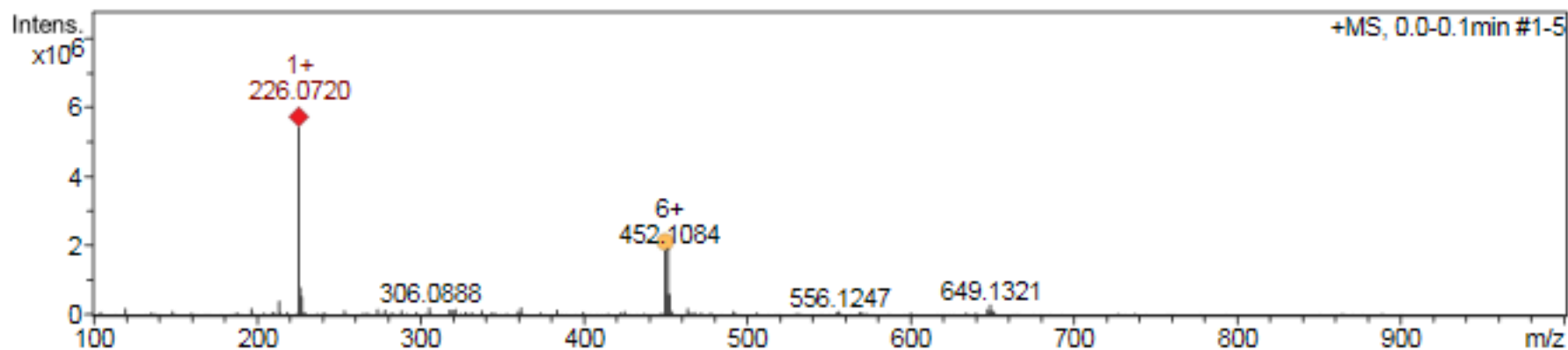


Fig D.14: GC-MS of 2-(furan-2-yl)-6-(5-(furan-2-yl)-4,5-dihydro-1H-pyrazol-3-yl)-3-phenylquinoline-4-carboxylic acid (XIV).

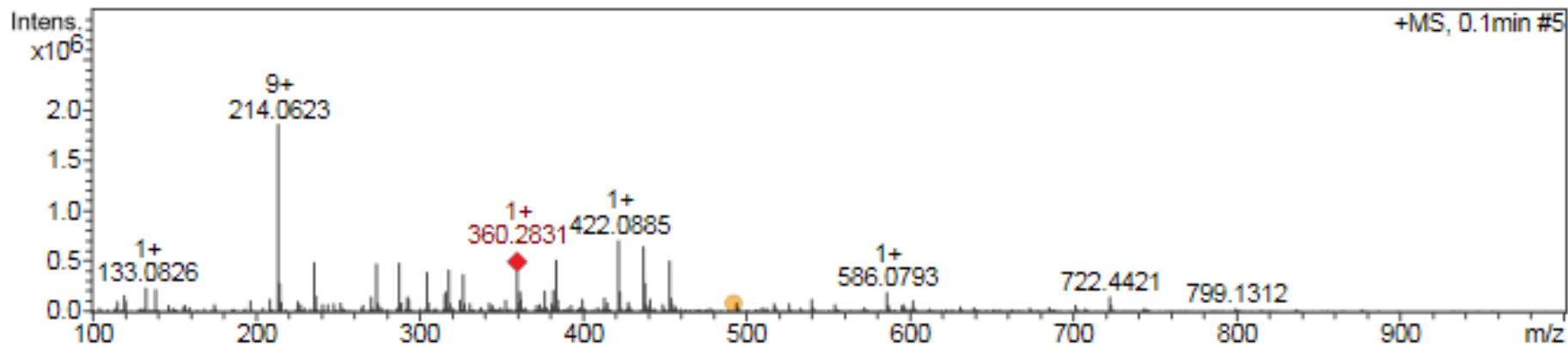


Fig D.15: GC-MS of 6-(1-carbamoyl-5-(furan-2-yl)-4,5-dihydro-1H-pyrazol-3-yl)-2-(furan-2-yl)-3-phenylquinoline-4-carboxylic acid (XV).

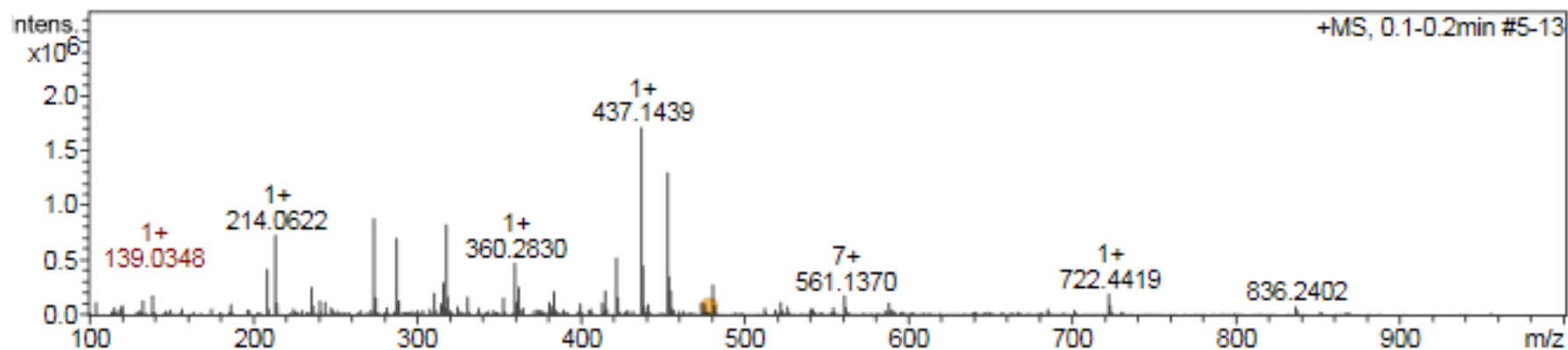


Fig D.16: GC-MS of 2-(furan-2-yl)-6-(7-(furan-2-yl)-2,3,6,7-tetrahydro-1,4-oxazepin-5-yl)-3-phenylquinoline-4-carboxylic acid (XVI).

Appendix E

2D model interactions of designed quinoline-4-carboxylic acid derivatives with dihydroorotate dehydrogenase enzyme (DHODH).

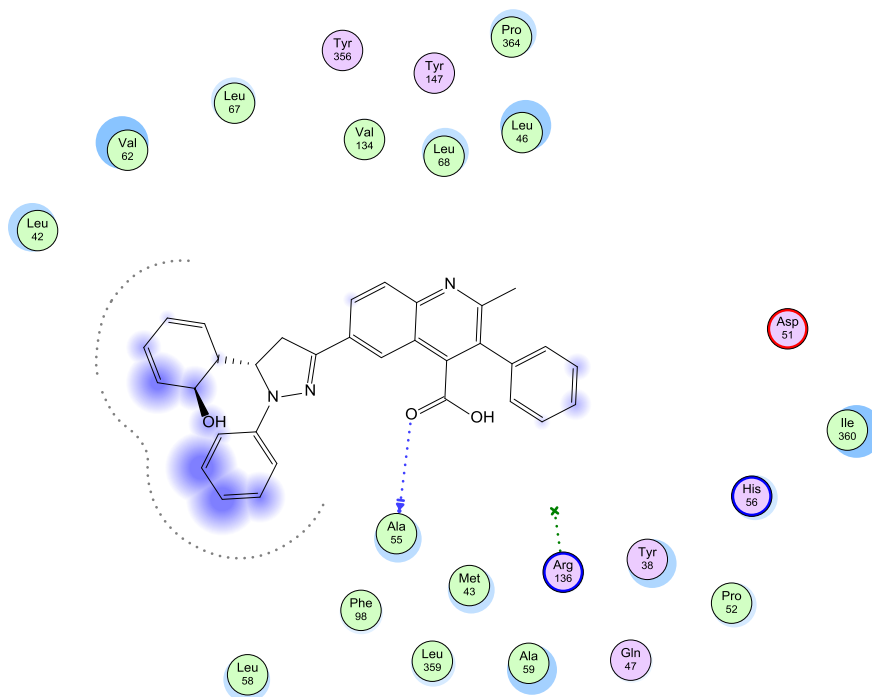


Fig E.1: Interactions of compound (A11).

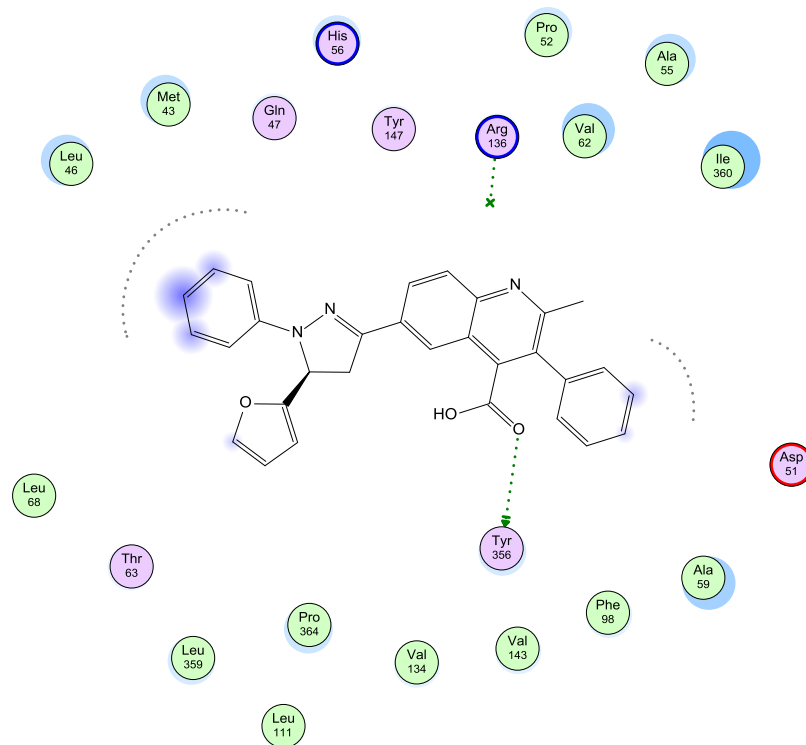


Fig E.2: interactions of compound (A25).

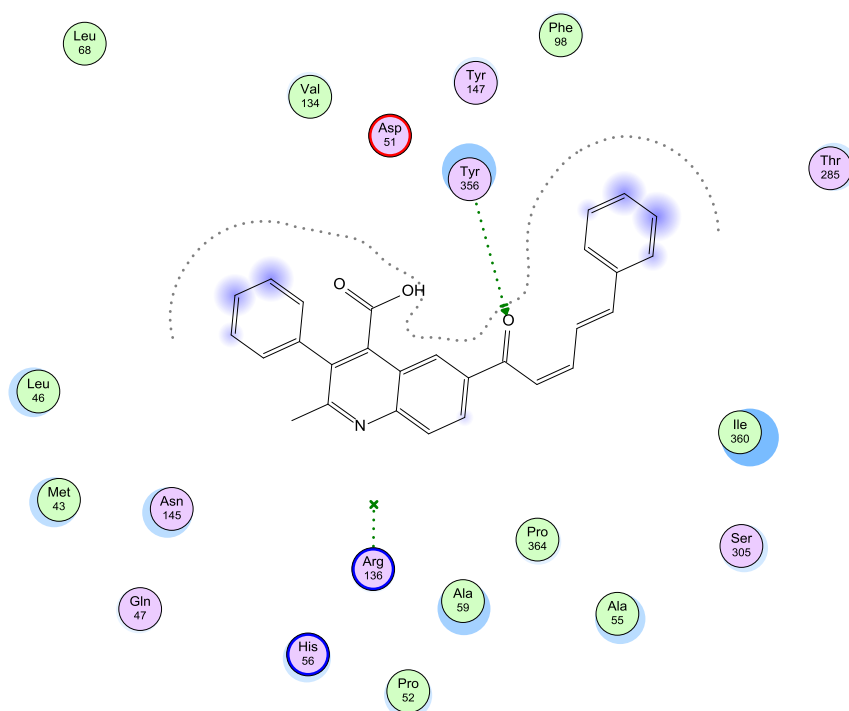


Fig E.3: interactions of compound (A29).

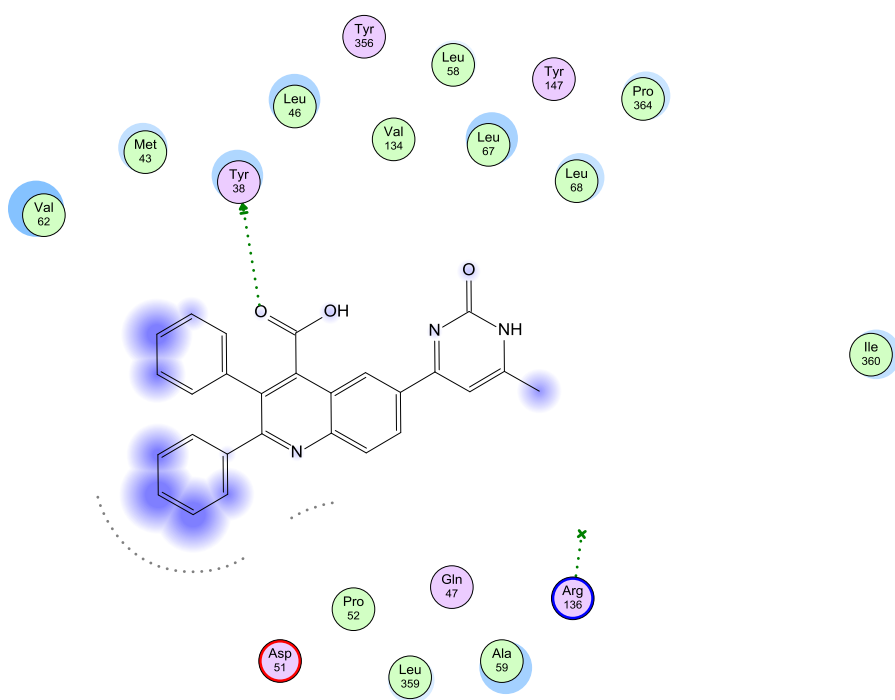


Fig E.4: interactions of compound (B2).

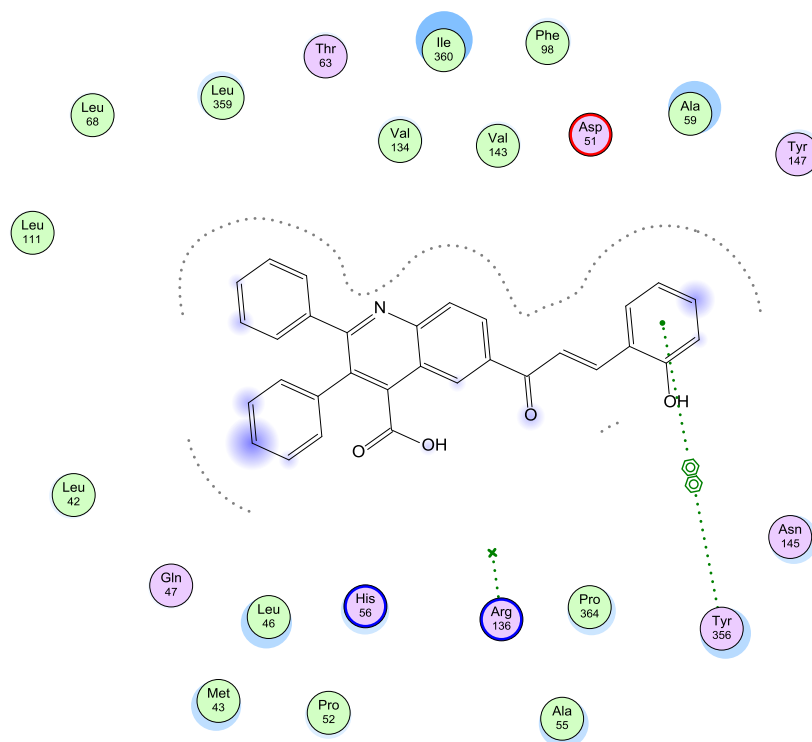


Fig E.5: interactions of compound (B8)

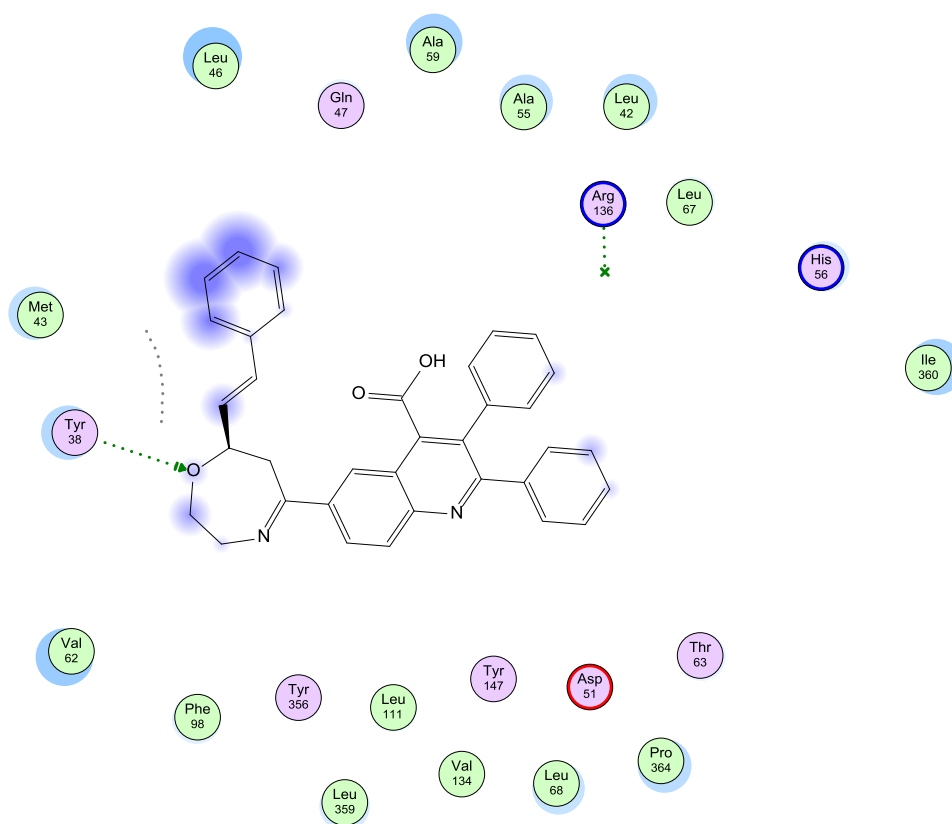


Fig E.6: interactions of compound (B35)

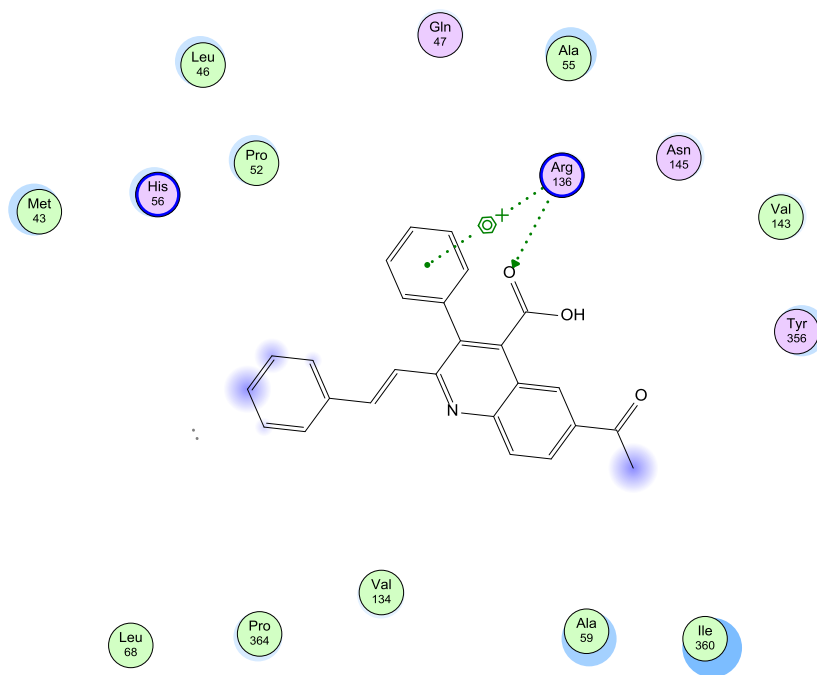


Fig E.7: interactions of compound (C)

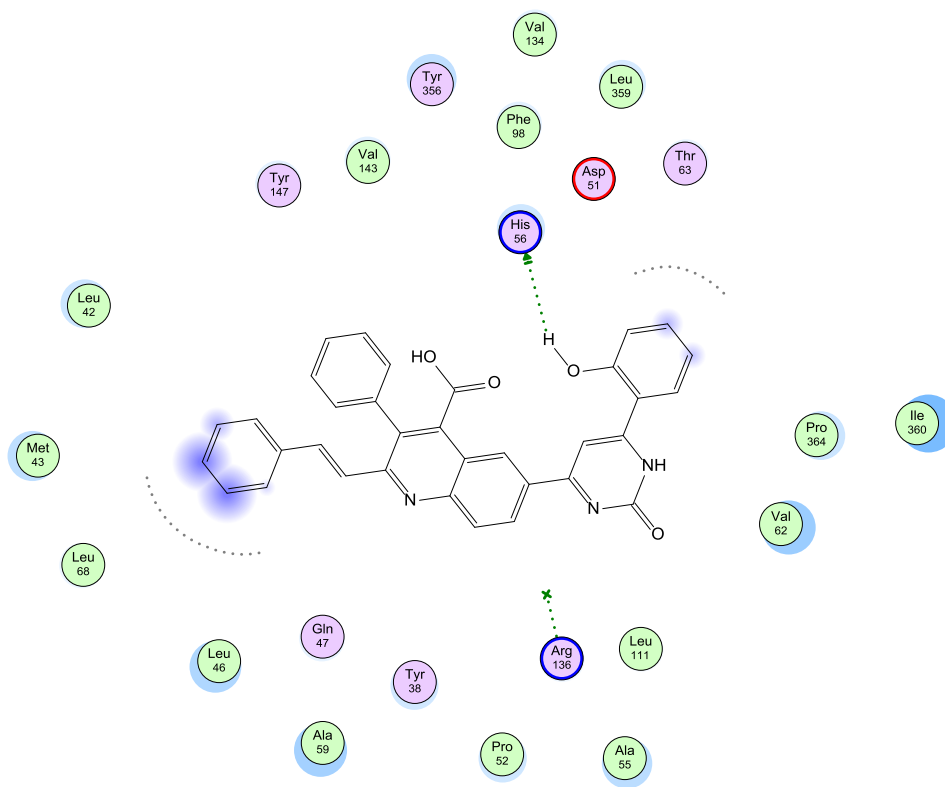


Fig E.9: interactions of compound (C9)

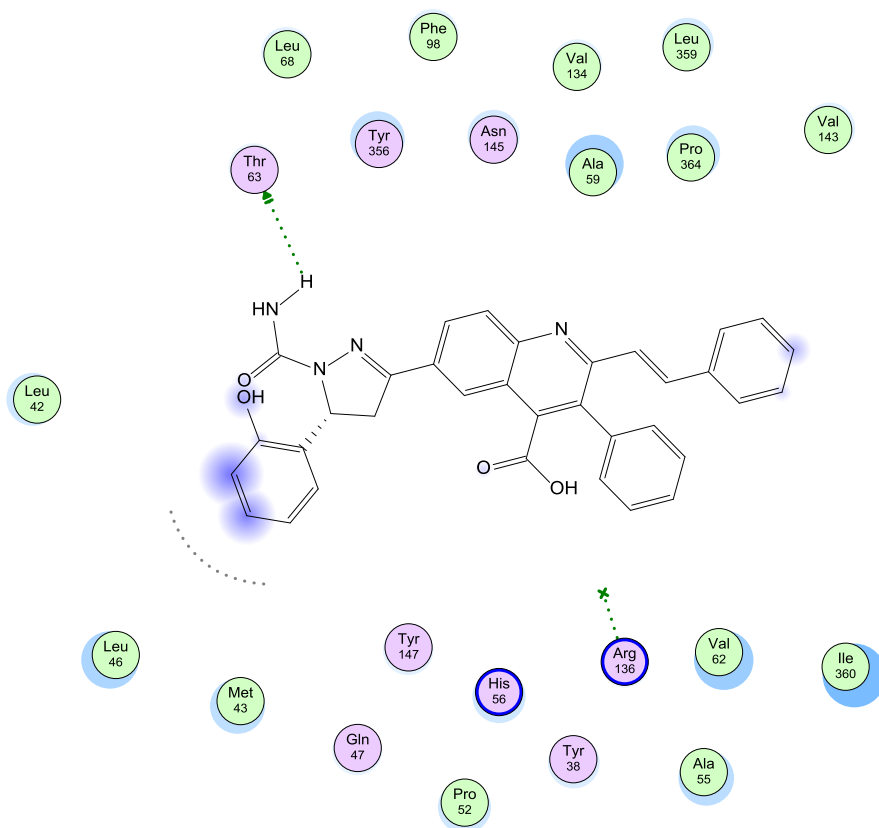


Fig E.10: interactions of compound (C13)

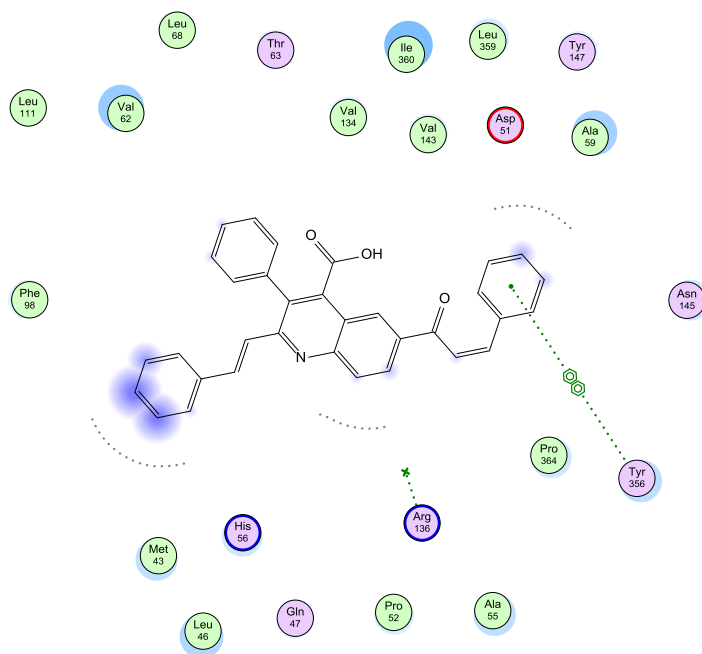


Fig E.11: interactions of compound (C15)

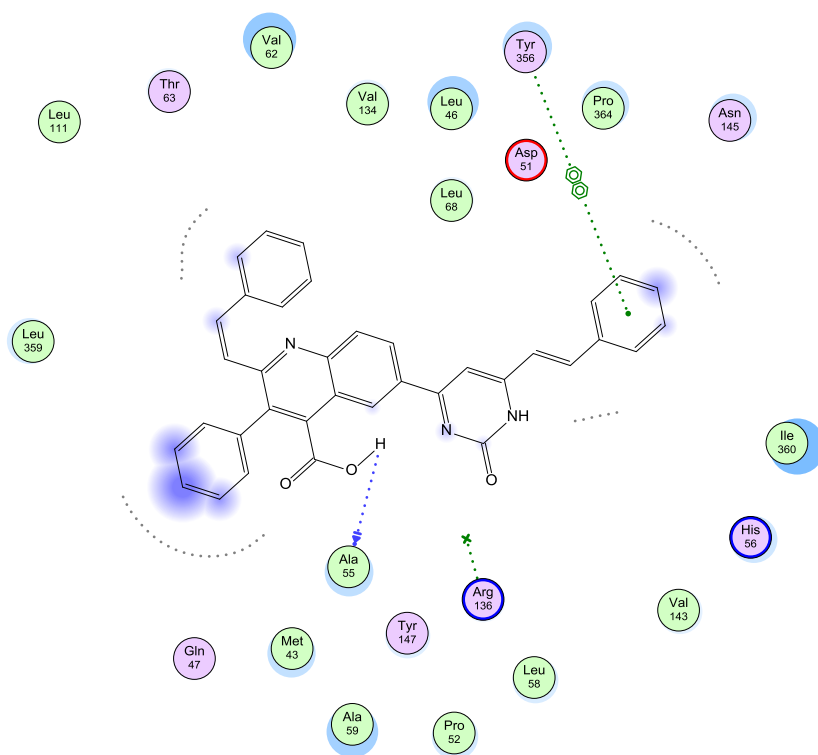


Fig E.14: interactions of compound (C32)

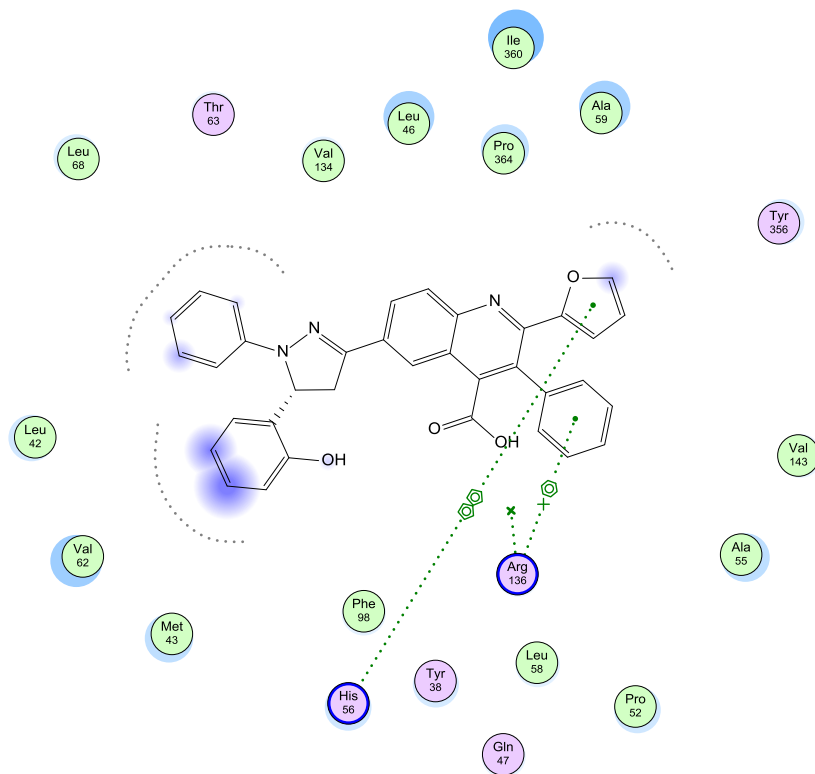


Fig E.15: interactions of compound (D11)

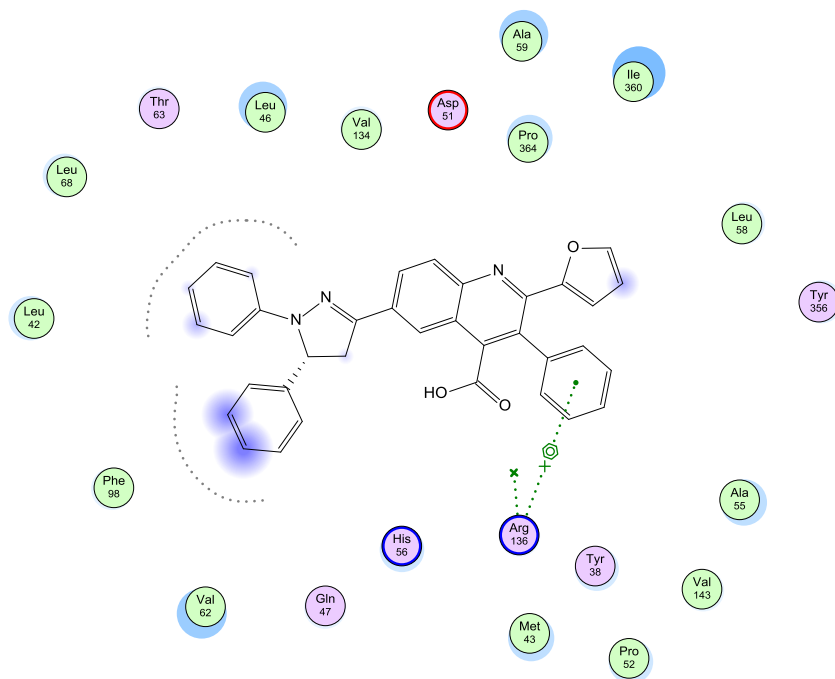


Fig E.16: interactions of compound (D18)

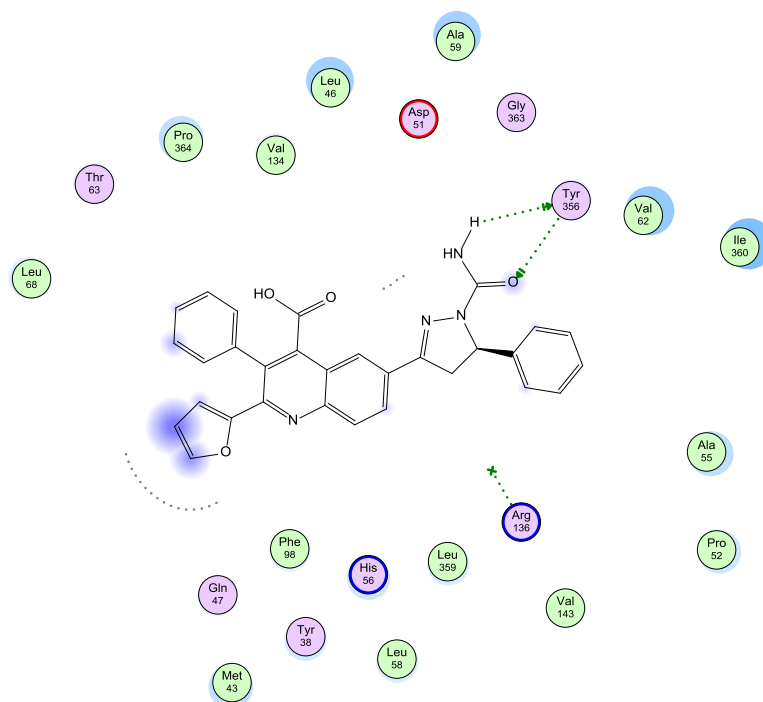


Fig E.17: interactions of compound (D20)

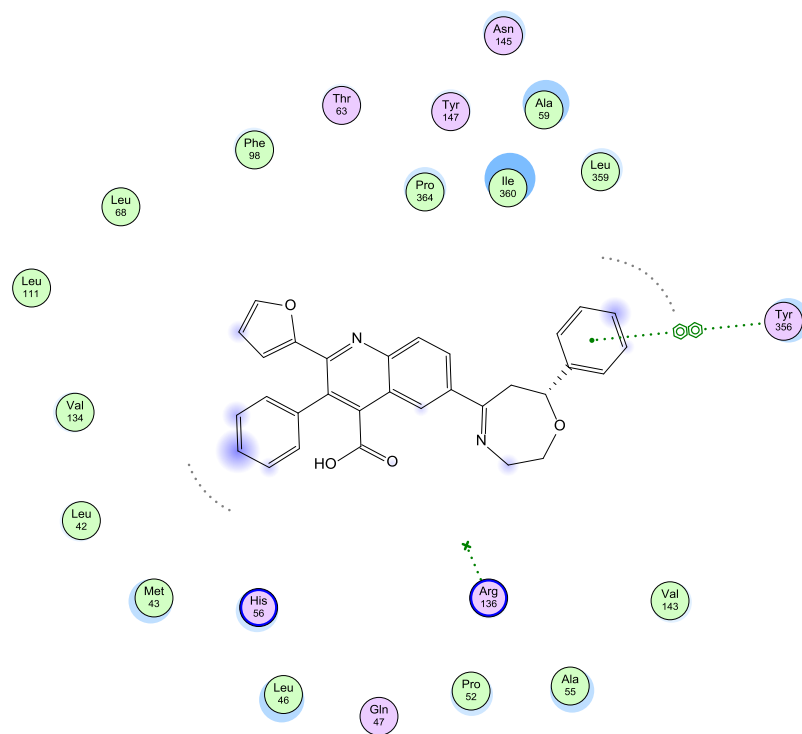


Fig E.18: interactions of compound (D21)

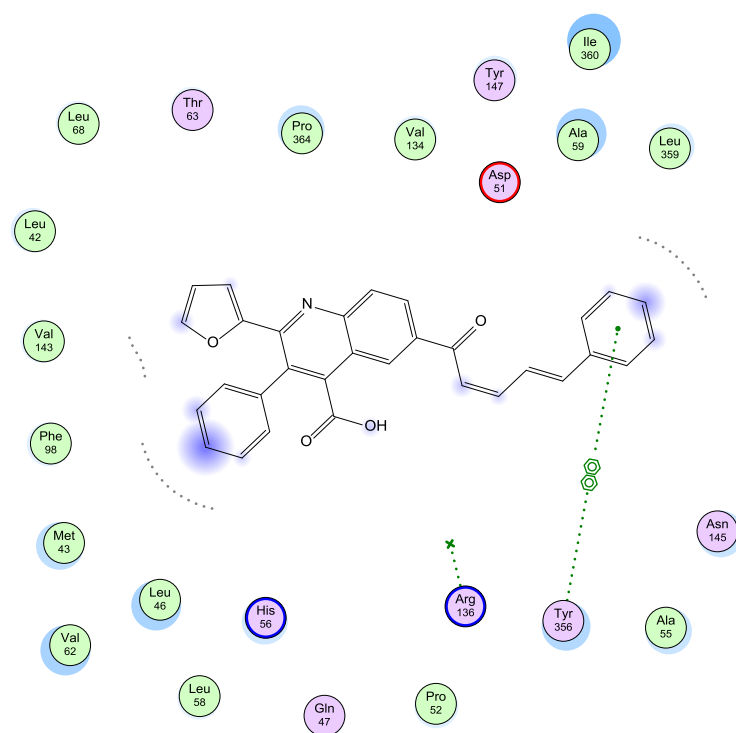


Fig E.19: interactions of compound (D29)

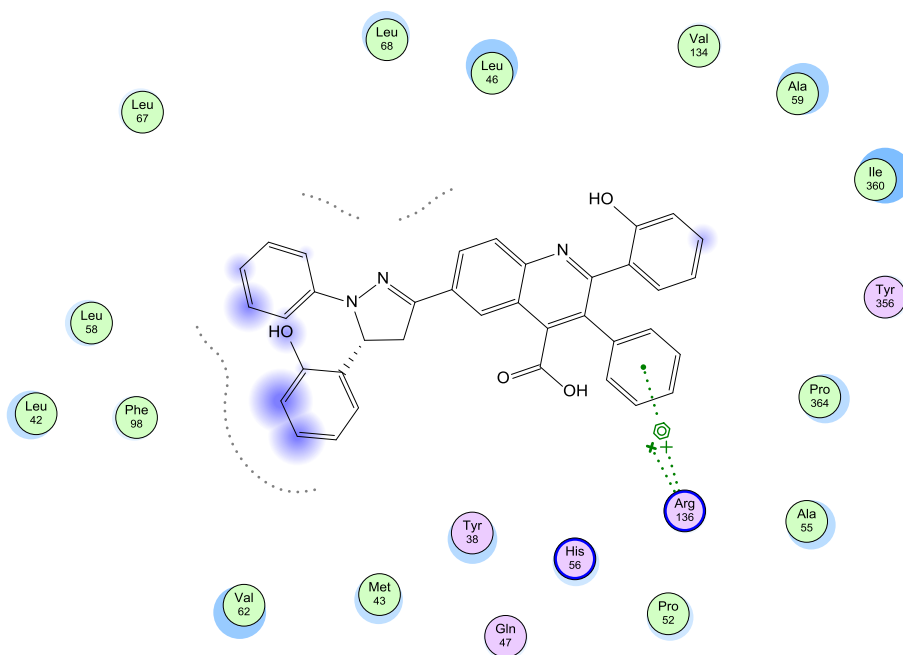


Fig E.20: interactions of compound (E11)

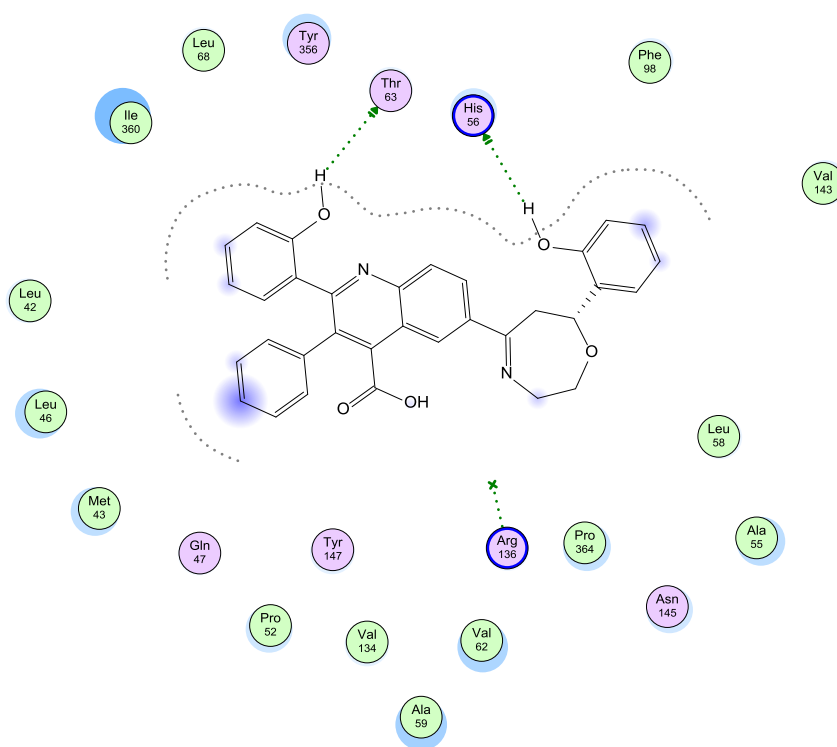


Fig E.21: interactions of compound (E14)

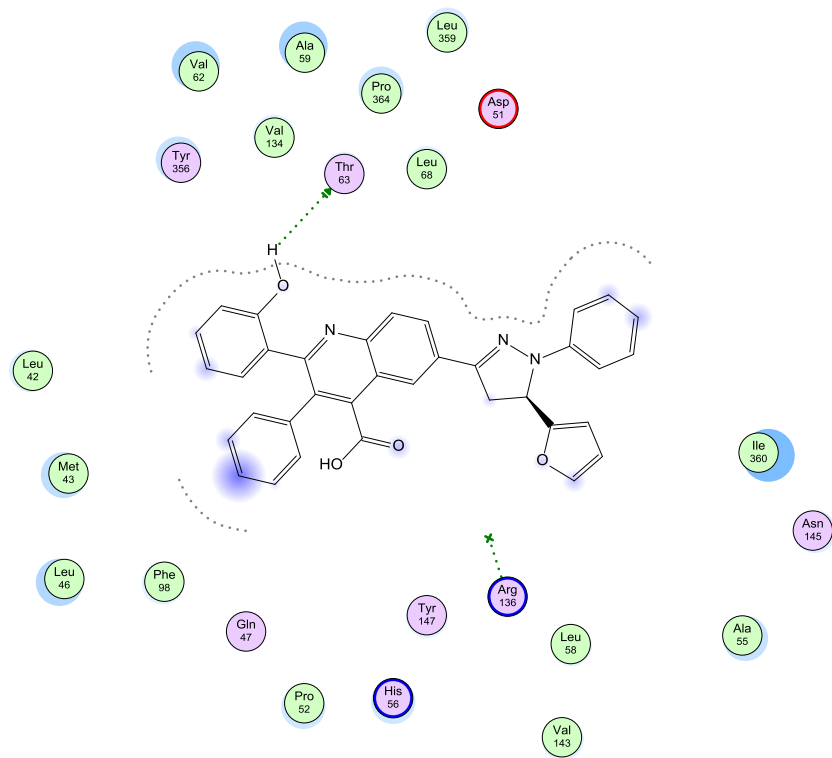


Fig E.22: interactions of compound (E25)

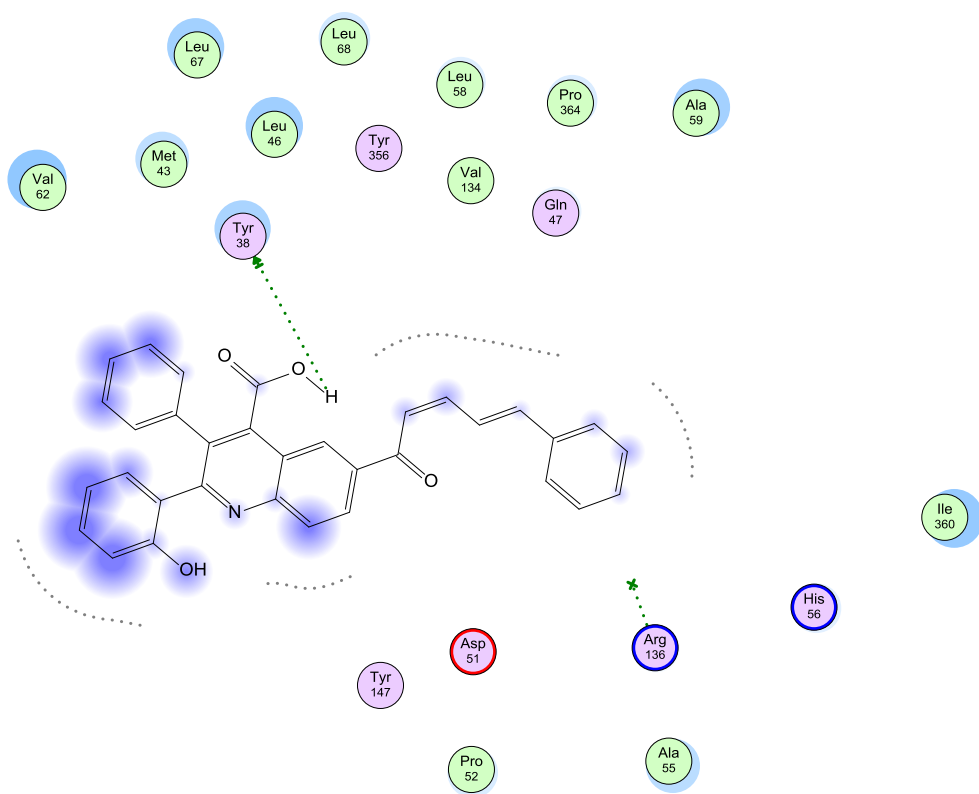


Fig E.23: interactions of compound (E26)

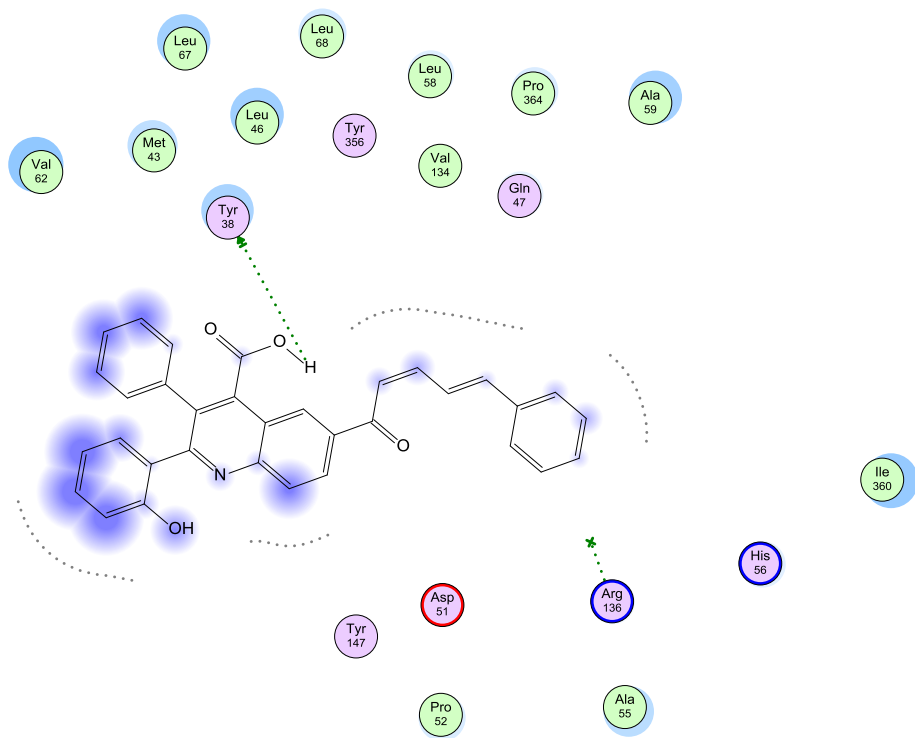


Fig E.24: interactions of compound (E29)

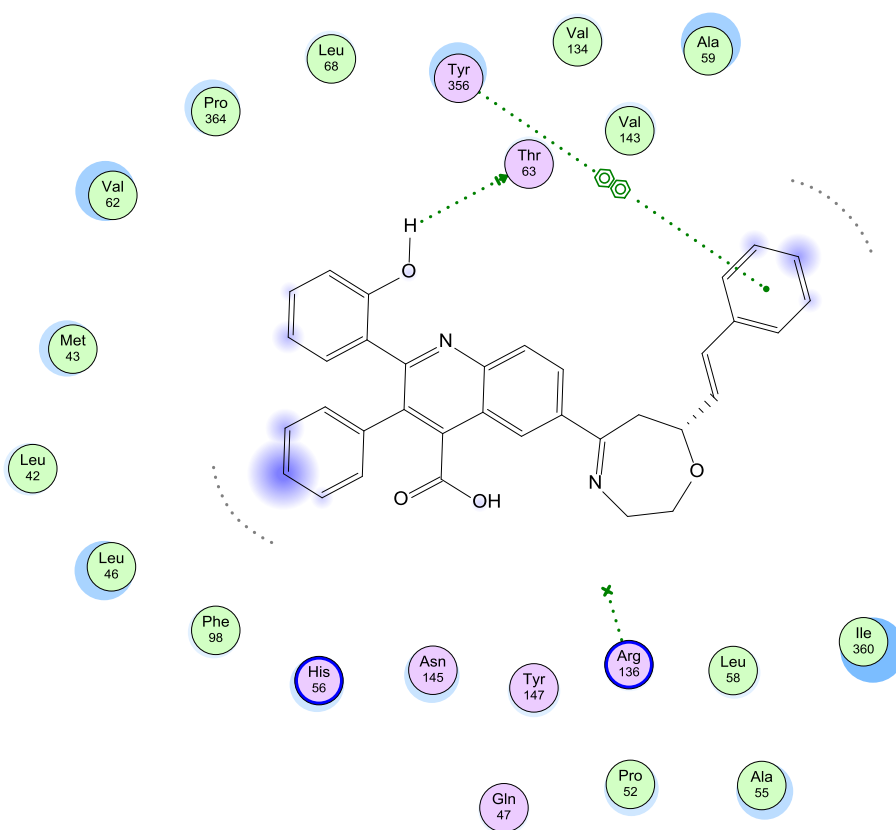


Fig E.25: interactions of compound (E35)